OXYGEN, CARBON DIOXIDE AND AMMONIA EXCHANGE IN THE GASTROINTESTINAL TRACT OF TELEOST FISH

by

Hyewon (Ellen) Jung

B.Sc., The University of British Columbia, 2014

M.Sc., The University of British Columbia, 2018

A THESIS SUBMITTED IN PARTIAL FULFILLMENT OF

THE REQUIREMENTS FOR THE DEGREE OF

DOCTOR OF PHILOSOPHY

in

THE FACULTY OF GRADUATE AND POSTDOCTORAL STUDIES

(Zoology)

THE UNIVERSITY OF BRITISH COLUMBIA

(Vancouver)

July 2022

The following individuals certify that they have read, and recommend to the Faculty of Graduate and Postdoctoral Studies for acceptance, the dissertation entitled:

Oxygen, Carbon Dioxide and Ammonia Exchange In The Gastrointestinal Tract Of Teleost Fish

submitted by Hyewon (Ellen) Jung in partial fulfillment of the requirements for

the degree of Doctor of Philosophy

in Zoology

Examining Committee:

Chris M. Wood, Adjunct professor, Department of Zoology, UBC
Co-Supervisor

Colin J. Brauner, Professor, Department of Zoology, UBC
Co-Supervisor

Juan Fuentes, Senior Researcher, Centre of Marine Sciences, Universidade do Algarve
External Examiner

William K. Milsom, Emeritus, Department of Zoology, UBC
University Examiner

Bill Sheel, Professor, School of Kinesiology, UBC
University Examiner

Additional Supervisory Committee Members:

Anthony Farrell, Professor, Department of Zoology, UBC
Supervisory Committee Member

Philip Matthews, Associate professor, Department of Zoology, UBC
Supervisory Committee Member

Abstract

The gastrointestinal tract (GIT) of teleost fish is a multifunctional organ system involved in digestion, assimilation of nutrients, immune responses, neuroendocrine functions and osmoregulation. Many of these processes have implications for gas exchange, acid-base regulation and ion regulation. However, there is a current lack of knowledge on the basic physiology of the three respiratory gases - oxygen, carbon dioxide and ammonia - in the GIT. My thesis expands our current understanding of the basic profiles of the three respiratory gases in the GIT lumen, their potential exchange with the vascular system, and the changes associated with feeding. In addition, the potential influence of osmoregulatory functions on these parameters was investigated by conducting a comparative study between freshwater and seawater species; the rainbow trout (*Oncorhynchus mykiss*) was used as a freshwater model species for in depth investigations and the English sole (*Parophrys vetulus*) as a comparative seawater species. A combination of *in vivo*, *in situ* and *in vitro* techniques was used to assess these areas at the whole animal, tissue and cellular levels. Based on findings from 5 research chapters, I conclude that both freshwater rainbow trout and seawater English sole have nearly anoxic, hypercapnic and high ammonia environments in the GIT lumen in both fasting and fed conditions. Feeding increases carbon dioxide and ammonia levels, but the GIT epithelia regulates the diffusion of the three respiratory gases into the vascular system regardless of feeding status. The different osmoregulatory requirements in seawater *versus* freshwater did not greatly affect these conclusions. Furthermore, the intestinal tissues have the capacity to handle and transport two nitrogenous products: urea and ammonia. Throughout the GIT, there were expressions of both a potential NH_4^+ transporter (NKCC) and NH_3 channels (Rhbg, Rhcg2), but ammonia transport was independent of the PNH_3 gradient. The thesis also highlights the importance of the

stomach in absorbing ammonia despite a reverse PNH_3 gradient at physiologically relevant pH levels.

Lay Summary

The gastrointestinal tract, recognized as a “second brain” in mammals, also serves many functions including digestion and water balance in fish. In fish, the gases inside the GIT lumen can potentially impact blood oxygen delivery, acid-base regulation and nitrogenous waste removal, and thus on overall physiology. This thesis identified extreme conditions in the system with a near absence of oxygen, and high levels of both carbon dioxide and ammonia – all of which could have lethal effects on the animal. Digestive processes elevated the latter two gases, yet different water regulation requirements of freshwater versus seawater fish did not affect the conditions. Differential handling of ammonia, as well as another nitrogenous waste urea by different sections of the tract occurred. However, the transport of all three gases into the bloodstream was largely regulated, allowing fish to maintain relative homeostasis despite the extreme conditions inside the gastrointestinal tract.

Preface

Chapter 1 is a General Introduction providing the research objectives of the thesis, relevant background information and brief summaries of research Chapters 2 – 6. The following research Chapters 2 – 6 are replicates of manuscripts either published in or submitted to peer-reviewed journals. Please note that throughout these research Chapters, the pronoun "we" is used, as in the original manuscripts, because while I led the investigations, all authors take responsibility for the contents. However, in Chapter 1 (General Introduction), Chapter 7 (Conclusions and Future Directions), and the Appendix, the pronoun "I" is used, as I take sole responsibility for the ideas therein.

Chapter 2 has been published as Jung EH, Eom J, Brauner CJ, Martinez-Ferreras F, Wood CM (2020) entitled "The gaseous gastrointestinal tract of a seawater teleost, the English sole (*Parophrys vetulus*)" in Comparative Biochemistry and Physiology A, 247, 110743. Doi.org/10.1016/j.cbpa.2020.110743. I performed all the experiments, with help from Dr. Eom for PCO_2 measurements. Dr. Martinez-Ferreras supplied the custom-built PCO_2 optodes employed in the study and advice on their use. I analyzed the data in consultation with Dr. Wood. I wrote the first draft of the manuscript, which was edited by Dr. Wood and Dr. Brauner, and revised by all authors.

Chapter 3 has been published as Jung EH, Brauner CJ, Wood CM (2022) entitled "Post-prandial respiratory gas and acid-base profiles in the gastrointestinal tract and its venous drainage in freshwater rainbow trout (*Oncorhynchus mykiss*) and seawater English sole (*Parophrys vetulus*)" in Comparative Biochemistry and Physiology A, 265, 111123. Doi.org/10.1016/j.cbpa.2021.111123. This paper was invited by the Editors for a special issue entitled "Digestion Physiology". I performed all the experiments and analyzed the data in

consultation with Dr. Wood. I wrote the first draft of the manuscript, which was edited by Dr. Wood and Dr. Brauner.

Chapter 4 has been submitted as Jung EH, Brauner CJ, Wood CM (2022) entitled "Do extreme postprandial levels of oxygen, carbon dioxide, and ammonia in the digestive tract equilibrate with the bloodstream in the freshwater rainbow trout (*Oncorhynchus mykiss*)?" to a peer-reviewed journal and is under revision. I performed all the experiments and analyzed the data in consultation with Dr. Wood. I wrote the first draft of the manuscript, which was edited by Dr. Wood and Dr. Brauner.

Chapter 5 has been published as Jung EH, Smich J, Rubino JG, Wood CM (2021) entitled "An *in vitro* study of urea and ammonia production and transport by the intestinal tract of fed and fasted rainbow trout: responses to luminal glutamine and ammonia loading" in the Journal of Comparative Physiology B, 191, 273-287. Doi.org/10.1007/s00360-020-01335-9. This was a data analysis and writing project performed during the COVID-19 pandemic lockdown. The experiments were directly relevant to the thesis objectives. The data had previously been collected by an Honours student Joanna Smich, mentored and assisted by a M.Sc. student Julian Rubino, both supervised by Dr. Wood. I analyzed the data in consultation with Dr. Wood. I wrote the first draft of the manuscript, which was edited by Dr. Wood and revised by all authors.

Chapter 6 has been submitted as Jung EH, Nguyen J, Nelson C, Brauner CJ, Wood CM (2022) entitled "Ammonia transport is independent of PNH_3 gradients across the gastrointestinal epithelia of the rainbow trout; a Role for the Stomach" to a peer-reviewed journal and is under revision. I performed all the experiments, with help from summer student Jessica Nguyen on the gut sac work and Ph.D. student Charlotte Nelson on the qPCR work. I analyzed the data in

consultation with Dr. Wood and Dr. Brauner. I wrote the first draft of the manuscript, which was edited by Dr. Wood and Dr. Brauner, and revised by all authors.

Chapter 7 provides Conclusions and Future Directions. This chapter summarizes the major findings of my work and points to research questions arising from it

The Appendix presents my preliminary findings (unpublished) on the vascular morphology of the gut, specifically the potential for a countercurrent exchanger in the intestinal blood vessels.

All experiments performed for this thesis followed the guidelines of the Canada Council for Animal Care, under joint approval of the animal care committees at the University of British Columbia (AUP#: 14-0251, 18-0271 and A18-0271), Bamfield Marine Sciences Centre (AUP#: RS-18-20, RS-19-15, RS-20-17) and McMaster University (AUP#: 12-12-45).

Table of Contents

List of Tables

List of Figures

List of Abbreviations

AE	bicarbonate-chloride anion exchanger
BMSC	Bamfield Marine Sciences Centre
CA	carbonic anhydrase
CCE	countercurrent exchanger
cDNA	complementary deoxyribonucleic acid
CMA	coeliacomesenteric artery
CO_2	carbon dioxide
CPS	carbamoyl phosphate synthetase
DA	dorsal aorta
FW	freshwater
GDH	glutamate dehydrogenase
GIT	gastrointestinal tract
GLN	glutaminase
GS	glutamine synthetase
h	hours
Hb	hemoglobin
Hct	hematocrit
HPV	hepatic portal vein
I.U.	international unit
Jm_{amm}	mucosal ammonia flux rate
Js_{amm}	serosal ammonia flux rate
Jt_{amm}	endogenous tissue ammonia production rate

$Jm_{urea\text{-}N}$	mucosal urea flux rate
$Js_{urea\text{-}N}$	serosal urea flux rate
$Jt_{urea\text{-}N}$	endogenous tissue urea production rate
K^+	potassium
min	minutes
mm Hg	millimeter of mercury
$\dot{M}O_2$	oxygen consumption rate
mRNA	messenger ribonucleic acid
MS-222	tricaine methanesulfonate
NH_3	gaseous ammonia
NH_4^+	ionic ammonium
NH_4OH	ammonium hydroxide
NKA	sodium-potassium adenosine triphosphatase
NKCC	sodium-potassium-two chloride cotransporter
NKCC1	sodium-potassium-two chloride cotransporter type 1
NKCC2	sodium-potassium-two chloride cotransporter type 2
O_2	oxygen
OUC	ornithine-urea cycle
PCA	perchloric acid
PCO_2	partial pressure of carbon dioxide
P_aCO_2	partial pressure of carbon dioxide in the arterial blood
P_vCO_2	partial pressure of carbon dioxide in the venous blood
PNH_3	partial pressure of ammonia

PO_2	partial pressure of oxygen
P_aO_2	partial pressure of oxygen in the arterial blood
P_vO_2	partial pressure of oxygen in the venous blood
Rh	rhesus glycoproteins
Rhag	rhesus glycoproteins type a
Rhbg	rhesus glycoproteins type b
Rhcg1	rhesus glycoproteins type c1
Rhcg2	rhesus glycoproteins type c2
s	seconds
SDA	specific dynamic action
SIV	subintestinal vein
SW	seawater
Tamm	total ammonia concentration
TCO_2	total CO_2 content
UBC	University of British Columbia
UT	urea transporter

Acknowledgements

I would like to express my sincere gratitude to my supervisors, Dr. Chris Wood and Dr. Colin Brauner, for providing guidance and feedback throughout the course of my PhD degree. Chris, your infinite passion for research was truly inspirational and has been really influential in shaping my way of approaching science. Colin, I remember sitting in your undergraduate class and becoming so fascinated about physiology. Thank you for giving me the opportunity to find my own passion in research. Over the years, Chris and Colin have given me the chance to broaden my perspectives about science by supporting research trips to the Amazon, Vietnam and Bamfield, through which I grew tremendously as a scientist. My gratitude extends to my committee members, Dr. Anthony Farrell and Dr. Philip Matthews, for their immense knowledge and plentiful feedbacks. Special thank you to Dr. Junho Eom for his continuous support as a friend and a mentor since undergraduate years. To the fellow friends in academia – especially Charlotte Nelson, Anne Kim, Jasmin Wong – our "wine" sessions pulled me through the tough times. My forever officemate Charlotte, thank you for riding the PhD rollercoaster journey with me. Most importantly, my family deserves endless gratitude for their unconditional, unequivocal, and loving support. Thank you for always believing in me and giving me the confidence to complete this degree. Thanks again to everyone who made this thesis and me possible.

Chapter 1: Introduction

1.1 Overview

The primary functions of the gastrointestinal tract (GIT) include digestion, absorption, excretion, and protection. Understanding the complex physiology of this organ system is proving to be crucial, especially in the midst of increasing evidence of the bidirectional link with the brain and thus its importance in overall health (i.e. Kalantar-Zadeh et al., 2019; Liu et al., 2022; Rogers et al., 2016; Sharon et al., 2016). Various gases exist in the mammalian GIT lumen that originate from swallowed air, production *via* internal chemical reactions, or bacterial fermentation of dietary substrates. In teleost fish, the levels of luminal gases in the GIT and their interactions with other physiological systems, especially the bloodstream, are largely unexplored. There are three respiratory gases that can diffuse through biological membranes and enter the blood circulation in teleosts: O_2, CO_2 and ammonia (NH_3 & NH_4^+; Randall and Ip, 2006).

In mammals, the luminal O_2 originates from swallowed air and becomes depleted down the GIT, reaching near anoxia in the intestine (Bettinger, 2015; Espey, 2013; Friedman et al., 2018; Kalantar-Zadeh et al., 2019; Kurbel et al., 2006). The luminal CO_2 arises as a byproduct of chemical reactions involved in digestion (e.g. neutralization of gastric HCl secretion by pancreatic and biliary $NaHCO_3$ secretions) and microbial breakdown of feed, and thus exists in high levels (Lacy et al., 2011; Tomlin et al., 1991). Ammonia also exists in the lumen in high levels originating from ammonia liberation during digestion as well as urea hydrolysis by microbes in the GIT (Lin and Visek, 1991; Moran and Jackson, 1990; Mouillé et al., 2004; Vince and Burridge, 1980). Luminal CO_2 and/or ammonia are either absorbed across the intestinal epithelia and enter the blood circulation, used by microbes, breathed out, or released as

flatulence (Ghoos et al., 1993; Imler et al., 1988; Lacy et al., 2011; Ohashi et al., 2007; Oliphant and Allen-Vercoe, 2019; Summerskill and Wolpert, 1970).

Prior to the investigations in this thesis, there was very little information on respiratory gases in the GIT of fish - indeed none at all on PO_2, a few measurements showing luminal ammonia considerably higher than blood ammonia (Bucking and Wood, 2012; Rubino et al., 2014) and one recent report that directly measured PCO_2 in the lumen of two fish species found considerably higher levels than that of the blood (Wood and Eom, 2019). The latter is supported by indirect calculations of high PCO_2 in the GIT lumen in a number of other species (summarized by Wood, 2019). Thus, to a large extent, the basic GIT gas profiles and their significance in fish are unexplored.

Moreover, the equilibration of these high luminal levels of PCO_2 and ammonia with the blood circulating past the GIT could be very harmful to the fish. Certainly, if a human's blood PCO_2 and ammonia increased to the levels measured in their GIT, the result would likely be toxic (Raabe, 1990; Shigemura et al., 2017). Likewise in fish, the PCO_2 and ammonia levels recorded so far in the GIT lumen would likely cause toxicity if equilibrated with the blood (e.g. Fivelstad et al., 2003; Lee et al., 2003; Randall and Tsui, 2002; Söderström and Nilsson, 2000). Thus, understanding the physiology of GIT luminal gases in teleost fish can give insight into GIT related disorders (i.e. Li et al., 2017; Sundh et al., 2011; Tran et al., 2018; Zhang et al., 2015), possibly illuminate the gut-brain-axis, and also contribute to improvements in aquaculture targeting the GIT of commercially important species and in its relation to improving growth performance (e.g. Couto et al., 2016; Krogdahl et al., 1999) and immune system function (e.g. Hoseinifar et al., 2017; Ramos et al., 2017; Ringø et al., 2010). This thesis aims to lay the physiological groundwork in understanding the GIT luminal gases in fasting and fed states and

the consequent blood gas levels in fish. Furthermore, I aim to broaden the thesis by investigating the luminal CO_2 and ammonia dynamics in depth. In marine teleost fish, the GIT serves an additional function of maintaining water balance. This involves movements of acid-base equivalents across the epithelia of the GIT, and potentially further contributes to the high PCO_2 in the lumen (see Section 1.5). Thus, the potential effects on luminal and blood gases accompanying this osmoregulatory role are investigated by comparing freshwater (FW) species (rainbow trout; *Oncorhynchus mykiss*) and seawater (SW) species (English sole; *Paroprys vetulus*). In addition, despite findings of high ammonia in the intestine and its potential transport into the blood circulation (see Section 1.6), there is insufficient information on how different GIT tissues handle and absorb the nitrogenous products. Therefore, another key objective of this thesis is to illuminate how nitrogenous wastes, particularly ammonia, are handled by different sections of the GIT.

1.2 GIT Metabolism and Cardiovascular system

1.2.1 GIT Metabolism

The GIT of teleosts exhibits high tissue metabolic demand that relies on the circulatory system for O_2 supply and CO_2 removal (see Section 1.2.2). In SW, the additional osmoregulatory function of the GIT (see Section 1.5) consequently requires greater metabolic supply (Brijs et al., 2016; Brijs et al., 2018) that is supported by greater blood flow to the GIT (Brijs et al., 2015). In fasting rainbow trout, the entire GIT takes up about 11-25 % of the whole-animal O_2 consumption measured *in vivo* (Brijs et al., 2018), indicating it represents a significant proportion of total metabolic demand in the whole animal. In mammals, the GIT is approximately 6 % of

body mass but uses 20-25 % of the whole animal O_2 consumption in the resting, fasted state (Duée et al., 1995; Vaugelade et al., 1994; Wolff, 2007; Yen et al., 1989).

Following feeding, increased metabolic demand associated with increased gut motility, increased active transport of nutrients, the synthesis and activation of digestive enzymes, and most importantly the post-absorptive protein synthesis of both the GIT and the whole animal lead to an increase in overall O_2 consumption ($\dot{M}O_2$). The elevation in postprandial $\dot{M}O_2$, termed Specific Dynamic Action (SDA), can reach a value more than double that of fasting animals (Alsop and Wood, 1997; Brown and Cameron, 1991a; Brown and Cameron, 1991b; Chabot et al., 2016; Jobling, 1981; McCue, 2006; Secor, 2009). *In vitro*, the $\dot{M}O_2$ of isolated toadfish *(Opsanus beta*) intestinal tissues sampled following feeding was significantly higher relative to tissues sampled from fasting animals, peaking at 187 % at 6 h following feeding (Taylor and Grosell, 2009).

1.2.2 Cardiovascular system

The blood flow to the GIT is important in supplying required O_2, removal of CO_2, ammonia and other waste products, and in carrying away absorbed nutrients to the liver and other tissues. In teleosts, the coeliacomesenteric artery (CMA) is the major vessel that branches off from the dorsal aorta (DA) and supplies the stomach, intestine, liver and gonads (Farrell et al., 2001; Thorarensen et al., 1991). In some species with larger and very-well vascularized GITs such as shorthorn sculpin (*Myoxocephalus scorpius*), the branchial arteries unite to form the CMA that receives oxygenated blood from the gills directly (reviewed by Seth et al., 2011). The intestinal blood then predominantly drains *via* the subintestinal vein (SIV) that joins with the venous blood from the stomach to form the hepatic portal vein (HPV). The liver consequently

receives venous blood from the GIT and also oxygenated arterial blood supply from branches of the CMA.

In a fasting SW teleost under routine conditions, the total blood flow to the GIT is typically 10-40 % of cardiac output, similar to mammals (see references within Seth and Axelsson, 2011). After feeding, the GIT blood flow increases greatly (by 70-150 %) with an increase in cardiac output through elevations in both stroke volume and heart rate (Axelsson and Fritsche, 1991; Axelsson et al., 1989; Axelsson et al., 2000; Gräns et al., 2009a; Seth et al., 2009; Thorarensen and Farrell, 2006). This serves to supply the extra O_2 needed to supply the GIT demands of SDA. An alteration of the blood flow to specific tissues is made possible by changing the total cardiac output and/or the vascular resistance through vasoconstriction/vasodilation. Since the visceral (GIT) circulation and the somatic circulation are organized in parallel, their blood flow affects each other. Upon feeding, a vasodilation of the GIT vessels, regulated by the enteric nervous system (Seth and Axelsson, 2010) and hormones (Fara et al., 1972), and an increase in vascular resistance of other peripheral tissues, creates a local hyperemia to meet the high demand and to carry away the absorbed nutrients.

In situations where blood flow to the GIT is unnecessary, fish temporarily suppress the visceral circulation and redirect the blood to the other tissues where it is critically needed (Farrell et al., 2001). For example, exercising salmonids increase cardiac output, decrease the blood flow to the GIT by 70-90 % and redirect the blood to the locomotory muscles that require additional O_2 and nutrient supply (see references within Seth and Axelsson, 2011). Thus, it may be that any stressful situations that require redirection of blood flow, such as exercise, can compromise GIT function, including digestion, osmoregulation and acid-base regulation.

1.3 Alkaline tide

As a consequence of H^+ secretion into the stomach for HCl formation, there is an equimolar increase in plasma HCO_3^- after feeding, causing an alkalinisation of the blood ("alkaline tide"). While originally described in mammals (reviewed by Niv and Fraser, 2002), this is now well documented to occur in fish as well (Bucking and Wood, 2009; Cooper and Wilson, 2008; Wood et al., 2005; reviewed by Wood et al., 2019). The H^+ is pumped from the blood into the gastric lumen *via* H^+/K^+ ATPase (HKA), and the HCO_3^-, originating from hydration of CO_2 by intracellular carbonic anhydrase (CA), is pumped out into the bloodstream in exchange for extracellular Cl^- *via* a basolateral Cl^-/HCO_3^- anion exchanger (Hersey and Sachs, 1995; Niv and Fraser, 2002). Ectothermic amphibians and reptiles compensate the alkaline tide by voluntary respiratory acidosis (hypoventilation) to retain CO_2, but fish cannot use this route, as it would compromise O_2 uptake during SDA. Instead, fish species such as the dogfish shark (*Squalus acanthias*) and rainbow trout have been observed to compensate by excreting metabolic base across the gills (Bucking and Wood, 2008; Tresguerres et al., 2007; Wood et al., 2007; Wood et al., 2009). SW species appear to be especially well equipped to deal with the elevated metabolic base load of the alkaline tide due to their capacity for HCO_3^- secretion into the intestinal lumen for osmoregulation (Bucking et al., 2009b; see Section 1.5). Contrary to the gastric (with stomach) species, agastric (without a stomach) species seem to lack an alkaline tide due to the absence of digestive HCl secretion. In fact, an agastric FW-acclimated killifish (*Fundulus heteroclitus*) experience the opposite phenomenon of a postprandial metabolic acidosis ("acidic tide") due to the high net intestinal base secretion accompanying feeding (Wood et al., 2010).

1.4 Luminal PO_2 and PCO_2

1.4.1 Luminal PO_2 and villus countercurrent exchanger in mammals

This section will mainly discuss the luminal PO_2 and villus countercurrent exchanger (CCE) in the mammalian systems, as there are currently no studies that have investigated these in teleosts. In mammals, the O_2 originating mainly from swallowed air becomes increasingly depleted throughout the tract with the increasing abundance of anaerobic microbes (Bettinger, 2015; Kalantar-Zadeh et al., 2019) and oxidative reactions of the GIT fluids (Friedman et al., 2018). Additionally, there is a cross-sectional PO_2 gradient which decreases to near anoxia at the midpoint of the lumen (Espey, 2013). This diverse PO_2 range provides microenvironments suitable for different microbes. As discussed in the above sections, the respiratory physiology of the GIT in fish has been relatively well studied with respect to O_2 supply by the blood (reviewed by Seth et al., 2011), but prior to this thesis, no study had been done on the luminal PO_2.

In mammals, the villi of the intestine and the papillae of the ruminant stomach are densely packed with capillary beds and lymph capillaries called lacteals (Jodal and Lundgren, 1986). Although the shape of the villi and their vascular arrangements vary among species, they all have a supplying artery and a draining vein (Jodal and Lundgren, 1986). These capillary beds within the villus exhibit a small diffusion distance between the artery and vein of 20-30 μm, high capillary density and permeability, and slow blood transit time, all of which facilitate exchange between the vessels and create a site of potential countercurrent exchange (Jodal and Lundgren, 1986; Shepherd and Kiel, 1992). The arterial O_2 diffusing into the nearby O_2-poor venous blood, combined with O_2 consumption by tissues results in the tips of the villi being relatively hypoxic (Bustamante et al., 1989; Shepherd and Kiel, 1992), and contact with glucose (i.e., a nutrient)

further decreases villi PO_2 (Bohlen, 1980). However, the venous PO_2 remains relatively higher than the nearly anoxic lumen (Kurbel et al., 2006).

As such, the villus CCE short-circuits any small lipid-soluble and water-soluble molecules like O_2, either shunting or trapping them at the tips (Jodal and Lundgren, 1986). The lipid-soluble and low molecular mass CO_2 presumably diffuses from venous to arterial vessels and gets trapped in the exchanger similar to other measured gases (H_2, He, CH_4, etc.) (Bond et al., 1977). It is possible that the CO_2 carried away in the venous vessels diffuses back into the arterial vessels, trapping the CO_2 at the villi. The resulting high CO_2 tension would be expected to lower the O_2 affinity of the hemoglobin (Bohr effect) or even decrease the O_2-carrying capacity of hemoglobin (Root effect) (Dejours, 1975). Generally, more than 90 % of CO_2 is hydrated by CA and exists in blood as HCO_3^-. The H^+ produced in the process of hydration disrupts acid-base balance if not removed quickly by buffering, largely by hemoglobin (Hb). Hbs, particularly those of teleosts, are sensitive to pH changes (Berenbrink et al., 2005). The cooperativity of the Hb tetramer gives rise to a sigmoidal O_2-Hb dissociation curve. An increase in PCO_2 or decrease in pH shifts the curve down and to the right, illustrating a reduction in Hb-O_2 affinity (Bohr effect) (Bohr et al., 1904) and capacity (Root effect; Root, 1931). The increased $\dot{M}O_2$ of GIT tissues (see Section 1.2.1) and CO_2 generated in the chyme (see Section 1.4.2) can both contribute to high luminal PCO_2 which can diffuse to the villi CCE after feeding, resulting in localized acidification of blood passing by the GIT. This trapped CO_2 in the villi CCE may compensate for the shunted O_2 by decreasing Hb-O_2 affinity and/or carrying capacity and thereby enhance O_2 unloading from the blood, although this concept has not yet been experimentally validated. Moreover, whether the fish GIT possesses a functional CCE is

currently unknown, but similar CCEs have been found in the gas gland of the swim-bladder that serves in secreting and maintaining high gas tensions for buoyancy (Pelster, 2021).

1.4.2 Luminal PCO_2

In mammals, the luminal PCO_2 is high (Steggerda, 1968; Suarez et al., 1997) mainly as a result of the chemical reactions of the digestive enzymes and from the metabolism of bacterial colonies (Altman, 1986; Kurbel et al., 2006; Tomlin et al., 1991). A similar situation may occur in teleosts, where throughout the GIT, there is substantial movement of acid and base molecules for the purpose of digestion as well as for osmoregulation (see Section 1.5) that gives rise to high luminal PCO_2. The stomach secretes HCl for chemical breakdown of the food and activation of the enzyme pepsinogen before HCO_3^- is added in the intestine to bring the pH back up (Bucking and Wood, 2009), thereby forming CO_2 in the lumen. Indeed, recent studies found high luminal PCO_2 in the GIT in both gastric and agastric teleosts, which significantly increases following feeding (Wood and Eom, 2019). In FW fish, mean PCO_2 values of approximately 40 mm Hg (rainbow trout) and 16 mm Hg (goldfish; *Carassius auratus*) have been directly measured in the lumen after feeding. These luminal PCO_2 values are significantly higher than those seen in the arterial blood of these two species, which range between 2-4 and 5-7 mm Hg, respectively (Wood and Eom, 2019). In Atlantic salmon (*Salmo salar*), a species closely related to rainbow trout, the HPV PCO_2 was reported to be within similar levels of 2.8-4.8 mm Hg in its post-absorptive state (Eliason et al., 2007). In SW teleosts, additional PCO_2 in the lumen may result from secretion of H^+ and HCO_3^- for osmoregulation (see Section 1.5), but this has not been measured. Blood PCO_2 levels of SW teleosts seem to be similar to those of FW teleosts. For example, Cooper et al. (2014) reported indirect measurements of PCO_2 in the arterial blood of ~3

mm Hg and SIV of 4.7 mm Hg in SW-acclimated rainbow trout. Such indirect measurements rely on re-arrangements of the Henderson-Hasselbalch equation:

$$Tco_2 = [HCO_3^-] + \alpha_{CO2} \times P_{CO2}$$

$$pH = pK' + log \frac{[HCO_3^-]}{[\alpha_{CO2} \times P_{CO2}]}$$

where TCO_2 is the total concentration of CO_2 and αCO_2 is the solubility constant for CO_2 (Boutilier et al., 1984). Comparable equations using pH and TCO_2 measurements in chyme or gastrointestinal fluids have been used to indirectly calculate GIT luminal PCO_2 levels in other fish studies (reviewed by Wood, 2019).

1.5 Osmoregulatory function of the GIT

The GIT of SW teleosts performs an additional function: osmoregulation. It compensates for osmotic water loss in hypersaline environments by actively drinking seawater at rates up to 2-10 ml kg^{-1} h^{-1} (Evans et al., 2005; Fuentes and Eddy, 1997a; Marshall and Grosell, 2005; Rankin et al., 2001; Rodríguez et al., 2002). The current knowledge about the exchangers and transporters of the intestinal enterocytes in SW fish is summarized in Figure 1.1. The movement of acid and base equivalents (e.g. H^+ or HCO_3^-) across GIT epithelia for osmoregulation can have an effect on GIT PO_2 and PCO_2 as discussed in the preceding sections. Furthermore, the additional active transport mechanisms for osmoregulation in SW fish requires a greater $\dot{M}O_2$ than in FW fish (Brijs et al., 2015; Brijs et al., 2016; Brijs et al., 2018). Thus, gas exchange across the GIT of SW teleost was of interest in this thesis.

The ions, particularly Na^+ and Cl^-, in the ingested seawater are actively transported into the bloodstream and water follows osmotically. The basolateral Na^+/K^+ ATPase **(**NKA) provides the

electrochemical gradient for Na^+ that drives most of the other transporters important for osmoregulation, including the apical $Na^+/K^+/2Cl^-$ cotransporter (NKCC2) and HCO_3^-/Cl^- anion exchanger (AE) (Grosell, 2006; Grosell and Genz, 2006; Skou, 1990; Skou and Esmann, 1992). Consequently in euryhaline teleosts, NKA mRNA expression and enzymatic activity in the intestine increase following transfer to SW (Brijs et al., 2017; Fuentes et al., 1997; Jensen et al., 1998; MacKay and Janicki, 1979; Seidelin et al., 2000). The movement of these ions drives water absorption across the tight junctions (paracellular pathways) and/or transcellular pathways of the intestinal epithelium. Some evidence supports a greater importance of the transcellular pathway (Wood and Grosell, 2012) possibly involving aquaporins or even other transporters (e.g. NKCC; Hamann et al., 2005; Loo et al., 2002) expressed in the intestine. Correspondingly, aquaporin expression and protein abundance generally increase following SW acclimation (Aoki et al., 2003; Martinez et al., 2005; Raldúa et al., 2008). However, the exact mechanism of water absorption and direct function(s) of aquaporin in the intestine are yet to be elucidated.

Concurrent with ion absorption in marine teleosts, HCO_3^- is secreted to the lumen and forms carbonate precipitates with divalent ions (Ca^{2+} and Mg^{2+}) in the ingested SW, which allows reduction of osmolality of the intestinal fluids and facilitates water absorption (Genz et al., 2008; Marshall and Grosell, 2005; McDonald and Grosell, 2006; Wilson et al., 2002). This intestinal HCO_3^- secretion in marine teleosts is an endocrine-regulated process (Ferlazzo et al., 2012; Fuentes et al., 2010; Gregório et al., 2014), with HCO_3^- provided by both transepithelial transport from the blood and/or by hydration of endogenous CO_2 (Grosell, 2011). The basolateral Na^+:HCO_3^- co-transporter (NBC) can import plasma HCO_3^- into the enterocytes, which then is secreted into the lumen *via* an apical AE (Grosell and Genz, 2006). The major contributor of the secreted HCO_3^-, however, is the hydration of metabolic CO_2 mediated by cytosolic carbonic

anhydrase (CA) that facilitates anion exchange by creating a high local concentration of HCO_3^- (Grosell, 2006). The intracellular CO_2 hydration also yields H^+ within the cell that is extruded in both apical and basolateral directions to avoid reversal of the reaction and to protect intracellular pH (pH_i) (Genz et al., 2008; Grosell, 2011; Grosell and Genz, 2006; Grosell et al., 2005; Grosell et al., 2009; Wilson et al., 2002; Wood et al., 2010). The HCO_3^- and H^+ secreted to the lumen form CO_2 with the aid of membrane bound CA-IV (Grosell et al., 2009), resulting in high luminal total CO_2 concentrations first observed by Smith (1930). Theoretically, the magnitude of this effect would increase with salinity. Modeling of European flounder (*Platichthys flesus*) Hbs suggested that red blood cell pH_i passing by the intestine is reduced by 0.14-0.33 units depending on the salinity, and this was supported by lower SIV blood pH of SW-acclimated rainbow trout relative to that of FW-acclimated animal (Cooper et al., 2014).

Due to the capacity for HCO_3^- secretion described above, marine teleosts including SW-acclimated rainbow trout are well equipped to deal with the elevated metabolic base load of the alkaline tide (Bucking et al., 2009b). However, interestingly, a recent study by Wood and Eom (2019) found that FW-acclimated rainbow trout and goldfish that do not need to drink also have high HCO_3^- levels in the intestine that increases after feeding. High HCO_3^- secretion rates were also seen in *in vitro* intestinal preparations from FW-acclimated individuals of the euryhaline common killifish, especially after feeding (Wood et al., 2010). These observations suggest that the HCO_3^- may be secreted for more than just osmoregulatory purposes, although the details remain unclear.

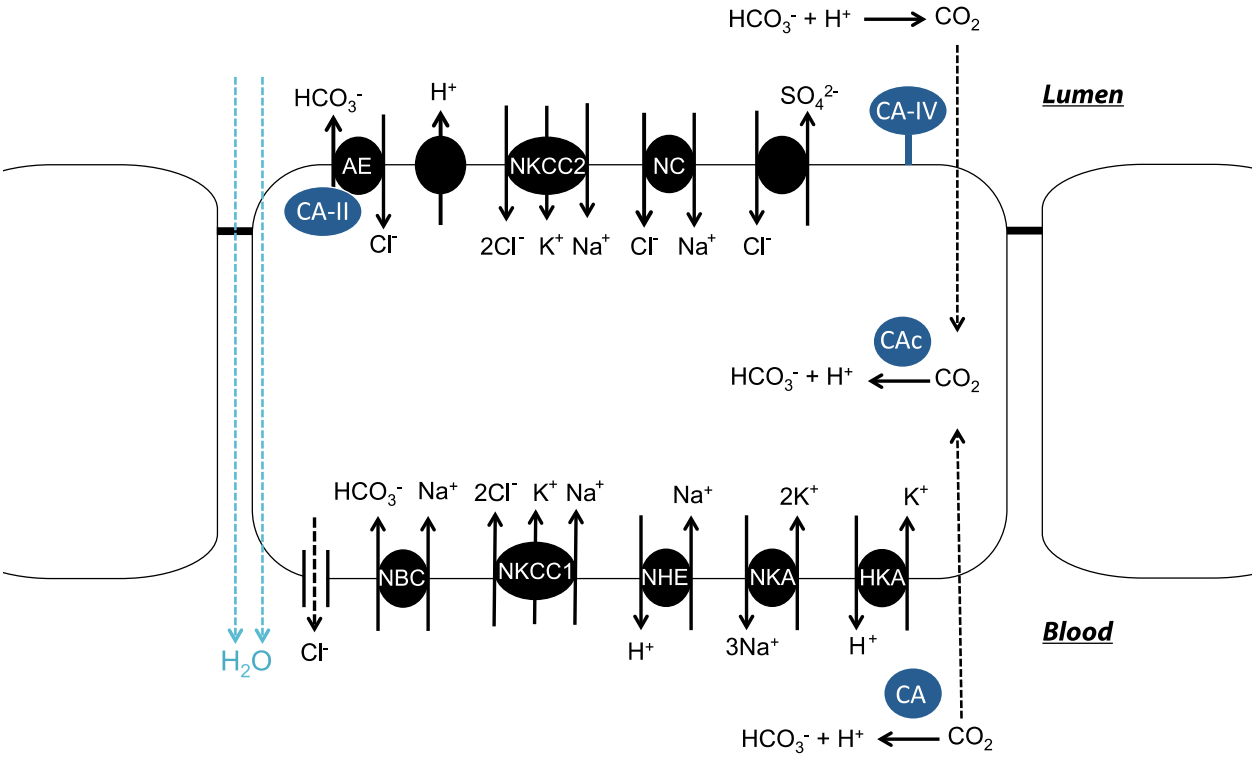

Figure 1.1 A summary of the ion exchangers and transporters found on the enterocytes of marine teleosts, adapted from Grosell (2007), Grosell et al. (2009), Gregório et al. (2013), and Ruiz-Jarabo et al. (2017). The Na^+ and Cl^- absorption *via* NKA and NKCC drives transcellular and/or paracellular H_2O absorption. On the apical membrane are: Cl^-/HCO_3^- anion exchanger (AE); H^+ pump; $Na^+/K^+/2Cl^-$ cotransporter (NKCC2); Na^+/Cl^- co-transporter (NC); Cl^-/SO_4^{2-} transporter. On the basolateral membrane are: Cl^- channel; Na^+/HCO_3^- co-transporter (NBC); $Na^+/K^+/2Cl^-$ cotransporter (NKCC1); Na^+/H^+ exchanger (NHE); Na^+/K^+ ATPase (NKA); H^+/K^+ ATPase (HKA).

1.6 GIT nitrogenous waste production and handling

The metabolism of amino acids and nucleic acids produces nitrogenous wastes, water and CO_2. Some of this nitrogen is retained for growth, and the rest is excreted. Most aquatic animals excrete the great majority of their nitrogenous waste as ammonia (NH_3 and/or NH_4^+), and hence are termed ammoniotelic (see Section 1.6.1). Some species produce urea depending on the environment they inhabit, and are hence termed ureotelic (see Section 1.6.2). Our current understanding of ammonia and/or urea pathways in the liver and GIT enterocytes are illustrated in Figures 1.2 and 1.3 respectively.

Ammonia is produced either as ammonia gas (NH_3) or ionized ammonium (NH_4^+), but the two forms redistribute as a function of pH. From here on, the term total ammonia (Tamm) will be used to refer to the combined concentration of NH_3 and NH_4^+. When the surrounding pH is equal to the pK' of ammonia, the ratio of NH_3 to NH_4^+ is 1:1. However, because the pK' of ammonia is about 9-10 depending on the temperature and ionic strength (Emerson et al., 1975) and the pH of the plasma is ~7.6-8.2, most of the total ammonia is present as NH_4^+ in teleosts. The Henderson-Hasselbach equation allows us to calculate the molar ratio of the pair of [NH_3] and [NH_4^+] given the pK' and pH values.

Dissociation constant: $$K' = \frac{[H^+][conjugate\ base]}{[conjugate\ acid]}$$

For ammonia, NH_3 acts as a weak base and NH_4^+ acts as a weak acid:

$$NH_3 + H^+ \leftrightarrow NH_4^+$$

$$K' = \frac{[H^+][NH_3]}{[NH_4^+]}$$

Rearrangement of this equation gives:

$$-\log[H^+] = -logK' + log\frac{[NH_3]}{[NH_4^+]}$$

Since:

$$pH = -log[H^+]$$

$$pK' = -log\ K'$$

$$pH = pK' + log\frac{[NH_3]}{[NH_4^+]}$$

The NH_3 form is considered to be more permeable to biological membranes and highly soluble in water, moving between compartments largely in the gaseous state and diffusing out to the environment through Rhesus glycoproteins (Rh proteins) at the gills (Nawata et al., 2010; Wright and Wood, 2009). An acidic environment enhances ammonia excretion because the NH_3 combines with H^+ and forms NH_4^+, which is unable to diffuse back in, while the partial pressure gradient for NH_3 movement is maintained (Knepper and Agre, 2004). Thus, at the gills, the diffusion of NH_3 is enhanced by simultaneous CO_2 and H^+ excretion and/or HCO_3^- uptake, all of which acidify the boundary layer. With this knowledge, we can speculate that the fate of the ammonia load produced in the lumen after feeding (see Section 1.6.1) can also be linked to the movements of ions and CO_2.

1.6.1 Postprandial ammonia

Within 24 hours of feeding, approximately 40-60 % of the nitrogen from the fish feed is excreted as ammonia (Brett and Zala, 1975; Randall, 2011; Zimmer et al., 2010). This is considered the "exogenous fraction" (Wood, 2001). Fasted fish break down their own muscle proteins for energy thereby also producing ammonia (the "endogenous fraction"). In rainbow trout, Rubino et al. (2014) estimated that close to half of the excess ammonia excretion after a

meal could result from processes in the lumen and the enterocytes. Following feeding, the intestinal Tamm can increase up to 1-2 mM in teleosts (Bucking and Wood, 2012; Bucking et al., 2013a; Rubino et al., 2014) and even higher in elasmobranchs (Wood et al., 2019). At the same time, the plasma Tamm concentrations rise up to 3-fold relative to those in fasted fish (~0.1 mM), and may stay elevated for up to 24 hours after feeding (Bucking and Wood, 2008; Bucking and Wood, 2012; Bucking et al., 2013a; Karlsson et al., 2006; Rubino et al., 2014). The increase in Tamm in the HPV draining the GIT is particularly marked (Karlsson et al., 2006). These luminal Tamm levels are high considering that a Tamm concentration of 0.5-5 mM in the external water can be lethal to teleosts as well as other vertebrates and invertebrates (Randall, 2011). Thus in recent years, the teleost and elasmobranch intestines have been gaining attention with respect to their ammonia handling mechanisms (e.g. Bucking et al., 2013; Mommsen et al., 2003; Rubino et al., 2014; Rubino et al., 2015; Wood et al., 2007; Wood et al., 2019).

Accordingly, studies have shown the presence of Rh proteins in the intestines of teleosts (Bucking et al., 2013b; Bucking et al., 2013a) and elasmobranchs (Anderson et al., 2010), with evidence that mRNA expression of Rhbg1 increases after feeding (Bucking and Wood, 2012). The Rh proteins in fish appear to serve as facilitated diffusion channels for NH_3 movement (Nawata et al., 2010). NH_4^+, on the other hand, may substitute for K^+ on the K^+ sites on NKA, NKCC and K^+ channels in the intestine (Rubino et al., 2015; Rubino et al., 2019). These potential NH_3 and NH_4^+ channels and transporters are speculated to facilitate the flux of ammonia through the enterocytes (Figure 1.3). However, it is still an open question as to what is the ratio of NH_4^+ to NH_3 moving through the intestinal membranes into the bloodstream.

Most of the absorbed free amino acids and Tamm from the intestine are transferred to the liver, where they are recycled to form other amino acids and nucleic acids or used to regenerate

α-ketoglutarate (Figure 1.2). Some of the postprandial glutamine may be deaminated by glutaminase (GLN) and used directly as an oxidative fuel by the intestinal enterocytes, thereby liberating ammonia. Under ammonia loading conditions such as feeding, the ammonia can be "trapped" in a less toxic form as glutamine by glutamine synthetase (GS) and as glutamate by glutamate dehydrogenase (GDH) (Figure 1.3) and then used in protein synthesis and/or effectively stored until the body ammonia level decreases back to normal (Bucking and Wood, 2012; Bucking et al., 2013a; Wicks and Randall, 2002a; Wright et al., 2007). The majority of the surplus ammonia is excreted across the gills (Forster and Goldstein, 1969) and a small amount is excreted *via* the urine (Bucking et al., 2010). Consequently, an increase in ammonia excreton rate following feeding has been observed in many species of teleosts (e.g. Bucking and Wood, 2008; Fehsenfeld and Wood, 2018; Ferreira et al., 2019; Weinrauch et al., 2018; Wilkie et al., 2017; Wood et al., 2010). A comprehensive understanding of how the nitrogenous products are handled by the enterocytes and to what extent they are transported into the bloodstream is as yet lacking.

1.6.2 Postprandial urea

Urea is a less toxic nitrogenous waste product than ammonia, produced *via* the ornithine-urea cycle (OUC) or arginase-mediated hydrolysis of dietary arginine (Wright et al., 1995). Despite the anabolism of urea being energetically costly (Ip and Chew, 2010), some species are forced to produce urea in environmental conditions where ammonia excretion is restricted. An example of this is the ureotelic Lake Magadi tilapia (*Alcolapia graham*) which inhabits an alkaline environment (Randall et al., 1989; Wood et al., 1989) where the water pH (10) is above the pK' of ammonia. Since NH_3 cannot diffuse out of the gills against the PNH_3 gradient, the fish

further process the ammonia to urea. Ureotelism exists in a very few other adult species but is found in early life stages of all teleost fish investigated to date (Braun et al., 2009; Chadwick and Wright, 1999; Dépêche et al., 1979; Felskie et al., 1998; Julsrud et al., 1998; Kong et al., 1998; Randall et al., 1989; Terjesen et al., 2002; Wood et al., 1995; Zimmer et al., 2017). Overall, these studies have shown that the OUC is present in the embryos so as to detoxify ammonia, but is usually lost in juveniles as the gills start to function for ammonia excretion, and it is generally believed to be absent in most adult teleosts.

Urea is capable of diffusing freely across the lipid bilayer, but urea transporters (UT) are also present in the gills, kidney and brain that greatly facilitate its transport (e.g. McDonald et al., 2006; Smith and Wright, 1999; Walsh et al., 2000; Walsh et al., 2001). Interestingly, the UTs are found not only in the intestines of the ureotelic toadfish (which unusually expresses the OUC), but also in the intestine of the closely related ammoniotelic plainfin midshipman (*Porichthys notatus*) that is thought to lack the OUC (Bucking et al., 2013b). The authors speculated that the luminal ammonia absorbed into the enterocytes is converted to urea *via* OUC enzymes localized to these cells, and then transported back to the lumen for use by ureolytic bacteria or later excretion *via* the anus (Bucking et al., 2013b). One study found an increased urea concentration in the HPV following feeding in rainbow trout (Karlsson et al., 2006), implying a possible production and/or transport of urea by the enterocytes. However, little is known about the capacity of the intestinal cells to produce and/or transport urea in ammoniotelic teleosts.

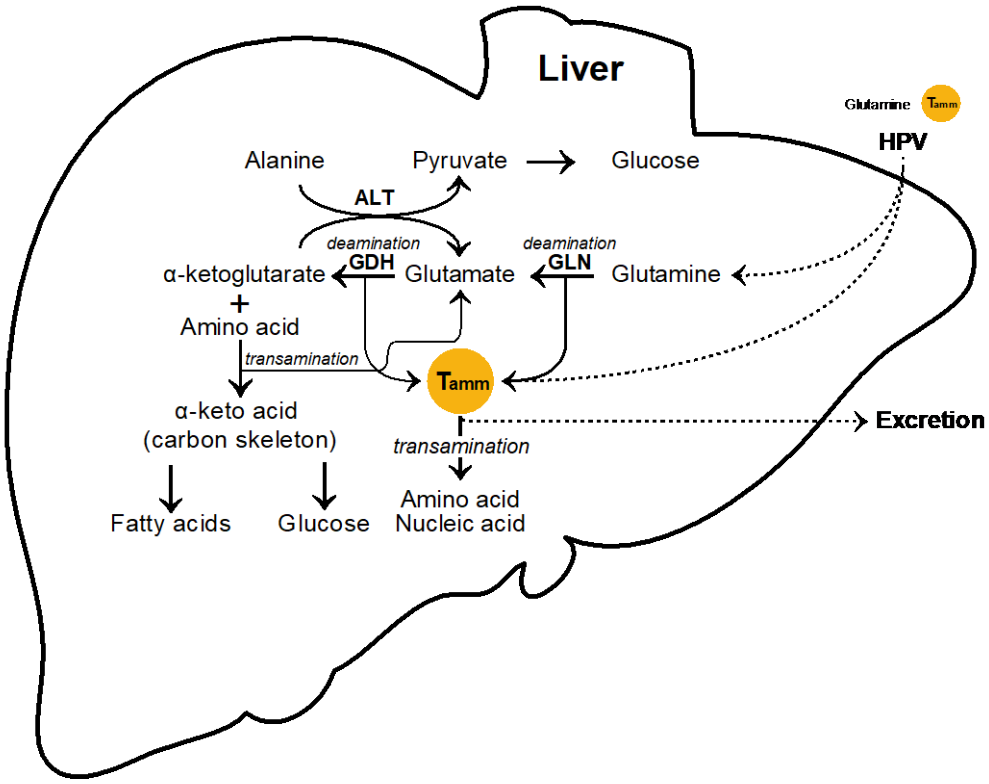

Figure 1.2 Ammonia handling in the hepatocytes.

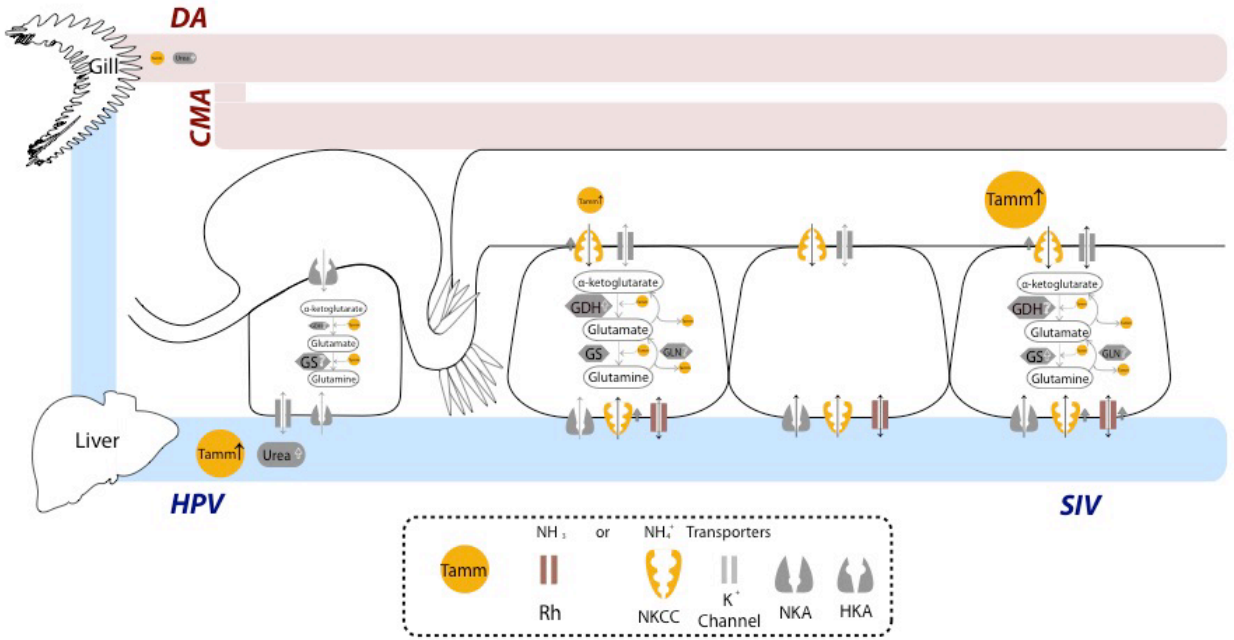

Figure 1.3 Ammonia and urea profiles & ammonia pathways in the GIT and the vascular system of FW rainbow trout. The size of the Tamm (NH_4^+ + NH_3) and urea symbol indicates relative concentrations. Arrows indicate the increase in concentration or activity of either enzymes or transporters after feeding. Data extrapolated from other studies: HKA (Bucking and Wood, 2012); postprandial upregulation of Rhbg1 (Bucking and Wood, 2012); postprandial upregulation of NKCC (Rubino et al., 2019); K^+ channels (Loretz, 1995; Movileanu et al., 1998); NKA (Gjevre and Naess, 1996); postprandial [urea] (Karlsson et al., 2006); postprandial GS and GDH activities (Bucking and Wood, 2012; Mommsen et al., 2003a; Mommsen et al., 2003b; Rubino et al., 2015).

1.7 Study organisms: FW rainbow trout and SW English sole

I used a widely studied FW-acclimated species, the rainbow trout (*Oncorhynchus mykiss*) for a detailed examination of gas exchange and ammonia handling in the GIT, and a SW species, the English sole (*Parophrys vetulus*) for comparative study on the osmoregulatory effect.

1.7.1 FW Rainbow trout (*Oncorhynchus mykiss*)

The rainbow trout is a model teleost for respiratory and acid-base physiology with an extensive body of scientific literature. The species has also been used to study GIT functions, nitrogenous product handling, and more (e.g. Bucking and Wood, 2008; Bucking and Wood, 2012; Bucking et al., 2009; Bucking et al., 2013b; Karlsson et al., 2006a; Rubino et al., 2014; Rubino et al., 2015; Rubino et al., 2019; Wood and Eom, 2019), thereby providing considerable background information for my investigation.

1.7.2 SW English sole (*Parophrys vetulus*)

Similar to the rainbow trout, the English sole is a carnivorous and gastric teleost that I used as a model SW species. Its choice was dictated partly by its ready availability at Bamfield Marine Sciences Centre where it is much easier to do seawater studies. The English sole has a relatively well studied intestinal physiology in areas such as silver toxicity (Grosell and Wood, 2001), ammonia handling (Wright et al., 1988), acid-base regulation (Cooper et al., 2014; McDonald et al., 1982), and there have been relevant investigations in other closely related flatfish species (e.g. Grosell and Jensen, 1999; Grosell et al., 2001; Grosell et al., 2005; Milligan and Wood, 1987; Taylor et al., 2007).

1.8 Thesis objectives and chapter summaries

The objectives of this study were to investigate the regulation of the three respiratory gases – oxygen (O_2), carbon dioxide (CO_2), and ammonia (NH_4^+ & NH_3) - in the gastrointestinal tract (GIT) and the associated vascular system during fasting and after feeding in fish, and to survey potential adaptive physiological differences in fish living in freshwater (FW) *versus* seawater (SW) environments. The thesis consists of 5 experimental chapters outlined below, where investigations focused on the FW gastric rainbow trout for Chapters 3 (comparative study), 4, 5, & 6, and on the SW gastric English sole for Chapters 2 and 3.

1.8.1 Chapter 2: "Pre and Postprandial GIT luminal PO_2 and PCO_2 profiles of English sole"

The primary goal of Chapter 2 was to directly measure the luminal PO_2 and PCO_2 levels in the GIT of the SW English sole under fasted and fed conditions. Measurements were made with direct insertion of PO_2 or PCO_2 micro-optodes in anaesthetized and artificially ventilated animals. These were the first ever measurements of the luminal PO_2 in any teleost, and only the second of luminal PCO_2. I found the lumen was virtually anoxic ($PO_2 \leq 0.3$ mm Hg) throughout the GIT in both fasted and fed animals. The luminal PCO_2 was high in fasted animal (14-17 mm Hg) and further increased following feeding (34-50 mm Hg). Regardless of feeding, the arterial blood PCO_2 values were significantly lower than those of the lumen. Measurements made with direct insertion of micro-optodes into the subintestinal vein (SIV) indicated elevated PCO_2 and low PO_2 values but both were variable. Comparisons of calculated *versus* directly measured PCO_2 were also made. To further investigate whether the osmoregulatory role of the GIT in the

SW English sole has an effect on luminal gas levels, the following chapter (Chapter 3) directly compares that of the SW English sole to the FW rainbow trout after feeding.

1.8.2 Chapter 3: "Comparison of postprandial luminal PO_2, PCO_2 and ammonia in the GIT between FW rainbow trout and SW English sole"

The primary goal of Chapter 3 was to compare postprandial PO_2, PCO_2 and ammonia (Tamm and PNH_3) profiles in the lumen and the circulatory systems supplying and draining the GIT of anaesthetized, artificially ventilated FW rainbow trout and SW English sole. Possibly, in a SW teleost, intestinal HCO_3^- secretion for osmoregulation may raise luminal PCO_2 levels higher than in a FW teleost. However, both species had similar luminal PCO_2 levels (stomach: 112-115 mm Hg and intestine: 20-38 mm Hg) and very low luminal PO_2 (< 1 mm Hg). There were species differences in luminal Tamm and [HCO_3^-], where SW English sole had higher intestinal Tamm and [HCO_3^-] but lower stomach Tamm than FW rainbow trout. Despite the extreme conditions inside the lumen, SIV blood draining from the tract experienced lesser disturbance with relatively lower PCO_2, Tamm and higher PO_2 than in the lumen, implying limited equilibration between the two compartments. Overall, there were minimal differences between the species, except for luminal Tamm and [HCO_3^-] levels that were potentially due to feed differences. Similar to the results of Chapter 2, however, the directly measured values with micro-optodes in the SIV and hepatic portal vein (HPV) were variable. These results suggested the need for the *in vivo* sampling approach employed in Chapter 4.

1.8.3 Chapter 4: "Potential equilibration of PO_2, PCO_2 and ammonia between the GIT lumen and systemic bloodstream in FW rainbow trout"

The primary goal of Chapter 4 was to investigate the degree of equilibration of the three respiratory gases (O_2, CO_2, and ammonia) between the GIT lumen and systemic bloodstream. In the two previous chapters, I had established that the lumen was very low in PO_2 and high in PCO_2 and Tamm, with feeding further increasing both PCO_2 and Tamm levels. To resolve the data variability in SIV and HPV measurements in Chapters 2 and 3, I sampled blood from indwelling catheters in the dorsal aorta (DA) and the SIV near the posterior intestine of non-anaesthetized FW rainbow trout during the fasting state and at 4 h to 48 h following feeding by an indwelling gastric catheter. This chapter also used *in situ* blood sampling in anaesthetized rainbow trout to compare ammonia levels between the SIV that drains only the posterior tract and the HPV that additionally drains the entire GIT. Overall, there was minimal equilibration of all three gases between the GIT lumen and the SIV blood, with the latter maintaining pre-feeding levels of PO_2, PCO_2 and Tamm. Importantly, HPV Tamm increased following feeding in contrast to the SIV Tamm that remained unchanged. This difference between SIV and HPV Tamm suggested postprandial luminal ammonia absorption occurring mainly in the anterior region of the GIT, a finding that was explored in the following Chapters 5 and 6.

1.8.4 Chapter 5: "Intestinal zonation in nitrogenous product handling and transport"

The primary goal of Chapter 5 was to investigate the potential handling and transport of ammonia and urea by different intestinal sections of FW rainbow trout. An earlier study had shown that urea as well as ammonia concentrations increase in the HPV following feeding (Karlsson et al., 2006), but whether the intestinal tissues have the capacity to produce urea is

unknown. *In vitro* gut sac preparations were used with specific focus on feeding *versus* fasting and on responses to loading of the lumen with 2 mM glutamine or 2 mM ammonia to simulate postprandial lumen conditions. Intestinal tissues from fed trout had increased urea production and transport relative to those from fasted trout, but neither glutamine or ammonia loading resulted in elevated urea production. The increased urea production associated with feeding occurred in conjunction with increased arginase activity but minimal carbamoyl phosphate synthetase III (CPS III activity). Overall, the intestinal tissues exhibited some limited capacity to produce urea, likely by direct arginolysis, rather than by the ornithine urea cycle (OUC) pathway. The fed intestinal tissues also exhibited increased ammonia production and transport relative to the fasted intestinal tissues. Results from glutamine or ammonia loadings of the gut sac preparations suggested that the intestinal tissues can deaminate glutamine thereby releasing ammonia, but can also downregulate ammonia generating pathways in the face of excess ammonia. Lastly, there were sectional differences among different parts of the intestine in ammonia production and handling, where the anterior sections from fed animals had higher absorptive ammonia flux rates and lower tissue ammonia levels. These results suggested intestinal zonation in the handling of ammonia, in which the anterior intestine is more involved in transporting ammonia to the bloodstream. To follow up these findings, Chapter 6 further elaborated the potential zonation in ammonia transport by comparing different intestinal sections as well as the stomach, focusing specifically on ammonia movement in the form of NH_3, and the potential transporters involved.

1.8.5 Chapter 6: "Potential NH_3 transport across GIT epithelia and ammonia transport in the stomach"

The primary goal of Chapter 6 was to investigate the potential for NH_3 transport in all three sections of the intestine and also the stomach by changing the PNH_3 gradients across the epithelia using *in vitro* gut sac preparations. An additional, related goal was to survey the expression of Rh proteins (Rhbg, Rhcg1, Rhcg2; channels which are known to facilitate the diffusion of NH_3) as potential NH_3 transporters, and NKCC as a potential ammonium ion (NH_4^+) transporter along the entire GIT of the FW rainbow trout. In Chapter 5, it was found that the intestinal tissues are able to transport ammonia *in vitro*, but whether they transport NH_3 or NH_4^+ was unknown. Moreover, the zonation in transporting ammonia found in Chapter 5 was also in agreement with findings from Chapter 4 where HPV Tamm was higher than that of the SIV following feeding. In this chapter, by experimentally manipulating mucosal pH at constant mucosal Tamm, I found that ammonia absorption is not dependent on the PNH_3 gradient despite expression of Rhbg and Rhcg2 in the intestinal tissues. There was no detectable expression of Rhbg in the stomach and no expression of Rhcg1 in any of the GIT sections. There was also a lack of correlation between ammonia transport and the NH_4^+ concentration gradient despite NKCC expression in all GIT tissues, a finding which requires further investigation. Importantly, the stomach had the greatest ammonia absorption and net tissue consumption regardless of the PNH_3 gradient. Indeed, at a stomach pH of 4.0 (typical of fed animals *in vivo*), ammonia absorption continued unchanged despite reversal of the PNH_3 gradient. The findings from this chapter, with the support from data of Chapters 4 and 5, suggest zonation of the GIT in ammonia handling and transport where the anterior region of the GIT including the stomach serves as an important site.

Chapter 2: Pre and Postprandial GIT luminal PO_2 and PCO_2 profiles of SW English sole

2.1 Summary

There has been considerable recent progress in understanding the respiratory physiology of the gastrointestinal tract (GIT) in teleosts, but the respiratory conditions inside the GIT remain largely unknown, particularly the luminal PCO_2 and PO_2 levels. The GIT of seawater teleosts is of special interest due to its additional function of water absorption linked to HCO_3^- secretion, a process that may raise luminal PCO_2 levels. Direct measurements of GIT PCO_2 and PO_2 using micro-optodes in the English sole (anaesthetized, artificially ventilated, 10-12 ºC) revealed extreme luminal gas levels. Luminal PCO_2 was 14-17 mm Hg in the stomach and intestinal sections of fasted sole, considerably higher than arterial blood levels of 5 mm Hg. Moreover, feeding, which raised intestinal HCO_3^- concentration, also raised luminal PCO_2 to 34-50 mm Hg. All these values were higher than comparable measurements in freshwater teleosts, and also greater than environmental CO_2 levels of concern in aquaculture or global change scenarios. The PCO_2 values in subintestinal vein blood draining the GIT of fed fish (28 mm Hg) suggested some degree of equilibration with high luminal PCO_2, whereas subintestinal vein PO_2 levels were relatively low (9 mm Hg). All luminal sections of the GIT were virtually anoxic ($PO_2 \leq 0.3$ mm Hg), in both fasted and fed animals, a novel finding in teleosts.

2.2 Introduction

The respiratory physiology of the gastrointestinal tract (GIT) in fish has been relatively well-studied with respect to O_2 supply by the blood (reviewed by Seth et al., 2011) but relatively little is known about the respiratory conditions inside the lumen of the tract, or about how the

other two respiratory gases (CO_2 and ammonia) are handled by the GIT. For example, to our knowledge there have been no measurements of PO_2 in the GIT lumen of any fish species, while a few recent investigations have reported ammonia levels that are many fold greater than blood levels (Bucking et al., 2013a; Pelster et al., 2015; Rubino et al., 2014; Wood et al., 2019). A very recent study (Wood and Eom, 2019) was the first to directly record PCO_2 levels *in vivo* using a needle-type fibre-optic PCO_2 sensor ("micro-optode"). Surprisingly, in two freshwater (FW) teleosts, the carnivorous gastric rainbow trout (*Oncorynchus mykiss*) and the omnivorous agastric goldfish (*Carassius auratus*), PCO_2 levels in the gastrointestinal fluids/chyme of various parts of the GIT were much higher than in arterial blood. Thus, in fasted fish of both species, GIT PCO_2 values were approximately 10 mm Hg (1 mm Hg = 0.1333 kPa), 2-3 fold higher than arterial blood values. With feeding, luminal PCO_2 increased moderately in the goldfish but dramatically in the trout to 20-41 mm Hg.

As in mammals (Altman, 1986; Kurbel et al., 2006; Steggerda, 1968; Suarez et al., 1997; Tomlin et al., 1991), these high PCO_2 values were speculatively attributed to a combination of endogenous metabolism of the GIT tissues, metabolism of the gut microbiome, and to the reaction of gastric HCl with endogenous carbonates in the food, as well as with biliary, pancreatic, and/or intestinal HCO_3^- secretion. Additionally, simultaneous H^+ and HCO_3^- secretion by the intestinal epithelium can occur in fish (Grosell, 2011; Guffey et al., 2011; Wood et al., 2010) and could also contribute to elevations in luminal PCO_2.

A subsequent survey of indirectly measured PCO_2 values (calculated *via* the Henderson – Hasselbalch equation from terminal measurements of pH and total CO_2 concentration in the GIT fluids, as reported in the literature) in a wide variety of teleost and elasmobranch species yielded comparably high values, with a tendency for greater values in fed animals (Wood, 2019). As

discussed subsequently, there are multiple uncertainties in terminal values obtained in this manner, but they nevertheless support the patterns seen in the direct measurements on FW trout and goldfish. Overall, these findings raise questions about how this high PCO_2 is generated, whether it equilibrates with the venous blood draining the GIT, and how it might impact blood O_2 transport *via* Bohr and Root effects (Nikinmaa, 2006).

The primary goal of the present study was to use this same technology (PCO_2 micro-optodes) to make the first direct measurements of luminal PCO_2 values in the GIT of a seawater (SW) teleost, under fasted and fed conditions. We selected the carnivorous, gastric English sole because it is abundant, has suitable anatomy, readily eats in captivity, and has a relatively well studied intestinal physiology (Grosell et al., 1999; Grosell et al., 2001; Grosell and Wood, 2001). A parallel objective of our experiments was to use PO_2 micro-optodes to make the first ever direct measurements of PO_2 in the GIT of any teleost.

We hypothesized that luminal PCO_2 values in the English sole would be much higher than arterial blood levels, and even higher than in the carnivorous FW rainbow trout since the metabolic rate and blood flow requirements of the GIT appear to be higher in SW than FW teleosts (Brijs et al., 2015), likely due to the major role of intestinal HCO_3^- and H^+ secretion in the osmoregulation of SW teleosts (Grosell, 2011; Guffey et al., 2011; Wood et al., 2010). Following feeding, we hypothesized that stomach pH would decrease due to digestive HCl secretion, and intestinal pH would increase due to HCO_3^- secretion. We hypothesized that these acid-base movements would also result in a higher luminal PCO_2 value in fed relative to fasting fish. Based on limited reports on venous blood draining from the GIT (Eliason et al., 2007; Cooper et al., 2014; Wood and Eom, 2019), we speculated that the subintestinal venous blood would not equilibrate with the luminal PCO_2, but would instead maintain a low PCO_2. Despite

quite extensive studies on the cardiovascular system of the GIT (reviewed by Seth et al., 2011), there has been no investigation on the PO_2 profile of the lumen in fish, to our knowledge. Based on the mammalian GIT that is known to be virtually anoxic (Espey, 2013; Kurbel et al., 2006), we hypothesized that the teleost lumen would exhibit similarly low luminal PO_2.

2.3 Materials and Methods

2.3.1 Experimental animals

Experiments were performed at Bamfield Marine Sciences Centre (BMSC; Bamfield, BC, Canada) in August – September 2018 and 2019. English sole (436.9 ± 27.7 g; N = 5 in 2018 and N = 14 in 2019) were caught from the wild (Barkley Sound, BC) by line fishing under Department of Fisheries and Oceans Canada collection permits XR-204.18 and XR-212.19, and transferred to outdoor seawater flow-through tanks filled with 4 cm of sand to allow the animals to burrow. Fish were held at 10-12 ˚C and 32 ppt salinity under natural photoperiod. All fish were allowed to recover from capture for at least 1 week before experimentation. The fasted group was not fed for 7 days prior to experimentation. Fed fish were fed thawed, previously frozen anchovies, then moved to a separate tank and experimented upon within 48 hours. Only those that were caught in 2019 were measured for total body length and GIT length (N = 14). With respect to individual measurements, occasional measurements could not be made because of experimental problems. All experiments were approved by the Animal Care Committees of the University of British Columbia (AUP 14-0251 and 18-0271) and Bamfield Marine Science Centre (RS-18-20 and RS-19-15).

2.3.2 Cannulation and blood measurements

The fish were anaesthetized with 0.1-0.2 g L^{-1} NaOH-neutralized MS-222 (Syndel Laboratories, Parksville, British Columbia, Canada) and placed on a flat surgery table. Due to the anatomical orientation of the fish, the gills were irrigated through the upper operculum with temperature-controlled water (10-12 ˚C). The anaesthetic level was adjusted as necessary so as to maintain Stage 5 anaesthesia (i.e. "loss of reflex activity, total loss of reactivity, shallow opercular movements" - McFarland, 1959) throughout the following cannulation and subsequent experiment. The caudal artery was cannulated for blood sampling as described by Watters and Smith (1973), using polyethylene tubing (Clay-Adams™ PE50, Becton and Dickinson Co., Franklin Lakes, NJ, USA) filled with Cortland's saline (Wolf, 1963; See Table S.1 for composition). The Cortland's saline was modified for SW teleosts by the addition of 20 mM NaCl, and was heparinized at 100 I.U. ml^{-1} with lithium heparin (Sigma-Aldrich, St. Louis, MO, USA). Approximately 1-ml samples of blood were collected from the catheter by blood pressure-driven flow into 2-ml microcentrifuge tubes. Measurements of pH, PO_2, and PCO_2 were made by inserting the micro-optodes to the bottom of the tube during and after collection. The Hct was determined by drawing blood into heparinized microhematocrit capillary tubes that were then centrifuged at 10,000 g for 5 min. The [Hb] was measured as described by Kampen and Zijlstra (1961).

The pH of the blood sample was measured using an oesophageal pH microelectrode (MI-508; 1.4-1.6 mm OD) and a flexible micro-reference electrode (MI-402; Microelectrodes Inc., Bedford, NH, USA) connected to a model 220 pH meter (Corning Instruments, Corning, NY, USA) in 2018, and using a thermo-jacketed Orion ROSS glass combination micro-electrode (Fisher Scientific, Toronto, ON, Canada) coupled to an Accumet™ meter (Fisher Scientific) in

2019. The electrodes were calibrated with precision buffers (Fisher Scientific and Radiometer-Copenhagen, Copenhagen, Denmark). The partial pressures of gases (PO_2, PCO_2) were measured using micro-optodes (manufactured by PreSens Precision Sensing GmbH Regensburg, Germany) mounted in #23 hypodermic needles. The micro-optodes were precisely positioned to the bottom of the collection vials using micro-manipulators (World Precision Instruments, Sarasota, FL, USA), and the blood samples were kept at experimental temperature and measured immediately during and after collection. The PO_2 micro-optodes were calibrated with air-equilibrated and sodium sulfite saturated saline kept in gas-tight bottles. The PCO_2 needle-housing type micro-optodes were prototype devices (PreSens 200001368) connected to an electronic transmitter (PreSens 300000114), with the output displayed on a personal computer running prototype software (PreSens 200001488). These PCO_2 optodes were calibrated with physiological salines equilibrated to 0.04, 0.3, 1, 3, 5, and 8 % CO_2 (0.04-7.93 kPa, 0.3-59.5 mm Hg) using CO_2/air mixtures created by a 301aF precision gas-mixing pump (Wösthoff Messtechnik GmbH, Bochum, Germany). The higher PCO_2 levels were needed to cover the range of values found in the GIT. All calibration solutions were in modified Cortland's saline kept at the experimental temperature. After measurement of the gases, blood and gastrointestinal fluid samples (sampled as described below) were centrifuged (2 min, 5000 *g*), and the plasma and supernatant were flash-frozen in liquid N_2. The samples were later thawed over ice and measured for total CO_2 content (TCO_2) using a Corning 965 CO_2 analyser (Ciba-Corning Diagnostics, Halstead, Essex, UK) calibrated with $NaHCO_3$ standards. Previous validation tests in the lab demonstrated that the flash-frozen samples thawed on ice and assayed quickly thereafter exhibited TCO_2 values that were unchanged from those of fresh samples.

2.3.3 GIT measurements

Immediately following blood collection, the peritoneal cavity was surgically opened for direct *in vivo* measurements of PO_2, PCO_2 and pH in the GIT fluids. Similar measurement and gastrointestinal fluid sampling procedures were used as in Wood and Eom (2019). The same micro-optodes were directly inserted into stomach, pyloric caeca, and anterior, mid and posterior intestines of the anaesthetized fish. In fed fish, the PO_2 and PCO_2 micro-optodes were additionally inserted into the engorged subintestinal vein for gas measurements in the venous blood draining from the GIT to the liver. These measurements were made immediately following the measurements in the lumen of the adjacent intestinal section. In fasted fish, the subintestinal vein was generally collapsed so we were not able to make the same measurements. After gas measurements, small incisions were made in each section for pH microelectrode insertion. Again, all insertions were made using micro-manipulators to correctly position the tips of the probes.

At the end of the experiment, the fish was euthanized by an overdose of neutralized MS-222, weighed and measured for total length. The length of the GIT from stomach to the end of posterior intestine was measured. The four sections of the GIT (stomach, anterior intestine, mid intestine, posterior intestine) were ligated and excised, and the gastrointestinal fluid was collected into 2-ml centrifuge tubes. The samples were centrifuged (2 min, 5000 g), and the supernatants were flash-frozen for TCO_2 assay as described above.

2.3.4 Calculation and statistical analyses

All graphs were made and statistical analyses were performed using Graphpad Prism software (version 7.0a). Data are expressed as means ± SEM (N = number of fish). Calculated

PCO_2 and $[HCO_3^-]$ values were derived from rearrangements of the Henderson-Hasselbach equation (see Wood et al., 1983) using values for pK' and CO_2 solubility for teleost plasma (Boutilier et al., 1984). The limitations with respect to this calculation for gastrointestinal fluid are assessed in the Discussion. Relative GIT length was calculated as: GIT length × total fish length^{-1}.

Two-way ANOVA and *post hoc* Tukey's multiple comparison tests were performed on all GIT measurements. Differences in blood gas values between treatment groups and between arterial and venous blood were analyzed using two-tailed Student's unpaired and/or paired t-test as appropriate. The PCO_2 and PO_2 measurements of subintestinal venous blood and the lumen of the nearby GIT section from which it was draining were compared using two-tailed Student's paired t-test. Blood pH, $[HCO_3^-]$, Hct, [Hb], and relative GIT length were also compared between treatment groups using the Student's unpaired t-test. A significance level of $p < 0.05$ was used in all tests.

2.4 Results

2.4.1 Overview

The total body length and body weight between fasted (31.7 ± 1.0 cm; 391.7 ± 24.7 g; N = 8) and fed (32.9 ± 1.0 cm; 497.3 ± 47.3 g; N = 6) groups were not significantly different (p = 0.40; p = 0.08 respectively). The relative GIT length was also not significantly different: fasted group 0.92 ± 0.03 (N = 6) and fed group 0.97 ± 0.06 (N = 6) (p = 0.50). Feeding had no effect on either hematocrit or hemoglobin concentration (p = 0.26 and 0.70 respectively). The Hct value of the fasted group was 21.8 ± 1.5 % and of the fed group was 24.4 ± 0.9 % (N = 5-6). The [Hb] of the fasted group was 6.2 ± 0.4 g dL^{-1} (N = 7) and of the fed group was 6.4 ± 0.4 g dL^{-1} (N = 7).

2.4.2 PCO_2

The mean stomach PCO_2 of the fasted fish was the lowest (13.5 mm Hg) measured amongst all GIT sections in both groups but was not significantly different from measurements in the other sections of fasted fish (Figure 2.1). All other GIT sections of fasted fish exhibited similar mean PCO_2 values (16.9-17.3 mm Hg). Using two-way ANOVA, we found a significant overall effect of feeding on luminal PCO_2 of all GIT sections ($p < 0.0001$), but no effect of GIT section on luminal PCO_2 ($p = 0.71$) and no significant interaction ($p = 0.62$). Among the intestine sections only, there was also a significant overall effect of feeding ($p < 0.0001$), but no effect of intestine section ($p = 0.56$) and no significant interaction ($p = 0.57$). In both fasted and fed groups, we found that the inter-individual values tended to be more variable than intra-individual values across GIT sections. We varied the measurement order of GIT sections among individuals, and detected no influence on the order of measurement. The subintestinal blood was always measured after the final GIT measurement to ensure all tissue was getting sufficient blood supply.

The mean luminal PCO_2 values in all sections, except for the pyloric caecae, were significantly higher in the fed fish than the corresponding levels of the fasted group ($p < 0.05$). In the fed group, the mean pyloric caeca PCO_2 was the lowest measured value (34.1 mm Hg) and was not significantly different from that of the fasted group. The mean PCO_2 values of all other sections were similar (49.4-50.3 mm Hg) and about 2.7-3.6 fold higher than those of the fasted group.

Relative to a substantial increase in luminal PCO_2 after feeding, the difference between mean arterial blood PCO_2 in fasted (4.9 mm Hg) and fed (9.3 mm Hg) groups was modest and

not significant ($p = 0.06$; Figure 2.1). After feeding, the PCO_2 values in the subintestinal venous blood and arterial blood were significantly different ($p = 0.014$). The subintestinal PCO_2 values were quite variable among the 5 fed individuals measured: one fish at 4 mm Hg; two fish at ~17 mm Hg; two fish at ~ 50 mm Hg (Table 2.1). A comparison of the PCO_2 of the subintestinal venous blood and the lumen at the point of measurement by paired t-test revealed no significant difference ($p = 0.15$; N = 5).

2.4.3 pH

There was a significant overall effect of feeding ($p = 0.007$) and a significant overall effect of GIT section on luminal pH ($p < 0.001$), as well as a significant interaction ($p < 0.0001$) (Figure 2.2). However, the only GIT section that exhibited a statistically significant change in pH associated with feeding was the stomach ($p < 0.001$): mean gastric pH decreased from 6.8 to 4.9 after feeding. The stomach pH after feeding was also significantly lower than any other intestinal sections in fed fish ($p < 0.05$). In the intestine alone (stomach excluded from the analysis), there was no significant effect of feeding ($p = 0.87$), no significant effect of the intestinal section ($p = 0.84$), and no significant interaction ($p = 0.30$) for pH. The arterial blood pH did not change after feeding ($p = 0.35$), with mean values of ~7.6 in both treatments.

2.4.4 Calculated $[HCO_3^-]$

Mean $[HCO_3^-]$ values as calculated by the Henderson-Hasselbalch equation were close to zero in the stomach, but ranged from about 40 to over 100 mM in the intestinal sections of both fasted and fed fish (Figure 2.3). There was no overall significant effect of feeding ($p = 0.18$) on the GIT $[HCO_3^-]$ (Figure 2.3) and no significant interaction ($p = 0.29$), but there was a significant

effect of GIT section on [HCO_3^-] (p = 0.0002). In the fed group, the posterior intestine [HCO_3^-] was significantly higher than that of other sections. There were no differences among sections in the fasted group. In the intestine alone (stomach excluded from the analysis) there was also no significant effect of feeding (p = 0.17) and no significant interaction (p = 0.33), but a significant effect of GIT section on [HCO_3^-] (p = 0.028), with a tendency for higher values in posterior regions. The arterial blood [HCO_3^-] was not significantly different between fasted and fed groups (p = 0.32).

2.4.5 PO_2

All sections of the GIT were almost anoxic with mean values ≤ 0.3 mm Hg in both groups (Figure 2.4). Nevertheless there was a significant overall effect of feeding on GIT PO_2 *(p* = 0.008), but no effect of GIT section on PO_2 (p = 0.67) and no significant interaction (p = 0.67; Figure 2.4). The fasted group had higher mean PO_2 values (0.06-0.24 mm Hg) than the fed group (0.00 mm Hg throughout). The mean arterial blood PO_2 after feeding (27.5 mm Hg) was significantly lower by 50 % (p = 0.022) than that of the fasted group (54.7 mm Hg). In the fed group, the mean PO_2 of the subintestinal venous blood (8.8 mm Hg) was approximately one third of that of arterial blood (27.5 mm Hg; p = 0.033).

2.5 Discussion

2.5.1 Overview

In this study, we have made the first direct measurement of PCO_2 inside the GIT of a SW teleost (Figure 2.1). Consistent with our original hypotheses, PCO_2 values in the GIT lumen of the English sole were greatly elevated relative to arterial blood levels, and were higher even than

recent direct measurements in the carnivorous FW rainbow trout, and much higher than in the omnivorous FW goldfish (Wood and Eom, 2019). Our fasting mean values were 14-17 mm Hg, whereas those in the trout were 7-13 mm Hg. Furthermore, after feeding, GIT PCO_2 values increased to 34-50 mm Hg in the English sole, relative to 20-41 mm Hg in the post-prandial trout (Wood and Eom, 2019). These internal PCO_2 levels were much higher than environmental values of common concern in aquaculture (Skov, 2019) and global climate change scenarios (McNeil and Matsumoto, 2019). Moreover, the projected levels of water PCO_2 associated with climate change have been shown to significantly increase luminal HCO_3^- secretion to maintain water balance in another seawater teleost (Heuer and Grosell, 2016), and water PCO_2 levels in intensive aquaculture can be even greater. Clearly, these could further exacerbate luminal PCO_2 conditions. The present measurements support our hypotheses that greater acid-base transport rates associated with both life in SW and feeding result in higher luminal PCO_2 levels. Certainly, as predicted, pH in the stomach dropped markedly after feeding in the English sole, opposite to the pattern in the trout, and pH values then increased again to fasting levels in the intestine. This presumably reflected greatly increased gastric secretion of HCl and greatly elevated intestinal HCO_3^- secretion, respectively. With respect to whether the blood in the subintestinal vein equilibrates with the high PCO_2 levels in the GIT lumen, our results are not clear-cut but suggest, contrary to our hypothesis, that there may be some degree of equilibration, because most of the subintestinal vein PCO_2 values were very high and close to GIT lumen values. Finally, by making the first direct measurements of PO_2 in the GIT lumen, we have confirmed the hypothesis that the inside of the teleost digestive tract is virtually anoxic throughout, consistent with that observed in mammals (Espey, 2013; Kurbel et al., 2006).

2.5.2 CO_2 in the GIT

Our data on English sole are in agreement with a recent review by Wood (2019) that surveyed the PCO_2 values calculated *via* the Henderson-Hasselbalch equation from pH and total CO_2 measurements in the intestinal fluids reported for a variety of fish species. While there are uncertainties in this approach (discussed below), 11 of the 15 SW species had values greater than 5 mm Hg, with a few above 20 mm Hg. A similar phenomenon is known to occur in the human intestine, with luminal PCO_2 levels up to 8-fold greater than blood levels (Steggerda, 1968; Suarez et al., 1997). In teleosts, the high PCO_2 is presumably a result of the metabolism of the GIT tissue itself and of the gut microbiome, as well as osmoregulatory processes occurring in the GIT in SW species.

The GIT has a very high mass-specific metabolic rate relative to other tissues in teleosts (Brijs et al., 2018; Taylor and Grosell, 2009) and in mammals (Britton and Krehbiel, 1993; Duée et al., 1995). In unfed teleosts, the blood flow to the GIT typically ranges from 10 to 40 % of cardiac output, and may increase greatly after feeding (Seth et al., 2011), indicating a significant functional importance. As a result, the respiratory CO_2 production by the enterocytes is presumably high. There are also some reports (Clements et al., 1994; Mountfort et al., 2002) of intestinal microorganisms which ferment amino acids and carbohydrates in fish to produce short chain fatty acids. Recent studies suggest that GIT microbiome composition, metabolic activity and enzyme activities change depending on the diet (Desai et al., 2012; Liu et al., 2016) as well as a variety of other environmental conditions such as geographical location (reviewed by Talwar et al., 2018). Fine flounder (*Paralichthys adspersus*) raised in the aquaculture setting were found to have different GIT microbiomes from those in the wild. However, in another flounder species (*Pleuronectes platessa*), microbiome composition was uniform and was not

influenced by environmental parameters (Heindler et al., 2019). In the human large intestine, CO_2, along with H_2, CH_4, and H_2S is also produced by the breakdown of these fatty acids (Macfarlane and Macfarlane, 2003) but this area has not been fully elucidated in teleosts.

The GIT of SW teleosts has an additional osmoregulatory function (Carrick and Balment, 1983; Fuentes and Eddy, 1997b; Lin et al., 2001; Perrott et al., 1992; Smith, 1930). With an increase in ambient water salinity, there is an increase in drinking rate (see references within Grosell, 2007) and increase in blood flow to the GIT (Brijs et al., 2015). The ingested SW, along with additional [HCO_3^-] secreted in the esophagus during the desalination process (Esbaugh and Grosell, 2014; Takei et al., 2017), enters the stomach. Note that the calculated stomach [HCO_3^-] of fasted sole (3.7 mM; Figure 2.3) was actually higher than typical SW levels (~2.3 mM).

Following feeding, the secretion of HCl reduces stomach pH (Koelz, 1992; Krogdahl et al., 2011) to values between 1-5 depending on a number of factors including species and time after a meal (reviewed by Bakke et al., 2011). In a non-digesting state, some species such as trout maintain an acidic stomach (e.g. Bucking and Wood, 2009; Wood and Eom, 2019) and some species keep the stomach pH high (e.g. Papastamatiou and Lowe, 2005; reviewed by Wood, 2019). The latter appears to be the case in English sole, as its stomach pH decreased from circumneutrality by almost 2 units following feeding (Figure 2.2). In a previous study of SW European flounder (*Platichthys flesus*), stomach pH decreased to an even greater degree with time after feeding (Taylor et al., 2007), suggesting that flatfish in general may maintain stomach pH high during the non-digesting state, and decrease it with HCl secretion following food intake. The low pH favors dehydration of HCO_3^- to CO_2, both from ingested SW and carbonates in food, producing a significant increase in PCO_2 in the stomach after feeding (Figure 2.1). This then

suggests that the high [HCO_3^-] levels in the intestine arise mainly from endogenous intestinal HCO_3^- secretion that occurs posterior to the stomach to neutralize the GIT fluid (Figure 2.3).

The gastrointestinal fluid entering the intestine is progressively depleted of Na^+ and Cl^- by transport processes of solute-coupled water absorption, leaving behind high concentrations of divalent ions such as Ca^{2+} and Mg^{2+}. The intestine secretes HCO_3^- to precipitate these ions (Genz et al., 2008; Marshall and Grosell, 2005; McDonald and Grosell, 2006), reducing the osmotic pressure and facilitating intestinal water absorption (Wilson et al., 2002). Thus, the SW teleosts typically have higher [HCO_3^-] in the lumen than FW teleosts (Wood, 2019). Fasted English sole had high calculated [HCO_3^-] in the intestine (36-62 mM; Figure 2.3), similar to direct measurements in a previous study on the same species (23-42 mM; Grosell et al., 2001). The secreted HCO_3^- seems to be supplied by the respiratory CO_2 that is reabsorbed into the enterocytes and hydrated by intracellular carbonic anhydrase (reviewed by Grosell, 2019). In SW European flounder, a significant part of the endogenous enterocyte CO_2 produced from aerobic respiration supplies the HCO_3^- that is secreted *via* apical Cl^-/HCO_3^- exchangers (Grosell et al., 2005). The additional HCO_3^- secretion for osmoregulation may also then contribute to high PCO_2 in the intestine, especially since some H^+ secretion by the intestinal epithelium occurs in parallel to the HCO_3^- secretion (Grosell, 2011; Grosell., 2019; Guffey et al., 2011; Wood et al., 2010). In fact, *in vitro* gut sac experiments of killifish (*Fundulus heteroclitus*) showed higher mucosal PCO_2 when the fish were acclimated to SW than FW, and this increased further after feeding (Wood et al., 2010). Furthermore, our *in vivo* measurements of intestinal PCO_2 and calculations of intestinal [HCO_3^-] (~17 mm Hg and 36-62 mM and respectively; Figures 2.1 and 2.3) in the English sole were higher than those found in unfed FW rainbow trout (7-13 mm Hg and 6-15 mM respectively; Wood and Eom, 2019). The presence of high PCO_2 in the intestinal fluid of

English sole then likely helps to promote CO_2 recycling by diffusion back into the enterocytes (Grosell, 2019; Wood, 2019).

The GIT PCO_2 of English sole is further elevated following feeding, which probably is associated with the significant doubling in the calculated [HCO_3^-] in the posterior intestine (62 to 131 mM; Figure 2.3). To neutralize acidic stomach fluid and allow digestive enzymes to function optimally in the intestine, fish secrete HCO_3^-. At present most evidence (e.g. Bucking et al., 2009; Ferlazzo et al., 2012; Grosell and Genz, 2006; Perry et al., 2010; Taylor and Grosell, 2009) points to the intestinal tissue itself as the major source of this HCO_3^- secretion (Wood, 2019). The role of the liver (e.g. Boyer et al., 1976; Grosell et al., 2000) appears modest, while exocrine HCO_3^- secretion by the fish pancreas has not been detected (reviewed by Bakke et al., 2011). The rate of [HCO_3^-] secretion into the intestine in both SW rainbow trout (Bucking et al., 2009) and SW gulf toadfish (*Opsanus beta*) (Taylor and Grosell, 2009) increased after feeding. Similarly, SW European flounder had high total CO_2 (11-45 mM) in the intestine 12 hours following feeding (Taylor et al., 2007). Moreover, feeding also significantly increased the calculated intestinal [HCO_3^-] and measured PCO_2 of fed FW rainbow trout (43-50 mM and 36-41 mm Hg, respectively; Wood and Eom, 2019), but to a lesser extent than in fed English sole (38-131 mM and 34-50 mm Hg, respectively). It is, however, important to note that the English sole were fed whole anchovies containing carbonate-rich bones, which may have resulted in an even greater PCO_2 than that associated with the use of commercial pellets used by Wood and Eom, (2019) in rainbow trout. The increased PCO_2 could also be a result of increased O_2 consumption of the GIT tissue (Taylor and Grosell, 2009) and increased metabolism of bacterial colonies associated with feeding (Altman, 1986; Kurbel et al., 2006; Tomlin et al., 1991), however, it was beyond the scope of this study to investigate these different potential contributors.

2.5.3 Measurements *versus* calculations of PCO_2 and $[HCO_3^-]$ in gastrointestinal fluids

In the present study, we have made direct measurements of gastrointestinal fluid PCO_2 levels using micro-optodes. With the exception of Wood and Eom (2019), all previous values of intestinal fluid PCO_2 levels in fish (summarized by Wood, 2019) were calculated *via* the Henderson-Hasselbalch equation from terminal measurements of pH and total CO_2. In the present study, we made some terminal measurements of these same parameters, so we could make paired comparisons with the directly measured *in vivo* PCO_2 values (Figure 2.5A). While calculated and measured PCO_2 values were significantly correlated ($p = 0.007$, $r^2 = 0.41$, N = 16), quantitative agreement for any individual point was generally poor. Similarly, when calculated $[HCO_3^-]$ values (computed from directly from measured PCO_2 and pH) were regressed against measured $[HCO_3^-]$ values (from terminally sampled total CO_2), the relationship was again significant (Figure 2.5B; $p = 0.022$, $r^2 = 0.32$, N = 16), but agreement for individual points was poor. Similar conclusions were reached by Wood and Eom (2019) for parallel comparisons in FW trout and goldfish. As discussed by these authors and by Wood (2019), possible reasons include uncertainties in pK' and CO_2 solubility coefficients for gastrointestinal fluid, micro-heterogeneity in the gastrointestinal fluid, absence of equilibrium conditions due to insufficient carbonic anhydrase activity in the gastrointestinal fluid, and post-mortem changes. The conservative conclusion is that while calculated values provide useful semi-quantitative indications, directly measured values are far more reliable.

2.5.4 O_2 in the GIT

We measured PO_2 in the GIT of English sole *via* direct insertion of PO_2 micro-optodes into the lumen and found very low PO_2 throughout the tract (Figure 2.4), similar to the virtually anoxic mammalian GIT (Kurbel et al., 2006). The mammalian tract exhibits a steep PO_2 gradient from very low PO_2 (relative to arterial blood) at the outer margins, dropping to anoxia at the luminal midpoint. While usually attributed to respiration by aero-tolerant microbes (Espey, 2013), a recent study suggests that the unusual oxidative chemistry of the GIT fluids also contributes to O_2 depletion (Friedman et al., 2018). We did not attempt to measure a PO_2 gradient in English sole, and our measurements were made by blind puncture, with most micro-optode placements probably close to the midpoint of the lumen. Clearly, virtual anoxia predominates, but in future, it will be of interest to investigate potential PO_2 gradients (as well as pH, PCO_2, ion, and ammonia gradients) from margin to mid-lumen in both fed and fasted fish. Our findings raise questions about the oxygenation status of the enterocytes (discussed in the next section), and also call into question the relevance of gassing salines on the luminal surface of the gut with normoxia or hyperoxia, as is commonly done in transport studies *in vitro* (e.g. Bucking et al., 2013; Grosell et al., 2001; Grosell and Genz, 2006; Rubino et al., 2014).

2.5.5 Blood

We found the arterial blood pH (Figure 2.2) and $[HCO_3^-]$ (Figure 2.3) of English sole did not change significantly following feeding, despite a significant decrease in stomach pH (Figure 2.2). In many fish, as a consequence of H^+ secretion into the stomach for HCl formation, there is an equimolar increase in plasma HCO_3^- after feeding, causing an alkalinisation of the blood ("alkaline tide"; Bucking and Wood, 2009; Cooper and Wilson, 2008; Wood et al., 2005). Some

fish such as the SW dogfish shark and FW rainbow trout compensate by excreting metabolic base across the gills (Bucking and Wood, 2008; Tresguerres et al., 2007; Wood et al., 2007; Wood et al., 2009). However, SW species may be equipped to deal with the elevated metabolic base load of the alkaline tide due to their higher capacity for HCO_3^- secretion into the intestinal lumen for osmoregulation as mentioned above. This has been seen previously in SW gulf toadfish (Taylor and Grosell, 2006) and SW European flounder (Taylor et al., 2007) that appear to not exhibit a postprandial alkaline tide. The same may be true in English sole, as indicated by the very high [HCO_3^-] in the posterior intestine (Figure 2.3).

We are aware of no previous investigation on blood O_2 transport in English sole, but the starry flounder (*Platichthys stellatus*), with which it commonly hybridizes (Garrett et al., 2007), has been well studied (e.g. Milligan and Wood, 1987; Watters and Smith, 1973; Wood et al., 1979). Based on blood gases and blood O_2 dissociation curves reported by Wood et al. (1979) and Milligan and Wood (1987) for *P. stellatus*, our arterial blood measurements (PO_2, PCO_2, pH) in fasted animals were in the normal range for resting animals, yielding about 90 % arterial O_2 saturation. However the increases in arterial PCO_2 (Figure 2.1) and decreases in arterial PO_2 (Figure 2.4) seen in fed fish would have depressed arterial O_2 saturation to about 70 %. As there appear to be no previous data on fed flatfish, we cannot determine whether these are artifacts of anaesthetization and artificial ventilation, or a normal response to feeding. The mean PO_2 (8.8 mm Hg; Figure 2.4) measured in the subintestinal vein draining the GIT of fed English sole was lower than mixed venous PO_2 in the starry flounder (13.4 mm Hg, from the caudal vein) which gave 66 % O_2 saturation in resting, fasted *P. stellatus* (Wood et al., 1979). In combination with the very high (but variable) PCO_2 in the subintestinal vein (mean = 27.8 mm Hg, Table 2.1, Figure 2.1) of English sole, this would have greatly reduced the O_2 saturation in the blood

leaving the intestine to less than 20 %, based on blood O_2 dissociation curves reported by Milligan and Wood (1987) for *P. stellatus*. This could partly be due to the increase in metabolism of the GIT, an artifact of the anaesthesia and artificial gill irrigation, or a combination of both. Certainly the high PCO_2 would be beneficial in releasing blood O_2 from the venous reserve to the enterocytes by Bohr and Root effects (Jensen, 2004; Nikinmaa, 2006; Wells, 2009). However these elevated subintestinal PCO_2 values (Table 2.1) were quite variable amongst animals, and did not agree with generally low subintestinal vein PO_2 values reported in fasted (Cooper et al., 2014) and fed salmonids (Eliason et al., 2007; Wood and Eom, 2019), so it would be premature to draw firm conclusions. The diffusion of both O_2 and CO_2 between the lumen and blood as well as their consequent effects on the O_2 delivery to the metabolically active enterocytes still requires further investigation.

2.5.6 Conclusion

This study investigated the CO_2 and O_2 profiles in the GIT and part of its circulatory system in the marine English sole. We found that this SW teleost has relatively higher PCO_2 levels than two FW species, with levels increasing even further with feeding. We also found extremely low PO_2 levels throughout the GIT, a novel finding in teleosts. Thus, the influence of the high PCO_2 in the GIT on blood O_2 transport, especially given the anoxic lumen, would be of interest in the future. This study had a limitation of working with fish artificially ventilated under anesthesia, which may have had some influence on the gas levels. Thus *in vivo* gas measurements in the GIT and blood of unanaesthetized free-swimming fish prior to and following feeding would be a very informative next step. The possible presence of PO_2 gradients in the lumen, the extent of gas diffusion between the GIT and blood, the fine details of the

vasculature of the GIT villi, and the effect of various feeds on gas levels would all be of potential interest in future studies. Furthermore, in accord with a few previous reports on other teleosts (see Section 2.2), we have measured levels of ammonia, which is another respiratory gas in fish (Randall and Ip, 2006), in the gastrointestinal fluid of the English sole that were much higher than blood levels (Chapter 3; Jung et al., 2022). Therefore, in future, the ammonia profile in the GIT and its influence on O_2 and CO_2 exchange dynamics would also be of great interest.

Table 2.1 The subintestinal venous blood PCO_2 values of 5 fed fish, and the intestinal PCO_2 values of the intestinal section at the point of measurement.

Fed fish	Subintestinal vein PCO_2 (mm Hg)	Intestinal section PCO_2 (mm Hg) at the point of measurement
#1	17.5	24.2; posterior
#2	48.3	76.5; anterior
#3	51.8	45.2; anterior
#5	17.1	21.9; mid
#7	4.1	38.6; anterior

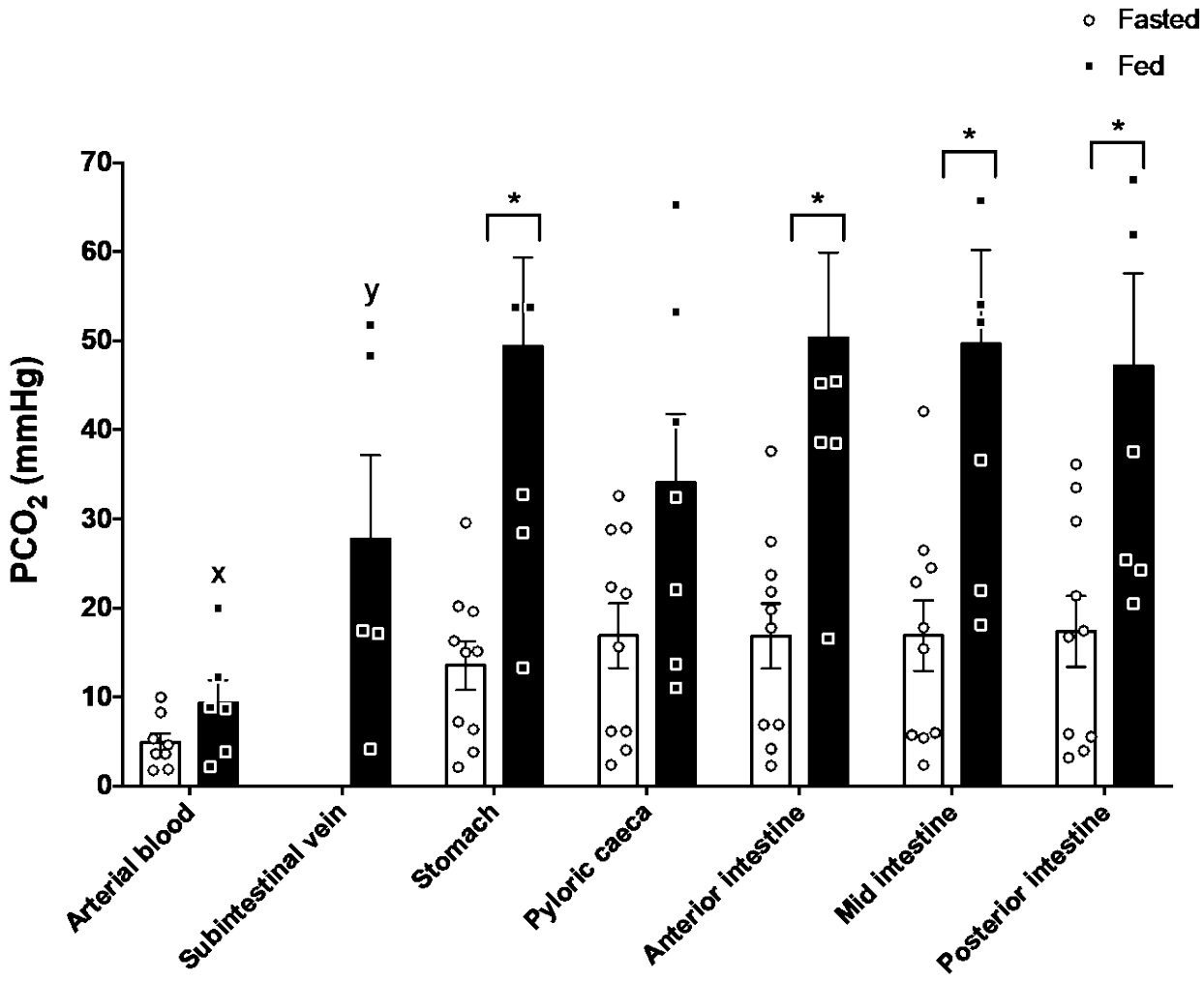

Figure 2.1 Measurements of PCO_2 in the arterial blood, subintestinal venous blood, and GIT sections of fasted (N = 8-10) and fed (N = 5-7) English sole treatment groups. The subintestinal venous blood PCO_2 was not measured in the fasted group. Values are means ± SEM. Asterisk indicates a significant difference between fasted and fed groups within the respective GIT section. Letters that differ indicate significant differences between arterial and venous blood within the fed group. There were no significant differences among GIT section within a given treatment.

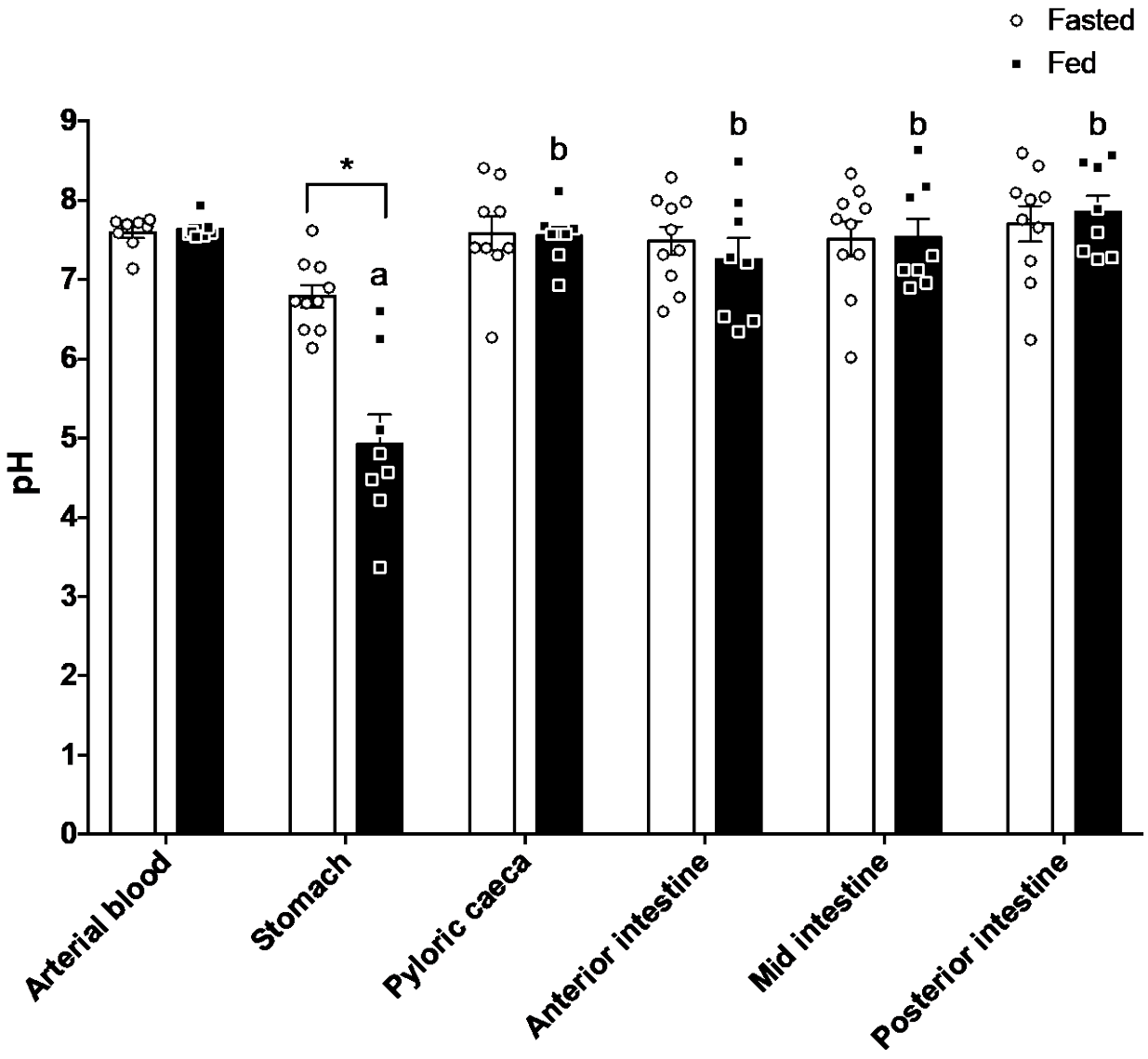

Figure 2.2 Measurements of pH in the arterial blood and GIT sections of fasted (N = 8-10) and fed (N = 7-8) English sole treatment groups. Values are means ± SEM. Asterisk indicates a significant difference between fasted and fed groups within a GIT section. Letters that differ represent significant differences among GIT sections within a fed group. There were no significant differences among GIT sections in the fasted group.

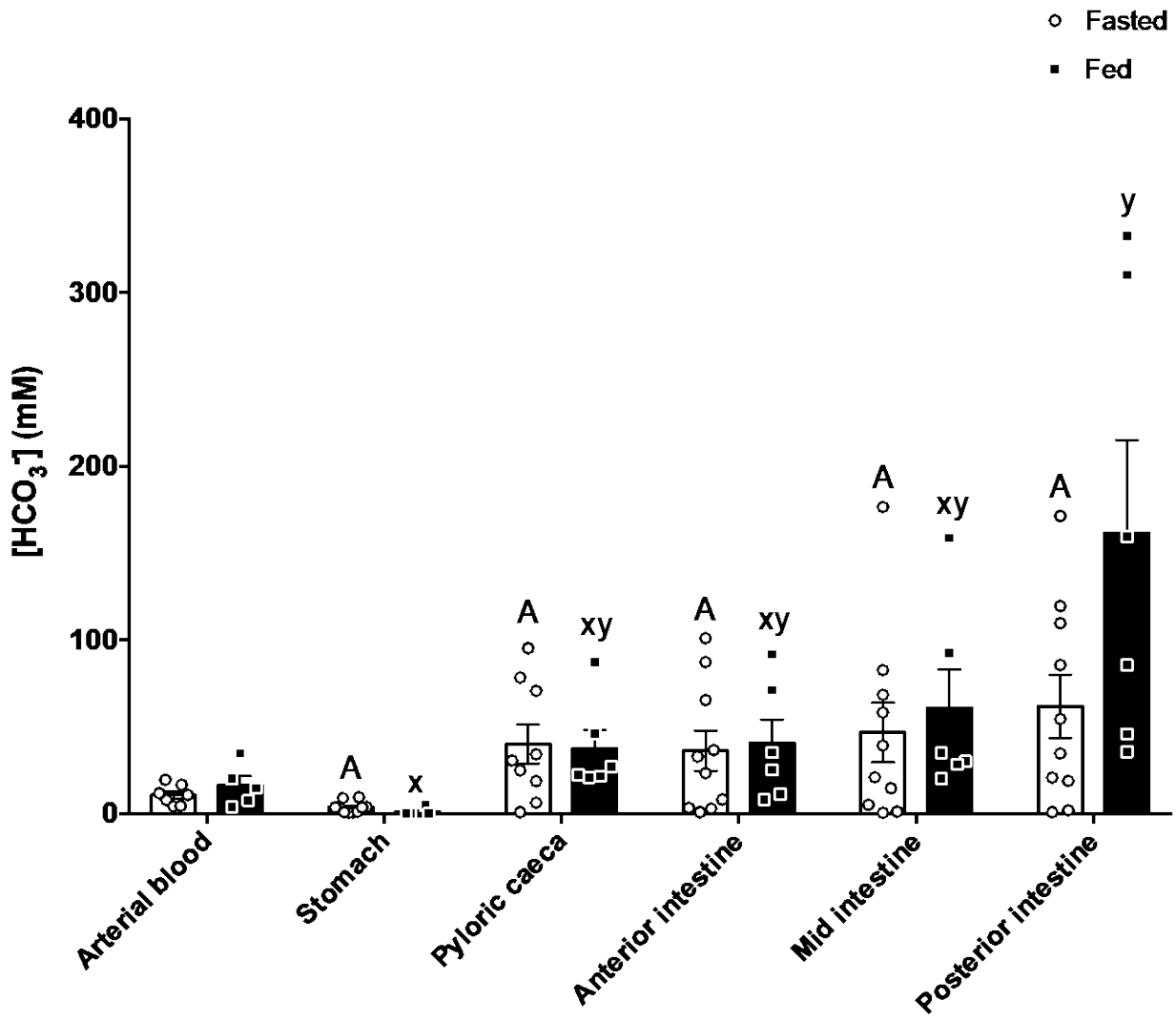

Figure 2.3 Calculated [HCO_3^-] values using measured *in vivo* PCO_2 (Figure 2.1) and pH (Figure 2.2) values of fasted (N = 7-10) and fed (N = 5-6) English sole treatment groups. Values are means ± SEM. Letters that differ indicate significant differences among GIT sections within a treatment group.

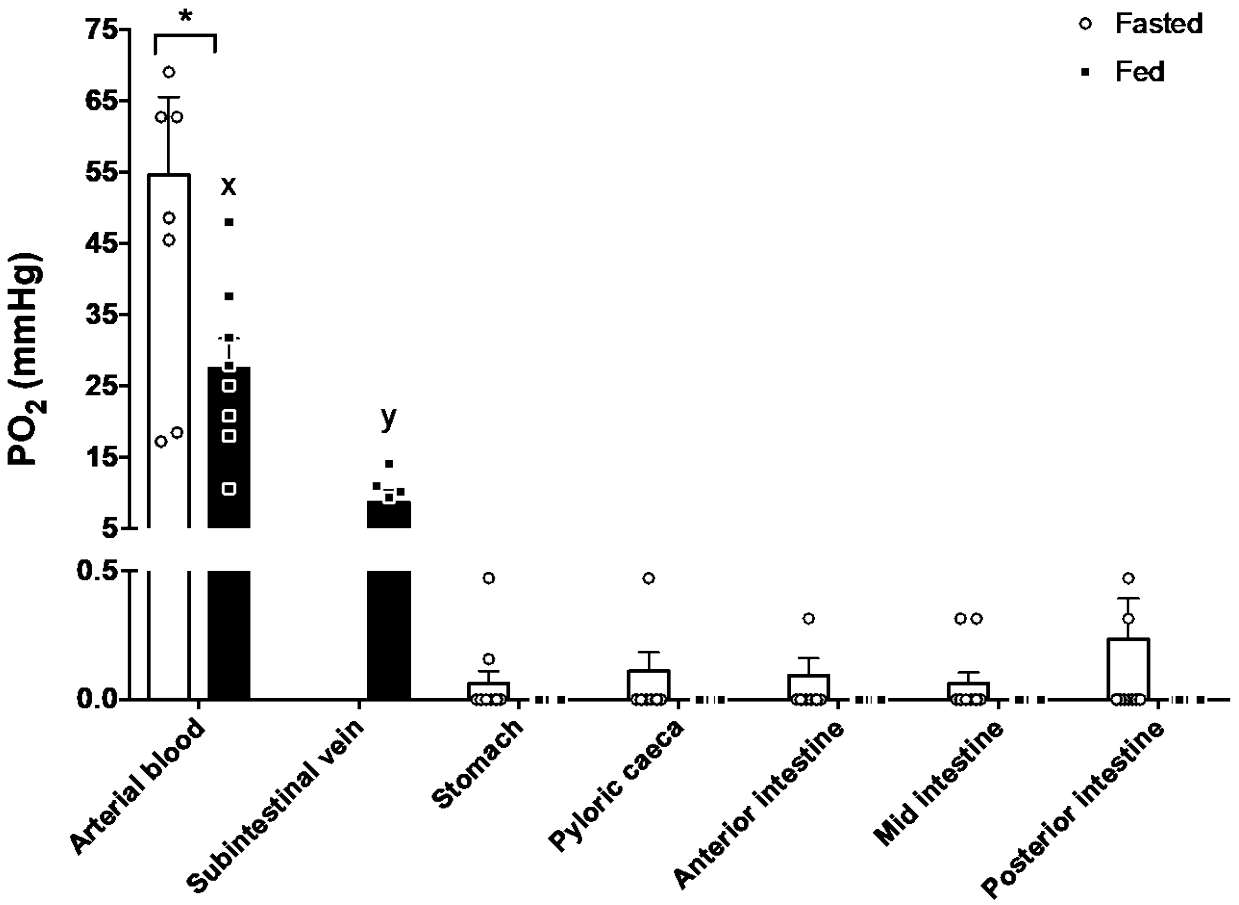

Figure 2.4 Measurements of PO_2 in the arterial blood, subintestinal venous blood and GIT sections of fasted (N = 8-10) and fed (N = 6-9) English sole treatment groups. The subintestinal venous blood PO_2 was not measured in the fasted group. Values are means ± SEM. Asterisk indicates a significant difference of arterial blood values between treatment groups. Letters that differ indicate significant differences between arterial and venous blood values in the fed group. Note the break in the scale on the Y-axis. All mean GIT PO_2 values were ≤ 0.3 mm Hg in the fasted fish, and 0.0 mm Hg in the fed group, and there were no significant differences among GIT sections or between treatment groups.

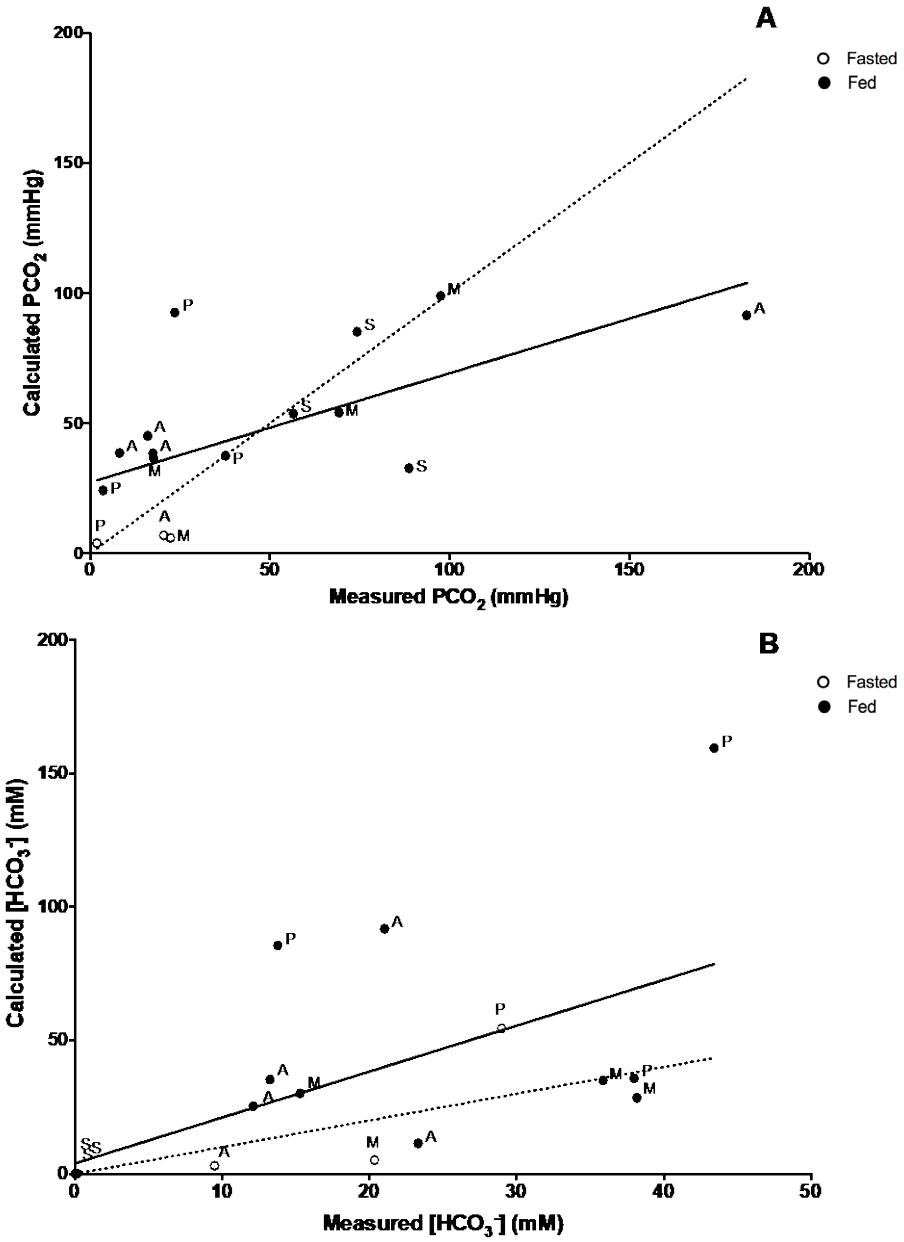

Figure 2.5 Scatter plot of the calculated and measured (A) PCO_2 and (B) $[HCO_3^-]$ values of different GIT sections (S = stomach; A = anterior intestine; M = mid intestine; P = posterior intestine). The dotted lines represent the lines of equality and the solid lines represent best-fit linear regressions. (A: slope = 0.4195 ± 0.13; b = 27.31 ± 8.72; $r^2 = 0.413$; $p = 0.0073$; N = 16) (B: slope = 1.719 ± 0.67; b = 3.93 ± 16; $r^2 = 0.32$; $p = 0.0224$; N = 16).

Chapter 3: Comparison of postprandial luminal PO_2, PCO_2 and ammonia in the GIT between FW rainbow trout and SW English sole

3.1 Summary

The basic respiratory gas and acid-base conditions inside the lumen of the gastrointestinal tract (GIT) and blood draining the tract are largely unestablished in teleost fishes after feeding, though there have been some recent novel discoveries on freshwater rainbow trout and seawater English sole. The present study examined in greater detail the gas (PO_2, PCO_2, PNH_3) and acid-base profiles (pH, $[HCO_3^-]$, Tamm (total concentration of ammonia) in the lumen of the stomach, the anterior, mid, and posterior intestine, as well as the venous drainage (subintestinal and/or hepatic portal vein) of the GIT in these two species 20 h post-feeding. Both species had high PCO_2, PNH_3, and Tamm, and low PO_2 (virtual anoxia) in the lumens throughout all sections of the GIT, and high $[HCO_3^-]$ in the intestine. Tamm, PNH_3, and $[HCO_3^-]$ increased from anterior to posterior intestine in both species. English sole had higher intestinal Tamm and lower $[HCO_3^-]$ than rainbow trout post feeding, but Tamm was much higher in the stomach of rainbow trout. Despite the extreme conditions in the lumen, both arterial and venous blood showed relatively lower PCO_2, Tamm and higher PO_2, implying limited equilibration between the two compartments. The higher $[HCO_3^-]$ and lower Tamm in the intestinal lumen of the freshwater rainbow trout than the seawater English sole suggest the need for future comparative studies using conspecifics fed identical diets but acclimated to the two different salinities in order to understand the potential role of environmental salinity and associated osmoregulatory processes underlying these differences.

3.2 Introduction

The fish gastrointestinal tract (GIT) is a metabolically dynamic tissue, being a site for endogenous tissue metabolism, microbiome metabolism, acid-base and osmoregulatory ion and water transport, and nutrient degradation and transport following feeding. In combination, these processes generate high levels of CO_2 (Wood, 2019) and ammonia (Bucking et al., 2013a; Pelster et al., 2015; Rubino et al., 2014) and a virtually anoxic luminal environment (Jung et al., 2020; Chapter 2). Indeed, recent direct measurements showed high PCO_2 (2 – 10 fold greater than blood levels) in the lumen of freshwater (FW) rainbow trout and goldfish (*Carassius auratus*) (Wood and Eom 2019), and in the seawater (SW) English sole (Jung et al. 2020; Chapter 2). Despite these extreme luminal conditions, it remains unclear to what degree the blood passing through the GIT is affected by these conditions.

Digestion can generate PCO_2 in the digestive tract as a result of a combination of increased endogenous metabolism of the GIT tissues, reaction of gastric HCl with endogenous carbonates in the food and HCO_3^- secretion in the lower tract, and bacterial fermentation (Grosell, 2011; Guffey et al., 2011; Kurbel et al., 2006; Suarez et al., 1997; Tomlin et al., 1991; Wood, 2019; Wood and Eom, 2019; Jung et al., 2020; Chapter 2). Thus, feeding could further elevate the luminal PCO_2, creating greater PCO_2 diffusion gradients between the lumen and the blood, and thus potentially increase blood PCO_2 (Wood and Eom, 2019; Jung et al., 2020; Chapter 2). In these earlier studies on rainbow trout (Wood and Eom, 2019) and English sole (Jung et al., 2020; Chapter 2), the blood in the subintestinal vein (SIV) draining the intestine exhibited higher (but variable) PCO_2 values than in the arterial blood. Notably, these PCO_2 levels were higher than the typical values reported for mixed venous blood in fish (reviewed by Tufts

and Perry, 1998), which suggests some degree of equilibration between the high luminal PCO_2 and the blood passing through the GIT.

If the high luminal PCO_2 diffuses into the blood, it could benefit in unloading O_2 to the tissues *via* Bohr and Root effects (Cooper et al., 2014; Nikinmaa, 2006; Rummer and Brauner, 2015). This could be especially important in delivering O_2 to the metabolically active transport epithelia of the intestine where it may be virtually anoxic on the apical side, as first reported in English sole (Jung et al. 2020; Chapter 2). The PO_2 in the subintestinal venous blood in fed English sole was low (8.8 mm Hg) but still significantly higher than the lumen (≤ 0.3 mm Hg) suggesting incomplete equilibration between the lumen and the blood. The luminal PO_2, however, did not seem to be affected by feeding in English sole. PO_2 in the GIT lumen of rainbow trout is completely unknown, and was measured for the first time in the present study. To understand the potential effect of feeding on the lumen and blood gas profiles, post-prandial conditions of both species were investigated. Due to an insufficient blood flow in the SIV of English sole in fasting conditions, we were unable to insert micro-optodes into the vessel for comparison with fasting rainbow trout.

Furthermore, the catabolism of dietary proteins generates high concentrations of ammonia in the lumen reaching up to 1-2 mM during digestion in rainbow trout (Bucking and Wood, 2012; Rubino et al., 2014), creating a concentration gradient for ammonia into the plasma (Kaushik and de Oliva Teles, 1985; Wicks and Randall, 2002a). A portion of this ammonia could be detoxified by GIT bacteria (Turner and Bucking, 2019) or absorbed into the enterocytes, which exhibit some capacity to metabolically detoxify ammonia loads (Rubino et al., 2014; Jung et al., 2021; Chapter 5). The plasma ammonia level of mixed systemic blood (Bucking and Wood, 2008) and hepatic portal vein (HPV) blood (Karlsson et al., 2006) both increased

significantly post feeding, suggesting transport of dietary-sourced ammonia into the blood. The majority of the plasma ammonia surplus is then excreted to the environment through the gills (Beamish and Thomas, 1984; Karlsson et al., 2006), and to a much lesser extent by the kidneys (Bucking et al., 2010). The possible transport of ammonia across the GIT membrane could be *via* K^+ channels, Rhesus (Rh) glycoproteins, and/or linked to Na^+ uptake partly through NKCC and aquaporins (Bucking and Wood, 2012; Bucking et al., 2013b; Rubino et al., 2015; Rubino et al., 2019; Wright and Wood, 2009). All of the above information was generated on FW rainbow trout, and nothing is known about ammonia handling in the GIT of SW English sole. Given the necessity of Na^+ uptake for osmoregulation, SW teleosts may experience greater uptake of ammonia into the blood than FW teleosts.

These previous novel findings indicated that that there is much more of interest to be learned about respiratory gas exchange in the GIT of FW and SW teleosts. The present study surveyed the profiles of the three respiratory gases - O_2, CO_2, and ammonia - inside the lumen and in the blood in FW rainbow trout and SW English sole. Questions of particular interest were whether the virtually anoxic conditions seen in English sole GIT lumen would also occur in rainbow trout, whether there would be differences between the two species possibly linked to environmental salinity, and whether luminal gases would equilibrate with the bloodstream. Specifically, we hypothesized that the extreme conditions of PO_2, PCO_2 and ammonia in the lumen would be reflected in the blood draining the tract, and would become more marked after feeding.

3.3 Material and Methods

3.3.1 Experimental animals

Rainbow trout (N = 12; 112 – 470 g) were obtained from Little Cedar Falls Hatchery (Nanaimo, BC) and transferred to University of British Columbia (UBC) where they were held for several months prior to experiments. Fish were held at 9 ˚C in flowing dechlorinated Vancouver tap water (Na^+ = 0.09, Cl^- = 0.10, Ca^{2+} = 0.10, Mg^{2+} = 0.011, K^+ = 0.004 mM, hardness as $CaCO_3$ = 3.3 mg L^{-1}, pH = 7.0). During this time, rainbow trout were fed to satiation daily with commercial pellet food (BioTrout 4.0 mm, Bio-Oregon^{TM}, Long-view, WA, USA). English sole (N = 21; 195-565 g) experiments were performed at Bamfield Marine Sciences Centre (BMSC; Bamfield, BC) in August-September 2019 and 2020. Fish were collected from the wild (Barkley Sound, BC) by angling under Department of Fisheries and Oceans Canada collection permits XR-204.18 and XR-212.19, and transferred to outdoor seawater flow-through tanks at 10-12 ˚C and 32 ppt salinity at BMSC. Tanks were filled with 4 cm of sand to allow the animals to burrow; during this time English sole were fed previously frozen anchovies (*Engraulis mordax*).

We investigated rainbow trout in starved and fed states, while only the fed state of English sole was measured. For both species, in the fed groups, fish were fed 20 h prior to experimentation while in the fasted group feeding was withheld for 7 days prior to experimentation. All experiments were approved by the UBC (AUP 14-0251 and 18-0271) and BMSC Animal Care Committees (RS-18-20, RS-19-15, and RS-20-17).

3.3.2 Cannulation

Fish were anaesthetized with 0.1-0.2 g L^{-1} NaOH-neutralized MS-222 (Syndel Laboratories, Parksville, BC) in either freshwater (rainbow trout) or seawater (English sole). Once anaesthetized, the fish were transferred to an operating table and their gills were continuously irrigated with temperature-controlled (acclimation temperature and salinity), anesthetic (~0.03 g L^{-1}; Stage 5; McFarland, 1959) water. The dorsal aorta of rainbow trout was cannulated according to the procedure described in Soivio et al. (1972). The caudal artery of English sole was cannulated as previously described by Watters and Smith (1973) and Jung et al. (2020; Chapter 2). Anaesthesia and gill irrigation were then maintained at the same level throughout the ensuing *in situ* measurements, following which fish were euthanized.

3.3.3 PCO_2, PO_2, total O_2 content ($[O_2]$) and hemoglobin ([Hb]) measurements

The PCO_2 micro-optodes (PreSens, Regensburg, Germany), mounted in #23 hypodermic needles, were prepared and calibrated as described in Chapter 2 (Jung et al., 2020). These PCO_2 micro-optodes were prototype devices (PreSens 200 001 368) connected to an electronic transmitter (PreSens 300 000 114), with the output displayed on a personal computer running prototype software (PreSens 200 001 488). All PO_2 measurements were made using micro-optodes (PreSens, Regensburg, Germany) mounted in #23 hypodermic needles and calibrated with air-equilibrated and sodium sulfite saturated saline kept in gas tight bottles. Arterial blood samples (approximately 1 ml) were collected from the catheter by blood pressure-driven flow into 2-ml microcentrifuge tubes, and then PCO_2 and PO_2 micro-optodes were inserted to the bottom of the tube sitting in the temperature-controlled bath. Whole blood O_2 content was measured using the Tucker method (Tucker, 1967); 10 μL of blood was collected using a gas-

tight syringe (Hamilton, Reno, Nevada, USA) and injected into a custom-made 2344 μL Tucker chamber with the PO_2 micro-optode inserted through a gas-tight septum. The chamber was filled with potassium ferricyanide and saponin to release O_2 bound by hemoglobin. The [Hb] was measured as described by Kampen and Zijlstra (1961).

Then, the peritoneal cavity was surgically opened and the PO_2 micro-optode was directly inserted into the lumen of the gastrointestinal tract (GIT) at four sites (stomach, anterior, mid, and posterior intestine) for luminal measurements. The PCO_2 and PO_2 micro-optodes were inserted into the subintestinal vein (SIV) near the posterior intestine of both species, and into the hepatic portal vein (HPV) of rainbow trout in random order. In fasted English sole, the SIV was not engorged enough for insertion of PO_2 and PCO_2 micro-optodes.

3.3.4 pH, total CO_2 content (TCO_2), and Tamm measurements

The pH of the collected arterial blood was measured using a micro-combination probe (MI-414; 6cm beveled tip; Microelectrodes Inc., Bedford, NH, USA). For both species, not enough blood could be taken from the SIV or HPV for pH, TCO_2 and Tamm measurements. After completion of all blood and luminal gas measurements, the fish was euthanized by an over-dose of anaesthetic, and weighed. The four sections of the GIT (stomach, anterior intestine, mid intestine, and posterior intestine) were ligated with 2-0 silk threads and excised. The GIT fluid/chyme was collected into 2-ml centrifuge tubes, centrifuged (2 min, 5000 g), and the pH of the supernatants was measured, using the same micro-electrode as for blood. The supernatants were then flash-frozen in liquid N_2. Samples were later thawed on ice and immediately assayed for TCO_2 using a Corning 965 CO_2 analyser (Ciba-Corning Diagnotstics, Halstead, Essex, UK)

and Tamm using a commercial ammonia kit (Raichem Cliniqa^{TM}; glutamate dehydrogenase method). Prior tests have demonstrated that chyme TCO_2 values do not change due to freezing.

3.3.5 Calculations and statistical analyses

Graphs were made and statistical analyses were performed using Graphpad Prism software (version 7.0a). All data are expressed as means ± SEM (N = number of fish). Calculated PCO_2 and [HCO_3^-] values were derived from rearrangements of the *Henderson-Hasselbach* equation (see Wood et al., 1983) using values for pK' and CO_2 solubility for teleost plasma (Boutilier et al., 1984). Partial pressures of ammonia (PNH_3) of both plasma and chyme were calculated from measured Tamm and pH using the solubility coefficient of rainbow trout plasma reported in Cameron and Heisler (1983). Species comparisons of data within the same blood or GIT section, as well as differences between fasted and fed treatment groups within a species employed Student's unpaired t-test. Comparisons between blood and GIT section within a species used one-way ANOVA and Tukey's *post hoc* test. All other data were analyzed using two-way ANOVA with blood and feeding state as factors, or species and blood or GIT sections as factors, followed by Tukey's *post hoc* tests. A significance level of $p < 0.05$ was used in all tests.

3.4 Results

3.4.1 Direct-measurement of blood and luminal O_2

The PaO_2 values of the two species in the fed state were not significantly different from each other, and the oxygenation status of arterial blood did not change with feeding in either species (Table 3.1). However, English sole had significantly lower levels of [O_2] and [Hb] than

rainbow trout, differences of about 75 % and 50 % respectively (Table 3.1). Feeding had no significant effect on the PO_2 of blood sampled at different locations of rainbow trout, but the PO_2 values of SIV and/or HPV were significantly lower than PaO_2 in both species, by 60 % or more (Table 3.1 and Figure 3.1). Luminal PO_2 was almost anoxic (< 1 mm Hg) in both species (Figures 3.1 A, B), and was not affected by feeding in rainbow trout; note the differences in scale between the left and right y-axis in Figure 3.1. Luminal PO_2 was significantly lower than SIV or HPV PO_2 in both species (Figure 3.1).

3.4.2 Direct-measurement of blood PCO_2

Rainbow trout had 4-fold higher SIV and HPV PCO_2 than that in the arterial blood, but for English sole, the 1.6-fold higher SIV PCO_2 was not significantly different than the arterial PCO_2 (Figure 3.2). There were no significant differences between species in either arterial or SIV PCO_2. However, as illustrated by the individual data symbols in Figure 3.2, direct measurements of PCO_2 in the veins draining the gastrointestinal tracts of both species (SIV and/or HPV) had greater variability (lowest – highest values: rainbow trout SIV = 11.1-27.1 mm Hg; HPV = 7.2-33.2 mm Hg; English sole SIV = 5.7-23.7 mm Hg) than in arterial blood samples (rainbow trout 2.6-6.4 mm Hg; English sole 3.2–11.0 mm Hg).

3.4.3 $[HCO_3^-]$, pH and calculated PCO_2 of blood and chyme

There was a significant 35 % increase in $[HCO_3^-]$ of the arterial blood after feeding in rainbow trout, but the increase in pH was not significant (Table 3.1). Stomach chyme contained almost no $[HCO_3^-]$ (< 0.3 mM), but $[HCO_3^-]$ gradually increased as chyme proceeded down the intestinal tract in both species, resulting in the highest concentration in the posterior intestine

(rainbow trout mean = 50.7 mM; English sole mean = 20.5 mM) (Figure 3.3A). In general, rainbow trout had 2- to 3-fold higher [HCO_3^-] in the arterial blood and intestinal chyme than English sole (Table 3.1 and Figure 3.3A). In both rainbow trout and English sole, the arterial blood pH values were typical of FW and SW teleosts respectively at these temperatures (Table 3.1). The stomach pH was the lowest in the GIT for both species (3.6 and 4.7 respectively), but pH increased close to blood levels in the intestine (7.7-8.1 and 7.1-7.6 respectively; Figure 3.3B). The direct measurements of total CO_2 and pH allowed calculation of PCO_2 in the arterial blood and chyme, for which there were no significant differences between the species (Figure 3.3C). In both species, the calculated PCO_2 was highest in the stomach at 112-115 mm Hg, but there were no differences among the intestinal sections (20–38 mm Hg). The calculated PCO_2 in the arterial blood was low in both species at 3.4 mm Hg for rainbow trout and 2.8 mm Hg for English sole. These were not significantly different from the directly measured values reported in Figure 3.2 for rainbow trout (p = 0.21), but measured values were significantly higher than calculated values in English sole (p = 0.0093).

3.4.4 Blood and chyme ammonia

English sole had approximately 5-fold higher Tamm in the arterial blood plasma than rainbow trout (Table 3.1 and Figure 3.4A). In both species, chyme Tamm was significantly higher (rainbow trout = 415–3709 μM; English sole = 2180–3062 μM) than that of the arterial blood (Figure 3.4A; rainbow trout = 46 μM; English sole = 238 μM). It was particularly high in the stomach of rainbow trout, followed by the posterior intestine then the anterior and mid intestines. English sole stomach chyme had the lowest Tamm, but it increased moving down the intestinal tract, as in rainbow trout. Therefore, rainbow trout had 1.7-fold higher stomach Tamm

than English sole, but much lower concentrations (by 60-80 %) in the intestine. There were no significant differences between species in chyme PNH_3 values (Figure 3.4B) calculated using measured pH (Figure 3.3B) and Tamm (Figure 3.4A). Both species had the greatest PNH_3 value in the posterior intestine, which was up to 30-fold higher than in the arterial blood.

3.5 Discussion

3.5.1 Overview

The present study found extreme conditions in the lumen of the GIT, with high PCO_2, PNH_3, and Tamm, concurrent with extremely low PO_2 (almost anoxic) in both FW rainbow trout and SW English sole. Overall, our findings did not support the original hypotheses. The venous blood draining from the tract did not seem to reflect the extreme luminal conditions. Furthermore, we did not find any remarkable differences in patterns between the species, though there were some interesting quantitative differences. Feeding had no effect on any of the blood measurements in rainbow trout with the exception of arterial blood [HCO_3^-], which was elevated (Table 3.1) likely as a consequence of HCl secretion into the stomach, inducing an alkaline tide (Hersey and Sachs, 1995). However, there were no significant differences in arterial blood pH or PCO_2 post feeding (Table 3.1). The lack of change in PCO_2 and consistent blood oxygenation status are indicative of an absence of respiratory compensation for the alkaline tide, similar to previous findings in teleosts (Bucking and Wood, 2008; Cooper and Wilson, 2008). The [O_2]/[Hb] did not change following feeding in English sole as well, indicating that both species may be compensating acid-base status using base excretion or other means, rather than by respiratory mechanisms observed in other vertebrates (Andrade et al., 2004; Busk et al., 2000; Niv and Fraser, 2002).

3.5.2 Direct-measurement of blood and luminal O_2

The present study is the first to report a nearly anoxic lumen in a FW teleost, similar to the previous observation in SW English sole (Jung et al., 2020; Chapter 2). We found there to be little or no equilibration of PO_2 between the lumen and the blood in the SIV in both species (Figure 3.1). The anoxic lumen is similar to that in mammals which is a requirement to maintain favorable conditions for the GIT microbiome (Espey, 2013; Tiso and Schechter, 2015). In fact, the average luminal PO_2 of a mouse is reported to be < 1 mm Hg, similar to our findings, but the mucosa near the intestinal tissue (< 200 μm from the epithelial surface) is relatively well-oxygenated and colonized by oxygen-tolerant bacteria (Albenberg et al., 2014; Espey, 2013). A more recent study on germ-free mice revealed that mechanisms other than microbial respiration such as respiration of the intestinal epithelium tissue itself, and/or oxidative chemical reactions may also contribute to O_2 depletion (Friedman et al., 2018). Chapters 2 and 3 found that the lumen was virtually anoxic regardless of feeding conditions in both species, implying oxygen depletion may not be dependent on the presence of food material. Whether similar heterogeneous PO_2 conditions and oxygen consumption pathways as those found in mouse also exist in fish requires further investigation.

3.5.3 Direct-measurement of Blood PCO_2

The PCO_2 values in both the SIV and the HPV were higher than that of the arterial blood in rainbow trout, but not in English sole, where only SIV PCO_2 could be measured (Figure 3.2). High venous PCO_2 could be due to an increase in luminal PCO_2, as observed after feeding in rainbow trout (Wood and Eom, 2019), where the measured PCO_2 in the lumen of the posterior

intestine was about 25-30 mm Hg. This is similar to the mean measured PCO_2 in the SIV and the HPV of approximately 20 mm Hg in the present study (Figure 3.2), values that were below the calculated PCO_2 in the intestinal chyme, and far below the calculated PCO_2 in the stomach (Figure 3.3C). If luminal PCO_2 does diffuse into the blood, it could potentially affect acid-base regulation and blood O_2 transport (Cooper et al., 2014; Nikinmaa, 2006). However, it is important to point out the variability of the venous blood PCO_2 measurements for both species, as illustrated in Figure 3.2. Such variability has also been seen previously by Wood and Eom (2019) in rainbow trout (2 – 34 mm Hg) and in English sole in Chapter 2 (4 – 48 mm Hg; Jung et al., 2020) and thus makes interpretation challenging. We speculate that this could be caused, at least in part, by the interruption of the blood flow during direct insertion of the PCO_2 micro-optodes. Further study with less invasive sampling will be required, perhaps by chronic cannulation of the SIV in much larger fish (Karlsson et al., 2006), before concluding that there is substantial PCO_2 diffusion from the lumen to the blood.

3.5.4 $[HCO_3^-]$, pH and calculated PCO_2 of blood and chyme

We found there to be almost no $[HCO_3^-]$ in the stomach and that $[HCO_3^-]$ increases as chyme moves down the intestinal tract in both species (Figure 3.3A). The secretion of $[HCO_3^-]$ into the intestinal lumen may be part of general digestive function in FW as well as in SW teleosts, but may be additionally utilized for osmoregulation in SW teleosts (Grosell, 2011). Calculated PCO_2 in the lumen was high in both species as predicted, but calculated stomach PCO_2 was higher (almost double) than directly measured values in previous studies (Figure 3.3C; Wood and Eom, 2019; Jung et al., 2020; Chapter 2). Goodrich et al. (2020) also calculated particularly high stomach PCO_2 in FW climbing perch (*Anabas testudineus*) relative to the

intestinal values. There may be a discrepancy between calculated and measured values as shown in Chapter 2 (Jung et al., 2020), but the same study also reported significant correlation between calculated and measured PCO_2 values. Thus, while some discretion should be used for interpreting absolute values, species comparisons using calculated PCO_2 could be relatively reliable. Nonetheless, arterial blood pH and PCO_2 showed no disturbance with feeding despite dynamic levels in the GIT.

English sole had lower [HCO_3^-] in the chyme and similar chyme and SIV PCO_2 levels to rainbow trout (Figures 3.2 and 3.3 A&C). Comparison between salinities is confounded by differences in diet (commercial pellets versus anchovies), temperature (9 ºC versus 10-12 ºC), and of course species. Nevertheless, there is no indication that the additional role of the intestine in osmoregulation in SW fish (Grosell, 2011) and the accompanying greater blood flow to the GIT (Brijs et al., 2015) is associated with more extreme levels of PCO_2 and [HCO_3^-] in the lumen. In SW teleosts, intestinal Cl^-/HCO_3^- exchange results in elevated luminal HCO_3^- concentrations, which help to precipitate Ca^{2+} and Mg^{2+} from the ingested seawater, thereby increasing the osmotic gradient for water absorption across the GIT (Grosell, 2011; Grosell et al., 2009; Guffey et al., 2011; Wood et al., 2010), with associated acid-base relevant ion movements between the lumen and the blood (Cooper et al., 2014). Our data, together with other recent data (Goodrich et al., 2020; Wood, 2019) question the general belief that high [HCO_3^-] in the intestine is exclusive to SW teleosts. As summarized in Wood (2019), the majority of the high intestinal [HCO_3^-] values measured in SW teleosts are for fasted animals. The few data on fed animals in SW summarized in Wood (2019) and our data for fed English sole in the Chapters 2 and 3 are more comparable to those measured in fed FW teleosts, including other species investigated by Goodrich et al. (2020). A comparative study of FW and SW teleosts in the fasting state to

eliminate feeding effects would be informative in teasing out these differences. Nevertheless, our observations indicate the need for further studies on conspecifics acclimated to FW and SW (e.g. the euryhaline rainbow trout) on similar diets to understand the effect of environmental salinity on luminal and blood gas conditions.

3.5.5 Blood and chyme ammonia

Luminal Tamm was high in both species, but particularly high in the stomach of rainbow trout (Figure 3.4A). To our knowledge, this is the first study to report Tamm in the chyme of the stomach, a region that has often been overlooked in ammonia handling abilities. This high [ammonia] disappears once the chyme moves into the intestine, suggesting that a large portion of the ammonia load may be absorbed in the stomach, similar to dietary Na^+ and K^+ ions (Bucking and Wood, 2006). If true, ammonia may be moving against the PNH_3 gradient in the stomach (Figure 3.4B), because the low gastric pH (Figure 3.3B) results in very low luminal PNH_3, despite high Tamm (Figure 3.4A). In the mouse, Rh isoforms are expressed in the stomach (Handlogten et al., 2005), which may be involved in secreting and absorbing ammonia (Gips, 1973; Summerskill et al., 1966). At present, there is no information on possible ammonia absorptive pathways in the teleost stomach. An alternative explanation would be a very rapid absorption of large amounts of ammonia in the very first part of the anterior intestine, which could be driven by an increase in chyme PNH_3 (Figure 3.4B) in response to the almost 4 unit increase in pH encountered as chyme leaves the stomach (Figure 3.3B). Future experiments with isolated gut sac preparations (e.g. Rubino et al., 2014) may be able to address this uncertainty.

To date, there has been a focus on the intestine as a site of ammonia detoxification, excretion and absorption. Rubino et al. (2014) estimated that almost half of the ammonia

produced from feeding in rainbow trout originates from ammonia being generated in the chyme or synthesized within the intestinal tissue, both of which may enter the blood. In various ammoniotelic teleosts, ammonia detoxifying enzymes such as glutamine synthetase (GS) and glutamate dehydrogenase (GDH) have been discovered in the enterocytes (Bucking and Wood, 2012; Bucking et al., 2013a; Mommsen et al., 2003a; Pelster et al., 2015; Tng et al., 2008; Turner and Bucking, 2019). The same enzymes are also found in intestinal bacteria (Andersson and Roger, 2003; Müller et al., 2006; Turner and Bucking, 2019), indicating the importance of the microbiome in handling ammonia as well.

Concurrent with the assumed ammonia load in the lumen after feeding in their study, Karlsson et al. (2006) found a significant increase in plasma Tamm levels in the HPV. While nothing is known about possible gastric ammonia absorption in fish, the mechanism of absorption of ammonia across the intestinal epithelium has now been investigated in some detail (Bucking et al., 2013a; Bucking et al., 2013b; Rubino et al., 2014; Rubino et al., 2015; Rubino et al., 2019; Jung et al., 2021; Chapter 5). Pathways include substitution for K^+ at K^+ channels and NKCC, and possibly passage through aquaporins (Rubino et al., 2015; Rubino et al., 2019). Another possible route is *via* Rh glycoproteins that are present in the mammalian intestine (Handlogten et al., 2005; Weiner, 2006; Worrell et al., 2008), and are also expressed and responsive to feeding in the intestine of teleosts (Bucking and Wood, 2012; Bucking et al., 2013b; Rubino et al., 2015). Present evidence indicates that rainbow trout Rh glycoproteins transport NH_3 rather than NH_4^+ (Nawata et al., 2010), but this remains unproven. The HPV receives venous blood draining from the stomach as well as from the intestine (SIV), so the large ammonia load in the stomach found in the present study (Figure 3.4A) could be an additional or major source of elevated HPV ammonia levels reported in Karlsson et al. (2006). If the PNH_3

gradient is a driver of ammonia uptake, the posterior intestine could be a major site of ammonia absorption (Figure 3.4B). Overall, our data argue for the importance of measuring ammonia in the SIV to compare to the HPV levels, on a paired basis, in concert with simultaneous measurements of ammonia levels in stomach and intestinal chyme.

In the species comparison, English sole had higher plasma and intestinal Tamm levels than rainbow trout (Figure 3.4). Initially, given the necessity of Na^+ uptake in the gut for osmoregulation, we speculated that SW teleosts may experience greater uptake of ammonia into the blood than FW teleosts, due to ammonia transport through Na^+ linked NKCC and aquaporins (Rubino et al., 2015; Rubino et al., 2019). Although we did find higher plasma ammonia levels in English sole, this may simply be due to the greater intestinal ammonia level in this species. Once ammonia is absorbed *via* the GIT, the fish is able to excrete some, but not all, of this ammonia across the gills, before the arterial blood sampling site (Bucking and Wood, 2008; Bucking et al., 2013a; Karlsson et al., 2006).

3.5.6 Conclusion

We performed a survey study on FW rainbow trout and SW English sole of their postprandial profiles in the lumen and the circulatory systems supplying and draining the GIT, with respect to O_2, CO_2, ammonia, and pH. Despite the extreme conditions inside of the lumen, blood experienced much less disturbance. Therefore, there was no or limited equilibration of PCO_2, PO_2, or ammonia between the lumen and blood in both species. There was a significant increase in post-intestinal venous PCO_2 in rainbow trout, but the variability in the data need to be addressed with a less invasive and/or *in vivo* sampling approach. We found minimal differences between the species, except for luminal Tamm and $[HCO_3^-]$ levels that are potentially due to feed

differences. Thus, our study suggests the need for further comparative investigation between FW and SW conspecifics under standardized conditions of diet and temperature, in order to understand any effects of the osmoregulatory role of the intestine in SW on the O_2, CO_2, ammonia, and acid-base conditions in the GIT lumen and the vascular system.

Table 3.1 Effect of feeding on arterial blood characteristics of rainbow trout (N = 5-6) and English sole (N = 7-13). Means ± SEM. Asterisk (*) represent significant differences between fasted and fed states within a species. Dagger (†) represents significant difference between species in the same feeding state.

	Rainbow trout		English sole	
	Fasted	Fed	Fasted	Fed
PO_2 (mm Hg)	99.5 ± 6.5	90.3 ± 3.5	-	80.3 ± 7.9
PCO_2 (mm Hg)	3.5 ± 0.7	4.7 ± 0.8	-	7.5 ± 1.1
Tamm (μM)	37.9 ± 11.4	45.9 ±14.0	-	238.3 ± 49.9†
PNH_3 (μmm Hg)	9.0 ± 2.4	15.8 ± 3.4	-	49.3 ± 14.3†
$[HCO_3^-]$ (mM)	10.5 ± 0.3	14.3 ±1.2*	-	3.9 ± 0.7†
pH	7.80 ± 0.09	7.94 ± 0.14	-	7.66 ± 0.10
$[O_2]$ (mM)	3.9 ± 0.2	4.4 ± 0.6	0.8 ± 0.2†	1.0 ± 0.2†
[Hb] (mg ml^{-1})	106.0 ± 19.2	126.5 ± 14.7	62.1 ± 3.5†	63.8 ± 5.0†
$[O_2]$/[Hb] (mmoles g^{-1})	0.042 ±0.006	0.038 ± 0.007	0.012 ± 0.002†	0.014 ± 0.004†

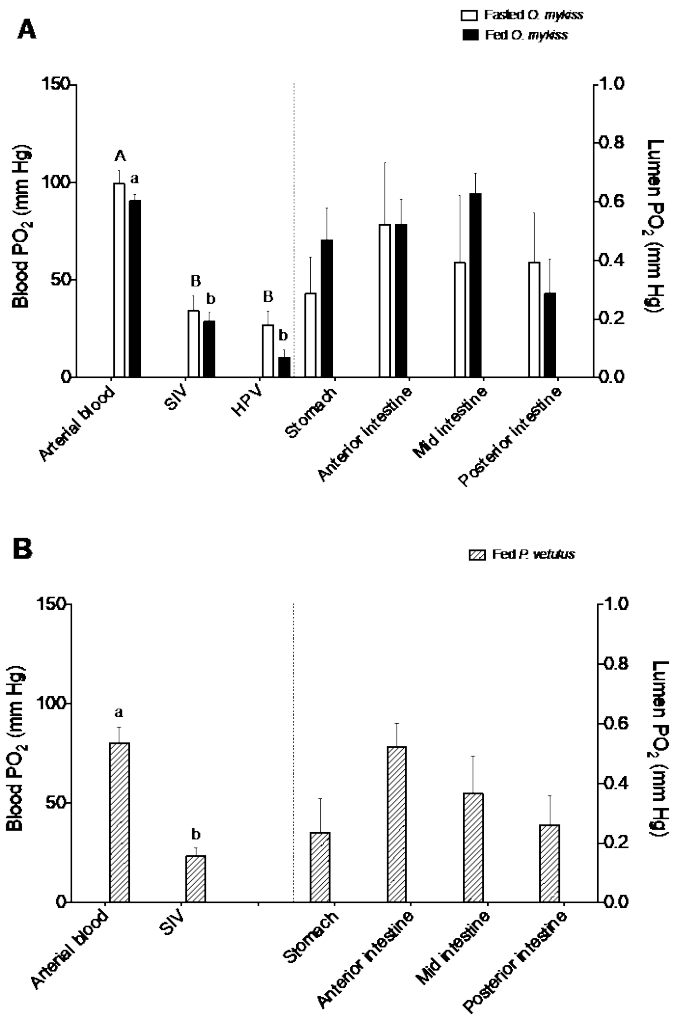

Figure 3.1 Direct measurements of PO_2 in the blood and four sections of the gastrointestinal tract (GIT) lumen of (A) fasted and fed rainbow trout (N = 5-6) and (B) fed English sole (N = 6-7). Means ± SEM. Blood data are reproduced from Table 3.1 to permit direct comparison with the luminal PO_2 values. Note that the left y-axis is for blood values, and right y-axis is for GIT lumen values. Upper case letters represent significant difference between blood samples from different sites in (A) fasted fish, and lower case in (A & B) fed fish. There were no significant differences between fasted and fed states in (A) rainbow trout, and there were no significant difference between fed species in either blood samples or luminal measurements. All luminal PO_2 values were significantly lower than blood PO_2 in both species.

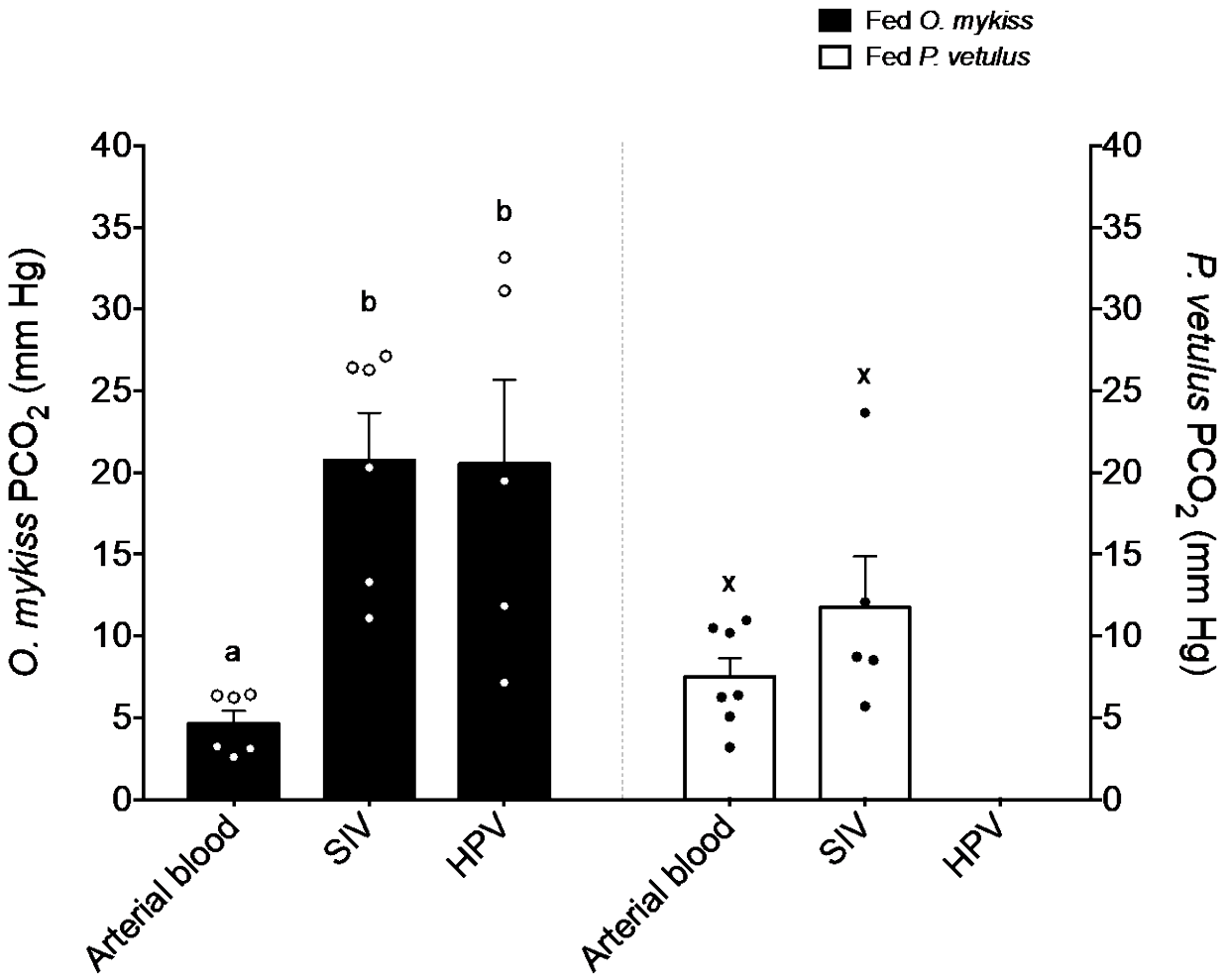

Figure 3.2 Direct measurements of PCO_2 in arterial, subintestinal vein (SIV) and hepatic portal vein (HPV) blood after feeding in rainbow trout (left y-axis; N = 5-6) and English sole (right y-axis; N = 5-7). Means ± SEM. Letters represent significant difference between blood measurements within a species. Arterial blood PCO_2 data are reproduced from Table 3.1 to permit direct comparison with SIV and HPV values. There were no significant differences between species. Individual data are overlaid on the bars as round symbols to illustrate the data distribution.

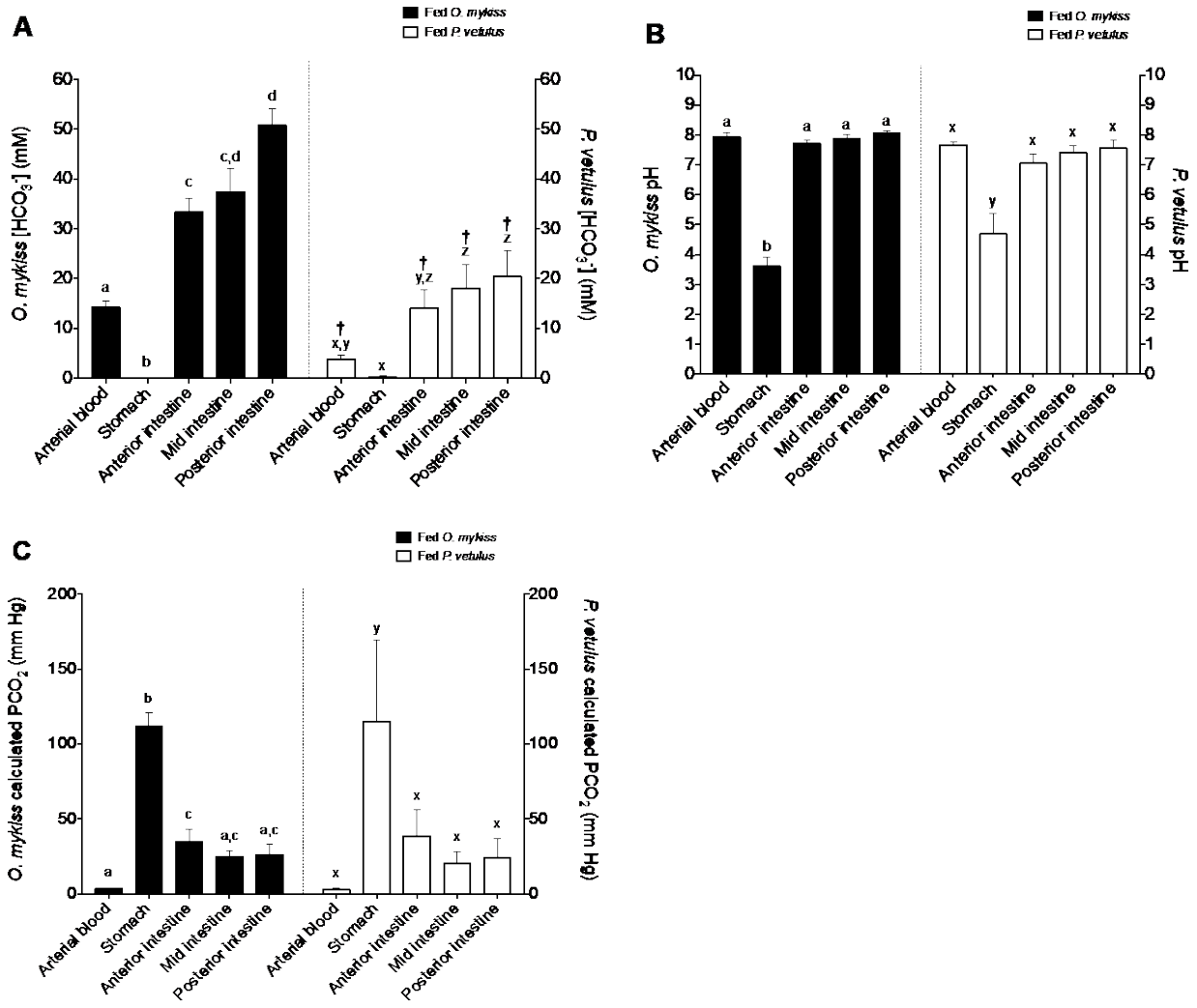

Figure 3.3 (A) Measured [HCO_3^-], (B) pH, and (C) calculated PCO_2 of blood and chyme in fed rainbow trout (left y-axis; N = 6), and English sole (right y-axis; N = 7). Means ± SEM. Arterial blood pH values are reproduced from Table 3.1 to permit direct comparison with the luminal values. Letters that differ represent significant differences between blood and sections of the GIT within a species. Dagger represents significant difference between species.

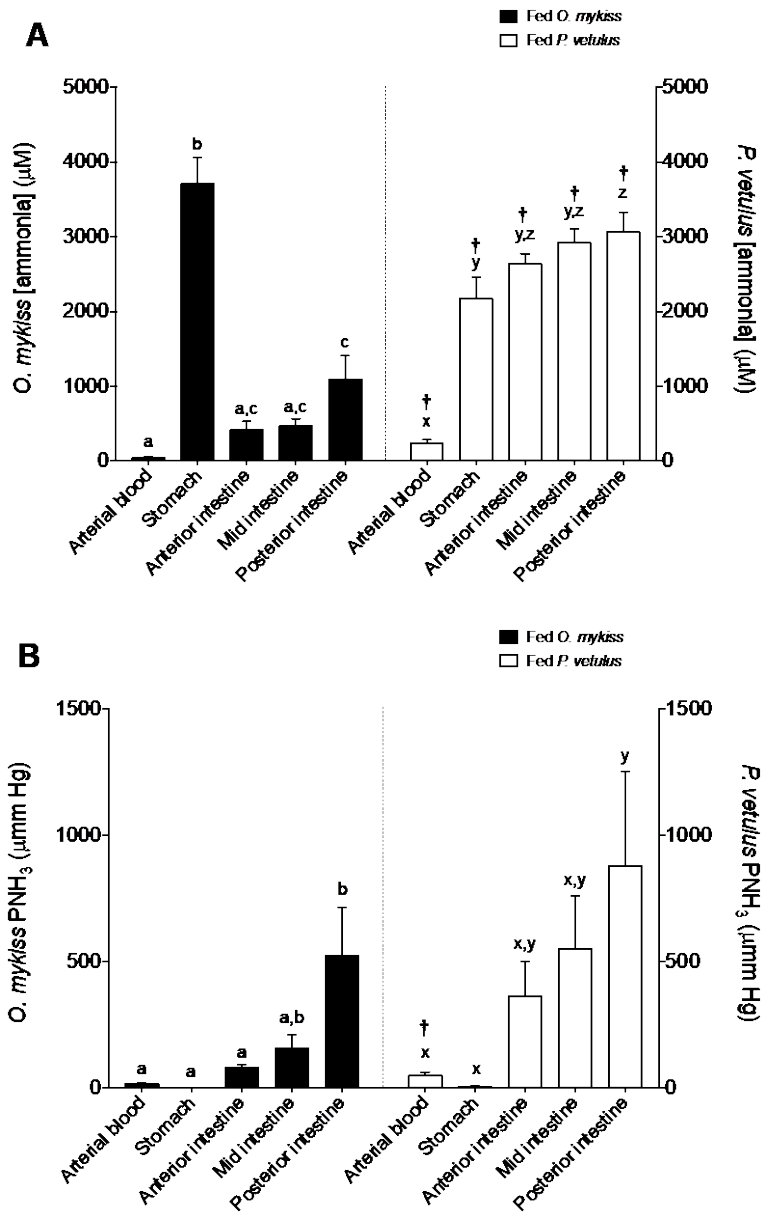

Figure 3.4 Measured (A) Tamm of arterial blood and chyme and (B) calculated PNH_3 from direct measurements of pH (Figure 3.3B) and Tamm (panel A) in fed rainbow trout (left y-axis; N = 5-6), and English sole (right y-axis; N = 6-7). Means ± SEM. Letters that differ represent significant differences between blood and sections of the GIT within a species. Dagger represents significant difference between species. Arterial blood pH and PNH_3 values are repeated from Table 3.1 for comparison with the luminal values.

Chapter 4: Potential equilibration of PO_2, PCO_2 and ammonia between the GIT lumen and systemic bloodstream in FW rainbow trout

4.1 Summary

Teleosts experience extreme conditions in the lumen of the gastrointestinal tract (GIT), especially after feeding: high PCO_2 (20-115 mm Hg), total ammonia (415-3710 μM), PNH_3 (79-1760 μmm Hg in the intestine), and virtual anoxia (PO_2 < 1 mm Hg). These levels could be dangerous if they were to equilibrate with the bloodstream. Previous findings have proven equivocal. Thus, we investigated the potential for equilibration of O_2, CO_2, and ammonia across the GIT epithelia in freshwater rainbow trout by monitoring postprandial arterial and venous blood gases *in vivo* and *in situ*. *In vivo*, blood was sampled from the indwelling catheters in the dorsal aorta (DA) and subintestinal vein (SIV) draining the posterior intestine in the fasting state and at 4 to 48 h following catheter-feeding. To investigate possible ammonia absorption in the anterior part of the GIT, blood was sampled from the DA, SIV and hepatic portal vein (HPV) from anaesthetized fish *in situ* following voluntary feeding. We found minimal equilibration of all three gases between the GIT lumen and the SIV blood, with the latter maintaining pre-feeding levels (PO_2 = 25-49 mm Hg, PCO_2 = 6-8 mm Hg, and total ammonia = 117-134 μM and PNH_3 = 13-30 μmm Hg at 48 h post-feeding). In contrast to the SIV, we found that the HPV total ammonia more than doubled 24 h after feeding (128 to 297 μM), indicative of absorption in the anterior GIT. Overall, the GIT epithelia of trout, although specialized for absorption, prevent dangerous levels of PO_2, PCO_2 and ammonia from equilibrating with the blood circulation.

4.2 Introduction

Conditions to improve fish health and maximize growth efficiency have been of growing interest in support of aquaculture, which is currently one of the fastest expanding industries globally (Food and Agriculture Organization, 2020). Despite such interest, relatively little is known about the conditions in the gastrointestinal tract (GIT) and its significance to fish productivity. The GIT is an important multifunctioning organ in fish not only for digestion and nutrient absorption, but also for ionic and osmotic regulation, neuroendocrine regulation, immune responses, and even air breathing in some species (Grosell et al., 2011).

The GIT lumen is a unique extracorporeal environment containing a complex microbiome, lined with specialized GIT cells (enterocytes) interacting closely with other organ systems. In mammals, the lumen contains high carbon dioxide (CO_2) and low oxygen (O_2) levels derived from chemical reactions and bacterial fermentation of dietary substrates during digestion (reviewed by Kalantar-Zadeh et al., 2019). Recent research has shown that this is similar in fish. Direct measurements in the lumen of fasted freshwater rainbow trout and seawater English sole have revealed low PO_2 (< 1 mm Hg) and high in PCO_2 (7-17 mm Hg) values (Wood and Eom, 2019; Jung et al., 2020; Chapter 2). Feeding further elevates the luminal PCO_2 in fish (20-115 mm Hg), whereas PO_2 remains nearly anoxic (Wood and Eom, 2019; Jung et al., 2020; Jung et al., 2022; Chapters 2 and 3). These luminal PO_2 and PCO_2 levels are much more extreme than normal blood levels, more extreme than predicted future levels induced by climate change, and even more extreme than levels considered harmful in the natural environment (Alabaster et al., 1957; Ellis et al., 2017). Moreover, a third respiratory gas for fish, ammonia (Randall and Ip, 2006), is also high in the lumen (415-3710 μM as total ammonia; 79-1760 μmm Hg in the intestine as PNH_3) as a result of breakdown of proteins in the food (Bucking and Wood, 2012;

Rubino et al., 2014; Jung et al., 2022; Chapter 3). This also exceeds the water ammonia levels considered toxic for fish (Randall and Tsui, 2002; Solbé and Shurben, 1989).

Ultimately, there are significant gradients of both PCO_2 and ammonia from the lumen into the arterial blood perfusing the GIT, while the opposite is true for PO_2. Notably, plasma ammonia concentrations in mixed caudal blood (Bucking and Wood, 2008; Kaushik and de Oliva Teles, 1985), and in the hepatic portal vein (HPV) draining the GIT (Karlsson et al., 2006) are elevated significantly after feeding This excess ammonia is then excreted *via* the gills, and to a lesser extent *via* the kidney (Beamish and Thomas, 1984; Bucking et al., 2010; Karlsson et al., 2006; Wicks and Randall, 2002b). However, transport of luminal ammonia into the systemic bloodstream must be carefully controlled as it can be a toxicant (Randall and Tsui, 2002). Similarly, if the high luminal PCO_2 were to equilibrate with the blood, it would result in a very unfavourable blood acid-base disturbance (extreme respiratory acidosis) in fish (Perry and Gilmour, 2006), though at the same time it potentially could help to release O_2 from hemoglobin by Bohr and Root effects (Nikinmaa, 2006; Rummer and Brauner, 2015) thereby fueling active transport processes in the enterocytes. In mammals, some of the luminal CO_2 and other gases can be absorbed across the intestinal epithelia and enter the blood circulation, but they are also either removed by microbes or released as flatulence (Lacy et al., 2011; Ohashi et al., 2007). Whether or not high luminal PCO_2 and ammonia are also moving into the vascular system in fish is still largely unproven. A few calculated PCO_2 values in the venous blood draining from the GIT are reported to be low (Cooper et al., 2014; Eliason et al., 2007), but direct measurements in the subintestinal vein (SIV) have proven to be quite variable (Wood and Eom, 2019; Jung et al., 2020; Jung et al., 2022; Chapters 2 and 3). This variability may reflect the fact that these direct measurements were taken from anaesthetized, artificially ventilated fish by direct micro-optode

puncture of the SIV (*in situ*) rather than from conscious animals. Anaesthesia and/or blockade of blood flow may have confounded the results.

Therefore, the purpose of this study was to investigate the degree of equilibration of the three respiratory gases, O_2, CO_2, and ammonia between the GIT lumen and systemic bloodstream, using *in vivo* measurements on non-anaesthetized fish fitted with a stomach feeding tube and indwelling catheters for sampling inflowing blood from the dorsal aorta (DA) and outflowing blood from the subintestinal vein (SIV). We investigated this in freshwater-acclimated rainbow trout sampled in the fasting state and at 4, 8 12, 24, and 48 h after feeding (*in vivo* series; 1 % body mass ration). We extended our *in vivo* ammonia findings with *in situ* experiments on anaesthetized trout that permitted sampling of blood from both the SIV that drains only the posterior tract and the hepatic portal vein (HPV) which additionally drains the entire GIT (*in situ* series; voluntarily fed to satiation). Plasma ammonia concentrations at the two sites were compared during the fasting state and at 24 and 48 h after voluntarily feeding (*in situ* series). In general, we hypothesized there would be minimal equilibration of these gases across the intestinal epithelia into the venous drainage. We also hypothesized that feeding would have little effect, so that SIV PO_2, PCO_2 and ammonia would remain largely unchanged during digestion. Finally, in light of the findings of Karlsson et al (2006), We hypothesized that postprandial luminal absorption of excess ammonia would be seen in the anterior part of the GIT, and thus higher plasma ammonia concentrations in blood sampled from the HPV than from the SIV.

4.3 Material and Methods

4.3.1 Experimental animals

Rainbow trout (220-620 g) were obtained from Little Cedar Falls Hatchery (Nanaimo, BC, Canada) and transferred to the University of British Columbia (UBC) where they were held for several months prior to experiments. Fish were held at 9 ˚C in flowing dechlorinated Vancouver tap water (Na^+ = 0.09, Cl^- = 0.10, Ca^{2+} = 0.10, Mg^{2+} = 0.011, K^+ = 0.004 mM, hardness as $CaCO_3$ = 3.3 mg L^{-1}, pH = 7.0). During this time, fish were fed to satiation daily with commercial pellet food (BioTrout 4.0 mm, Bio-Oregon^{TM}, Long-view, WA, USA). Food was withheld for 7 days prior to experimentation. For the *in vivo* series, fish were anaesthetized and surgery was performed as described below. For the *in situ* series, fish were sampled either at 7 days of fasting (control), or at 24 or 48 h after voluntary feeding to satiation. For both series, we measured or calculated P_aO_2, hemoglobin-O_2 saturation (Hb-O_2 saturation), pH_a, $[HCO_3^-]_a$, P_aCO_2, total ammonia (Tamm), and/or P_aNH_3 from blood sampled from the dorsal aorta (DA). Venous drainage was sampled from the subintestinal vein (SIV) and measured for P_vO_2, Hb-O_2 saturation, pH_v, $[HCO_3^-]_v$, P_vCO_2, SIV Tamm, and/or P_vNH_3. All experiments were approved by the UBC Animal Care Committee (AUP 14-0251 and 18-0271) and conformed to national regulations of the Canada Council for Animal Care.

4.3.2 Cannulation and blood sampling

For both *in vivo* and *in situ* series, the same DA and SIV cannulation techniques were performed. Fish were anaesthetized with 0.1-0.2 g L^{-1} NaOH-neutralized MS-222 (Syndel Laboratories, Parksville, BC). Once anaesthetized, the fish were transferred to an operating table and their gills were continuously irrigated with temperature-controlled anesthetic (~0.03 g L^{-1}) to

achieve stage 5 anaesthesia (McFarland, 1959) water. The DA was cannulated according to the procedure described in Soivio et al. (1972). The SIV was cannulated near the proximal end of the posterior intestine, as described by Cooper et al. (2014). In brief, a 3-cm incision in the midline anterior to the anus was made, the SIV was located, and then the most posterior end of the vessel was tied with 2-0 silk thread to occlude posterior blood flow. About 2 cm of polyethylene tubing-10 (PE10; Clay-Adams^{TM}, Becton and Dickinson Co., Franklin Lakes, NJ, USA) was fitted to stretched PE50 tubing and filled with heparinized (150 I.U. ml^{-1}; Sigma-Aldrich, St. Louis, MO, USA) Cortland's saline (Wolf, 1963; See Table S.1 for composition). An opening for the cannula in the SIV was made with a hypodermic needle, then the PE10-tipped cannula was pushed forward anteriorly about 2 cm and tightly secured around the vessel using 2-0 surgical silk.

For *in vivo* series, blood flow through the cannula was checked, which was then flushed with heparinized saline. The cannula was secured to the anal fin and the incision was sutured closed with silk suture. In addition, flared PE240 was inserted down the oesophagus into the stomach and securely sutured through a hole next to the nostril to serve as a feeding tube. Fish were then transferred to black Plexiglas chambers and were left to recover overnight. The chambers were supplied with flow-through 9 ˚C freshwater and were aerated throughout the experiment. After overnight recovery, blood was sampled from both the DA and SIV cannulae while the fish was still in the fasting state, which will be referred to as the "control" from hereon. Approximately 0.5 ml of blood was sampled from each cannula by blood pressure-driven and/or gravity driven flow into 0.6-ml heparinized microcentrifuge tubes, taking care to minimize air exposure. Equivalent volumes of saline were immediately injected to replace the blood removed by sampling. Immediately after, fish were fed a 1 % body mass ration of pellet food (delivered as

a slurry of homogenized food pellets in two volumes of water; Cooper and Wilson 2008; Bucking et al. 2010) *via* the oesophageal feeding tube. Postprandial blood samples were collected at 4, 8, 12, 24 and 48 h after feeding.

For the *in situ* series, fish were implanted with the same DA and SIV cannulae on a surgery table with anaesthesia and gill irrigation maintained at the same level throughout. Experiments lasted approximately 1 hour. Blood samples were collected *via* the cannulae into 0.6-ml heparinized microcentrifuge tubes. In addition, the hepatic portal vein (HPV) blood was sampled by direct insertion of the needle of a heparinized gas-tight 100 μL-syringe (Hamilton, Reno, Nevada, USA) into the blood vessel.

4.3.3 Whole blood measurements

Collected blood samples were first measured for pH, PO_2 and PCO_2 by inserting the micro-electrode and micro-optodes to the bottom of the tube, while kept at the experimental temperature. The pH was measured using an oesophageal pH microelectrode (MI-508; 1.4-1.6 mm OD) and a flexible micro-reference electrode (MI-402; Microelectrodes Inc., Bedford, NH, USA) connected to a model 220 pH meter (Corning Instruments, Corning, NY, USA). The electrodes were calibrated with precision buffers (Fisher Scientific and Radiometer-Copenhagen, Copenhagen, Denmark).

The PO_2 and PCO_2 were measured using micro-optodes (PreSens Precision Sensing GmbH Regensburg, Germany) positioned into the collection tubes using micro-manipulators (World Precision Instruments, Sarasota, FL, USA). The PO_2 micro-optodes were calibrated with air-equilibrated and sodium sulfite saturated saline kept in gas-tight bottles. The PCO_2 micro-optodes were prototype devices (PreSens 200 001 368) connected to an electronic transmitter

(PreSens 300 000 114), with the output displayed on a personal computer running prototype software (PreSens 200 001 488). These PCO_2 micro-optodes were prepared and calibrated as described in Jung et al. (2020; Chapter 2), with salines equilibrated to 0.04, 0.5, 1, 3, and 5 % CO_2 using CO_2/air mixtures created by a 301aF precision gas-mixing pump (Wösthoff Messtechnik GmbH, Bochum, Germany). All calibration solutions were kept at the experimental temperature of 9 ˚C.

The hemoglobin-O_2 saturation (%) was calculated from the measured blood O_2 content ($[O_2]$) and hemoglobin concentration ([Hb]) by taking 4 O_2 molecules per Hb (tetramer) into account. Blood $[O_2]$ was measured using the Tucker method (Tucker, 1967). During collection of the blood from cannulae into the microcentrifuge tubes, 10 µL of blood was taken using a gas-tight syringe and injected into a custom-made 2344 µL Tucker chamber with the PO_2 micro-optode inserted through a gas-tight septum. The chamber was filled with a potassium ferricyanide and saponin solution to release O_2 bound by hemoglobin. The [Hb] was measured as described by Kampen and Zijlstra (1961). After all measurements were completed, the remaining blood was centrifuged (2 min, 5000 *g*), and the plasma was removed and flash-frozen in liquid N_2 and stored at –70 ˚C in an ultra-cold freezer.

4.3.4 Plasma and chyme measurements: Tamm and TCO_2

At the end of the experiment, fish were euthanized by an overdose of neutralized MS-222. The four sections of the GIT (stomach, anterior intestine, mid intestine, posterior intestine) were ligated and excised, and the chyme was collected into 2-ml centrifuge tubes. The chyme samples were centrifuged (2 min, 5000 g), and the pH values of the supernatants were measured. The samples were then flash-frozen in liquid N_2 for storage at –70 ºC in an ultra-cold freezer.

Plasma and chyme supernatant were later measured for total CO_2 content (TCO_2) using a Corning 965 CO_2 analyser (Ciba-Corning Diagnostics, Halstead, Essex, UK) calibrated with $NaHCO_3$ standards. The samples were also analyzed for total ammonia (Tamm; μM) by an enzymatic assay based on the glutamate dehydrogenase/NAD method using a commercial kit (Raichem; San Diego, CA, USA).

4.3.5 Calculations and statistical analyses

The [HCO_3^-] values in plasma and chyme, and the PCO_2 values in chyme were derived from measurements of pH and TCO_2 *via* rearrangements of the Henderson-Hasselbach equation (see Wood et al., 1983) using values for pK' and CO_2 solubility for teleost plasma (Boutilier et al., 1984). Partial pressures of ammonia (PNH_3) of both plasma and chyme were similarly calculated *via* the Henderson-Hasselbach equation using measured Tamm and pH values with the pK and solubility coefficients reported in Cameron and Heisler (1983).

Graphs were made and statistical analyses were performed using Graphpad Prism software (version 7.0a). Data have been expressed as means ± SEM (N = number of fish). For both series, comparisons between DA and SIV at each postprandial sampling time were made using two-way ANOVA with Sidak's *post hoc* test. Comparisons of the measured parameter of either DA or SIV from different postprandial sampling times to that of the control value were done using two-way ANOVA with Dunnett's *post hoc* test. Tamm and PNH_3 data were log transformed to meet assumptions of homogeneity of variance, and comparison between plasma and chyme Tamm or PNH_3 values were done using one-way ANOVA with Sidak's *post hoc* test. One-way ANOVA with Tukey's *post hoc* test were performed to compare chyme pH, [HCO_3^-], PCO_2 between GIT compartments. Comparison of pH, [HCO_3^-] or PCO_2 between posterior

chyme and SIV were done using two-way ANOVA with Sidak's *post hoc* test. A significance level of $p < 0.05$ was used in all tests.

4.4 Results

4.4.1 Postprandial blood O_2 (*in vivo*)

Within 4 h of feeding, P_aO_2 in the DA increased significantly from about 100 to 140 mm Hg, remained high for about 8 h, then gradually came back down to control level by 24 and 48 h after feeding (Figure 4.1A). Feeding had no significant effect on the P_vO_2 in the SIV (25-49 mm Hg), which remained lower than P_aO_2 throughout the series. The difference between P_aO_2 and P_vO_2 was approximately 64 mm Hg in fasting fish (control) then increased to 98 mm Hg at 4 h following feeding. Despite these changes and the observed increase in P_aO_2 in response to feeding, the Hb-O_2 saturation did not change in either arterial (DA) or venous (SIV) blood, averaging 77.3 ± 2.4 % and 44 ± 3.1 % respectively (Figure 4.1B).

4.4.2 Postprandial blood and chyme pH, $[HCO_3^-]$, PCO_2 (*in vivo*)

We observed a metabolic alkalosis (also known as an alkaline tide) at 24 h post-feeding where plasma pH_a and $[HCO_3^-]_a$ were elevated significantly relative to the control values (Figures 4.2 A&B). A 5.6 mM increase in $[HCO_3^-]_a$ at 24 h led to a 0.4 unit increase in pH_a. Both parameters then came back down to the control level by 48 h. In contrast, the pH_v and $[HCO_3^-]_v$ remained unchanged throughout digestion. DA and SIV values were similar except at 4 and 24 h for pH, and at 24 h for $[HCO_3^-]$. Throughout the experiment, the measured P_vCO_2 values in the SIV were generally higher than P_aCO_2 by approximately 1.5 mm Hg (Figure 4.2C). Both P_aCO_2 and P_vCO_2 increased similarly at 12 h (by ~1.7 and 1.4 mm Hg respectively), but came back

down to control levels by 24 h. Interestingly, in both DA and SIV blood, the PCO_2 remained below 8 mm Hg throughout digestion.

The cannulated animals were sacrificed for chyme sampling at 48 h post-feeding. Visual inspection showed that most of the chyme was in the posterior intestine at this time, with small amounts in the more anterior sections of the intestine and stomach. Levels of pH and $[HCO_3^-]$ in the chyme collected at 48 h increased from anterior to posterior sections of the GIT (Table 4.1). Consequently, the calculated PCO_2 was the highest in the stomach chyme despite the lowest $[HCO_3^-]$ due to its low pH. The intestinal chyme $[HCO_3^-]$ was much higher than that of the $[HCO_3^-]_v$ in the SIV blood plasma (Table 4.1 and Figure 4.2B; p = 0.005), especially in the posterior intestine where the SIV blood was sampled. However, the pH (8.0 ± 0.1) and PCO_2 values (15.3 ± 7.7 mm Hg) in the posterior intestinal chyme were not significantly different from those (7.7 ± 0.1, 5.8 ± 0.4 mm Hg respectively) in the SIV blood plasma (Table 4.1 and Figures 4.2 A&C; p = 0.14 and 0.31 respectively).

4.4.3 Postprandial plasma and chyme ammonia (*in vivo* and *in situ)*

In both the *in vivo* and *in situ* series, venous (SIV and/or HPV) plasma Tamm were generally slightly higher than arterial (DA) plasma Tamm (Figures 4.3 A&B; denoted by †). Interestingly, both series showed that DA and SIV Tamm did not increase with feeding. In fact, in the *in situ* series, SIV Tamm decreased by 52 % at 48 h after feeding (Figure 4.3B), a trend that was not seen in the *in vivo* series (Figure 4.3A). Using the Henderson-Hasselbalch equation with measured Tamm and pH, we calculated PNH_3 in plasma and chyme in both series (Figure 4.4). The DA and SIV plasma PNH_3 were not significantly different from each other, with values of 30-43 μmm Hg in the *in vivo* series and 8-13 μmm Hg in the *in situ* series.

The chyme Tamm (Figures 4.4 A&B) was highest in the stomach in both the *in vivo* and the *in situ* series (2184 and 2024 μM respectively), followed by posterior intestine (1027 and 567 μM respectively), and anterior and mid intestines (495-722 and 114-160 μM respectively). Reflecting the pH gradient along the GIT (Table 4.1), however, PNH_3 was the lowest in the stomach in both series, with 0.02-3.1 μmm Hg. The intestinal chyme PNH_3 gradually increased down the tract, with posterior intestine being significantly higher (*in vivo* 262; *in situ* 371 μmm Hg) than all other measurements including plasma values in both series. The SIV plasma Tamm and PNH_3 at 48 h were 79-96 % lower than posterior chyme Tamm or PNH_3 collected immediately afterwards in both series (Figure 4.4). In contrast, HPV Tamm increased by 132 % at 24 h after feeding and remained high until 48 h (Figure 4.3B).

4.5 Discussion

4.5.1 Overview

Here, we investigated potential equilibration of the three respiratory gases, O_2, CO_2, and ammonia across the GIT epithelia in rainbow trout by monitoring arterial and venous blood status *in vivo* following feeding. Overall, feeding had no significant effect on subintestinal venous blood plasma PO_2, PCO_2, and ammonia sampled near the posterior intestine, and these were notably different from the posterior intestine chyme values measured in this study and those previously reported. Thus, our data support the overall hypotheses that there is minimal equilibration between the lumen and the blood circulation, and that blood gas levels in the venous drainage of the intestine remain largely unchanged after feeding. However, we did observe a significant increase in HPV plasma ammonia level after feeding, which agrees with our hypothesis that ammonia absorption occurs in the anterior part of the GIT.

4.5.2 Postprandial blood O_2 (*in vivo*)

The control P_aO_2 measured in this study is similar to previously reported values of fish starved for 48 h or more (Perry and Reid, 1992; Tetens and Lykkeboe, 1985). Feeding significantly increased this value within 4 h, which then gradually dropped back to the control level by 48 h (Figure 4.1A; open circles). Interestingly, the arterial blood Hb-O_2 saturation (%) was not affected by feeding (Figure 4.1B) and remained similar to previously measured values of fasted animals (Milligan and Wood, 1987) and within the typical range of rainbow trout blood (Rummer and Brauner, 2015). This suggests a ventilatory response to feeding, rather than an increase in O_2 carrying capacity or blood-O_2 affinity. This is an opposite response to that known in air-breathing terrestrial vertebrates that reduce ventilation to retain CO_2, thereby triggering a rise in P_aCO_2 following feeding so as to minimize the rise in blood pH (reviewed by Wang et al., 2001). In water-breathing fish, for which O_2 solubility in the media is much less than CO_2 solubility, it has been understood that hypoventilation would detrimentally compromise O_2 uptake at a time when metabolic demand ($\dot{M}O_2$) is elevated during digestion. Thus, hypoventilation is assumed to be an impractical response to feeding in fish, but a detailed study is lacking. To our knowledge, this is the first study to suggest a postprandial change in ventilation in fish.

Although P_aO_2 increased after feeding, SIV P_vO_2 and Hb-O_2 saturation did not change throughout digestion (Figure 4.1; closed circles). This agrees with our initial hypothesis where we expected to see no effect of low luminal PO_2 on P_vO_2. The lumen of the rainbow trout GIT remains nearly anoxic (< 1 mm Hg) even during digestion (Jung et al., 2022; Chapter 3). Concurrently, feeding induces an increase in whole-animal $\dot{M}O_2$ by ~96 % by 27 h in adult

rainbow trout (Eliason et al., 2008), which is likely accompanied by a simultaneous increase in GIT tissue $\dot{M}O_2$ (Taylor and Grosell, 2009). Although the difference between P_aO_2 and P_vO_2 was greater following feeding (63 mm Hg in control vs. 88-99 mm Hg during digestion), there was no change in SIV Hb-O_2 saturation (Figure 4.1B). In fish, however, the GIT blood flow can be controlled and quickly increased to supply metabolically active organs at the time of need (Dupont-Prinet et al., 2009; Gräns et al., 2009a; Gräns et al., 2009b; Sundh et al., 2018). In various species including rainbow trout, feeding is shown to induce redistribution of blood flow to the stomach and intestine, with elevations of 72-136 % (Axelsson and Fritsche, 1991; Axelsson et al., 1989; Axelsson et al., 2000; Eliason et al., 2008; Thorarensen and Farrell, 2006). Thus, the postprandial increase in GIT O_2 requirement could be presumably met by an increase in blood flow regardless of the luminal PO_2 status.

4.5.3 Postprandial blood and chyme pH, $[HCO_3^-]$, and PCO_2 (*in vivo*)

Under control (fasting) conditions, pH_a, $[HCO_3^-]_a$, and P_aCO_2 were similar or slightly elevated relative to previous findings (e.g. Bucking and Wood, 2008; Cooper and Wilson, 2008; Milligan and Wood, 1987; Perry and Reid, 1992; Wood and Eom, 2019). This study found a classic postprandial alkaline tide, where arterial pH and $[HCO_3^-]$ increased (Figures 4.2 A&B) presumably due to acid secretion by the stomach (reviewed by Hersey and Sachs, 1995). In both voluntarily and catheter-fed rainbow trout, plasma $[HCO_3^-]$ level increases by ~3-4 mM, causing blood pH to rise by ~0.2-0.3 units (Bucking and Wood, 2008; Bucking et al., 2009; Cooper and Wilson, 2008). In this study, we found $[HCO_3^-]$ and pH values peaked at 24 h after feeding with elevations of 5.6 mM and 0.4 units, respectively (Figures 4.2 A&B). The delayed alkaline tide observed in this study (24 h *vs* 3-12 h; e.g. Bucking et al., 2009; Bucking and Wood, 2008;

Cooper and Wilson, 2008) could be due to the relatively small ration (reviewed by Wood 2019) introduced *via* the feeding tube (Cooper and Wilson, 2008) or delayed digestion due to stress from the surgery (Eliason et al., 2008). Moreover, the lower acclimation temperature used here (9 ˚C) can slow down digestion (Jobling, 1981; McCue, 2006) relative to the temperatures used in studies mentioned above (10-15.5 ˚C). Nonetheless, the increase in pH_a and $[HCO_3^-]_a$ were indicative of animals undergoing digestion.

We found no change in P_aCO_2 following feeding (Figure 4.2C), similar to the observations of Bucking and Wood (2008) in voluntarily fed rainbow trout. Our finding and other recent studies suggest fish have a compensatory mechanism for dealing with alkaline tide that is different from the hypoventilatory CO_2 retention strategy of air-breathing terrestrial vertebrates (e.g. Andrade et al., 2004; Busk et al., 2000; Higgins, 1914; Wang et al., 2001). Nonetheless, fish are able to minimize blood pH disturbance relative to the postprandial metabolic base load (Bucking and Wood, 2008; Bucking et al., 2010; Wood et al., 2007) by excreting HCO_3^- *via* branchial Cl^-/HCO_3^- exchange mechanisms (Bucking and Wood, 2008; Tresguerres et al., 2007; Wood et al., 2005; Wood et al., 2007), as well as *via* the urine (Bucking et al., 2010). However, it is interesting that the increase in $[HCO_3^-]$ seen in DA plasma was not observed in SIV plasma (Figure 4.2B). Some of the base load from the stomach is likely excreted on the first pass through the gills, and the remaining fraction is what was seen in our DA samples. This base load was not detected in the SIV sampling site, downstream of the gills and DA sampling site. In seawater fish, the intestine has the capacity to compensate the plasma base load by HCO_3^- secretion into the lumen where it is used for osmoregulation (Grosell and Genz, 2006; Grosell et al., 2007; Taylor et al., 2010; Wilson and Grosell, 2003; Wilson et al., 2002) and possibly even for postprandial HCO_3^- excretion in rectal fluid and feces (Bucking et al., 2009;

Taylor and Grosell, 2006; Wilson et al., 1996). Presumably, the intestine in freshwater fish may also be a potential site for postprandial base excretion to alleviate the alkaline tide in addition to export by the gills and kidney. However, an *in vitro* study found that freshwater rainbow trout intestine tissue had minimal involvement in removing a metabolic base load (Bucking et al., 2009). Additional studies are required to evaluate this possibility further.

Here, we have recorded the first *in vivo* measurements of PCO_2 in the SIV blood during digestion (Figure 4.2C; closed circles). During the period of active digestion, luminal PCO_2 is found to be very high (calculated value of 25-111 mm Hg and direct measurement of 20-40 mm Hg; Wood and Eom, 2019; Jung et al., 2022; Chapter 3). In mammals, microbial metabolic production, reaction of gastric HCl with food carbonates, and endogenous HCO_3^- secretion contribute to high luminal PCO_2 (Altman, 1986; Kurbel et al., 2006; Steggerda, 1968; Suarez et al., 1997; Tomlin et al., 1991). In fish, endogenous HCO_3^- secretion by the intestinal epithelium for neutralizing chyme (Bucking and Wood, 2009; Goodrich et al., 2020; Wood and Eom, 2019) and for osmoregulatory purpose, particularly in seawater fish, can contribute to the high luminal PCO_2. We found that luminal PCO_2 remained elevated even at 48 h after feeding, and at particularly high levels in the stomach in parallel to its low pH (Table 4.1).

Until now, it has been difficult to conclude whether such high luminal PCO_2 will equilibrate with the venous bloodstream draining the GIT. In seawater-acclimated rainbow trout (presumably) fasted for 72 h, calculated SIV PCO_2 was low at 4.7 mm Hg (Cooper et al., 2014). Moreover, in Atlantic salmon fed 24-48 h prior to measurement, calculated HPV PCO_2 was low at 4.8 mm Hg and remained low at 2.9-3.6 mm Hg for 7 days (Eliason et al., 2007), implying that PCO_2 may not be equilibrating into the blood draining the stomach as well. Both Jung et al. (2022; Chapter 3) and Wood and Eom (2019) found highly variable measured SIV PCO_2 levels

(11-27 mm Hg, 2-34 mm Hg respectively) using anaesthetized fed fish sampled *in situ*, even with direct insertion of the PCO_2 micro-optode into the SIV. The present study was able to measure SIV PCO_2 in non-anaesthetized fish and found low and constant levels during digestion, similar to the control fasting values. There was a slight elevation at 12 h, but in general, all measurements were below 8 mm Hg, much lower than previously reported levels measured in the lumen. The calculated PCO_2 of chyme collected at 48 h following feeding was not significantly different from measured SIV plasma PCO_2, but we suspect the animals to be near completion of digestion at the time of sampling. In fact, our calculated intestinal chyme PCO_2 levels (12-15.5 mm Hg; Table 4.1) are similar to those directly measured in fasted rainbow trout (7-13 mm Hg; Wood and Eom 2019). Thus, despite the high luminal PCO_2 found during active digestion, this study and previous reported values support that minimal equilibration of PCO_2 is occurring across the GIT epithelium.

4.5.4 Postprandial plasma ammonia (*in vivo* and *in situ*)

In both the *in vivo* and the *in situ* series, control fish had DA plasma Tamm concentrations typical of those measured in other studies (Figures 4.3 A&B; Bucking et al., 2009; Karlsson et al., 2006; Knoph and MåsØval, 1996). The Tamm levels in DA plasma sampled from fish *in situ* was higher than *in vivo*, which could be due to anaesthetic in the water reducing the ammonia excretion rate (Guo et al., 1995). More significantly, SIV Tamm did not increase after feeding in both series, supporting our initial hypothesis. Our chyme measurements are in agreement with earlier studies (Bucking and Wood, 2012; Rubino et al., 2014; Jung et al., 2022; Chapter 3) showing that chyme Tamm throughout the intestine is typically very high (Figure 4.4 A&B; 495-1027 μM *in vivo*; 114-566 μM *in situ*) following feeding in rainbow trout.

This likely reflects the catabolism of amino acids within the GIT lumen after ingestion of protein. Importantly, these data also confirm our recent finding (Jung et al., 2022; Chapter 3) that chyme Tamm levels are even higher in the stomach (2024-2181 μM) than in the more posterior sections of the GIT (Figure 4.4 A&B). This suggests considerable absorption of ammonia in the anterior tract, perhaps in the stomach and/or anterior intestine. And many studies have shown that plasma ammonia level increases up to 3-fold after feeding (Bucking and Wood, 2008; Bucking and Wood, 2012; Kaushik and de Oliva Teles, 1985; Wicks and Randall, 2002b).

Previous studies found that feeding stimulates the endogenous ammonia production rate of the intestinal epithelia and increases the efflux rate to the serosal solution *in vitro* (Rubino et al., 2014; Jung et al., 2021; Chapter 5). Whole-body ammonia excretion rate increases after feeding (Alsop and Wood, 1997; Bucking et al., 2010; Taylor et al., 2007), of which up to 47 % can originate from the GIT, mainly by endogenous production (Rubino et al., 2014). However, we measured 5-7 fold lower Tamm in venous drainage relative to the posterior intestine chyme (Figure 4.4 A&B). With measured Tamm and pH, we calculated PNH_3 of both plasma and chyme (Figure 4.4 C&D). Although our chyme PNH_3 values were lower than reported values at earlier stage of the digestion (24 h after feeding; Rubino et al., 2014; Jung et al., 2022; Chapter 3), they were still significantly higher than SIV PNH_3 in both series. Thus, like PCO_2 (Section 4.2), there was minimal equilibration of PNH_3 between the lumen and SIV.

In contrast, there was a clear increase in HPV Tamm sampled *in situ* (Figure 4.3B), similar to findings by Karlsson et al. (2006). The HPV differs from the SIV by additionally collecting venous drainage from the stomach and anterior intestine, suggesting that the anterior part of the GIT could be a greater site of ammonia absorption. In fact, an ammonia transporter NKCC is more highly expressed in the anterior intestine than in the mid and posterior intestine of

fed rainbow trout (Rubino et al., 2019). Another possible ammonia NH_3 transporter – rhesus glycoprotein (Rh protein) – is expressed along the mice GIT including the stomach; both apical (Rhcg) and basolateral (Rhbg) isoforms are present throughout the tract (Handlogten et al., 2005). In rainbow trout, the Rhbg is expressed along the whole GIT including the stomach, with feeding elevating the relative expression in both the anterior and posterior intestines (Bucking and Wood, 2012). The Rhcg seems to be lacking in the intestine of rainbow trout (Nawata et al., 2007) and the situation is currently unknown in the stomach. However, two Rhcg isoforms, in addition to Rhbg, were expressed throughout the intestine in two marine Batrachoidid teleosts (Bucking et al., 2013b). Nonetheless, our data suggest that the posterior intestine is not the major source of postprandial ammonia absorption, and that ammonia may be transported in the anterior intestine and/or even the stomach. The NH_3 absorption across the stomach epithelia would be of particular interest, as it would mean moving against a large PNH_3 gradient (Figure 4.4 C&D; 0.02-3.1 μmm Hg in stomach *vs* 13-30 μmm Hg in SIV).

4.5.5 Conclusion

In summary, it is now clear that feeding and digestive processes establish a harsh environment in the GIT lumen of the rainbow trout: high PCO_2 (Wood and Eom, 2019; Jung et al., 2020; Jung et al., 2022; Chapters 2 and 3), high ammonia (Jung et al., 2022; Chapter 3), and virtual anoxia (Jung et al., 2020; Jung et al., 2022; Chapters 2 and 3). This study found that despite such conditions and increased blood flow to the system after feeding (Eliason et al., 2008), the composition of the venous blood draining the posterior intestine remains relatively unchanged, indicating minimal equilibration of the three respiratory gases.

Table 4.1 Measured pH, $[HCO_3^-]$, and calculated PCO_2 of chyme collected in different GIT sections 48 h post feeding of the rainbow trout in the *in vivo* series. Letters indicate significant difference between different sections for that particular variable. Values are means ± SEM (N = 7-9 for pH; N = 4-8 for $[HCO_3^-]$ and PCO_2).

	Stomach	Anterior intestine	Mid intestine	Posterior intestine
pH	5.3 ± 0.3^{x}	7.6 ± 0.1^{y}	7.7 ± 0.1^{y}	8.0 ± 0.1^{y}
$[HCO_3^-]$ (mM)	1.9 ± 0.9^{x}	19.4 ± 4.9^{y}	21.0 ± 5.1^{y}	40.1 ± 5.8^{z}
PCO_2 (mm Hg)	125.5 ± 15.8^{x}	12.0 ± 2.5^{y}	15.5 ± 7.0^{y}	15.3 ± 7.7^{y}

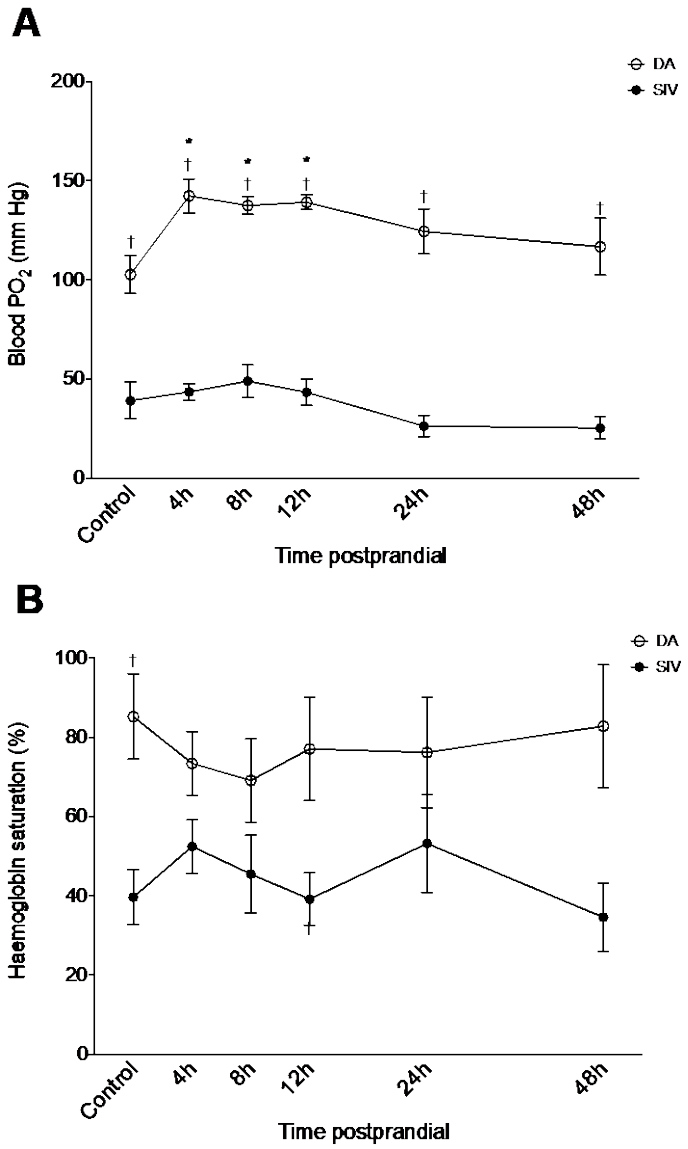

Figure 4.1 Postprandial dorsal aorta (DA; unfilled circles) and subintestinal vein (SIV; filled circles) blood (A) PO_2 (DA parameters indicated with subscript "a" and SIV with subscript "v"; P_aO_2 and P_vO_2 respectively; mm Hg; N = 5-9) and (B) hemoglobin saturation (%), measured from rainbow trout *in vivo*. Control represents fasting state prior to feeding which occurred immediately thereafter. Values are means ± SEM (N = 4-6). Dagger (†) indicates significant difference between DA and SIV values. All SIV PO_2 were significantly lower than DA PO_2. Asterisk (*) indicates a significant difference from control values for either DA or SIV.

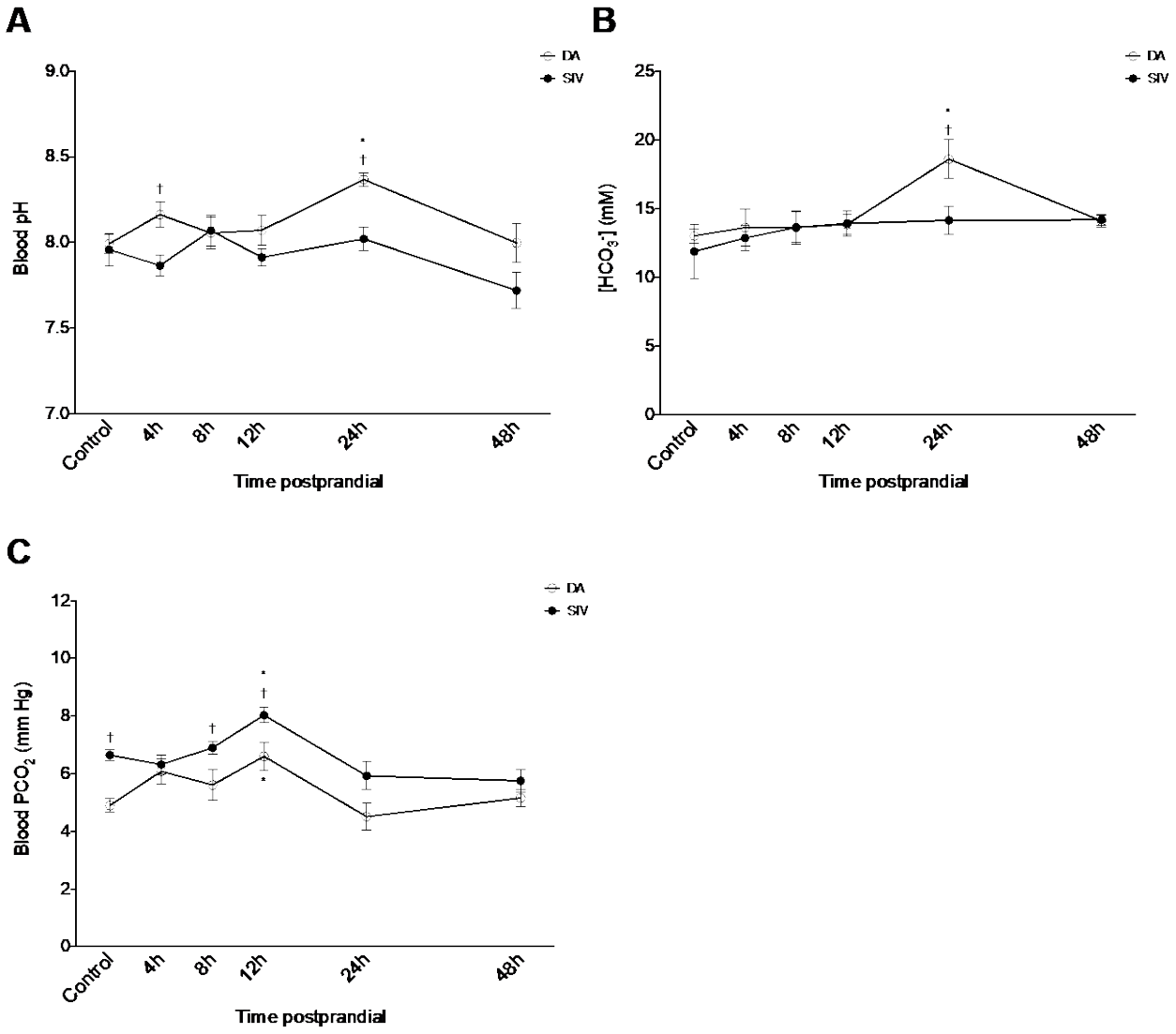

Figure 4.2 Postprandial DA (unfilled circles) and SIV (filled circles) blood (A) pH (pH_a and pH_v respectively; N = 5-9), (B) $[HCO_3^-]$ ($[HCO_3^-]_a$ and $[HCO_3^-]_v$ respectively; mM; N = 4-9), and (C) PCO_2 (P_aCO_2 and P_vCO_2 respectively; mm Hg; N = 4-9), measured from rainbow trout *in vivo*. See Figure 4.1 legend for further details.

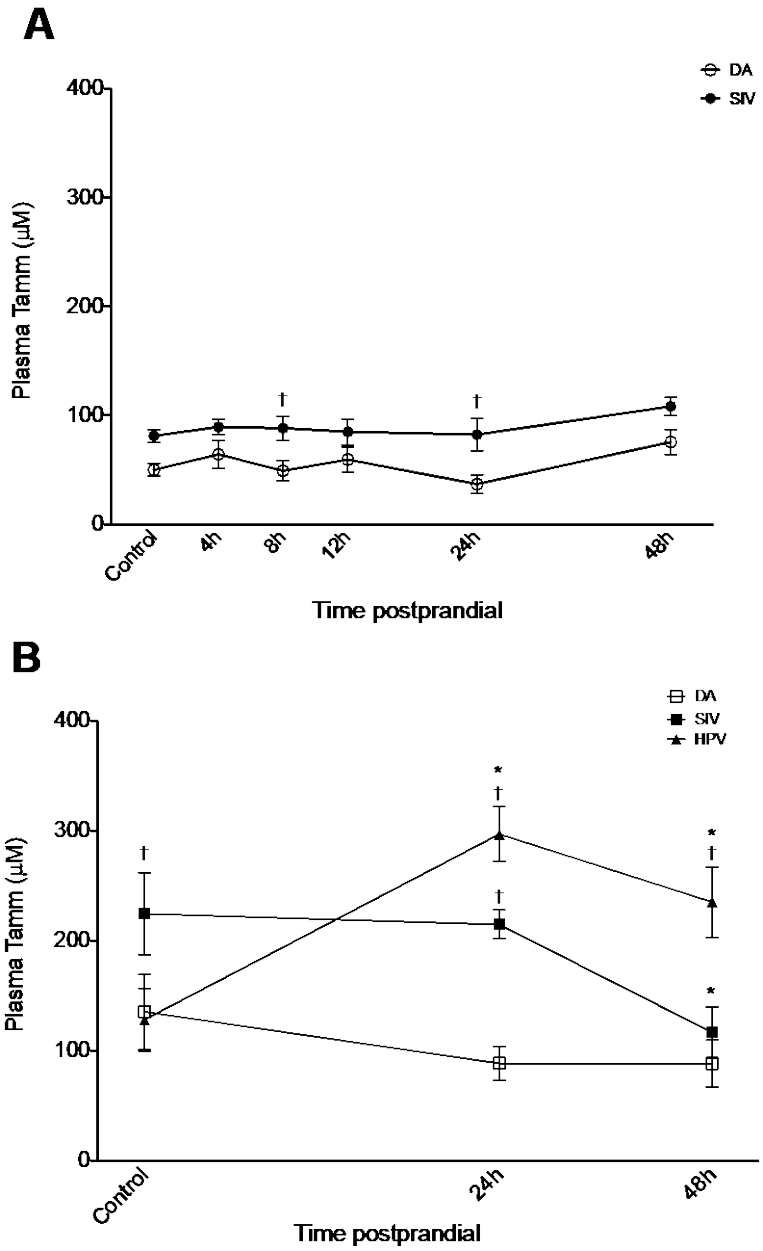

Figure 4.3 Comparison of postprandial plasma Tamm (μM) from DA (unfilled circle or square), SIV (filled circle or square), and HPV (filled triangle) blood sampled from rainbow trout (A) *in vivo* (N = 4-6) and (B) *in situ* (N = 5-7). Control represents fasting state, feeding occurred immediately after control sample was taken in (A). See Figure 4.1 legend for further details.

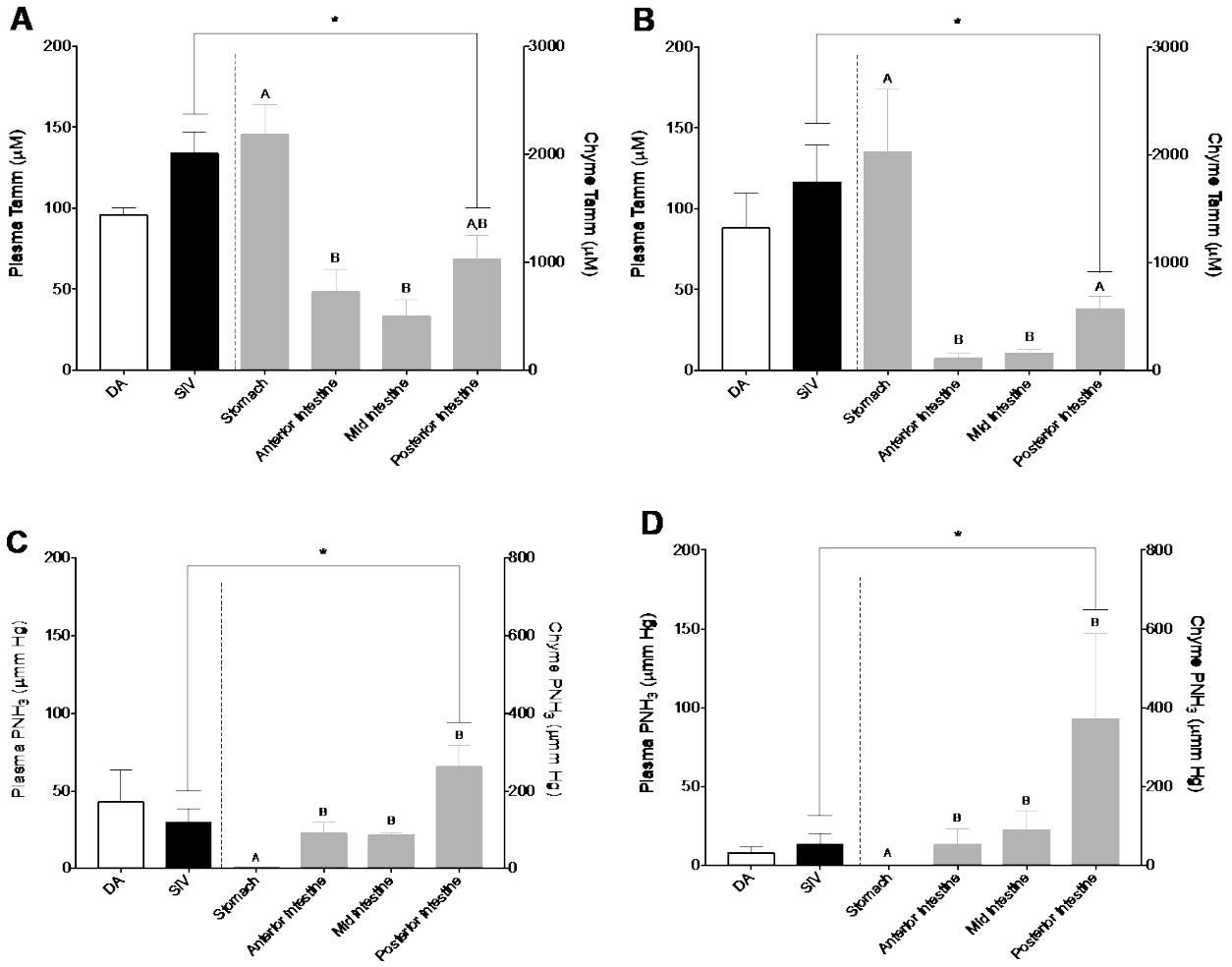

Figure 4.4 Comparison of measured plasma and chyme (A&B) Tamm (µM) and calculated (C&D) PNH_3 (µmm Hg) sampled 48 h post feeding in rainbow trout in (A&C) the *in vivo* series (N = 4-7) and in (B&D) the *in situ* series (N = 5-7). Plasma Tamm values are reproduced from Figure 4.3. In all graphs, left y-axis represents plasma values and right y-axis represents chyme values. Note different scales between left and right y-axes. Values are means ± SEM. DA and SIV plasma values were not significantly different from each other in all panels. Upper case letters indicate significant difference between chyme from different GIT compartments. Asterisk indicates a significant difference between SIV plasma and posterior intestine chyme values.

Chapter 5: Intestinal zonation in nitrogenous product handling and transport

5.1 Summary

Digestion of dietary protein in teleosts results in high ammonia levels within the intestinal chyme that may reach concentrations that are many-fold greater than blood plasma levels. We used *in vitro* gut sac preparations of the ammoniotelic rainbow trout (*Oncorhynchus mykiss*) to investigate the role of the intestine in producing and transporting ammonia and urea, with specific focus on feeding versus fasting, and on responses to loading of the lumen with 2 mM glutamine or 2 mM ammonia. Feeding increased not only ammonia production and both mucosal and serosal fluxes, but also increased urea production and serosal fluxes. Elevated urea production was accompanied by an increase in arginase activity but minimal CPS III activity, suggesting that urea may be produced by direct arginolysis. The ammonia production and serosal fluxes increased in fasted preparations with glutamine loading, indicating an ability of the intestinal tissue to deaminate glutamine and perhaps use it as an energy source. However, there was little evidence of urea production or transport resulting from the presence of glutamine. Furthermore, the intestinal tissues did not appear to convert surplus ammonia to urea as a detoxification mechanism, as urea production and serosal flux rates decreased in fed preparations, with minimal changes in fasted preparations. Nevertheless, there was indirect evidence of detoxification by another pathway, as ammonia production rate decreased with ammonia loading in fed preparations. Overall, our study suggests that intestinal tissues of rainbow trout have the ability to produce urea and detoxify ammonia, likely *via* arginolysis.

5.2 Introduction

In teleost fish, protein degradation during digestion produces amino acids (Cowey and Sargent, 1972), which are mainly absorbed into the blood and transported to the liver to be catabolized (Bakke-McKellep et al., 2000; Collie and Ferraris, 1995). Some deamination occurs within the intestinal lumen, such that ammonia levels in the chyme of teleosts may reach 1 mM or higher, concentrations that are many-fold greater than blood plasma levels (Bucking and Wood, 2012; Bucking et al., 2013a; Pelster et al., 2015; Rubino et al., 2014; Wood et al., 2019). The intestine itself also catabolizes some of the absorbed amino acids from ingested food as endogenous energy sources, producing additional ammonia (Ballantyne, 2001; Bucking and Wood, 2012; Bucking et al., 2013a). Most teleosts, such as rainbow trout, are ammoniotelic, excreting ammonia as the primary nitrogenous waste (Anderson, 2001; Randall and Wright, 1987; Wright and Wood, 2009). Following a meal, the intestine both absorbs ammonia from the chyme and produces ammonia by its catabolism of amino acids (Rubino et al., 2014), increasing systemic plasma ammonia concentration by up to 2- to 3-fold (Bucking and Wood, 2008, 2012; Karlsson et al., 2006). The plasma ammonia level after feeding is particularly high in the hepatic portal vein (HPV) draining from the gastrointestinal tract (GIT) (Karlsson et al., 2006). The ammonia originating from the intestine is first passed by the HPV to the liver where it may be used for amino acid synthesis, or else it escapes to the ventral aortic blood perfusing the gills, where much of it is excreted out to the water (e.g. Brett and Zala, 1975; Bucking et al., 2010; Bucking and Wood, 2008; Zimmer et al., 2010), leaving lower, but still elevated, plasma ammonia level in the dorsal aorta (Karlsson et al., 2006). In the rainbow trout, Rubino et al. (2014) estimated that approximately 47 % of post-prandial ammonia excretion was produced in the intestine.

In contrast, most terrestrial species are ureotelic, producing nitrogenous waste in a less toxic form, urea. Typically in mammals, the amino groups released when amino acids are oxidized feeds into the ornithine-urea cycle (OUC) in the liver and the resulting urea is excreted by the kidney as a component of urine (Schmidt-Nielsen, 1958). Although urea production is more energetically costly, a few species of teleosts are ureotelic (e.g. Magadi tilapia and gulf toadfish) and/or may synthesize urea to detoxify ammonia depending on the environment, life stage, or physiological condition (Felskie et al., 1998; Julsrud et al., 1998; Kong et al., 1998; Randall et al., 1989; Wood et al., 1995). Indeed, many species in their early life stages express OUC enzymes, producing urea and minimizing ammonia accumulation within the embryo, but lose this ureagenic pathway as development proceeds (Braun et al., 2009; Chadwick and Wright, 1999; Dépêche et al., 1979; Terjesen et al., 2002; Zimmer et al., 2017). Moreover, in the marine plainfin midshipman (*Porichthys notatus*, an ammoniotelic relative of the ureotelic gulf toadfish), Bucking et al. (2013b) presented evidence for a model in which ammonia is transported from the intestinal lumen into the enterocytes, where it is detoxified by conversion to urea *via* the OUC, and then transported back into the lumen for use by ureolytic bacteria or later excretion *via* the anus. However, in typical adult ammoniotelic teleosts such as freshwater rainbow trout, little is known about the capacity of the intestinal cells to produce and/or transport urea. Interestingly, Karlsson et al. (2006) showed a significant increase in urea concentration in the HPV and dorsal aorta (DA) after feeding, implying a possible production and/or transport of urea by the intestinal cells. Additionally, Kajimura et al. (2004) provided indirect evidence for urea production by the intestine and excretion by the anus in trout. Thus, in this study, we used a similar *in vitro* gut sac approach to that employed by Bucking et al. (2013b) and Rubino et al.,

(2014) to test whether the intestinal cells of rainbow trout are able to synthesize and transport urea.

With the gut sac preparation, we can test the production and direction of transport (to lumen or blood side) of the nitrogenous wastes in response to experimental treatments. If the intestinal cells have the ability to produce urea, we hypothesized that feeding would not only increase ammonia, but also urea production and flux rates. We also tested for two key enzymes involved in urea production (Anderson et al., 2002; Bucking et al., 2013a; Julsrud et al., 1998; Kajimura et al., 2006; Lindley et al., 1999). In the OUC of mammals and amphibians, carbamoyl phosphate synthetase (CPS) I catalyzes the ATP-dependent synthesis of carbamoyl phosphate from ammonia substrate. However, in most teleosts, CPS III prefers glutamine as the nitrogen-donating substrate (reviewed by Anderson, 1995). Arginase is also involved in the OUC, converting L-arginine to L-ornithine, producing urea directly in the process. If the intestinal cells have the ability to produce urea *via* the OUC, we hypothesized that there would be an increase in CPS III and arginase activities after feeding. Furthermore, the gut sac preparation allows us to examine the *in vitro* response of loading the lumen with potential substrates for urea production such as glutamine and ammonia. As glutamine is thought to be the immediate nitrogen-donating substrate for the OUC in fish (Anderson, 1995), we hypothesized that a luminal glutamine supply would increase both ammonia and urea production and flux rates as the intestinal cells break down the amino acid and/or feed it into the OUC. In addition, if the intestinal cells have the ability to detoxify high luminal ammonia, we hypothesized that they would convert the surplus ammonia to urea and thus increase urea production and flux rates.

5.3 Material and methods

5.3.1 Experimental animals

Freshwater rainbow trout (150-250 g) were obtained from Humber Springs Trout Hatchery, Ontario, Canada. Upon arrival, the trout were acclimated for 1-2 months to laboratory conditions in running, dechlorinated Hamilton tap-water with constant aeration (moderately hard water from Lake Ontario: $[Na^+]$ = 0.6 mequiv L^{-1}, $[Cl^-]$ = 1.8 mequiv L^{-1}, $[Ca^{2+}]$ = 0.8 mequiv L^{-1}, $[Mg^{2+}]$ = 0.3 mequiv L^{-1}, $[K^+]$ = 0.05 mequiv L^{-1}; titration alkalinity 2.1 mequiv L^{-1}, pH ~8.0; hardness ~140 mg L^{-1} as $CaCO_3$ equivalents; temperature 12.5–15 ˚C, water flow rate = 30 mL s^{-1}, background ammonia concentration ≤ 10 μmol L^{-1}). The trout were kept in aerated 500-liter tanks with approximately 30 fish per tank. Scheduled feedings occurred three times per week (Martin Profishent Aquaculture Nutrition, Tavistock, ON, Canada; crude protein 45 %, crude fat 9 %, crude fiber 3.5 %). Ration size was 3 % of body mass, which provided satiation. Experiments on fed fish occurred exactly 24 hours following a meal and fasted experiments occurred 7 days following the last meal. Animal handling was in compliance with an approved McMaster Animal Care Committee Animal Utilization Protocol 12-12-45.

5.3.2 *In vitro* gut sac experiments and calculations

Gut sac experiments were performed to quantify the changes in urea-N and ammonia fluxes (Js and Jm), as well as tissue ammonia and urea-N loads, based on the influence of the feeding state and varying composition of mucosal solutions used. Trout were euthanized using 0.07 g L^{-1} MS-222 (Syndel Laboratories, Parksville, British Columbia, Canada), neutralized with NaOH. The intestine was removed, thoroughly rinsed with Cortland's saline (in mM: NaCl 124, KCl 5.1, $CaCl_2$ 1.6, $MgSO_4$ 0.9, $NaHCO_3$ 11.9, NaH_2PO_4 3, glucose 5.5, pH = 7.4), then

sectioned into the anterior, mid, and posterior regions. Each of these sections was tied off at one end with a 2-0 silk thread while the other end had a flared polyethylene tube (Intramedic Clay-Adams PE 60; Becton-Dickinson and Company, Sparks, MD, USA) inserted and held securely with another silk thread. Saline, which had been pre-equilibrated with a 99.7 % O_2: 0.3 % CO_2 gas mix, was then injected into the gut sac through the open polyethylene tube using a syringe (termed mucosal saline hereafter). In the control group, the gut sacs were loaded with regular Cortland's saline. In the high luminal glutamine treatment, the sacs were loaded with Cortland's saline containing 2 mM of L-glutamine (Sigma-Aldrich, St. Louis, MO, USA) and in the high luminal ammonia group with Cortland's saline containing 2 mM of NH_4Cl (Fisher Scientific, Toronto, ON, Canada). The saline was infused and then withdrawn multiple times for thorough mixing. On the final filling, the saline was injected until the intestinal section became taut, and the remainder of the saline was collected as the initial mucosal sample. The PE tube was then sealed, and the sac was thoroughly blotted dried, then weighed to 0.0001 g accuracy for initial weight (W_i). It was then inserted into a centrifuge tube that contained regular Cortland's saline (termed serosal saline hereafter). Anterior intestine preparations were placed in a 50-mL centrifuge tubes while both mid and posterior intestine sacs were placed in 15-mL centrifuge tubes. The amount of serosal saline needed to fully immerse the preparations varied, and was exactly recorded, and an initial serosal sample was taken.

During a 2-hour flux period, the saline was bubbled with 99.7 % O_2: 0.3 % CO_2 gas mix to mimic physiological PCO_2 and to maximize O_2 supply in the preparation. Then, the gut sacs were removed, thoroughly blotted dry, and weighed again (W_f). Their internal contents were collected as the final mucosal sample. Finally, the drained gut sac was thoroughly blotted again and weighed to yield the empty weight (W_e) of the preparation. In the equations below, the final

mucosal volume (Vm_f) was calculated as $W_f - W_e$, and the initial mucosal volume (Vm_i) as $W_i - W_e$. The saline left in the centrifuge tubes was collected as the final serosal sample. The intestinal sections were traced onto 0.5-mm graph paper, which allowed each of their surface areas to be determined; a technique first outlined by Grosell and Jensen (1999). All samples, including the initial ones and the gut sac tissue itself, were frozen in liquid N_2, then stored at -80 ºC for later analysis of ammonia and urea-N concentrations. The following parameters were calculated.

Serosal urea ($Js_{urea\text{-}N}$) flux rate

$$Js_{urea-N} = \frac{[(Ts_{urea}f - Ts_{urea}i) \times Vs]}{SA \times t} \times 2 \qquad \text{Equation 1}$$

where $Js_{urea\text{-}N}$ is in µmol-N cm^{-2} h^{-1}, $Ts_{urea}f$ and $Ts_{urea}i$ are the final and initial urea concentrations (µmol L^{-1}) in the serosal saline, Vs is the volume of serosal solution (L), SA is intestinal surface area (cm^2), and t is time (h). Note that Equations 1 and 2 are multiplied by 2 due to the presence of two nitrogen in urea. All $Js_{urea\text{-}N}$ fluxes were positive, into the serosal saline.

Mucosal urea ($Jm_{urea\text{-}N}$) flux rate

$$Jm_{urea-N} = \frac{[(Tm_{urea}i \times Vmi) - (Tm_{urea}f \times Vmf)]}{SA \times t} \times 2 \qquad \text{Equation 2}$$

where $Jm_{urea\text{-}N}$ is in µmol-N cm^{-2} h^{-1}, $Tm_{urea}f$ and $Tm_{urea}i$ are final and initial urea concentrations (µmol L^{-1}) in the mucosal saline, Vmi and Vmf are initial and final volumes of mucosal saline (L). Positive $Jm_{urea\text{-}N}$ fluxes were out of the mucosal saline; negative $Jm_{urea\text{-}N}$ fluxes were into the mucosal saline.

Serosal ammonia (Js_{amm}) flux rate

$$Js_{amm} = \frac{[(Ts_{amm}f - Ts_{amm}i) \times Vs]}{SA \times t} \quad \text{Equation 3}$$

where Js_{amm} is in μmol cm^{-2} h^{-1}, $Ts_{amm}f$ and $Ts_{amm}i$ are the final and initial ammonia concentrations (μmol L^{-1}) in the serosal saline, Vs is the volume of serosal solution (L), SA is intestinal surface area (cm^2), and t is time (h). All Js_{amm} fluxes were positive, into the serosal saline.

Mucosal ammonia (Jm_{amm}) flux rate

$$Jm_{amm} = \frac{[(Tm_{amm}i \times Vmi) - (Tm_{amm}f \times Vmf)]}{SA \times t} \quad \text{Equation 4}$$

where Jm_{amm} is in μmol cm^{-2} h^{-1}, where $Tm_{amm}f$ and $Tm_{amm}i$ are final and initial ammonia concentrations (μmol L^{-1}) in the mucosal saline, Vmi and Vmf are initial and final volumes of mucosal saline (L). Positive Jm_{amm} fluxes were out of the mucosal saline; negative Jm_{amm} fluxes were into the mucosal saline.

Total tissue urea & ammonia production rates (Jt_{urea} & Jt_{amm})

$$Jt = Js - Jm \quad \text{Equation 5}$$

Jt (μmol cm^{-2} h^{-1}) represents the net rate of endogenous production of ammonia or urea-N by the intestinal tissue itself.

Total tissue urea & ammonia (T_{urea} & T_{amm})

$$T = \frac{[\text{urea-N or ammonia in tissue}]}{\text{weight of tissue}} \quad \text{Equation 6}$$

T (μmol g^{-1}) represents the concentration of urea-N or ammonia found in the tissue itself.

5.3.3 Analytical methods

Mucosal samples were deproteinized using ice-cold 20 % perchloric acid (PCA) before the ammonia assay was run to prevent potential protein interference with the assay, then spun at 13,000 rpm for 1 minute. After the supernatant was collected, samples were pH-neutralized using 1 mM KOH. Flash-frozen intestinal tissues were ground into fine powder using a liquid N_2-cooled mortar and pestle, then deproteinized using a solution of 8 % PCA and 1 mM ethylenediaminetetraacetic acid (EDTA), followed by pH neutralization using 1 mM KOH. Serosal samples showed no protein interference with the ammonia assay, thus were not deproteinized. The ammonia assay was performed *via* a commercial kit (Raichem Cliniqa™; glutamate dehydrogenase method) and read at 340 nm. The urea assay employed the colorimetric method of Rahmatullah and Boyde (1980) and was read at 525 nm.

5.3.4 Enzymatic analysis

Intestine tissue was taken from randomly selected trout that had been subjected to either fasted or fed pre-treatment, prior to euthanization as described above. The intestine was sectioned, cleaned and immediately flash frozen in liquid N_2. In some intestinal sections, the muscle layer was separated from the epithelial layer using a glass slide. This was done to further analyze enzymatic activity within these different constituents.

OUC enzyme CPS III activity was measured using a CPS assay similar to that employed by Bucking et al. (2013b) at 412 nm. The reaction involved in this assay proceeds in the forward direction. The reaction mixture contained 20 mM ATP, 25 mM $MgCl_2$, 25 mM N-acetyl glutamate (AGA), 2 mM dithiothreitol, 5 mM ornithine, 20 mM glutamine, 25 mM

phospho(enol)pyruvate, and 50 mM Hepes, pH 8.0. 20 mM glutamine was used to determine the activity of CPS III or CPS II while 1.7 mM UTP was used to inhibit CPS II. Arginase enzyme activity was analyzed using an arginase assay similar to that employed by Felskie et al. (1998). This reaction also proceeds in the forward direction. The reaction mixture contained 250 mM arginine, 1 mM $MnCl_2$, and 50 mM Hepes, pH 8.0. The enzyme was activated with mixture that contained 5 mM $MnCl_2$ in 50 mM Hepes. Activity units of all enzymes were quantified as the micromolar appearance of reaction product in the measured solution per minute (U g^{-1} tissue).

5.3.5 Statistical analysis

All graphs were made and statistical analyses were performed using Graphpad Prism software (version 7.0a). Data have been expressed as means ± SEM (N = number of fish). Two-way ANOVA and *post hoc* Tukey's multiple comparison tests were performed on the control group to look at the effect of feeding and the intestinal sections on flux rates, tissue urea or ammonia concentrations, and total tissue urea or ammonia levels, as well as on the CPS III and arginase activities. Comparisons between controls and either glutamine or ammonia treatment on all other flux rates, $Jt_{urea/amm}$ or $T_{urea/amm}$ were conducted using two-way ANOVA with intestinal section as the other factor, and *post hoc* Dunnett's multiple comparison tests. A significance level of $p < 0.05$ were used in all tests.

5.4 Results

5.4.1 Effects of feeding on urea and ammonia handling

In general, for both urea-N and ammonia, serosal flux rates (positive = appearance in the serosal fluid) were many fold higher on an absolute basis than mucosal flux rates (negative =

appearance in the mucosal fluid) (Table 5.1). There were significant overall effects of feeding on $J_{s\text{urea-N}}$ ($p < 0.0001$), $J_{t\text{urea-N}}$ ($p = 0.0015$), $J_{s\text{amm}}$ ($p < 0.0001$), $J_{m\text{amm}}$ ($p = 0.0034$), $J_{t\text{amm}}$ ($p < 0.0001$), and T_{amm} ($p = 0.0063$; Table 5.1). In all cases these effects were stimulatory, resulting in more positive serosal and total fluxes, more negative mucosal fluxes, and greater tissue contents. Feeding did not have a significant overall effect on $J_{m\text{urea-N}}$ ($p = 0.79$) and $T_{\text{urea-N}}$ ($p = 0.17$) (Table 5.1). Specifically, feeding significantly increased $J_{s\text{urea-N}}$ only in the anterior intestine ($p = 0.0055$), but there were no differences of $J_{t\text{urea-N}}$ between groups in each individual section, despite the significant overall difference. However, fed fish had more positive $J_{s\text{amm}}$ in all intestinal sections ($p < 0.05$), and more negative $J_{m\text{amm}}$ ($p = 0.0065$) and greater T_{amm} ($p = 0.0210$) in the posterior intestine than fasted fish. There were also significant effects of intestinal sections on $J_{s\text{urea-N}}$ ($p < 0.0001$), $J_{s\text{amm}}$ ($p < 0.0001$), both of which tended to be greater in the anterior section, and on $J_{m\text{amm}}$ ($p = 0.0008$), and T_{amm} ($p = 0.0460$), both of which tended to be greater in the more posterior sections. There was no significant interaction between feeding and intestinal sections for any of the measurements ($p > 0.05$).

5.4.2 CPS III and arginase enzyme activity levels after feeding

Feeding had a significant overall effect on the muscle CPS III activity, but not the epithelial scraping CPS III activity (Table 5.2; $p = 0.031$ and 0.20 respectively). The anterior intestine, specifically, had a significant decrease in CPS III activity in the muscle ($p = 0.0251$) and epithelial scraping ($p = 0.0209$) after feeding. There was no significant overall effect of intestinal section on either the muscle or epithelial scraping CPS III activity ($p = 0.23$ and 0.15 respectively). In contrast, feeding had a significant overall effect on arginase activity in the epithelial scrapings, but not in the muscle (Table 5.3; $p = 0.005$ and 0.74 respectively). In fed

fish, the arginase activity was significantly lower in the muscle of posterior intestine (p = 0.0105), but higher in the epithelial scraping of mid intestine ($p < 0.0001$). There was also a significant overall effect of intestinal section on the arginase activity in both muscle and epithelial scrapings (p = 0.0002 and 0.0013 respectively). There were significant interactions between feeding and intestinal sections in both muscle and epithelial scraping on CPS III activity (Table 5.2; p = 0.0016 and 0.0105 respectively) and arginase activity (Table 5.3; p = 0.0007 and 0.0003 respectively).

5.4.3 High luminal glutamine treatment

In general, there were minimal effects of high luminal glutamine on intestinal urea-N handling. There was no significant overall effect of high luminal glutamine on either serosal or mucosal urea-N flux rates in either fasted or fed fish (Figure 5.1; all p = 0.32-0.66). In both fasted and fed fish, there were also no overall effects of treatment on $Jt_{urea\text{-}N}$ (Figure 5.2; p = 0.31 and 0.62 respectively) and $T_{urea\text{-}N}$ (Figure 5.3; p = 0.66 and 0.06 respectively). When compared between treatment and control groups within intestinal sections, the glutamine treatment significantly increased $Js_{urea\text{-}N}$ in the anterior intestine of fed fish only (Figure 5.1B; p = 0.0105), which translated to higher $Jt_{urea\text{-}N}$ in the same anterior intestine (Figure 5.2B; p = 0.0275).

However, in contrast to urea-N handling, ammonia handling was substantially altered by high glutamine in both fasted and fed fish. High glutamine had a significant overall effect (p = 0.0111) to increase Js_{amm} in fasted fish (Figure 5.4A) with a significantly higher Js_{amm} in the anterior intestine only (Figure 5.4A; p = 0.0262). There were no significant effects of glutamine on Js_{amm} in fed fish (Figure 5.4B; p = 0.31). There were also significant overall effects of glutamine on Jm_{amm} in both treatments (Figures 5.4 C&D; p = 0.0159 in fasted fish and p =

0.0198 in fed fish). However, these effects were different between fasted fish where Jm_{amm} became more negative (Figure 5.4C), and fed fish where Jm_{amm} became less negative (Figure 5.4D). The more negative Jm_{amm} in the posterior intestine of fasted fish was significant (Figure 5.4C; p = 0.0456), but none of the section-specific differences in Jm_{amm} of fed fish were significant (Figure 5.4D). As a result, there were also significant effects on Jt_{amm} (Figure 5.5; p = 0.0012 in fasted fish and p = 0.0245 in fed fish), where Jt_{amm} became greater in fasted fish (Figure 5.5A; significant in all three intestinal sections, $p < 0.05$), but lower in fed fish, with no significant section-specific differences in the latter (Figure 5.5B). There was also a significant overall effect of glutamine elevating T_{amm} in fasted fish (Figure 5.6A; p = 0.0060), which was not seen in the fed fish (Figure 5.6B; p = 0.96). There was no significant interaction between treatment and intestinal sections for any of the measurements ($p > 0.05$) except for $Js_{urea\text{-}N}$ in fed fish (p = 0.045).

5.4.4 High luminal ammonia treatment

High luminal ammonia had minimal or negative effects on urea-N fluxes and production in both fasted and fed fish. There was a significant overall inhibitory effect of treatment on $Js_{urea\text{-}N}$ in fed fish (Figure 5.1B; p = 0.0007), but no effect on $Js_{urea\text{-}N}$ in fasted fish (Figure 5.1A; p = 0.09). In fed fish, ammonia treatment significantly decreased $Js_{urea\text{-}N}$ in mid and posterior intestines (Figure 5.1B; p = 0.0404 and 0.0314 respectively). There was no effect of high ammonia on $Jm_{urea\text{-}N}$ in either fasted or fed fish (Figures 5.1 C&D; p = 0.59 and 0.83 respectively). Thus, there were also no significant effects of treatment on $Jt_{urea\text{-}N}$ in fasted fish (Figure 5.2A; p = 0.22), but a significant overall inhibitory effect on $Jt_{urea\text{-}N}$ in the fed fish (p = 0.0067), which was significant in the posterior intestine (Figure 5.2B; p = 0.0257). In both fasted

and fed fish, the high luminal ammonia treatment also had a significant overall inhibitory effect on urea-N content, $T_{urea\text{-}N}$ (Figures 5.3 A&B p =0.0007 and <0.0001 respectively). With the exception of the anterior intestine of fasted fish (Figure 5.3A; p = 0.33), these inhibitory effects on $T_{urea\text{-}N}$ were significant in all intestinal sections in both fasted and fed fish (Figures 5.3 A&B; p = 0.0004-0.03).

There were also marked effects of high luminal ammonia on ammonia fluxes and ammonia production rates. However, while there were no significant overall effects of high ammonia on Js_{amm} in either fasted or fed fish (Figures 5.4 A&B; p = 0.19 and 0.99 respectively), the treatment had contrasting effects depending on the intestinal sections. It increased anterior intestine Js_{amm} in both fasted and fed fish (Figures 5.4 A&B; p = 0.0008 and 0.0004 respectively), but decreased Js_{amm} in the mid intestine of fed fish (Figure 5.4B; p = 0.0339). The high luminal ammonia treatment had a significant overall effect on Jm_{amm} in both fasted and fed fish (Figures 5.4 C&D; p = 0.0067 and p < 0.0001 respectively), converting the normally negative flux rates (appearance in the lumen) to positive values (removal from the lumen), at least in the anterior and mid intestine, and reducing the negative values in the posterior intestine. These effects on Jm_{amm} were significant in all three individual sections of fed fish (Figure 5.4D; p = 0.0009, 0.0198, and 0.0022 respectively). There was a significant interaction between treatment and intestinal sections on Js_{amm} in both fasted and fed fish (p < 0.0001). The net results were no significant overall effects of high ammonia on Jt_{amm} of fasted fish (Figure 5.5A; p = 0.17) but an overall reduction of Jt_{amm} in fed fish (Figure 5.5B; p = 0.0010), which was significant in the mid and posterior intestine (Figure 5.5B; p = 0.0017 and 0.0018 respectively). There was also a significant interaction between treatment and intestinal sections in both fasted and fed fish (p = 0.0014 and 0.0104 respectively). High ammonia increased T_{amm} overall in

fasted fish (Figure 5.6A; p = 0.0060) but had no effect on T_{amm} of fed fish (Figure 5.6B; p = 0.96).

5.5 Discussion

5.5.1 Overview

Our first hypothesis, that feeding would increase not only ammonia, but also urea production and flux rates in these trout gut preparations, was confirmed. While the finding on ammonia is confirmatory of previous trout studies (Rubino et al., 2014; Rubino et al., 2019), the urea result is novel, and in accord with the findings of Bucking et al. (2013b) on similar *in vitro* preparations of the plainfin midshipman. With respect to our second hypothesis, that the activities of both CPS III and arginase activities would increase if the OUC were involved in this urea production, our data do not provide support for OUC involvement, because CPS III activity did not increase with feeding. However, the observed increase in arginase activity suggests that an alternate pathway, direct arginolysis, may have contributed to elevated urea production. Our third hypothesis, that luminal glutamine supply would increase the production and flux rates of both ammonia and urea, was supported in part by observations of elevated ammonia production and transport in preparations from fasted fish, but not from fed fish. This indicates an ability of the intestinal tissue to deaminate glutamine, and perhaps use it as an oxidative fuel, similar to the observations of Bucking et al. (2013b). However, with the exception of the anterior intestine of fed trout, there was no evidence of increased urea production or flux resulting from the presence of glutamine, again arguing against the presence of a functional OUC in the intestine. Our final hypothesis, that elevated luminal ammonia supply would result in elevated urea production and flux rates, reflecting a detoxification mechanism, was not supported. There were negligible or

negative effects on urea-N fluxes and production in both fasted and fed fish, but indirect evidence of ammonia detoxification by another pathway.

5.5.2 The effect of feeding

This study provides further evidence (c.f. Rubino et al., 2019, 2014) that the intestinal cells of rainbow trout break down dietary amino acids, because feeding increased overall Js_{amm}, Jm_{amm}, Jt_{amm}, and T_{amm} (Table 5.1), in the absence of the original chyme. Most of this increased intestinal production was transported to the serosal side (Table 5.1; Rubino et al., 2019, 2014), explaining the greatly elevated blood ammonia levels measured in the HPV of trout after feeding (Karlsson et al., 2006). A novel finding of our study was that there were also overall significant increases in $Jt_{urea\text{-}N}$ and $Js_{urea\text{-}N}$ in the intestine of fed fish (Table 5.1). Again, as the original chyme was not present, this supports the idea that urea can be synthesized in some way from dietary amino acids by the intestinal tissues after feeding, then subsequently transferred to the blood, draining to the HPV, as also evidenced by Karlsson et al. (2006). Although Kajimura et al. (2004) provided indirect evidence (by anal suturing) that rectal excretion of both ammonia (especially) and urea increased after feeding in trout, only the increased ammonia flux to the lumen (Jm_{amm}) was significant in the present study, occurring mainly in the posterior intestine (Table 5.1). Nevertheless, the intestinal cells of ammoniotelic freshwater rainbow trout clearly have the ability to not only transport urea in a directional fashion, but also likely produce it after feeding. This agrees with previous whole animal studies on rainbow trout that showed an increase in urea excretion rate depending on the diet (Alsop and Wood, 1997; Kajimura et al., 2004; Kaushik et al., 1983). Similarly, isolated GIT tissues of plainfin midshipman significantly increased production and transport of urea across both mucosal and serosal surfaces following a

meal (Bucking et al., 2013a). In this particular species, the urea secreted into the GIT lumen appeared to be both excreted out in the feces and used by ureolytic GIT bacteria, with possible recycling of ammonia (Bucking et al., 2013a). Both ammonia (Rh glycoproteins) and urea transporters (UT) have been identified in the GIT of the plainfin midshipman, and the UT is upregulated after feeding (Bucking et al. 2013a, b). In trout intestine, Rhbg expression increases after feeding (Bucking and Wood, 2012), but as yet there is no information on the presence of UT.

5.5.3 CPS III and arginase enzyme activity levels after feeding

In association with the increased $Jt_{urea\text{-}N}$ and $Js_{urea\text{-}N}$ discussed above, we hypothesized that the intestinal cells would increase CPS III and arginase activity after feeding. However, feeding had minimal or negative overall effect on CPS III activity in either epithelial scrapings or muscle (Table 5.2). Previous studies also found below detectable or low levels of CPS III activity in adult rainbow trout intestine (Bucking et al., 2013a; Korte et al., 1997; Wright et al., 1995) and in the intestine of other adult teleosts (Felskie et al., 1998; Kong et al., 1998). This contrasts with the plainfin midshipman where intestinal CPS III activity increased greatly after feeding (Bucking et al., 2013a). Rainbow trout, similar to other teleosts, have relatively higher CPS and other OUC enzyme activities during embryogenesis to prevent possible ammonia toxicity, that is then reduced at about 70 days post fertilization (Korte et al., 1997; Wright et al., 1995; reviewed by Zimmer et al., 2017). Therefore, the low enzymatic activities we found may not have physiological importance for urea production, but rather simply represent the products of low-level gene expression left over from embryonic life.

On the other hand, arginase activity increased significantly after feeding, specifically in the mid intestine epithelial scraping (Table 5.3). In contrast to CPS III, arginase activity increases slowly during post-fertilization development of rainbow trout (Wright et al., 1995). This is similar to a previous finding on adult Atlantic cod (*Gadus morhua*) with undetectable level of CPS III but the presence of arginase in its intestine (Chadwick and Wright, 1999). Unlike CPS III that is exclusively involved with the OUC pathway, arginase is also involved in arginolysis, metabolizing dietary arginine directly to urea. This may explain the increase in urea production and transport after feeding. Another mechanism that may have contributed to intestinal urea production is uricolysis, by the conversion of uric acid to urea (reviewed by Anderson, 2001; Cvancara, 1969; Goldstein and Forster, 1965). This pathway should be investigated in future studies.

5.5.4 High luminal glutamine treatment

Glutamine can be metabolized to α-ketoglutarate as an energy source for immediate energy production by the citric acid cycle (or for carbon storage), releasing ammonia, or the amino group can be transferred by transamination to form other amino acids. It can also feed into the OUC pathway by CPS III, producing urea to be excreted. We predicted that the surplus supply of glutamine in the lumen would increase both ammonia and urea-N production and flux rates as the intestinal cells break down the amino acid. We found an increase in ammonia flux rates and production in intestinal preparations from fasted trout, but not fed trout (Figures 5.4, 5.5 and 5.6), suggesting that glutamine is deaminated and metabolized as an energy source in fasted fish, whereas in fed fish there may be alternate fuels available from the chyme. This response pattern differs from that of the plainfin midshipman where high mucosal glutamine

stimulated ammonia production in intestinal preparations from both fasted and fed fish (Bucking et al., 2013a).

There were minimal changes in urea-N handling in response to elevated mucosal glutamine (Figures 5.1, 5.2 and 5.3). This is in accord with the low and generally unresponsive CPS III activity we found (Table 5.2), further suggesting that the intestine does not use the OUC to make urea. However, at present we should not dismiss the significant stimulations of $Js_{urea\text{-}N}$ and $Jt_{urea\text{-}N}$ in the anterior intestine of fed trout only (Figures 5.1B and 5.2B) which occurred in parallel to significantly decreased CPS III activity in this tissue (Table 5.2); a puzzling result. Another puzzling result was reported by Bucking et al. (2013b) in the plainfin midshipman, which is thought to have an intestinal OUC. Plainfin midshipman intestinal preparations exhibited decreased urea production in response to high glutamine in the lumen (Bucking et al., 2013a). The authors speculated that ammonia was the substrate for the OUC in this species, and that the excess glutamine was interfering with the ammonia transport across mitochondrial matrix, thereby reducing the substrate available for the OUC.

5.5.5 High luminal ammonia treatment

The suggestion of Bucking et al. (2013b) that ammonia rather than glutamine could be the preferred substrate for the intestinal OUC of the plainfin midshipman is a rare but not an unprecedented phenomenon in fish, having been documented in the ureotelic Magadi tilapia (Lindley et al., 1999). Magadi tilapia increases urea excretion rate when exposed to high external ammonia (Wood et al., 1989; Wood et al., 2013). Ureogenic largemouth bass (*Micropterus salmoides*) also increase urea excretion in high ammonia water (Kong et al., 1998). To evaluate this suggestion in the rainbow trout intestine, we loaded high ammonia into the lumen to

investigate whether the rainbow trout has the ability to detoxify ammonia to less toxic urea. The treatment had significant effects on ammonia handling and production (Figures 5.4, 5.5 and 5.6), somewhat parallel to earlier studies with lower levels (1 mM) of ammonia loading (Rubino et al., 2014; Rubino et al., 2019). At this higher level (2 mM), there were no significant overall effects of high ammonia on Jt_{amm} of fasted fish (Figure 5.5A) but an overall reduction of Jt_{amm} occurred in fed fish, prominent in the mid and posterior intestine (Figure 5.5B). This suggests that ammonia detoxification was induced. However, there were minimal effects on urea-N handling in both fasted and fed fish (Figures 5.1, 5.2 and 5.3). Since the adult rainbow trout does not appear to use the OUC, the formation of urea may not be the primary mechanism for the detoxification of ammonia. In fact, there were some inhibitory effects on both the flux rates and production of urea. Presumably, this is because the primary mechanism for detoxification of ammonia in the intestine of the rainbow trout is by synthesis of glutamine, *via* the enzyme glutamine synthetase (GS), with potential transamination to other amino acids. We found the most marked changes in the posterior intestine and correspondingly, the GS enzyme activity is reported to be highest in this section in the trout (Mommsen et al., 2003a; Rubino et al., 2014). Although we have not demonstrated that the trout intestine was making glutamine specifically, glutamine in general acts as an ammonia storage molecule which can be used as energy immediately or later on (reviewed by Anderson, 2001).

Interestingly*, in vitro* preparations of the intestine of the plainfin midshipman also did not exhibit changes in urea production with high mucosal ammonia, possibly because an *in vivo* signal is needed to regulate the OUC enzymes (Bucking et al., 2013a). There are a few pieces of evidence suggesting that the intestinal bacteria community (microbiome) influences ammonia handling in some fish species. Ammonia appearance in the gut of plainfin midshipman was

greatly reduced with antibiotic treatment (Bucking et al., 2013a). Similarly, in the ureotelic dogfish shark, inhibition of bacterial urease decreased ammonia appearance in the mucosal chyme of the intestine (Wood et al., 2019). Intestinal bacteria and the activity of ammonia detoxifying enzymes were correlated in the herbivorous fish (*Campostoma anomalum*), but not in the carnivorous fish (*Etheostoma caeruleum*; Turner and Bucking, 2019). It is still unclear whether the rainbow trout also carries an intestinal bacteria community that is capable of detoxifying ammonia or glutamine, or converting urea to ammonia, but we assume that a lot of the flora was flushed out during our gut sac preparations. We used relatively high concentrations of ammonia and glutamine in short flux periods, which likely would have minimized the influence of any residual microbial activity. Clearly, there is a need for better mechanistic understanding of N-handling by the GIT in fish, including the contributions of the microbiome.

Table 5.1 Comparison of serosal (Js_{urea-N}) and mucosal (Jm_{urea-N}) urea-N flux rates, total tissue urea-N production rate (Jt_{urea-N}), tissue urea-N concentration (T_{urea-N}), ammonia flux rates (Js_{amm} & Jm_{amm}), total tissue ammonia production rate (Jt_{amm}), and tissue ammonia (T_{amm}) of fasted and fed fish. Single dagger (†) in the first column indicates a significant overall effect of intestinal section and double dagger (‡) in the second column indicates a significant overall effect of feeding ($p < 0.05$, two-way ANOVA). Letters represent significant difference among GIT sections in each row, using small letters for fasted fish and capital letters for fed fish ($p < 0.05$). Asterisk (*) represents significant differences between fasted and fed fish within the same intestinal section ($p < 0.05$). Values are means ± SEM (N = 5).

		Anterior intestine	Mid intestine	Posterior intestine
Js_{urea-N} (μmol urea-N cm^{-2} h^{-1}) †	Fasted	0.086 ± 0.019^{a}	0.020 ± 0.002^{b}	0.051 ± 0.006^{ab}
	Fed ‡	$0.171 \pm 0.027^{A*}$	0.077 ± 0.010^{B}	0.083 ± 0.010^{B}
Jm_{urea-N} (μmol urea-N cm^{-2} h^{-1})	Fasted	-0.019 ± 0.006	-0.006 ± 0.003	-0.029 ± 0.008
	Fed	-0.009 ± 0.007	-0.009 ± 0.003	-0.046 ± 0.034
Jt_{urea-N} (μmol urea-N cm^{-2} h^{-1})	Fasted	0.104 ± 0.020	0.026 ± 0.003	0.079 ± 0.010
	Fed ‡	0.180 ± 0.028	0.086 ± 0.011	0.129 ± 0.035
T_{urea-N} (μmol urea-N g^{-1} tissue)	Fasted	0.22 ± 0.02	0.29 ± 0.05	0.37 ± 0.02
	Fed	0.33 ± 0.02	0.27 ± 0.03	0.41 ± 0.05
Js_{amm} (μmol ammonia cm^{-2} h^{-1}) †	Fasted	0.305 ± 0.034^{a}	0.136 ± 0.014^{b}	0.112 ± 0.018^{b}
	Fed ‡	$0.595 \pm 0.038^{A*}$	$0.387 \pm 0.052^{B*}$	$0.292 \pm 0.038^{B*}$
Jm_{amm} (μmol ammonia cm^{-2} h^{-1}) †	Fasted	-0.041 ± 0.010	-0.039 ± 0.014	-0.094 ± 0.018
	Fed ‡	-0.071 ± 0.033^{A}	-0.088 ± 0.024^{A}	$-0.287 \pm 0.070^{B*}$
T_{amm} (μmol ammonia g^{-1} tissue) †	Fasted	2.19 ± 0.18	2.61 ± 0.49	2.45 ± 0.27
	Fed ‡	2.56 ± 0.07^{A}	$3.18 \pm 0.15A^{B}$	$4.39 \pm 0.75^{B*}$
Jt_{amm} (μmol ammonia cm^{-2} h^{-1})	Fasted	0.346 ± 0.035	0.174 ± 0.020	0.206 ± 0.026
	Fed ‡	$0.666 \pm 0.050^{*}$	0.475 ± 0.058	$0.579 \pm 0.079^{*}$

Table 5.2 CPS III activity (nmol min^{-1} g^{-1} tissue) of the anterior, mid, and posterior muscle and epithelial scrapings of fasted and fed fish. There were no significant overall effects of intestinal section, but double dagger (‡) in the second column indicates a significant overall effect of feeding; there were also significant interactive effects in both muscle and epithelial scrapings ($p < 0.05$, two-way ANOVA). Asterisk (*) represents significant difference of fed muscle or epithelial scraping in comparison to fasted muscle or epithelial scraping ($p < 0.05$). Values are means ± SEM (N = 5).

		Anterior intestine	Mid intestine	Posterior intestine
Muscle CPS III activity (nmol min^{-1} g^{-1} tissue)	Fasted	0.529 ± 0.152	0.111 ± 0.059	0.546 ± 0.102
	Fed ‡	0.112 ± 0.019*	0.358 ± 0.080	0.230 ± 0.035
Epithelial scraping CPS III activity (nmol min^{-1} g^{-1} tissue)	Fasted	0.355 ± 0.101	0.093 ± 0.037	0.091 ± 0.033
	Fed	0.074 ± 0.027*	0.149 ± 0.073	0.130 ± 0.027

Table 5.3 Arginase activity (μmol min^{-1} g^{-1} tissue) of the anterior, mid, and posterior muscle and epithelial scrapings of fasted and fed fish. Single dagger (†) in the first column indicates a significant overall effect of intestinal section and double dagger (‡) in the second column indicates a significant overall effect of feeding; there were also significant interactive effects in both muscle and epithelial scrapings ($p < 0.05$, two-way ANOVA). Asterisk (*) represents significant difference of fed muscle or epithelial scraping in comparison to fasted muscle or epithelial scraping ($p < 0.05$). Values are means ± SEM (N = 5).

		Anterior intestine	Mid intestine	Posterior intestine
Muscle arginase activity (μmol min^{-1} g^{-1} tissue) †	Fasted	0.417 ± 0.103	1.680 ± 0.349	2.397 ± 0.365
	Fed	0.873 ± 0.275	2.558 ± 0.380	0.821 ± 0.190*
Epithelial scraping arginase activity (μmol min^{-1} g^{-1} tissue) †	Fasted	0.807 ± 0.212	0.821 ± 0.214	1.234 ± 0.247
	Fed ‡	0.840 ± 0.247	3.175 ± 0.380*	1.035 ± 0.380

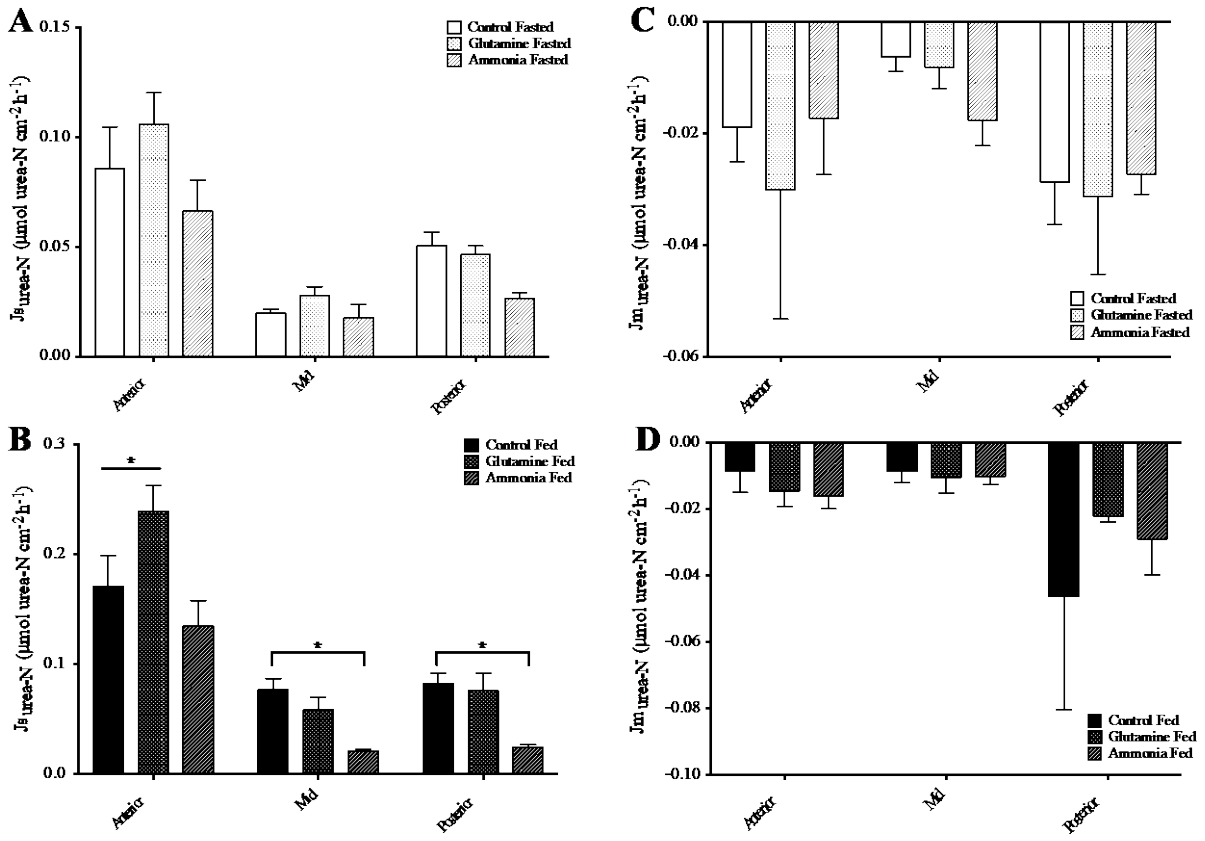

Figure 5.1 Serosal (A&B; $Js_{urea\text{-}N}$) and mucosal (C&D; $Jm_{urea\text{-}N}$) urea-N flux rates (µmol cm-2 h-1) of the anterior, mid, and posterior intestines of fasted (A&C; white bars) and fed (B&D; filled bars) fish in the presence of either control saline (no pattern), high glutamine (dotted pattern), or high ammonia (diagonal pattern) in the lumen. Asterisk (*) represents significant difference between high glutamine or high ammonia treated group relative to control group ($p < 0.05$). Values are means ± SEM (N = 5).

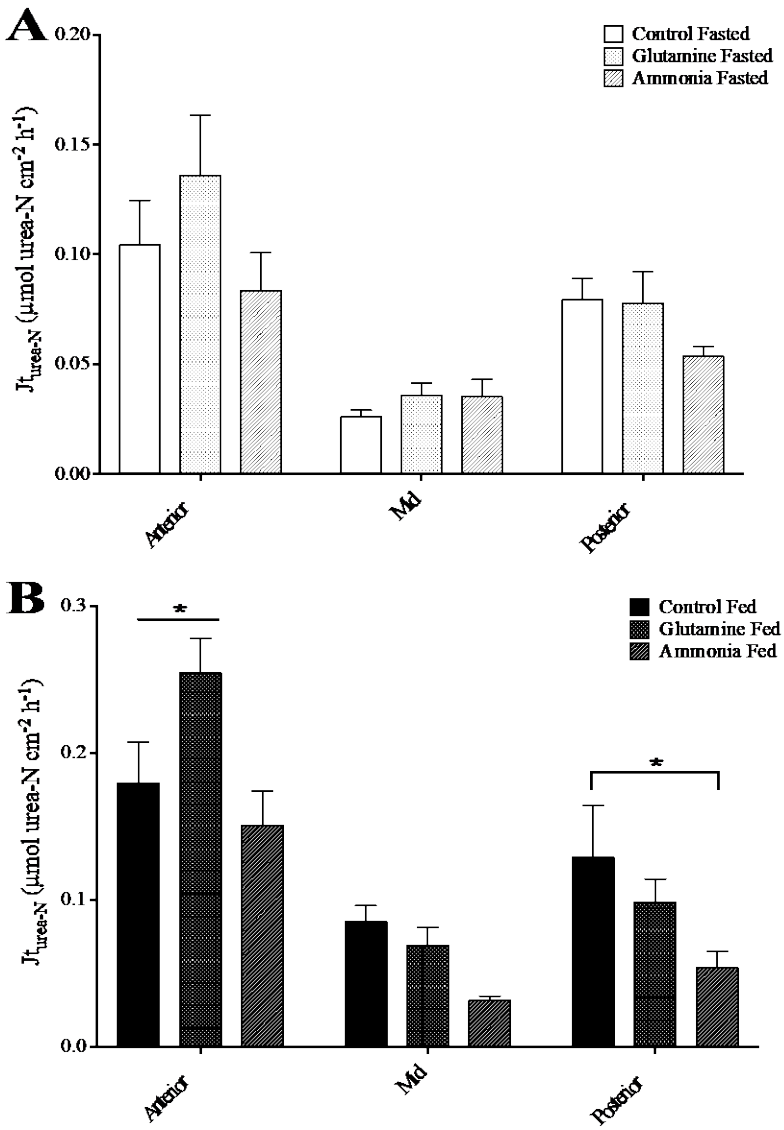

Figure 5.2 Total tissue urea-N production rates (Jt_{urea}: μmol cm^{-2} h^{-1}) of the anterior, mid, and posterior intestine of (A) fasted and (B) fed fish in the presence of either control saline (no pattern), high glutamine (dotted pattern), or high ammonia (diagonal pattern) in the lumen. Values are calculated from Figure 5.1 data. Asterisk (*) represents significant difference between high glutamine or high ammonia treated group relative to control group ($p < 0.05$). Values are means ± SEM (N = 5).

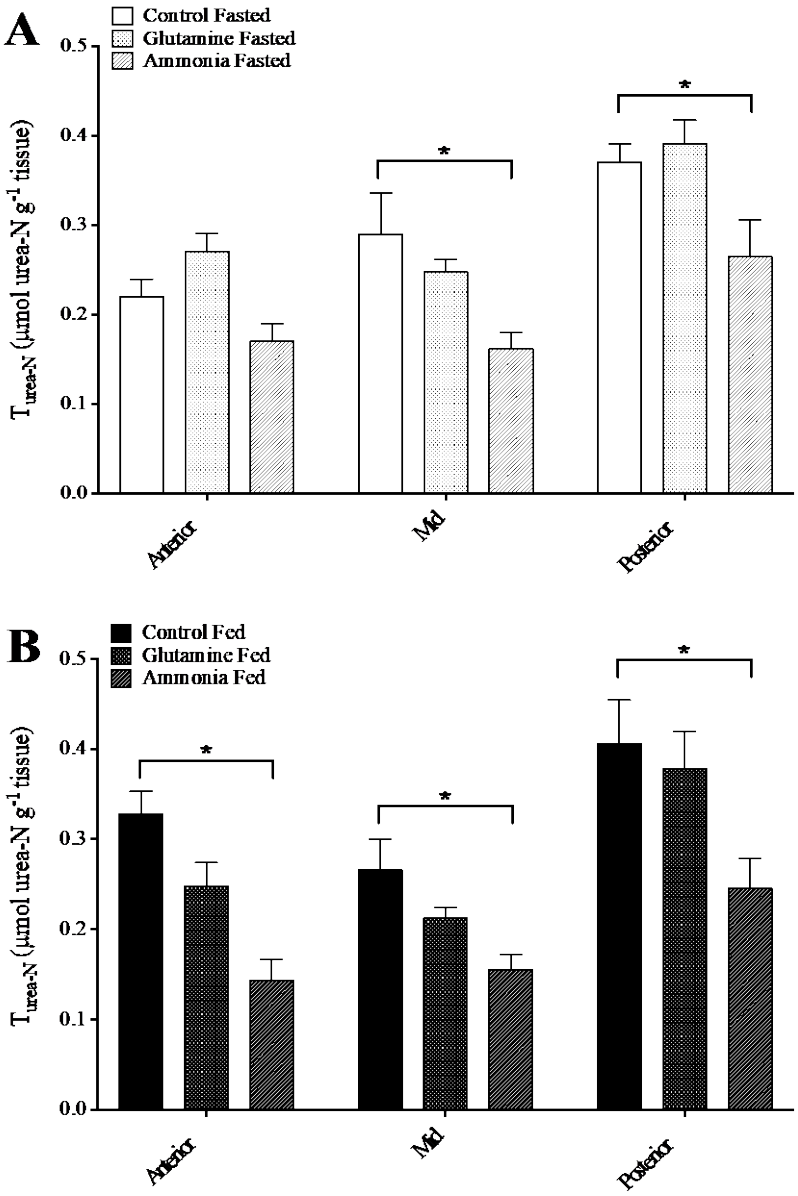

Figure 5.3 Total tissue urea-N concentration (T_{urea}, μmol g^{-1} tissue) of the anterior, mid and posterior intestines of (A) fasted and (B) fed fish in the presence of either control saline (no pattern), high glutamine (dotted pattern), or high ammonia (diagonal pattern) in the lumen. Asterisk (*) represents significant difference between high glutamine or high ammonia treated group relative to control group ($p < 0.05$). Values are means ± SEM (N = 5).

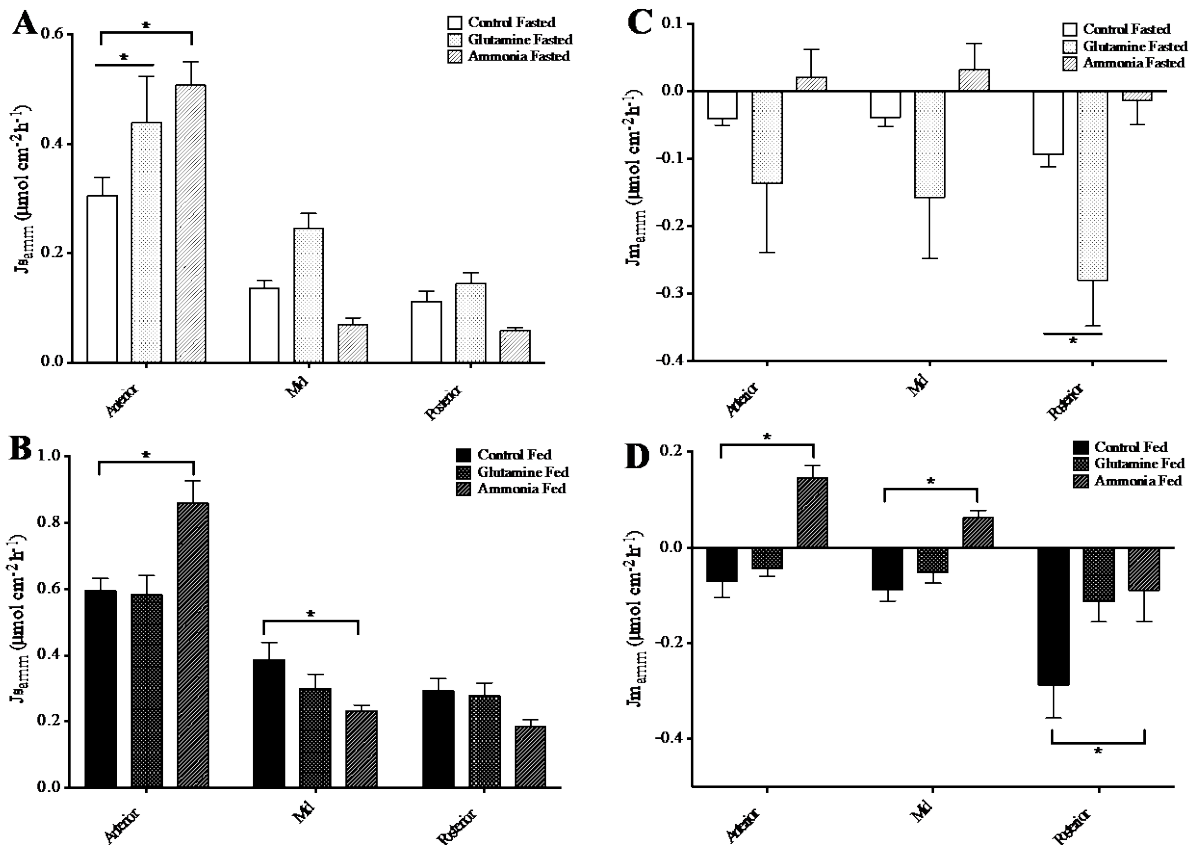

Figure 5.4 Serosal (A&B; Js_{amm}) and mucosal (C&D; Jm_{amm}) ammonia flux rates (µmol cm-2 h-1) of the anterior, mid, and posterior intestines of fasted (A&C; white bars) and fed (B&D; filled bars) fish in the presence of either control saline (no pattern), high glutamine (dotted pattern), or high ammonia (diagonal pattern) in the lumen. Asterisk (*) represents significant difference between high glutamine or high ammonia treated group relative to control group ($p < 0.05$). Values are means ± SEM (N = 5).

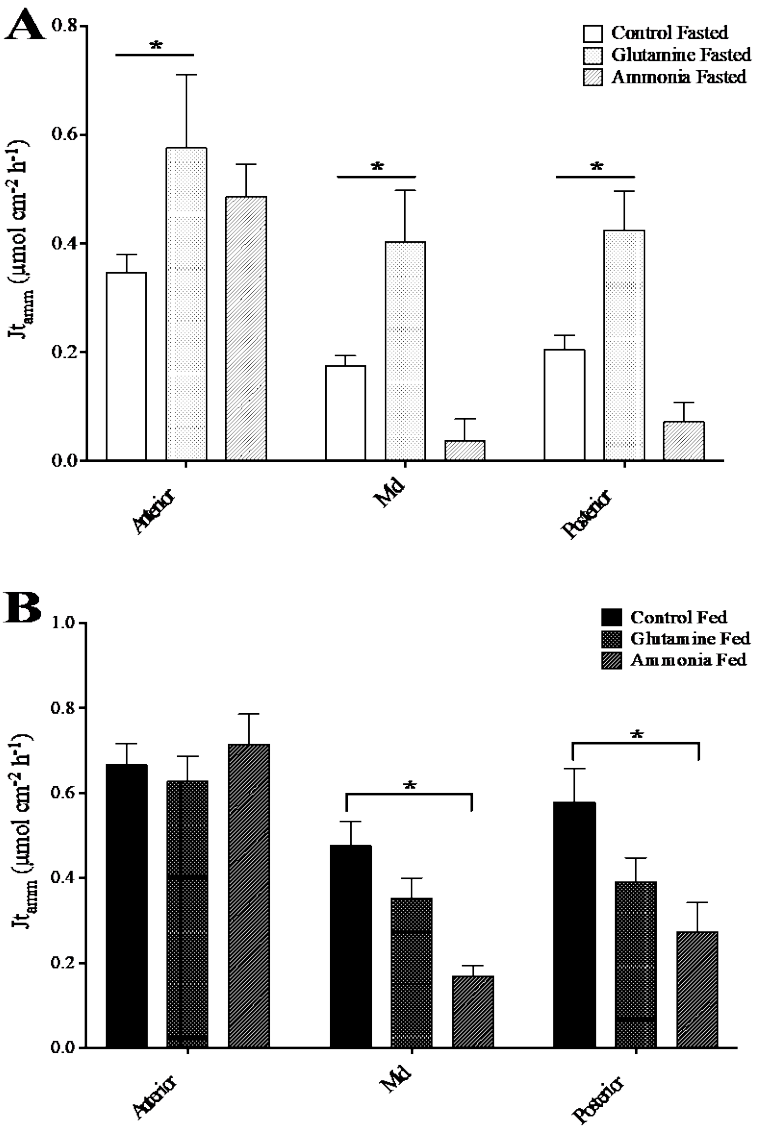

Figure 5.5 Total tissue ammonia production rates (Jt_{amm}: μmol cm^{-2} h^{-1}) of the anterior, mid, and posterior intestine of (A) fasted and (B) fed fish in the presence of either control saline (no pattern), high glutamine (dotted pattern), or high ammonia (diagonal pattern) in the lumen. Values are calculated from Figure 5.4 data. Asterisk (*) represents significant difference between high glutamine or high ammonia treated group relative to control group ($p < 0.05$). Values are means ± SEM (N = 5).

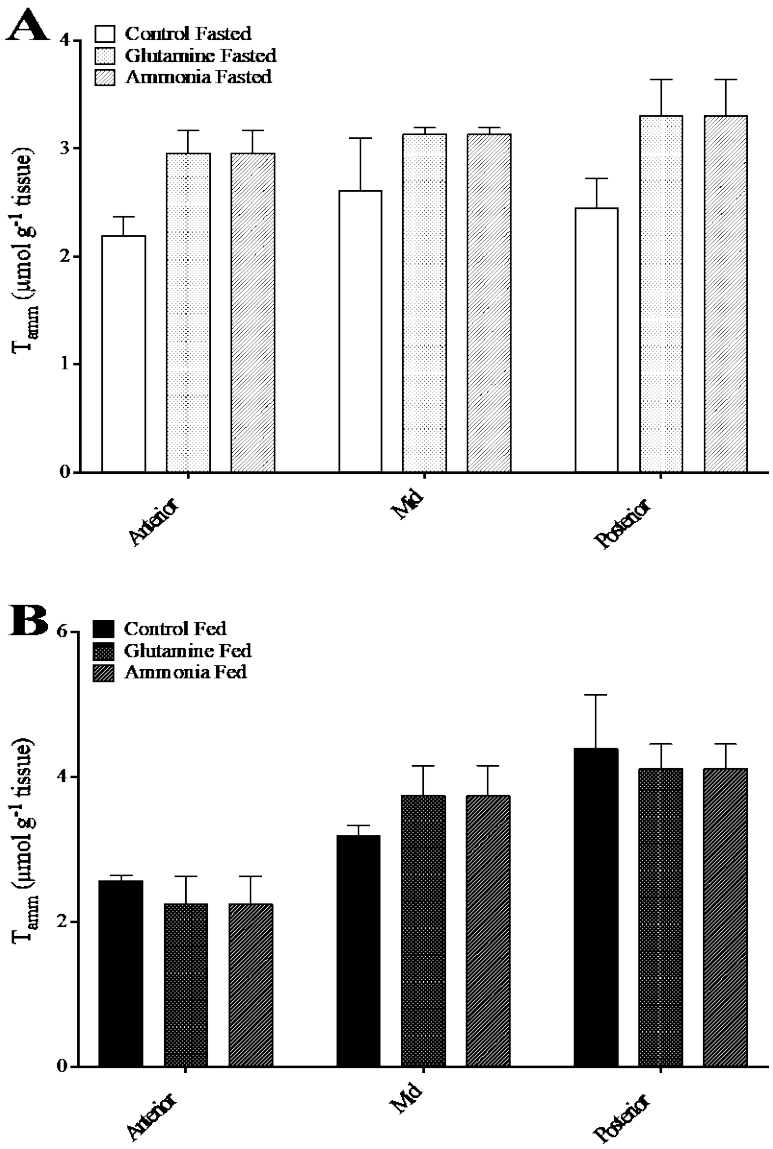

Figure 5.6 Total tissue ammonia concentration (T_{amm}, µmol g^{-1} tissue) of the anterior, mid and posterior intestines of (A) fasted and (B) fed fish in the presence of either control saline (no pattern), high glutamine (dotted pattern), or high ammonia (diagonal pattern) in the lumen. Asterisk (*) represents significant difference between high glutamine or high ammonia treated group relative to control group ($p < 0.05$). Values are means ± SEM (N = 5).

Chapter 6: Potential NH_3 transport across GIT epithelia and ammonia transport in the stomach

6.1 Summary

Although the gastrointestinal tract (GIT) is an important site for nitrogen metabolism in teleosts, the mechanisms of ammonia absorption and transport remain to be elucidated. Both protein catabolism in the lumen and the metabolism of the GIT tissues produce ammonia which, in part, enters the portal blood through the anterior region of the GIT. The present study examined the possible roles of different GIT sections of rainbow trout (*Oncorhynchus mykiss*) in transporting ammonia in its unionized gas form - NH_3 - by changing the PNH_3 gradient across GIT epithelia using *in vitro* gut sac preparations. We also surveyed mRNA expression patterns of three of the identified Rh proteins (Rhbg, Rhcg1, Rhcg2) as potential NH_3 transporters and NKCC as a potential ammonium ion (NH_4^+) transporter along the GIT of rainbow trout. We found that ammonia absorption is not dependent on the PNH_3 gradient despite expression of Rhbg and Rhcg2 in the intestinal tissues, and Rhcg2 in the stomach. We detected no expression of Rhbg in the stomach and no expression of Rhcg1 in all GIT tissues. There was also a lack of correlation between ammonia transport and [NH_4^+] gradient despite NKCC expression in all GIT tissues. Regardless of PNH_3 gradients, the stomach showed the greatest absorption and net tissue consumption. Overall, our findings suggest nitrogen metabolism zonation of GIT, with stomach serving as an important site for the absorption, handling and transport of ammonia that is independent of PNH_3 gradient.

6.2 Introduction

Following feeding in fish, it is now evident that total ammonia levels (Tamm = NH_3 and NH_4^+) increase in the systemic blood plasma (Kaushik and de Oliva Teles, 1985; Bucking and Wood, 2008) as well is in the blood plasma of the hepatic portal vein (HPV) (Karlsson et al., 2006, Chapter 4), likely as a result of ammonia production and absorption across the gastrointestinal tract (GIT) epithelia (Bakke et al., 2011; Rubino et al., 2014). Ammonia is produced during protein catabolism in the GIT, thus Tamm in the chyme is high (Bucking and Wood, 2012; Rubino et al., 2014; Jung et al., 2022; Chapter 3). Ammonia is also produced by the metabolism of the GIT tissue itself (Rubino et al., 2014). In *in vitro* preparations, intestinal tissues taken from fed rainbow trout (*Oncorhynchus mykiss*) display increases in both ammonia absorption rates and endogenous tissue ammonia production rates relative to tissues from fasted fish (Rubino et al., 2014; Jung et al., 2021; Chapter 5). Furthermore, Tamm levels in HPV blood are greater after feeding than in the arterial blood (Karlsson et al., 2006, Chapter 4), supporting the hypothesis that the postprandial increases in HPV Tamm originate from the GIT tissues. However, the specific sections of the GIT responsible, and the specific mechanisms involved, remain unknown and are the focus of this study.

Chyme Tamm concentration can reach over 20-fold greater than the arterial plasma Tamm level 48 h following feeding (Chapter 4) and likely even higher at earlier stages of digestion. If equilibrated with the bloodstream, such high ammonia levels would be toxic to fish (Liew et al., 2013; Tsui et al., 2009; Wicks and Randall, 2002a). Recent evidence shows that ammonia does not enter the blood of the subintestinal vein that drains the posterior intestine (Chapter 4), but rather enters somewhere in the anterior region of the GIT, increasing the HPV Tamm (Karlsson et al., 2006; Chapter 4). In solution, ammonia is present in two forms: an

unionized gas (ammonia; NH_3) and a protonated cation (ammonium ion; NH_4^+). NH_4^+ has been shown to move across intestinal epithelia *via* transporters energized by basolateral Na^+, K^+ ATPase (NKA) such as the Na^+, K^+, $2Cl^-$ co-transporter (NKCC) and K^+ channels (Rubino et al., 2019). In contrast, the potential transport of NH_3 across the GIT epithelia has not been investigated.

While NH_3 was originally considered to be highly permeable through biological membranes (Randall and Tsui, 2002), more recent findings suggest that it requires a transporter to move across membranes, possibly through Rhesus (Rh) glycoproteins (Wright and Wood, 2012). Fish express at least four glycosylated Rh isoforms: Rhag, Rhbg, and Rhcg1 and Rhcg2 (Bucking et al., 2013b; Huang and Peng, 2005; Hung et al., 2007; Nawata et al., 2007) that are homologous to the Amt/Mep proteins identified as ammonia transporters in bacteria, plants and yeasts (Khademi et al., 2004; McDonald and Ward, 2016; Weiner, 2006). When expressed in a model translation system (*Xenopus* oocytes), all four of these Rh proteins from rainbow trout have been shown to facilitate the diffusion of NH_3 (Nawata et al., 2010). In the GIT of rainbow trout, the basolateral isoform Rhbg is expressed along the entire GIT including the stomach (Bucking and Wood, 2012; Nawata et al., 2007). Rhcg, which is usually apical in location, has not been found in the intestine of rainbow trout (Nawata et al., 2007), but is expressed in both the stomach and in the intestine of mammals (Handlogten et al., 2005; Weiner, 2006). Therefore, it is unclear whether the postprandial increase in HPV Tamm is a result of NH_3 transport and whether the Rh proteins are expressed on both apical and basolateral membranes throughout the GIT.

The overall goals of this study were to survey mRNA expression patterns of three of the identified Rh proteins (Rhbg, Rhcg1, Rhcg2) in all four sections of the GIT tissues (stomach,

anterior, mid, and posterior intestine) in freshwater rainbow trout, and to investigate the potential for NH_3 transport in each of the sections by changing the PNH_3 gradient across GIT epithelia using *in vitro* gut sac preparations. The latter was achieved by using selected buffers to "clamp" the mucosal pH at different values, thereby changing PNH_3 at constant mucosal Tamm. Specifically, we hypothesized that increases in PNH_3 gradient across the intestinal epithelia of gut sacs would be positively correlated with increased mucosal ammonia flux rate (Jm_{amm}) as a result of increased NH_3 movement *via* Rh proteins serving as possible transcellular transporters. Accordingly, we also hypothesized that Rh proteins would be expressed throughout different sections of the GIT for NH_3 absorption. In particular, we predicted that these proteins would be more highly expressed in the anterior regions of the GIT, thus facilitating greater Jm_{amm} in this region, in parallel with recent findings (Chatper 4). Moreover, the stomach in particular has been shown to be involved in absorbing dietary cations such as Na^+ and K^+ in trout (Bucking and Wood, 2006). Therefore, we hypothesized that regardless of the PNH_3 gradient, the stomach would be an important absorptive site for ammonia in the form of NH_4^+. We hypothesized that in addition to the Rh proteins, NKCC would be expressed in the stomach and throughout the intestine (the latter has already been shown by Rubino et al., 2019) in order to transport NH_4^+ ions, thereby contributing to the increased postprandial Tamm.

6.3 Material and methods

6.3.1 Experimental animals

Rainbow trout (300-570 g) were obtained from Little Cedar Falls Hatchery (Nanaimo, BC, Canada) and transferred to the University of British Columbia (UBC) where they were held for several months prior to experiments. Fish were held at 9 ˚C in flowing dechlorinated

Vancouver tap water (Na^+ = 0.09, Cl^- = 0.10, Ca^{2+} = 0.10, Mg^{2+} = 0.011, K^+ = 0.004 mM, hardness as $CaCO_3$ = 3.3 mg L^{-1}, pH = 7.0). During this time, animals were fed to satiation every other day with commercial trout pellet food (BioTrout 4.0 mm, Bio-Oregon^{TM}, Long-view, WA, USA). All experiments were approved by the UBC Animal Care Committee (AUP A18-0271) and conformed to national regulations of the Canada Council for Animal Care.

6.3.2 Gut sac experiments and calculations

Gut sac preparations were used to measure the changes in the mucosal and serosal fluxes of total ammonia (Jm_{amm} and Js_{amm} respectively) based on the influence of the PNH_3 gradient across the GIT epithelium. Gut sacs were made according to the protocol of Rubino et al. (2014). Animals were fed within 24 h prior to experimentation and euthanized by an overdose of buffered MS-222 (0.07 g L^{-1}). The GIT was removed and sectioned into the stomach, anterior, mid, and posterior regions. The contents of each GIT section (referred to as chyme hereafter) were removed and centrifuged (13 000 g, 60s) and the supernatant pH was measured. The pH values of all chyme supernatant, mucosal and saline samples were measured using a micro-combination probe (MI-414; 6cm beveled tip; Microelectrodes Inc., Bedford, NH, USA) calibrated with precision buffers (Fisher Scientific and Radiometer-Copenhagen, Copenhagen, Denmark). All salines used for the experiment were pre-equilibrated with a 99 % O_2: 1 % CO_2 gas mix, then pH was measured.

The lumens of GIT sections were then thoroughly rinsed with Cortland's saline (in mM: NaCl 124, KCl 5.1, $CaCl_2$ 1.6, $MgSO_4$ 0.9, $NaHCO_3$ 11.9, NaH_2PO_4 3, pH = 7.4) to remove any leftover chyme. Each of the GIT sections was tied off at one end with a 2-0 silk thread while the other end had a flared polyethylene tube (PE 60; Clay-Adams, Sparks, MD, USA) inserted and

held securely with another silk thread. In all pH treatment groups, the gut sacs were filled with gas-equilibrated Cortland's saline with 1 mM of ammonium hydroxide (Sigma-Aldrich, St. Louis, MO, USA) and 50 mM of appropriate buffer (Sigma-Aldrich) through the open polyethylene tube using a syringe (termed mucosal saline hereafter). For pH 4 stomach gut sacs, 50 mM of formic acid was mixed into the mucosal saline. For pH 7 and 8 gut sacs, 50 mM of HEPES (4-(2-hydroxyethyl)-1-piperazineethanesulfonic acid) buffer was used. For pH 9 gut sacs, 25 mM of CHES (N-Cyclohexyl-2-aminoethanesulfonic acid) and 25 mM of AMPD (2-amino-2-methyl-1,3,-propanediol) buffers (total of 50 mM) were used. The saline was infused and then withdrawn multiple times for thorough mixing with a 1-mL syringe to ensure the remaining saline in the syringe was the same as the mucosal saline in the gut sacs. The saline was injected until the gut sacs became taut, and the remainder 0.3-0.5 mL of the saline was collected as the initial mucosal sample and pH was measured. The PE tube was then sealed, and the sac was thoroughly blotted dried, then weighed for initial weight (W_i).

The gut sacs were then placed in either 30-mL glass bottles or 100-mL glass beakers depending on the size, and bubbled with 99 % O_2: 1 % CO_2 gas mix throughout the flux period with PE50 tubing. All glass bottles and beakers were kept semi-submerged in 9 ˚C flow through tank. The opening of the bottles and beakers were sealed around the gas tubing with caps or parafilm to minimize evaporation. For all pH treatment groups, the serosal saline had 50 mM of HEPES buffer (pH 7.8). The amount of serosal saline needed to fully immerse the preparations varied and was exactly recorded. After about 30 sec of placement of gut sacs, 5-mL of initial serosal sample was taken (termed serosal saline hereafter) and pH was measured. Based on preliminary experiments that checked the efficacy of mucosal pH-stating with the various buffers, it proved necessary to limit the experiments to relatively short flux periods. Therefore, to

minimize pH shifts, fluxes in mucosal pH 4 stomach gut sacs were measured for 15 min, and all other pH treatment groups for 30 min.

At the end of the flux period, the gut sacs were blotted dry, and weighed again (final gut sac weight; W_f). Then, the internal contents of the gut sacs were collected (final mucosal saline), measured for pH, and the whole gut sac including the luminal side were thoroughly blotted dry again and weighed (empty weight of the preparation; W_e). The final mucosal volume (Vm_f) was calculated as $W_f - W_e$, and the initial mucosal volume (Vm_i) as $W_i - W_e$. The serosal saline was collected as the final serosal sample and measured for pH. The gut sac tissues were cut open and traced onto 0.5-mm graph paper to determine the surface areas. All samples were frozen in liquid N_2, then stored at -80 ºC for later analysis of total ammonia concentrations. Then the following parameters were calculated.

Serosal ammonia (Js_{amm}) flux rate

$$Js_{amm} = \frac{[(Ts_{amm}f - Ts_{amm}i) \times Vs]}{SA \times t} \qquad \text{Equation 1}$$

where Js_{amm} is in μmol cm^{-2} h^{-1}, $Ts_{amm}f$ and $Ts_{amm}i$ are the final and initial ammonia concentrations (μmol L^{-1}) in the serosal saline, Vs is the volume of serosal solution (L), SA is intestinal surface area (cm^2), and t is time (h). Positive Js_{amm} fluxes were into the serosal saline; negative Js_{amm} fluxes were out of the serosal saline.

Mucosal ammonia (Jm_{amm}) flux rate

$$Jm_{amm} = \frac{[(Tm_{amm}i \times Vmi) - (Tm_{amm}f \times Vmf)]}{SA \times t} \qquad \text{Equation 2}$$

where Jm_{amm} is in μmol cm^{-2} h^{-1}, where $Tm_{amm}f$ and $Tm_{amm}i$ are final and initial ammonia concentrations (μmol L^{-1}) in the mucosal saline, Vmi and Vmf are initial and final volumes of mucosal saline (L). Positive Jm_{amm} fluxes were out of the mucosal saline; negative Jm_{amm} fluxes were into the mucosal saline.

Total tissue ammonia production rates (Jt_{amm})

$$Jt_{amm} = Js_{amm} - Jm_{amm} \qquad \text{Equation 3}$$

Jt (μmol cm^{-2} h^{-1}) represents the net rate of endogenous production of ammonia by the gastric or intestinal tissue itself. Positive Jt_{amm} values represent net production and negative Jt_{amm} values represent net consumption of ammonia by the tissue.

Partial pressure of ammonia (PNH_3) and concentration of ammonium ions ($[NH_4^+]$)

$$[NH_3] = \frac{T_{amm} \times \text{anti}\log(pH - pK')}{1 + \text{anti}\log(pH - pK')} \qquad \text{Equation 4}$$

$$P_{NH3} = \frac{[NH_3]}{\alpha NH_3} \qquad \text{Equation 5}$$

$$NH_4^+ = T_{amm} - [NH_3] \qquad \text{Equation 6}$$

The PNH_3 (μmm Hg) was calculated from total ammonia and pH measurements using pK' and αNH_3 constants from Cameron and Heisler (1983). The initial PNH_3 gradient was calculated using measured Tamm and pH measured from both mucosal and serosal saline collected before the flux period.

6.3.3 Ammonia analytical methods

Mucosal samples were deproteinized using ice-cold 20 % perchloric acid (PCA) then pH-neutralized using 1 mM KOH before the ammonia assay was run to prevent potential protein interference with the assay. Quantification of ammonia in the deproteinized mucosal salines and chyme samples were performed with a commercial kit (Raichem Cliniqa™; glutamate dehydrogenase method; 340 nm). It proved unnecessary to deproteinize the serosal samples, and these were analyzed using a colorimetric assay (Verdouw et al., 1978).

6.3.4 Rh proteins and NKCC mRNA expression

Expression of rhesus glycoprotein types b (Rhbg) and c (Rhcg1 and Rhcg2) and NKCC genes in GIT tissues of fed rainbow trout were investigated. Animals were fed within 48 h prior to tissue sampling and euthanized by an overdose of buffered MS-222 (0.07 g L^{-1}). The stomach, anterior, mid, and posterior intestine tissue samples were collected in 5 volumes of RNAlater (ThermoFisher, AM7021, Waltham, MA, USA) and kept overnight at 4 ˚C before storage at -80 ˚C until use.

Tissues were homogenized using a Bullet Blender Storm 24 bead beater (Next Advance, Troy, NY, USA) with Precellys ceramic (zirconium oxide) beads (Bertin Corp., Rockville, MD, USA). mRNA was extracted according to the recommended protocol using Qiagen RNeasy mini kit (Qiagen, 74106, Germantown, MD, USA). Total RNA was quantified and assessed for purity using a Nanodrop 2000 (ThermoFisher, EN0521, Waltham, MA, USA). Samples were treated with DNase 1 (ThermoFisher, EN0521, Waltham, MA, USA) and cDNA was synthesized from 0.5 ng total RNA using RevertAid Reverse Transcriptase (ThermoFisher, EP0441, Waltham, MA, USA) and random hexamer primers (ThermoFisher, SO142, Waltham, MA, USA). Before

use in the qPCR reaction, cDNA was diluted 5 times in molecular water (ThermoFisher, BP28191, Waltham, MD, USA).

Quantitative real-time PCR (qPCR) was performed using 2X Maxima SYBR Green/ROX qPCR Master Mix (ThermoFisher, K0221, Waltham, MA, USA) on the CFX96™ real-time system qPCR machine (Bio-Rad) and primers listed in Table 1. Primer specificity was confirmed *via* gel electrophoresis in preliminary experiments on pooled gill samples. The qPCR protocol consisted of 40 cycles of 15 s at 95 ˚C for denaturation and 1 min at 60 ˚C for annealing. Melt-curve analysis confirmed production of single amplicon product in all cases. β-actin expression did not vary between tissues and was used for normalization. To ensure residual genomic DNA was not amplified, control samples were included in which no reverse transcriptase was added during cDNA synthesis. Reactions were set up in a final volume of 12.5 μL using 1 μL of cDNA template, 6.25 μL 2X SYBR Green Master Mix and final forward and reverse primer concentration of 200 mM for Rhbg and Rhcg2, and 400 mM for Rhcg1, NKCC, and β-actin. Expression was standardized to β-actin using the Pfaffl method (Pfaffl, 2001) and results are displayed as relative expression throughout. Standard curves generated by serial dilution of pooled rainbow trout gill cDNA were used to calculate amplification efficiencies.

6.3.5 Statistical analysis

The stomach gut sac Jm_{amm}, Js_{amm} and Jt_{amm} values were compared among all four pH treatment groups (4, 7, 8 and 9) using one-way ANOVA. Comparisons among gut sac pH treatments (7, 8 and 9; excluding pH 4 stomach gut sac) and GIT sections for initial PNH_3 gradient, Jm_{amm}, and Jt_{amm} were conducted using two-way ANOVA and *post hoc* Tukey's multiple comparison tests. In both Jm_{amm} and Jt_{amm}, there were no overall sectional effects in the

intestine gut sacs. When a two-way ANOVA was conducted with all the sections included – stomach and intestine – there was a significant effect of section in both Jm_{amm} and Jt_{amm}. The difference between stomach and intestine Jm_{amm} or Jt_{amm} was confirmed again using one-way ANOVA with pooled stomach gut sacs and pooled gut sacs of each of the intestinal sections. Pearson's correlation analysis was conducted to examine the correlation between Jm_{amm} or Jt_{amm} and gut sac PNH_3 or $[NH_4^+]$ gradients. All data were tested for normality and homogeneity of variance. In cases where these assumptions were not met, values were appropriately transformed, and the statistical analysis was repeated. The mRNA expressions were checked for outliers using Grubb's outlier test and for normality using the Shapiro-Wilk normality test. Comparison of expression levels between GIT sections were done on Ln transformed data using one-way ANOVA with *post hoc* Tukey's multiple comparison tests. A significance level of $p < 0.05$ was used in all tests. Data have been expressed as means ± SEM (N = number of fish).

6.4 Results

In chyme collected from voluntarily fed rainbow trout, we found the stomach to have the lowest pH and PNH_3, yet highest Tamm (Table 6.2). In the intestinal chyme, pH was similar in all sections, but both PNH_3 and Tamm were the lowest in the anterior intestine. Indeed, Tamm in the anterior intestine was less than 20 % of the concentration in the stomach. Thereafter, PNH_3 and Tamm values gradually increased towards the posterior intestine.

We were able to successfully modify the PNH_3 gradient across the GIT epithelia *in vitro* by manipulating the mucosal pH (Figure 6.1). There was a significant overall effect of pH treatment on PNH_3 gradient in the intestine gut sacs ($p < 0.0001$), but no effect of GIT section ($p = 0.16$) and no significant interaction ($p = 0.44$). In all three intestinal sections, the PNH_3

gradient was significantly higher at mucosal pH 9, than at pH 7 or 8. In stomach gut sacs, there was a significant overall effect of pH treatment ($p < 0.0001$), but a significant difference was observed only between pHs 4, 7, 8 *vs* pH 9. Although pH 4, 7 and 8 treatment groups were not significantly different, there was a clear stepwise increase in PNH_3 gradient with increasing pH. The PNH_3 gradient in the pH 9 treatment group was particularly high, reaching 4000-5500 µmm Hg. In the chyme collected, the PNH_3 values in the various sections of the intestine were 125-420 µmm Hg (Table 6.2). These are similar to the pH 7 and 8 treatment group PNH_3 gradients: 102-302 µmm Hg and 484-605 µmm Hg respectively. For the stomach gut sacs, the pH 4 treatment best represented the *in vivo* PNH_3 gradient as it was the closest to the stomach chyme PNH_3, (-7.4 and 0.2 µmm Hg respectively).

There was a significant overall effect of pH treatment ($p = 0.0031$) on mucosal ammonia flux rates (Jm_{amm}) in the intestinal gut sacs (Figure 6.2), but no effect of intestinal section ($p = 0.71$) and no significant interaction ($p = 0.99$). Within individual intestinal sections, however, there were no significant differences among pH treatment groups. Serosal flux rates (Js_{amm}) were generally low and highly variable (Table 6.3). There were no significant treatment, section, or interaction effects.

Similarly, within the intestinal sections, there was an overall effect of pH treatment ($p = 0.0007$) but no effect of section ($p = 0.68$) on endogenous ammonia production rates (Jt_{amm}) and no interaction ($p = 0.98$) (Figure 6.3). In stomach gut sacs, there was no overall effect of pH treatment for both Jm_{amm} ($p = 0.29$) and Jt_{amm} ($p = 0.28$). When all GIT sections were considered, excluding pH 4 stomach gut sacs, there was a significant overall effect of section for both Jm_{amm} and Jt_{amm} ($p = 0.0002$ and < 0.0001 respectively). The significant difference between the stomach and the intestine was confirmed by comparing pooled stomach values *versus* pooled values for

each of the intestinal sections ($p < 0.0001$ for both Jm_{amm} and Jt_{amm}), as indicated with asterisks in Figures 6.2 & 6.3.

The sectional difference was only observed in the pH 8 treatment group for both Jm_{amm} and Jt_{amm} (Figures 6.2 & 6.3; indicated with letters). All Jm_{amm} values were positive (out of the mucosal saline) and all Jt_{amm} values were negative (net consumption of ammonia by the tissue), except for the pH 8 intestinal gut sacs where Jm_{amm} was negative (into the mucosal saline) and Jt_{amm} was positive (net production). Thus, the pH 8 intestine gut sac Jm_{amm} and Jt_{amm} values were significantly different from those of the pH 8 stomach.

Overall, there were no significant correlations between Jm_{amm} and PNH_3 or $[NH_4^+]$ gradients (Figure 6.4; Table 6.4). When both GIT section-specific and pooled Jm_{amm} were compared to either PNH_3 or $[NH_4^+]$ gradients, all correlation coefficient values were low, between -0.42–0.38 (Table 6.4). Surprisingly, the only significant correlation was a negative one ($r = -0.250$, $p = 0.043$), rather than the expected positive relationship, for the pooled analysis of Jm_{amm} *versus* the $[NH_4^+]$ gradient.

The relative mRNA expressions of Rhbg, Rhcg1, Rhcg2 and NKCC were investigated in all sections of the GIT. There was no detectable expression of Rhbg mRNA in the stomach, but it was expressed in all three sections of the intestine (Figure 6.5). Rhcg1 mRNA was not detected in any of the GIT sections (data not shown), but Rhcg2 mRNA was expressed in the stomach and all three sections of the intestine (Figure 6.6). The NKCC mRNA was also expressed in the stomach and all three sections of the intestine (Figure 6.7). For all of these genes, expression levels were variable within sections, although less so for NKCC, and there were no significant differences among sections.

6.5 Discussion

6.5.1 Overview

Here, we investigated the potential PNH_3-dependent NH_3 transport in all sections of the GIT in freshwater rainbow trout *in vitro*, and surveyed the section-specific mRNA expression of Rh proteins as possible NH_3 transporters and NKCC as a possible NH_4^+ transporter. We found that ammonia absorption rate is not dependent on PNH_3 gradient across the GIT epithelia. However, the GIT does express Rh proteins in a section-specific manner, whereas NKCC is expressed throughout the GIT. Importantly, we found the stomach to be a significant site for ammonia absorption regardless of the PNH_3 gradient.

6.5.2 Lack of correlation between PNH_3 and ammonia flux rate

The pH treatment had an overall effect on mucosal ammonia flux rate (Jm_{amm}) and endogenous ammonia production rates (Jt_{amm}) (Figures 6.2 & 6.3), but in contrast to our hypothesis, there were no significant individual differences between pH treatment groups within the intestine sections. The pH 8 treatment in particular, which closely mimics the mucosal pH *in vivo* (Table 6.2) showed an opposite trend to other pH groups: net tissue production of ammonia, moving into the mucosal saline. This fits well with the progressive rise in chyme Tamm levels seen *in vivo* moving from the anterior to posterior intestine (Table 6.2). However, it is somewhat contradictory to previous findings where fed intestinal tissues were shown to have increased ammonia production rates that were followed by an increased efflux rate to the serosal solution (Rubino et al., 2014; Jung et al., 2021; Chapter 5). However, these studies measured the serosal flux rates over a much longer time period (2 h) than in the present study (0.5 h). Due to the limitations of buffering, we were only able to measure ammonia transport over this short flux

time, which provided good resolution for mucosal flux rates, where the volume is only a few ml but not for serosal flux rates where the volume is up to 80 ml. This probably explains the observed variability in Js_{amm} values (Table 6.3). In addition, recent evidence shows that bacteria inhabiting the lumen are involved in ammonia detoxification (Turner and Bucking, 2019). In the mucosal pH 8 treatment, which represents the most physiologically realistic pH condition (Table 6.2), enterocytes may be transporting ammonia apically to the bacteria in the lumen for a support in ammonia detoxification.

Contrary to our initial hypothesis, we found no correlation between Jm_{amm} and the PNH_3 gradient, either in individual GIT sections or overall (Figure 6.4A; Table 6.4). Perhaps this low permeability to NH_3 serves to prevent large influx of ammonia into the bloodstream as NH_3 is a neurotoxin at high concentrations (Chew et al., 2005). Similarly in mammals, it has been reported that several cell types in the GIT and urinary tracts have low permeability to NH_3 possibly to prevent high luminal ammonia from entering the vascular system (reviewed by Marcaggi and Coles, 2001). Rather than an energy-expensive investment in detoxification of the absorbed ammonia, a selectively permeable membrane is likely favourable in mitigating potentially lethal increases in plasma ammonia. In fact, the GIT of the weather loach (*Misgurnus anguillicaudatus*) under terrestrial conditions can serve as an ammonia excretion site when the fish cannot rely on its skin to volatilize ammonia (Tsui et al., 2002).

6.5.3 Expression of ammonia transport proteins in the intestine

Despite ammonia transport occurring independent of the PNH_3 gradient, both Rhbg (Figure 6.5) and Rhcg2 (Figure 6.6) were expressed at the mRNA level in the intestine, whereas Rhcg1 expression was undetectable. This expression pattern is consistent with findings in

mammals (Handlogten et al., 2005), but only to some degree with a previous study on rainbow trout where only Rhbg and neither Rhcg1 or Rhcg2 were expressed in the intestine (Nawata et al., 2007). The animals investigated in Nawata et al. (2007) were fasted for 7 days whereas the fish in our study were fed within 48 h prior to sampling, suggesting Rhcg2 upregulation may occur in response to feeding. In the intestines of both fasted ureotelic toadfish and ammoniotelic plainfin midshipman, Rhbg, Rhcg1 and Rhcg2 were all present as detected by immunohistochemistry (Bucking et al., 2013b), suggesting species-specific expression of Rh isoforms. The differences in expression of Rh isoforms among previous studies and the present study suggest that the regulation of these proteins likely depends on feeding condition and species, which will be an interesting area for future research.

The Rh proteins are known to be involved in PNH_3 gradient-dependent NH_3 movement across fish gills (reviewed by Weihrauch et al., 2009; Wright and Wood, 2009, 2012) and in excreting ammonia through the skin in mangrove killifish (Hung et al., 2007). However, the functional role of Rh proteins in the fish GIT yet remains uncertain. Although the majority of evidence suggests an ammonia transport function of the Rh proteins both in mammals (Weiner and Hamm, 2007) and fish (Nawata et al., 2010) or possibly an ammonia-sensing function (Weiner, 2006), some studies suggest that they may not be involved in ammonia transport at all (Chambrey et al., 2005; Chambrey et al., 2006). In addition, fish possess more copies of Rh genes compared to mammals (Huang and Peng, 2005), and only some of them were studied here. Future investigations should examine the expression of a wider range of Rh genes as a function of feeding regime.

This study also found a lack of correlation between Jm_{amm} and the $[NH_4^+]$ gradient (Figure 6.4B) despite consistent expression of NKCC in all sections of the GIT (Figure 6.7).

NKCC, along with K^+ channels, have been identified as possible pathways for the absorptive transport of NH_4^+ in the intestine of rainbow trout (Rubino et al., 2019). In the mammalian GIT, it is speculated that the NKCC is involved in secretion rather than absorption to prevent ammonia levels from rising too high in the portal bloodstream (Worrell et al., 2008). The situation is unknown in fish, but some ammonia is absorbed into the portal bloodstream (Karlsson et al., 2006) and recent findings suggest that this occurs in the anterior region of the GIT, including the stomach (Chapter 4). Note in Table 6.2, the large "disappearance" of ammonia from the chyme between the stomach and the anterior intestine.

Finally, it should be noted that conclusions about the lack of correlation between Jm_{amm} and $[NH_4^+]$ gradient should be taken with caution. The analysis done in this study is an oversimplification of the system, as only the chemical gradient was calculated, whereas the electrochemical gradient, taking into account the transepithelial potential as well as the NH_4^+ concentration difference, is the true driving force for diffusion of NH_4^+ (Wood and Nawata, 2011). Additionally, if transporters (e.g. NKCC) are involved, they may be regulated and therefore not respond in a simple manner to changes in the chemical gradient. In fact, although significant (p = 0.043), the low and negative correlation coefficient (r = -0.250) observed between Jm_{amm} values of all GIT sections in comparison to the simultaneous $[NH_4^+]$ gradients (Table 6.4) indicates that a more thorough investigation is required.

6.5.4 Ammonia handling by the stomach

Perhaps the most interesting observation of this study was the role of the stomach in absorbing ammonia, regardless of the pH, and regardless of the PNH_3 gradient. There was no overall effect of intestinal section on the Jm_{amm} and Jt_{amm}, but the stomach gut sacs in all pH

treatment groups showed the highest Jm_{amm} (Figure 6.2) and the most negative Jt_{amm} values – i.e. net consumption of ammonia (Figure 6.3). This fits well with the large decline in chyme Tamm between the stomach and the anterior intestine (Table 6.2). Our results agree with our initial hypothesis of the pronounced role of the stomach in absorbing and transporting ammonia. This functional zonation of the GIT also agrees with the recent *in vivo* findings where, after feeding, no change in Tamm was observed in the subintestinal vein draining the posterior intestine, but an increase was observed in the HPV (Chapter 4).

However, our prediction that Rh proteins would be more expressed in the anterior region of the GIT was not supported, as there were no significant differences between GIT sections. We found expression of Rhcg2 in the stomach, but not Rhbg, the latter in contrast to findings by Bucking and Wood (2012) on rainbow trout. The Rhbg expression in the stomach could have been downregulated by the time of sampling of this study (approximately 48 h postprandial) as solid chyme is moved down to the intestine by 8 h postprandial (Bucking and Wood, 2009). However, the positive expression of Rhcg2 in the intestine compared to 7-day fasted rainbow trout (Nawata et al., 2007) implies fish in this study were undergoing postprandial changes within the sampling time. Additionally, these Rh proteins may not be exclusively localized to either apical or basolateral membranes in mammals (reviewed by Weiner and Hamm, 2007), thus Rhbg could also be expressed on the apical membrane. In fact, Rhbg that is expressed in the basolateral membrane of the villi in plainfin midshipman (*Porichthys notatus*), is not expressed in the villi but in other tissue layers in gulf toadfish (*Opsanus beta*) (Bucking et al., 2013b), suggesting species-dependent localization of Rh isoforms. Nonetheless, the expression of Rhcg2 as well as NKCC as a possible NH_4^+ transporter (Figure 6.7) in the stomach support the hypothesis that stomach could be a site of ammonia absorption.

A basic mechanism to avoid ammonia toxicity, is “ammonia trapping” into glutamine by glutamine synthetase (GS) (Hakvoort et al., 2017). This can also start the process of synthesis of other amino acids by transamination. A distinct distribution pattern of GS activity has been observed in the fish GIT: it is highest in the stomach and posterior region of the intestine of different fish species including the rainbow trout (Anderson et al., 2002; Mommsen et al., 2003a). Following feeding, GS activity increases only in the posterior intestine of rainbow trout (Bucking and Wood, 2012). In mammals, higher GS activity is found in the stomach yet very low activity occurs in the small intestine (James et al., 1998; Remesar et al., 1985). Interestingly, in the sleeper fish (*Bostrichthys sinensis*), exposure to ammonia increased GS activity, GS protein and mRNA levels in all tissues including intestine except the stomach (Anderson et al., 2002). GS expression in rodent stomach is controlled by different mechanisms than in the intestine (Lie-Venema et al., 1998). However, this may not be the case in fish (Mommsen et al., 2003a) equipped with more complex GS subunits (Murray et al., 2003).

In addition to GS, other metabolic enzymes such as glutamate dehydrogenase (GDH) also display distinct zonation in the GIT tissues (Mommsen et al., 2003b). GDH, an enzyme that can also fix ammonia to make glutamate, increases in activity in the anterior intestine after feeding in rainbow trout (Rubino et al., 2014). The same was observed in marble goby (*Oxyeleotris marmorata*), where feeding increased both GS and GDH activities in the intestine tissues followed by increased in glutamate content (Tng et al., 2008). Interestingly, intestine tissue ammonia did not increase following feeding, and the authors calculated approximately 70 % of the ingested nitrogen was converted to glutamate to avoid postprandial ammonia toxicity and retained for somatic growth, and the rest was excreted to the environment (Tng et al., 2008). The situation is not clear for the stomach, but there is higher activity of GDH in the intestine than the

stomach (Mommsen et al., 2003b). Additionally, fed rainbow trout intestine tissues are found to have the capacity to produce urea likely *via* direct arginolysis (Jung et al., 2021; Chapter 5). Whether the stomach tissues are also able to produce urea is unknown, but urea level in the HPV plasma increases following feeding (Karlsson et al., 2006). These data along with the current findings indicate that different sections of the GIT have distinct roles in ammonia handling and transport, with the stomach specifically serving as an important site for ammonia absorption for the synthesis of glutamine, glutamate, and possibly other amino acids or urea, and transporting some ammonia to the portal blood to be processed by the liver, gill and other tissues.

6.5.5 Conclusion

Here we have provided an *in vitro* investigation of ammonia transport capacity and further describe patterns of Rhbg, Rhcg1, Rhcg2 and NKCC transporter mRNA expression along the GIT of rainbow trout. We found that the absorption of ammonia is not dependent on the PNH_3 or $[NH_4^+]$ gradient, although the latter in particular requires further investigation. Our findings suggest that an in-depth investigation of other isoforms of Rh proteins and the functional zonation of the GIT in absorbing ammonia, exporting it the portal bloodstream, and metabolizing it to amino acids, would be an exciting future research project.

Table 6.1 Primers used for qPCR

Gene	Accession no.; Reference	Forward sequence (5'-3')	Reverse sequence (5'-3')
Rhbg	EF051114; Nawata et al., 2007	CGACAACGACTTTTACTACCGC	GACGAAGCCCTGCATGAGAG
Rhcg1	EF051115; Nawata et al., 2007	CATCCTCAGCCTCATACATGC	TGAATGACAGACGGAGCCAATC
Rhcg2	AY619986.1; Eom et al., 2020	GGTAGTCTGCTTCGTCTGGC	TCATGGGCCTTGGTCTCTAC
NKCC	DQ864492; Rubino et al., 2019	AACTTTGTGGATCCGAGTGG	TATCAGCTTGTCCCCCAGAG

Table 6.2 pH, total ammonia (Tamm; mM), and calculated PNH_3 (μmm Hg) of chyme collected from different GIT sections. Letters that differ indicate statistically significant differences among sections. Values are means ± SEM (N = 16-19).

	Stomach	Anterior intestine	Mid intestine	Posterior intestine
pH	3.7 ± 0.1 [a]	7.9 ± 0.1 [b]	8.0 ± 0.1 [b]	8.0 ± 0.1 [b]
Tamm (mM)	3.5 ± 0.2 [a]	0.6 ± 0.1 [b]	0.8 ± 0.2 [b]	1.1 ± 0.2 [b]
Chyme PNH_3 (μmm Hg)	0.2 ± 0.1 [a]	125 ± 21 [b]	235 ± 48 [b]	420 ± 99 [b]

Table 6.3 Serosal ammonia flux rates (Js_{amm}; μmol cm^{-2} h^{-1}) of gut sacs loaded with pH-controlled mucosal saline containing 1 mM of NH_4OH. Values are means ± SEM (N = 5-7). There were no significant treatment, section, or interaction effects.

	Stomach	Anterior intestine	Mid intestine	Posterior intestine
pH 4	0.008 ± 0.028	-	-	-
pH 7	0.028 ± 0.015	0.002 ± 0.007	0.053 ± 0.049	0.007 ± 0.025
pH 8	0.016 ± 0.023	0.024 ± 0.027	0.089 ± 0.057	0.027 ± 0.041
pH 9	0.005 ± 0.002	0.018 ± 0.011	-0.002 ± 0.006	0.001 ± 0.003

Table 6.4 Pearson's correlation coefficient (r), p values, and the number of XY pairs between Jm_{amm} and PNH_3 or $[NH_4^+]$ gradient for each of the GIT sections and all sections combined tested in Figure 6.4.

Comparison		Stomach	Anterior intestine	Mid intestine	Posterior intestine	GIT sections combined
Jm_{amm} *vs* PNH_3 gradient	r	0.378	0.076	0.240	0.123	0.026
	p	0.183	0.779	0.371	0.704	0.840
	Number of XY pairs	14	16	16	12	58
Jm *vs* $[NH_4^+]$ gradient	r	-0.210	-0.229	-0.408	-0.422	-0.250
	p	0.472	0.394	0.117	0.151	0.043
	Number of XY pairs	14	16	16	13	59

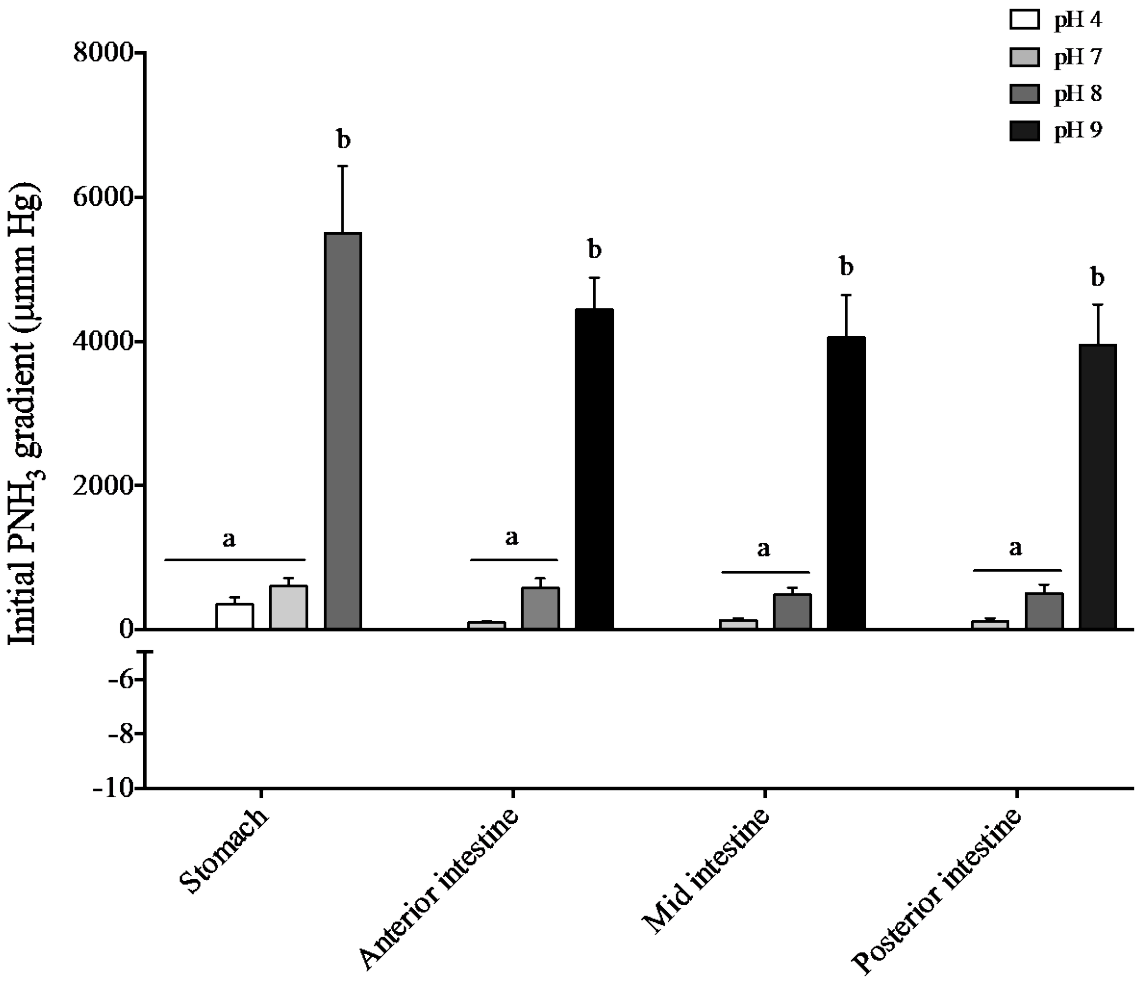

Figure 6.1 Initial PNH_3 gradient (µmm Hg) across the epithelia of gut sacs loaded with pH-controlled mucosal saline containing 1 mM of NH_4OH. Values are means ± SEM (N = 4-7). Letters that differ indicate statistically significant differences among pH treatment groups within each GIT section.

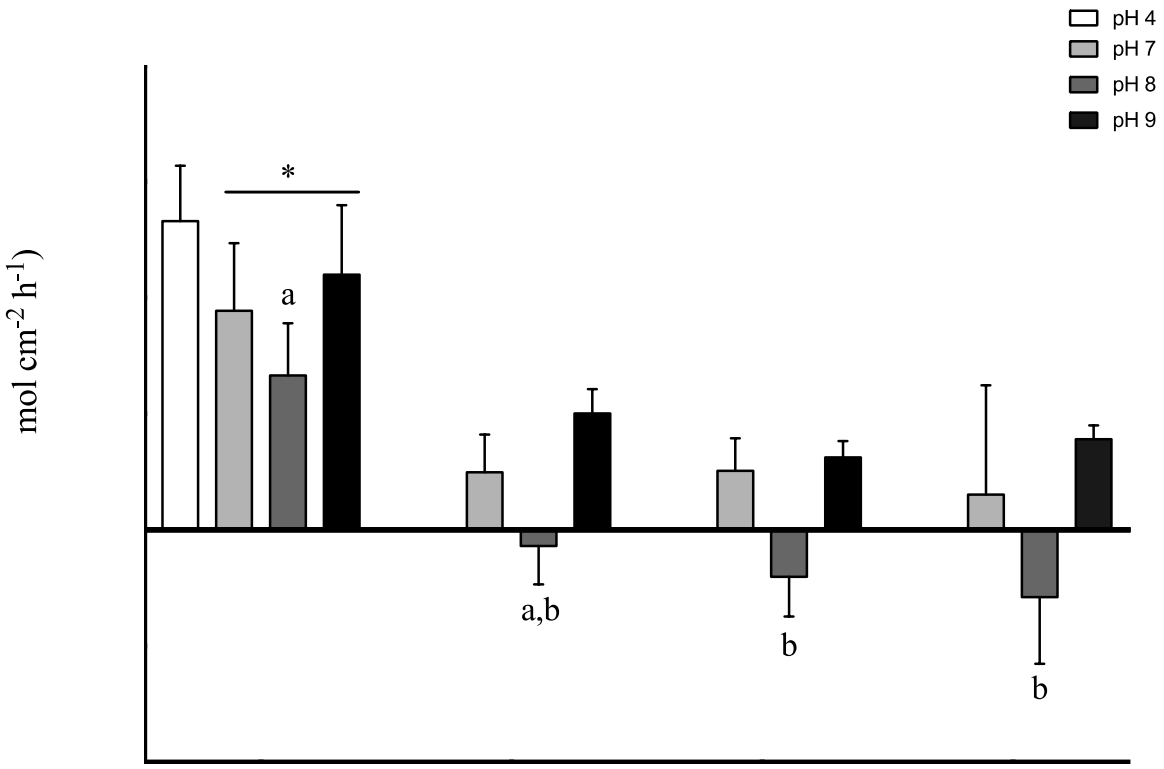

Figure 6.2 Mucosal ammonia flux rates (Jm_{amm}; μmol cm^{-2} h^{-1}) of gut sacs loaded with pH-controlled mucosal saline containing 1 mM of NH_4OH. Values are means ± SEM (N = 4-7). Positive values indicate net absorption from the lumen, negative values indicate net secretion into the lumen. There were no differences among pH treatment groups in the stomach gut sacs. There was no overall sectional effect on Jm_{amm} in the intestine gut sacs, but a significant effect was observed when stomach gut sacs were included. An asterisk indicates the stomach value differs significantly from all of the intestine gut sacs. Letters that differ indicate statistically significant differences among GIT sections within the same pH treatment group.

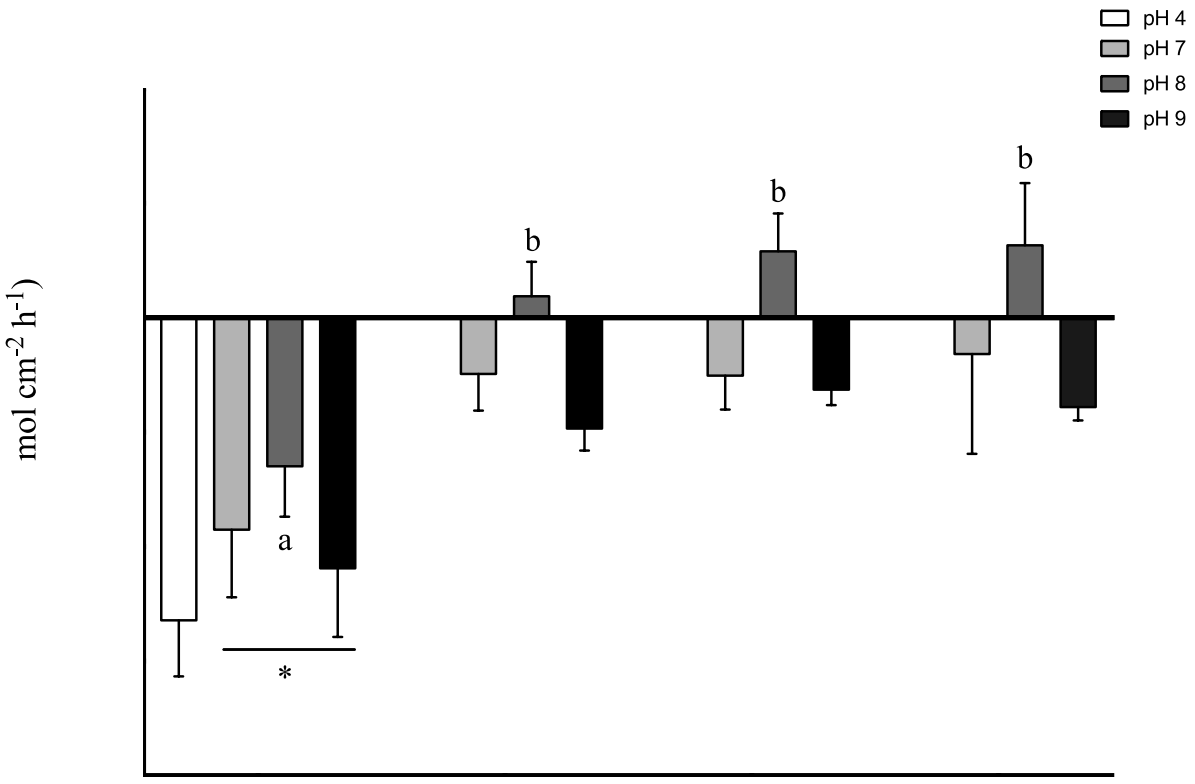

Figure 6.3 Total endogenous ammonia production rates (Jt_{amm}; μmol cm^{-2} h^{-1}) of gut sacs loaded with pH- controlled mucosal saline containing 1 mM of NH_4OH. Values are means ± SEM (N = 4-7). Positive values indicate net production, negative values indicate net consumption. There were no differences among pH treatment groups in the stomach gut sacs. There was no overall sectional effect on Jt_{amm} in the intestine gut sacs, but a significant effect was observed when stomach gut sacs were included. An asterisk indicates the stomach value differs significantly from all of the intestine gut sacs. Letters that differ indicate significant differences among GIT sections within the same pH treatment group.

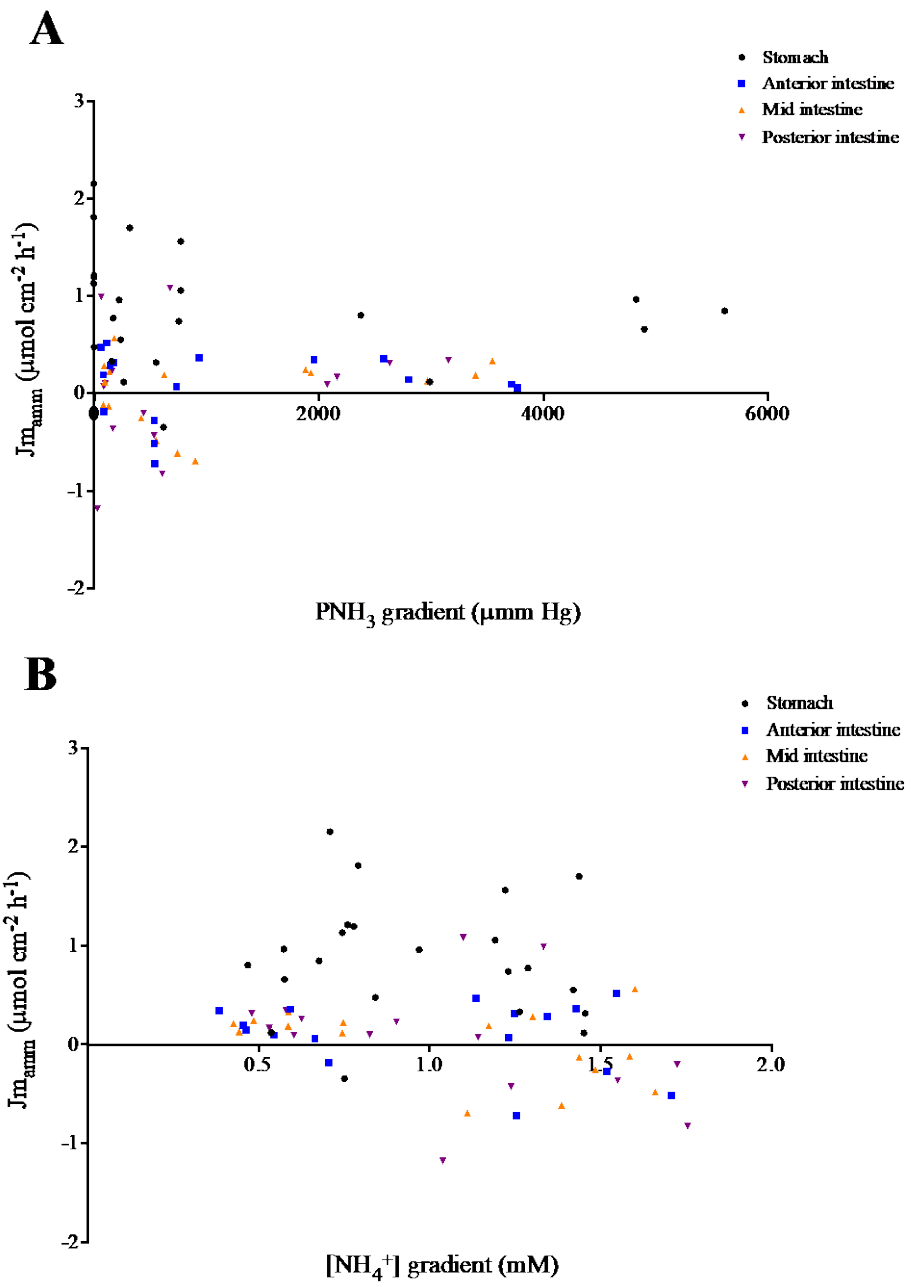

Figure 6.4 Mucosal ammonia flux rates (Jm_{amm}; µmol cm^{-2} h^{-1}) plotted against **(A)** PNH_3 gradient (µmm Hg) or **(B)** $[NH_4^+]$ gradient (mM). PNH_3 and NH_4^+ gradients were calculated using measured Tamm and pH. The Jm_{amm} values were reported in Figure 6.2. Values are means ± SEM (N = 58-59). For all data, there was no significant correlation between Jamm and either PNH_3 or $[NH_4^+]$ gradients (statistical details reported in Table 6.4).

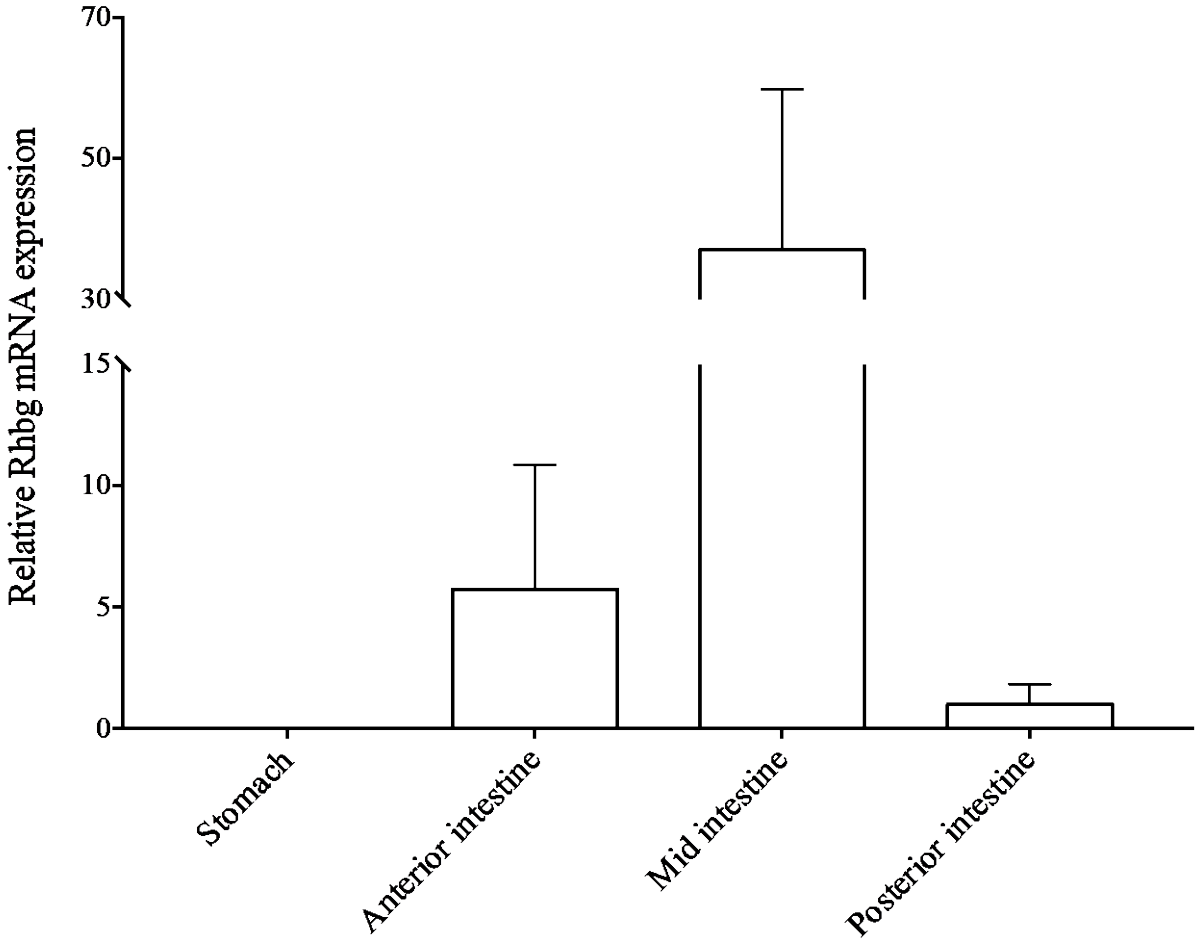

Figure 6.5 Relative (posterior intestine = 1) mRNA expression of Rhbg (normalized to β-actin) in different GIT sections in rainbow trout. Bars indicate means ± SEM (N = 5-6). There were no significant differences among GIT sections.

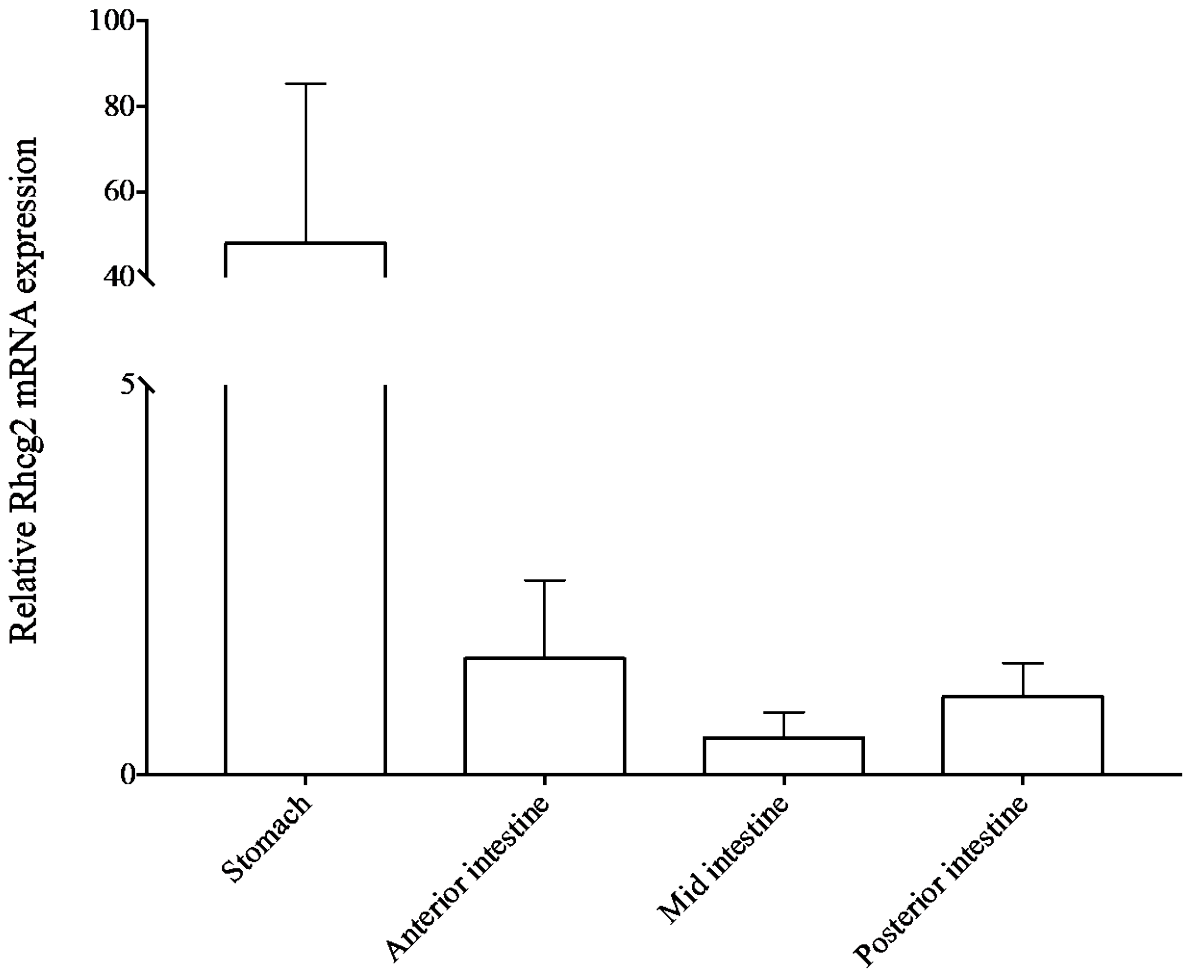

Figure 6.6 Relative (posterior intestine = 1) mRNA expression of Rhcg2 (normalized to β-actin) in different GIT sections in rainbow trout. Bars indicate means ± SEM (N = 5-6). There were no significant differences among GIT sections.

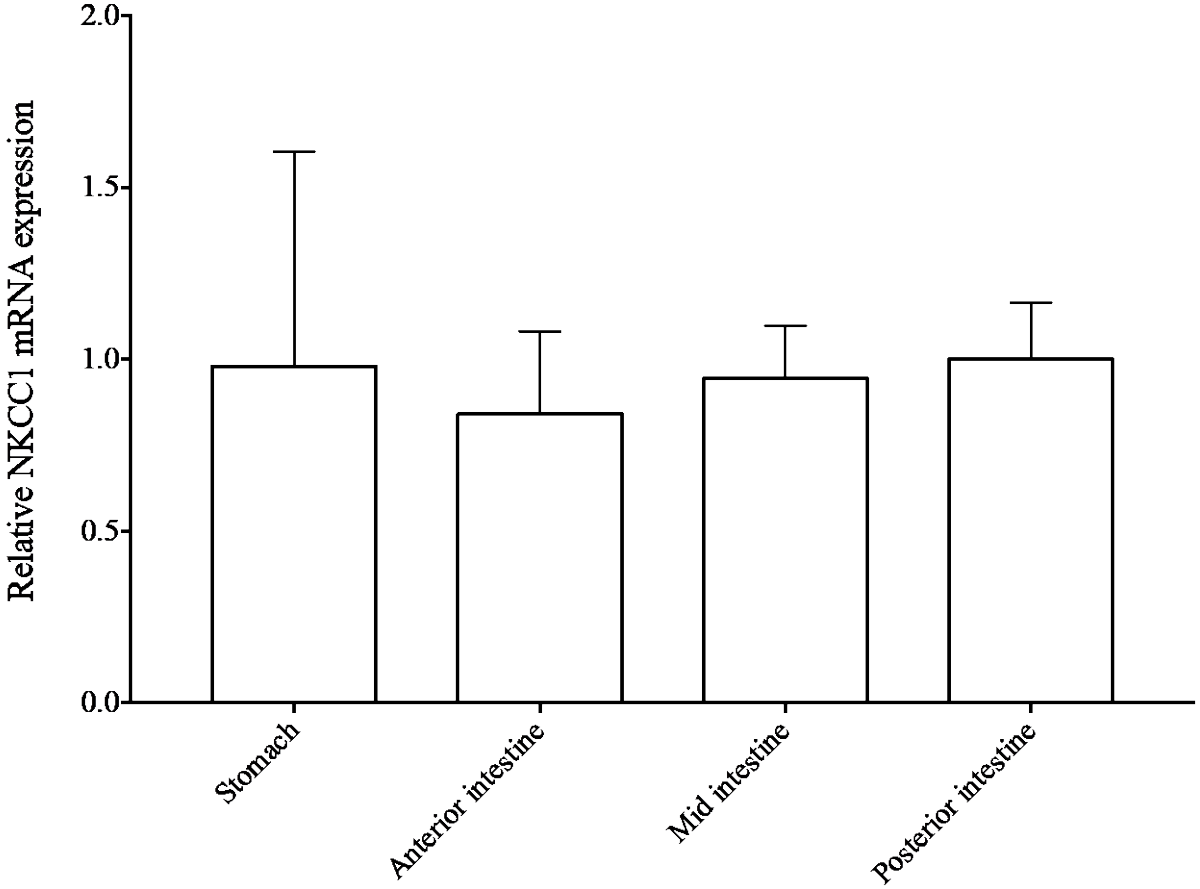

Figure 6.7 Relative (posterior intestine = 1) mRNA expression of NKCC1 (normalized to β-actin) in different GIT sections in rainbow trout. Bars indicate means ± SEM (N = 5-6). There were no significant differences among GIT sections.

Chapter 7: General discussion and conclusions

The overarching goal of my thesis was to expand our knowledge about the physiology of the three respiratory gases in the gastrointestinal tract (GIT) and their potential for equilibration with the vascular system supplying and draining the GIT in teleost fish, and associated changes with feeding and osmoregulatory roles. My thesis has shown that both FW rainbow trout (Chapters 3, 4, 5 & 6) and SW English sole (Chapters 2 & 3) have nearly anoxic, hypercapnic and high ammonia environments in the GIT lumen in both fasting and fed conditions, and that the GIT epithelia largely regulates the diffusion of these three respiratory gases into the vascular system. The thesis also gives insight into the nitrogenous product handling and transport of the intestinal tissues and the previously overlooked function of the stomach in transporting ammonia. In this general discussion, I have integrated the major findings from my thesis, described how my research extends the current knowledge on GIT gas exchange and provided some considerations for future research.

7.1 **Critique of methods**

While each technique used in this thesis contributed significantly to the understanding of GIT gas exchange and function in fish, there are challenges and limitations associated with each. I have discussed these in more detail in each Chapter, but here I have summarized all in brief.

The *in situ* measurements of luminal and blood parameters used in Chapters 2 and 3 involved working with fish that were artificially ventilated under anaesthesia, which likely would have had some influence on the blood gases (Guo et al., 1995; Iwama et al., 1989). The direct insertion of micro-optodes may have interfered with the blood flow, which is implied by the

variability in the SIV PCO_2 data in both species in Chapters 2 and 3, and confirmed by *in vivo* measurements in Chapter 4.

In Chapter 2, the difference between the traditionally used calculated PCO_2 and the new directly measured PCO_2 was addressed. However, due to the limited number of PCO_2 micro-optodes available, and their susceptibility to damage by high luminal PCO_2 levels, calculated luminal PCO_2 values based on measurements of chyme pH and TCO_2 were used in Chapter 3. Although quantitative luminal PCO_2 values obtained by this method should be interpreted with caution, species comparisons, which were the focus of the Chapter, are valid regardless since in both species PCO_2 values were obtained using the same technique. Furthermore, the insignificant difference between the species was confirmed by comparing the directly measured luminal PCO_2 of rainbow trout in both fasting and fed states to previous direct measurements from the literature (Wood and Eom, 2019).

Chapter 4 addressed these limitations of *in situ* techniques by sampling blood from indwelling catheters in a non-anesthetised rainbow trout. However, this technique involves fairly invasive surgeries that have been shown to have an effect on blood parameters such as pH, TCO_2 and $[HCO_3^-]$ (Eliason et al., 2007). The majority of such post-surgery stress effects are ameliorated within 1-2 days (Eliason et al., 2007), but the fish used in this thesis were fitted with 2 indwelling blood vessel catheters (DA and SIV) as well as a feeding tube that can exert additional stress. Nonetheless, these surgeries are necessary in sampling blood with the least disturbance so as to obtain the most physiologically reliable parameters, and therefore have been used in other GIT vascular studies (e.g. Cooper et al., 2014; Karlsson et al., 2006b) .

In Chapters 5 and 6, *in vitro* gut sac preparations were used to further explore some of the interesting findings from the previous Chapters. As discussed by Wood and Bucking (2010), gut

sacs are widely used in GIT work in fish (i.e. Rubino et al., 2014, 2019; Wood et al., 2019; Goodrich et al., 2020), providing relatively simple experimental preparations that allow efficient testing of a number of different treatments such as glutamine, ammonia and pH-adjusted mucosal saline loadings that were used in this thesis. It was also an advantageous technique to use in my thesis to explore possible section-specific differences in nitrogen handling and transport. However, one of the disadvantages of gut sacs is that they are not perfused with blood. *In vitro* preparations lack the hormonal, neural, chemical, and mechanical signals present *in vivo*, along with other endogenous components of the GIT such as chyme and microbiome. Other traditional *in vitro* preparations such as Ussing chambers (Ussing, 1949) suffer from many of the same shortfalls as gut sacs. The typical gas levels used for gut sacs (99.7 or 99 % O_2: 0.3 or 1 % CO_2) are also quite different from *in vivo* situations. Indeed, findings from Chapters 2, 3 and 4 illustrated that both the mucosal and serosal PO_2 are significantly lower *in vivo*, especially the lumen PO_2, than in the *in vitro* preparation. Furthermore, the lack of correlation between [NH_4^+] gradient and ammonia transport in Chapter 6 needs to be followed up with electrophysiological studies to understand the mechanisms of NH_4^+ transport (Loretz, 1995). Despite these shortcomings, the technique has produced a lot of new findings in this thesis that can lead to many new future research areas.

7.2 **Anoxic, hypercapnic and high ammonia environment in the lumen in both FW and SW species, in both fasting and fed states**

Prior to my studies, no comprehensive investigation into the gas profiles in the GIT lumen of teleost fish had been performed. Without this knowledge, it was impossible to decipher gas exchange across the GIT epithelia. Thus, Chapters 2 and 3 laid the groundwork with direct

insertion of PO_2 and PCO_2 micro-optodes into the lumen for more accurate measurements, in combination with *in situ* sampling of the chyme for ammonia and calculated PCO_2 levels in rainbow trout and English sole.

Prior to this thesis, there was no knowledge of the PO_2 profile of the lumen in fish. The lumen of the mammalian GIT remains virtually anoxic (Bettinger, 2015; Kalantar-Zadeh et al., 2019; Kurbel et al., 2006), due to the respiration of inhabiting microbes (Espey, 2013) and the oxidative chemistry of the GIT fluids (Friedman et al., 2018). Using PO_2 micro-optodes *in situ*, I discovered for the first time that both fish species also have comparable nearly anoxic lumens (< 1 mm Hg), a level which remains undisturbed regardless of feeding. Whether mechanisms similar to those of mammals cause the low PO_2 in teleosts remains to be investigated.

Despite the osmoregulatory function of the GIT in SW teleosts (Grosell, 2011; Guffey et al., 2011; Wood et al., 2010), the SW English sole had comparable and high calculated luminal PCO_2 levels to the FW rainbow trout (stomach: 112-115 mm Hg; intestine: 20-38 mm Hg in both species). A recent fabrication of a needle-type fibre-optic PCO_2 micro-optode, similar in size to the PO_2 micro-optode, allowed a direct measurement of the luminal PCO_2 *in situ* in English sole. The directly measured PCO_2 in the lumen was ~14 mm Hg in the stomach and ~17 mm Hg in the intestine in fasted animals (Chapter 2). Feeding increased the levels to ~49 and ~47-50 mm Hg respectively. These are similar to direct measurements of 7-13 mm Hg in fasted and 20-41 mm Hg in fed rainbow trout by Wood and Eom (2019). Overall, my results indicate no significant differences in luminal PCO_2 between the two species regardless of feeding status, and similar to the rainbow trout results in Wood and Eom (2019), feeding elevates the luminal PCO_2 in English sole.

The third respiratory gas for fish, ammonia (Randall and Ip, 2006), has previously been measured to be high in the chyme owing to protein catabolism (Bucking and Wood, 2012; Rubino et al., 2014). However, the stomach has generally been overlooked in ammonia handling abilities and thus there appear to be no previous measurements of stomach chyme ammonia concentrations in teleost fish. In my thesis, I measured the luminal Tamm in the chyme collected from the entire GIT including the stomach of both species. The stomach was found to have high Tamm (2179-3709 μM), but very low PNH_3 (0.1-5.5 μmm Hg) in both species (Chapter 3). The latter reflected the low gastric pHs (3.6-4.7) in both species. There were some species differences where rainbow trout had lower intestinal Tamm than English sole (415-1096 *vs* 2639-3061 μM respectively), yet stomach Tamm was significantly higher (2179 vs 3709 μM respectively) in the rainbow trout. However, due to the constraint of different feeding habits, these two species were given different feeds in differing amounts. This may have had an effect on the results.

Altogether, results from Chapters 2 and 3 revealed the lumen of both species to be virtually anoxic, hypercapnic and high in ammonia. Feeding exacerbated the luminal PCO_2 and Tamm, reaching levels that, if present in water, would be considered toxic (Ou et al., 2015; Randall and Tsui, 2002; Solbé and Shurben, 1989). However, no changes in luminal PO_2 levels associated with feeding were observed. An interesting yet challenging issue emerging from these two chapters was the extent of equilibration of respiratory gases between the lumen and the vascular system. Data collected by means of direct insertion of the micro-optodes into the SIV were variable, possibly due to an interference with the blood flow and anaesthesia. In addition, obtaining enough blood samples from the SIV for ammonia analysis was not feasible due to low blood pressure in anaesthetized fish. Thus, in Chapter 4, I investigated whether the luminal PO_2, PCO_2 and ammonia were reflected in the blood draining the GIT *in vivo*, as discussed below.

7.3 **GIT epithelial barrier: lack of equilibration of PO_2, PCO_2, and ammonia between the lumen and the bloodstream in FW rainbow trout**

The few previous measurements of venous blood PCO_2 draining from the GIT are low (Cooper et al., 2014; Eliason et al., 2007) and variable (Wood and Eom, 2019). Similarly, the findings in Chapters 2 and 3 were also variable and inconclusive as to whether the extreme luminal PO_2 and PCO_2 are equilibrating with the blood draining the GIT. However, plasma Tamm of blood sampled from the HPV increased in response to feeding in rainbow trout (Karlsson et al., 2006), which suggested a postprandial ammonia absorption from the lumen. In Chapter 4, I further investigated the potential equilibration of PO_2, PCO_2 and ammonia between the lumen and the vascular system of rainbow trout, and the possible functional zonation of GIT sections in ammonia absorption. This was accomplished by sampling blood from indwelling catheters in the DA and SIV near the posterior intestine in a non-anaesthetized rainbow trout throughout the 48-h digestion period. Additionally, both SIV and HPV blood were sampled from anaesthetized fish following voluntary feeding in order to analyze plasma Tamm. Overall, the SIV remained undisturbed with limited equilibration of PO_2, PCO_2 and ammonia between the lumen and the blood (Figure 7.1), but there was evidence of ammonia transport possibly occurring in the anterior region of the GIT as HPV Tamm increased following feeding.

While fish underwent an alkaline tide after feeding, there was no indication of compensatory hypoventilatory CO_2 retention seen in air breathing vertebrates (reviewed by Wang et al., 2001). Instead, feeding stimulated an increase in P_aO_2 within the first 4 h of a meal. This fits with recent measurements of increased ventilatory water flow after feeding in rainbow trout (J. Eom and C.M. Wood, unpublished results). It is now evident that fish compensate the

postprandial metabolic base load by excreting HCO_3^- *via* branchial Cl^-/HCO_3^- exchange mechanisms (Bucking and Wood, 2008; Tresguerres et al., 2007; Wood et al., 2005; Wood et al., 2007) and to a lesser extent *via* the kidney (Bucking et al., 2010). Importantly, the SIV P_vO_2 was significantly higher than the luminal PO_2 and did not change following feeding, indicating a lack of equilibration. In humans, systemic hypoxemia can downregulate many of the GIT transporters (Ward et al., 2014), hindering its functions in assimilation and absorption. The multifunctional GIT of fish (Grosell et al., 2011) also possesses many of the same transporters as in the human GIT, and so may be maintaining its bloodstream PO_2 to avoid such challenges. Thus, mechanisms appear to be present to prevent hypoxia such as increases in blood flow rate. Indeed, to meet the postprandial increase in GIT O_2 requirement, blood flow is increased and redistributed to the GIT (Axelsson and Fritsche, 1991; Axelsson et al., 1989; Axelsson et al., 2000; Eliason et al., 2008; Thorarensen and Farrell, 2006).

Similarly, the high luminal PCO_2 was also not reflected in the SIV even during digestion. In mammals, some of the luminal CO_2 is absorbed to the blood, breathed out (Ghoos et al., 1993), removed by microbes, and/or released as flatulence (Lacy et al., 2011; Ohashi et al., 2007; Oliphant and Allen-Vercoe, 2019). To large extent, the luminal epithelia in higher vertebrates appear to have limited permeability allowing only a small percentage of other diffusible gases such as H_2, He and CH_4 to diffuse from the lumen into the villus blood (Bond et al., 1977). As a result, feeding resulted in no change in arterial PCO_2 in humans (Mensink et al., 2006) and no difference between arterial and venous PCO_2 in chickens (*Gallus gallus domesticus*; Wideman et al., 2003).

Moreover, mammals possess a countercurrent arrangement of the capillary bed in the intestinal villi and in the ruminant stomach (see Section 1.4.1), that may possibly function to

recirculate and trap the CO_2. While the rainbow trout do not have intestinal villi (see Appendix), they have larger epithelial folds that are more prominent in the posterior intestine (Harder, 1975; Kapoor et al., 1975). Through casting of the vasculature followed by imaging by scanning electron microscopy (SEM) and both single and multi-photon microscopy of the rainbow trout posterior intestine, I found evidence for capillaries possibly arranged in a countercurrent exchange fashion within the intestinal folds (see Appendix). If true, the luminal PCO_2 could diffuse into and recirculate within the intestinal fold, thereby possibly helping with oxygen unloading to the enterocytes *via* the Bohr and Root effects (Cooper et al., 2014; Nikinmaa, 2006; Rummer and Brauner, 2015). Thus, it will be of great interest to further investigate the vascular anatomy of the GIT in the future studies.

The postprandial ammonia increase was not observed in the SIV but interestingly, there was a postprandial increase in HPV Tamm in agreement with previous findings (Karlsson et al., 2006). The implication of this finding is that there is zonation of the GIT, whereby the luminal ammonia is likely absorbed in the anterior region of the GIT such as the stomach, pyloric caeca and anterior intestine. The mechanism of ammonia absorption across the stomach epithelia is of interest as it would be moving against a large PNH_3 gradient *in vivo*. Indeed, results of Chapters 5 and 6 indicate GIT zonation of ammonia handling and an important role for the stomach in absorbing ammonia despite the unfavourable PNH_3 gradient, as discussed below.

In summary, I found minimal equilibration of the three respiratory gases across the GIT epithelia even after feeding in rainbow trout, reflected in large differences between the lumen and the SIV plasma gas tensions (Figure 7.1). Preventing the extreme extracorporeal environment of the GIT from equilibrating with the vascular system would be favourable in maintaining homeostasis in the rainbow trout. This may also be the case in English sole where

similar variability of SIV PCO_2 was observed in Chapter 3 using the same micro-optode technique as in rainbow trout, thus *in vivo* blood sampling of English sole will be of interest in future studies.

7.4 GIT zonation in handling of nitrogenous products: ammonia and urea

In Chapters 3 and 4, the high luminal Tamm in fed rainbow trout was not reflected in its SIV plasma, but a postprandial increase in plasma Tamm was observed in the HPV. To investigate the handling and transport of postprandial nitrogenous products - ammonia and urea - by different sections of the GIT, Chapters 5 and 6 employed *in vitro* gut sac preparations and molecular analyses of channels and transporters involved in the process. Specifically, the gut sacs of fasted or fed rainbow trout were loaded with either glutamine or ammonia in the mucosal saline (Chapter 5) and at different pHs to manipulate the PNH_3 gradients (Chapter 6). Enzymes involved in the synthesis of urea and transporters involved in moving either NH_4^+ or NH_3 were studied in different GIT sections. In this section, I will further discuss the main findings regarding zonation of the GIT in handling and transporting ammonia and urea, and the importance of stomach in the process.

As an ammoniotelic teleost, the rainbow trout excrete ammonia as their primary nitrogenous waste (Anderson, 2001; Randall and Wright, 1987; Wright and Wood, 2009), yet an increase in HPV plasma urea level was seen following feeding in Karlsson et al. (2006). The capacity of the intestinal cells of rainbow trout to handle and transport urea was largely unknown, and thus was of interest in Chapter 5. I found that after feeding, intestinal tissues produce urea, likely *via* direct arginolysis. This was accompanied by an increased serosal urea flux rate, but surplus glutamine and ammonia in the mucosal saline were not converted to urea.

No notable difference was observed among the intestinal sections in urea handling. Although it is not known whether rainbow trout have urea transporters (UT) in the intestine, another ammoniotelic teleost, the plainfin midshipman (*Porichthys notatus*) was found to have UT localized in the intestine (Bucking et al., 2013b).

Similar to the situation with urea, fed intestinal tissues had greater ammonia production and transport rates relative to fasted intestinal tissues of rainbow trout. Notably, the fed anterior intestinal tissue exhibited higher serosal and mucosal ammonia flux rates, and lower tissue ammonia concentrations relative to the posterior intestinal tissue. These results indicate a zonation of the intestine where the anterior intestine has greater ability to transport ammonia from the mucosal to the serosal saline. In Chapter 6, this ammonia transport was supported by the demonstration that at the mRNA level, both NKCC as a possible NH_4^+ transporter, and Rhbg and Rhcg2 proteins as possible NH_3 transporters, were expressed in the fed rainbow trout intestine. The expression levels in all GIT sections were similar, not supporting the intestinal zonation. However, the effect of feeding on the regulation of these transporters was not investigated in this thesis. In other studies, feeding stimulated an upregulation of Rhbg in the posterior intestine, and NKCC in the anterior and posterior intestines (Bucking and Wood, 2012; Rubino et al., 2019).

Furthermore, the ammonia transport was not dependent on the PNH_3 gradient across the intestinal epithelia (Chapter 6). Perhaps this agrees with the relatively low PCO_2 in the SIV. As discussed in Chapter 1 (Section 1.6), diffusion of NH_3 across the gill in fish is accompanied by simultaneous CO_2 excretion as it allows "ammonia trapping," which does not seem to be the case in the GIT. Thus, the higher ammonia transport to the vascular system of the anterior intestine

likely involves more complex mechanisms. Future studies should include examining the upregulation of NH_4^+ and/or NH_3 transporter expression levels.

To date, there has been a focus on the intestine as a site of ammonia handling and transport. In this thesis, I have reported for the first time that Tamm is very high in the stomach chyme, which disappears in the intestine. The stomach has often been considered mainly as a site for the mechanical and chemical breakdown of meals rather than an assimilation site, though it is known to play a major role in the absorption of Na^+ and K^+ ions from the diet in the rainbow trout (Bucking and Wood, 2006). In Chapter 6, I found that the stomach is an important site for ammonia absorption, similar to dietary Na^+ and K^+ ions. As ammonia transport throughout the GIT sections is independent of the PNH_3 gradient, this implies that ammonia is absorbed as NH_4^+ across the gastric epithelia. This could explain why Tamm in the SIV remains low after feeding, but becomes elevated in the HPV that additionally drains blood from the stomach (Chapter 4). Prior to this thesis, there was little information on possible ammonia absorptive pathways in the teleost stomach. I found mRNA expression levels of Rhcg2 and NKCC similar to those in the intestine, but no expression of Rhbg could be detected in the stomach. However, there are some inconsistencies among previous studies and this thesis regarding the expression of both Rhbg and Rhcg2 in the GIT of rainbow trout, possibly due to differences in feeding condition (Bucking and Wood, 2012; Nawata et al., 2007; Chapter 6), thus further research is needed. Nevertheless, the current possibilities for ammonia absorption pathways are incorporated into the conceptual model shown in Figure 7.2.

As discussed in more detail in Chapter 6, other previous studies found a distinct zonation in two key ammonia-fixing enzymes: GS and GDH (Figure 7.2). In brief, all intestinal tissues have similar GS activity, which increases with feeding in the posterior intestine (Bucking and

Wood, 2012; Mommsen et al., 2003a). The anterior intestine has the highest GDH activity, and this increases in response to feeding (Mommsen et al., 2003b; Rubino et al., 2015). Comparably, the stomach has similar GS activity but significantly lower GDH activity than the intestinal tissues (Mommsen et al., 2003b; Mommsen et al., 2003a). There seems to be some disagreement on postprandial upregulation of GS activity between studies (Bucking and Wood, 2012; Rubino et al., 2014). The authors speculated that these differences are of environmental and/or genetic origins that need to be addressed further in the future. Postprandial responses in enzyme activity appear to be completely unknown in the stomach. The presence of GS and GDH enzymes, however, indicate that the stomach tissues are also capable of fixing ammonia to glutamate or glutamine.

In summary, the findings in Chapters 5 and 6 indicate that the rainbow trout intestine has some capacity to produce urea, that there is a functional zonation of the GIT in ammonia handling and transport, and that ammonia absorption appears to be independent of the PNH_3 gradient. Concurrent with the *in vivo* findings in Chapter 4, postprandial ammonia absorption seems to occur in the anterior intestine and the stomach, to be used for amino acid synthesis or for circulatory transport to the liver, gills and/or other tissues for further processing.

7.5 **Perspectives for future research**

While my thesis discovered new information about the physiology of the GIT in rainbow trout and English sole, it also has raised many additional questions and interesting future research directions that I have noted in the individual chapters. Here, I have highlighted several of particular interest.

First, having established that the GIT lumen in fish is nearly anoxic, similar to that of mammals, a more elaborate study on the PO_2 profile of both the lumen and the blood draining the GIT should be considered. If enterocyte transporters in fish are vulnerable to hypoxemia as in mammals (Ward et al., 2014), they would require a mechanism in order to avoid such challenges. My initial trials on the vasculature of the intestinal folds (see Appendix) shed insight into a possible countercurrent exchanger that could potentially be used to enhance O_2 delivery to the enterocytes, while preventing equilibration of high GIT lumen CO_2 and ammonia levels with the blood draining the intestine. Information on whether CO_2 and moreover, NH_3, are able to recirculate in the fish intestinal vasculature is currently lacking. To the best of my knowledge, no study to date has looked at the effect of ammonia on Hb-O_2 dynamics in fish. Future investigations on whether such an arrangement exists throughout the GIT, including the stomach, and whether CO_2 and/or ammonia can enhance O_2 delivery would give us better insight into the aerobic metabolism of the GIT.

Moreover, the mammalian luminal PO_2 profile is complex with a steep PO_2 gradient allowing different anaerobic microbes to thrive (Espey, 2013). Whether similar PO_2 microenvironments exist in the fish lumen would be of interest. In relation, the GIT microbes are one of the largest contributors for not only the GIT PO_2, but for many of the other gases. Microbiome is the key player acting between the gut-brain-axis in humans (i.e. Kalantar-Zadeh et al., 2019; Rogers et al., 2016; Sharon et al., 2016) and it is also important in fish (Banerjee and Ray, 2017; de Bruijn et al., 2018; López Nadal et al., 2020; Nayak, 2010; Vargas-Albores et al., 2021). Moreover, ammonia-fixing enzymes are found in intestinal bacteria in some fish species (Andersson and Roger, 2003; Müller et al., 2006; Turner and Bucking, 2019), indicating the importance of the microbiome in handling ammonia as well. Thus, the potential contribution of

microbes to all of the luminal gases including the three respiratory gases examined in this thesis would be an interesting topic to pursue.

Lastly, further elaboration of my *in vitro* work on the GIT zonation in the handling and transport of nitrogenous wastes would be very informative. This could include additional qPCR work on postprandial ammonia transporter expression at the mRNA level, as well as protein expression and immunohistochemical localization of transporters before and at various times after feeding. Comparison of the blood draining the intestine and stomach with *in vivo* non-occlusive catheters inserted into the SIV in the upper anterior intestine and HPV would allow sectional differentiation of the relative ammonia transport. This should be feasible using much larger animals. Moreover, possible GIT zonation in the handling and transport of O_2 and CO_2 is a completely unexplored field. In addition, a comparative study between FW *versus* SW species on the GIT zonation in the three respiratory gases would be an interesting future study as similar GIT intestinal zonation for osmoregulatory functions such as water absorption, HCO_3^- secretion and NKA activities also exist in SW teleosts (Alves et al., 2019; Carvalho et al., 2012; Guffey et al., 2011). The intestinal folds are more prominent, if not exclusive, to the posterior intestine (see Appendix). Thus, the proposed countercurrent exchanger may be more prominent in the posterior intestine. These potential research areas will provide interesting routes for future research in further advancing our understanding the physiology of the GIT in fish.

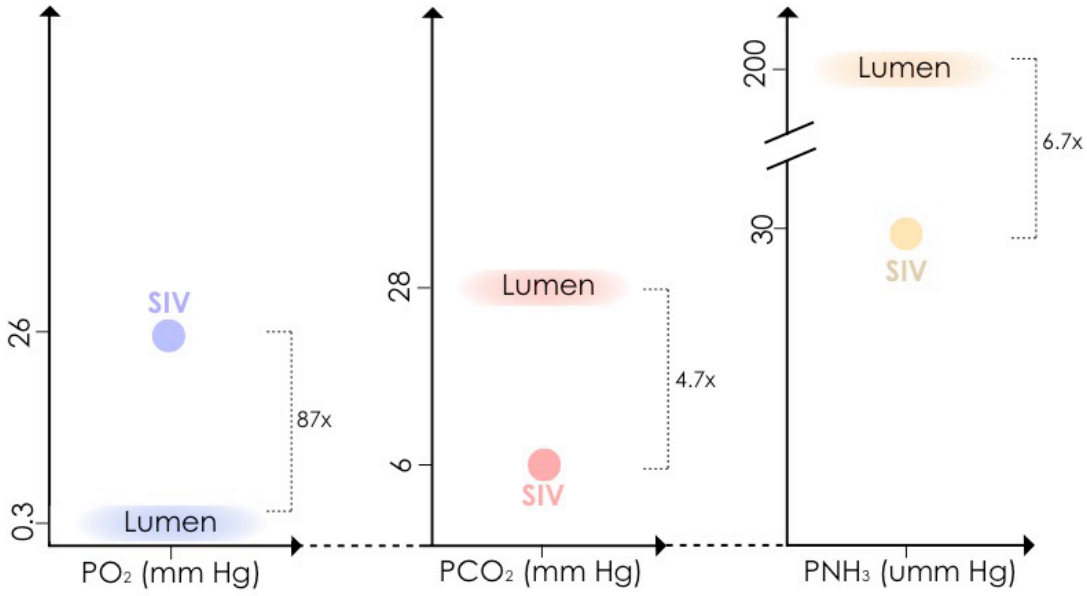

Figure 7.1 Combined figure representing luminal (intestine) and SIV PO_2, PCO_2 and PNH_3 48 h following feeding in FW rainbow trout based upon the findings of this thesis. The relative magnitude of differences between the luminal and SIV values are indicated on the respective panels.

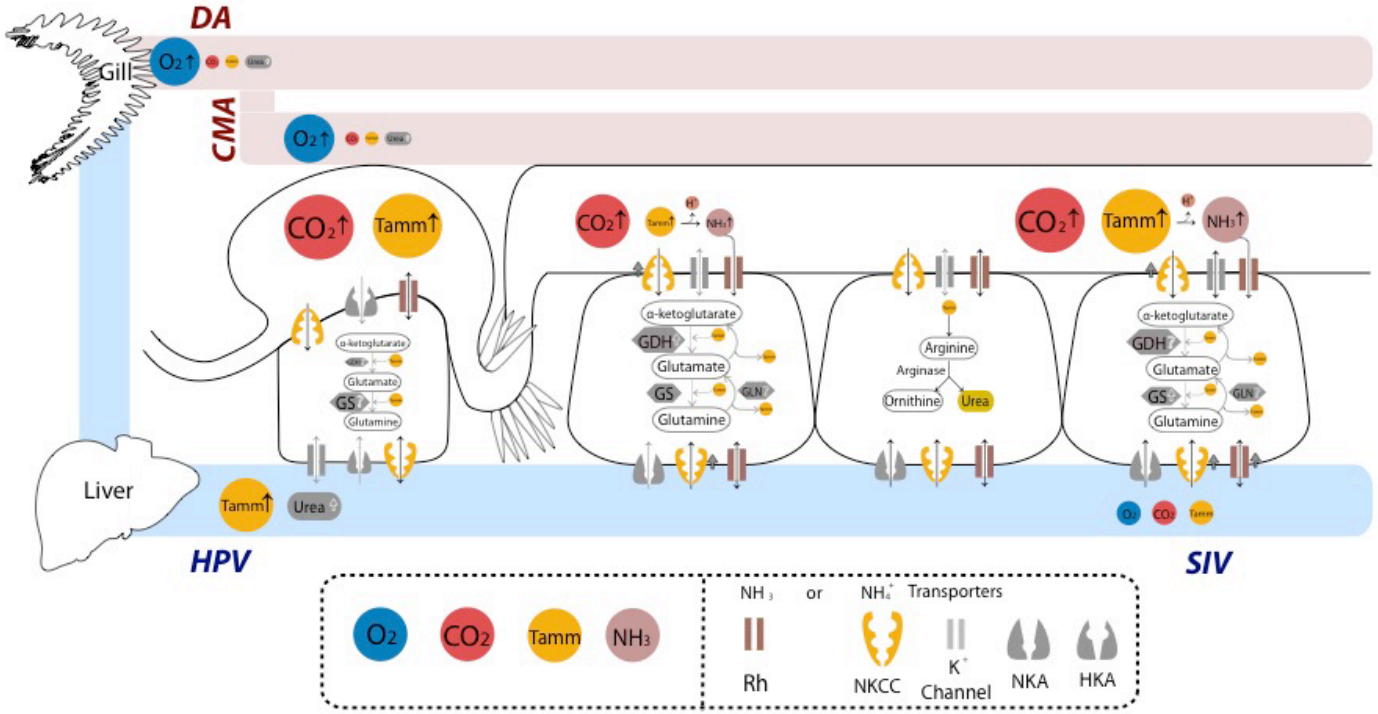

Figure 7.2 Model diagram of the PO_2, PCO_2, Tamm (NH_4^+ and NH_3), and PNH_3 profiles within the FW rainbow trout GIT lumen and the vascular system. The size of the O_2, CO_2, Tamm, and NH_3 symbols indicate relative partial pressure (PO_2, PCO_2, PNH_3) or concentrations (Tamm). Arrow indicates the increases in partial pressure, concentration or enzymatic activity after feeding. Data extrapolated from other studies are indicated with gray symbols: HKA (Bucking and Wood, 2012); postprandial upregulation of Rhbg1 (Bucking and Wood, 2012); postprandial upregulation of NKCC (Rubino et al., 2019); K^+ channels (Loretz, 1995; Movileanu et al., 1998); NKA (Gjevre and Naess, 1996); postprandial [urea] (Karlsson et al., 2006); postprandial GS and GDH activities (Bucking and Wood, 2012; Mommsen et al., 2003a; Mommsen et al., 2003b; Rubino et al., 2015).

Bibliography

Alabaster, J. S., Herbert, D. W. M. and Hemens, J. (1957). The survival of rainbow trout (*Salmo Gairdnerii* Richardson) and perch (*Perca Fluviatilis* L.) at various concentrations of dissolved oxygen and carbon dioxide. *Ann. Appl. Biol.* **45**, 177–188.

Albenberg, L., Esipova, T. V., Judge, C. P., Bittinger, K., Chen, J., Laughlin, A., Grunberg, S., Baldassano, R. N., Lewis, J. D., Li, H., et al. (2014). Correlation between intraluminal oxygen gradient and radial partitioning of intestinal microbiota. *Gastroenterology* **147**, 1055-1063.e8.

Alsop, D. H. and Wood, C. M. (1997). The interactive effects of feeding and exercise on oxygen consumption, swimming performance and protein usage in juvenile rainbow trout (*Oncorhynchus mykiss*). *J. Exp. Biol.* **200**, 2337–2346.

Altman, F. (1986). Downwind update-a discourse on matters gaseous. *West. J. Med.* 502–505.

Alves, A., Gregório, S. F., Egger, R. C. and Fuentes, J. (2019). Molecular and functional regionalization of bicarbonate secretion cascade in the intestine of the European sea bass (*Dicentrarchus labrax*). *Comp. Biochem. Physiol. - A Mol. Integr. Physiol.* **233**, 53–64.

Anderson, P. M. (1995). Urea cycle in fish: Molecular and mitochondrial studies. In *Fish Physiology* (ed. Wood, C. and Shuttleworth, T. J.), pp. 57–83. Academic Press.

Anderson, P. M. (2001). Urea and glutamine synthesis: Environmental influences on nitrogen excretion. In *Fish Physiology: Nitrogen Excretion* (ed. Wright, P. A. and Anderson, P. M.), pp. 239–277. Academic Press.

Anderson, P. M., Broderius, M. A., Fong, K. C., Tsui, K. N. T., Chew, S. F. and Ip, Y. K. (2002). Glutamine synthetase expression in liver, muscle, stomach and intestine of *Bostrichthys sinensis* in response to exposure to a high exogenous ammonia concentration.

J. Exp. Biol. **205**, 2053–2065.

Anderson, W. G., Dasiewicz, P. J., Liban, S., Ryan, C., Taylor, J. R., Grosell, M. and Weihrauch, D. (2010). Gastro-intestinal handling of water and solutes in three species of elasmobranch fish, the white-spotted bamboo shark, *Chiloscyllium plagiosum*, little skate, *Leucoraja erinacea* and the clear nose skate *Raja eglanteria*. *Comp. Biochem. Physiol. - A Mol. Integr. Physiol.* **155**, 493–502.

Andersson, J. O. and Roger, A. J. (2003). Evolution of glutamate dehydrogenase genes: Evidence for lateral gene transfer within and between prokaryotes and eukaryotes. *BMC Evol. Biol.* **3**, 1–10.

Andrade, D. V., De Toledo, L. F., Abe, A. S. and Wang, T. (2004). Ventilatory compensation of the alkaline tide during digestion in the snake *Boa constrictor*. *J. Exp. Biol.* **207**, 1379–1385.

Aoki, M., Kaneko, T., Katoh, F., Hasegawa, S., Tsutsui, N. and Aida, K. (2003). Intestinal water absorption through aquaporin 1 expressed in the apical membrane of mucosal epithelial cells in seawater-adapted Japanese eel. *J. Exp. Biol.* **206**, 3495–3505.

Axelsson, M. and Fritsche, R. (1991). Effects of exercise, hypoxia and feeding on the gastrointestinal blood flow in the Atlantic cod *Gadus morhua*. *J. Exp. Biol.* **158**, 181–198.

Axelsson, M., Driedzic, W. R., Farrell, A. P. and Nilsson, S. (1989). Regulation of cardiac output and gut blood flow in the sea rave, *Hemitripterus americanus*. *Fish Physiol. Biochem.* **6**, 315–326.

Axelsson, M., Thorarensen, H., Nilsson, S. and Farrell, A. P. (2000). Gastrointestinal blood flow in the red Irish lord, *Hemilepidotus hemilepidotus*: Long-term effects of feeding and adrenergic control. *J. Comp. Physiol. - B Biochem. Syst. Environ. Physiol.* **170**, 145–152.

Bakke-McKellep, A. M., Nordrum, S., Krogdahl, Å. and Buddington, R. K. (2000). Absorption of glucose, amino acids, and dipeptides by the intestines of Atlantic salmon (*Salmo salar* L.). *Fish Physiol. Biochem.* **22**, 33–44.

Bakke, A. ., Glover, C. and Krogdahl, Å. (2011). Feeding, digestion, and absorption of nutrients. In *Fish Physiology: Multifunctional Gut* (ed. Grosell, M., Farrell, A. P., and Brauner, C. J), pp. 57–111. Elsevier Inc.

Ballantyne, J. S. (2001). Amino acid metabolism. *Fish Physiol.* **20**, 77–107.

Banerjee, G. and Ray, A. K. (2017). Bacterial symbiosis in the fish gut and its role in health and metabolism. *Symbiosis* **72**, 1–11.

Beamish, F. W. H. and Thomas, E. (1984). Effects of dietary protein and lipid on nitrogen losses in rainbow trout, *Salmo gairdneri*. *Aquaculture* **41**, 359–371.

Berenbrink, M., Koldkjær, P., Kepp, O. and Cossins, A. R. (2005). Evolution of oxygen secretion in fishes and the emergence of a complex physiological system. *Science (80-.).* **307**, 1752–1757.

Bettinger, C. J. (2015). Materials advances for next-generation ingestible electronic medical devices. *Trends Biotechnol.* **33**, 575–585.

Bohlen, H. G. (1980). Intestinal tissue PO_2 and microvascular responses during glucose exposure. *Am. J. Physiol. Circ. Physiol.* **238**, H164–H171.

Bohr, C., Hasselbalch, K. and Krogh, A. (1904). Ueber einen in biologischer Ueziehung wichtigen Einfluss, den die Kohlensäurespannung des Blutes auf dessen Sauerstoffbindung übt. *Skand Arch Physiol* **16**, 401–412.

Bond, J. H., Levitt, D. G. and Levitt, M. D. (1977). Quantitation of countercurrent exchange during passive absorption from the dog small intestine. *J. Clin. Invest.* **59**, 308–318.

Boutilier, R. G., Heming, T. A. and Iwama, G. K. (1984). Appendix: Physicochemical parameters for use in fish respiratory physiology. In *Fish Physiology* (ed. Hoar, W. S. and Randall, D. J.), pp. 403–430. Academic Press.

Boyer, J., Schwarz, J. and Smith, N. (1976). Biliary secretion in elasmobranchs. I. Bile collection and composition. *Am. J. Physiol. Content* **230**, 970–973.

Braun, M. H., Steele, S. L. and Perry, S. F. (2009). The responses of zebrafish (*Danio rerio*) to high external ammonia and urea transporter inhibition: Nitrogen excretion and expression of rhesus glycoproteins and urea transporter proteins. *J. Exp. Biol.* **212**, 3846–3856.

Brett, J. R. and Zala, C. A. (1975). Daily pattern of nitrogen excretion and oxygen consumption of sockeye salmon (*Oncorhynchus nerka*) under controlled conditions. *J. Fish. Res. Board Canada* **32**, 2479–2486.

Brijs, J., Axelsson, M., Gräns, A., Pichaud, N., Olsson, C. and Sandblom, E. (2015). Increased gastrointestinal blood flow: An essential circulatory modification for euryhaline rainbow trout (*Oncorhynchus mykiss*) migrating to sea. *Sci. Rep.* **5**, 1–10.

Brijs, J., Gräns, A., Ekström, A., Olsson, C., Axelsson, M. and Sandblom, E. (2016). Cardiorespiratory upregulation during seawater acclimation in rainbow trout: effects on gastrointestinal perfusion and postprandial responses. *Am. J. Physiol. Integr. Comp. Physiol.* **310**, R858–R865.

Brijs, J., Sandblom, E., Sundh, H., Gräns, A., Hinchcliffe, J., Ekström, A., Sundell, K., Olsson, C., Axelsson, M. and Pichaud, N. (2017). Increased mitochondrial coupling and anaerobic capacity minimizes aerobic costs of trout in the sea. *Sci. Rep.* **7**, 1–12.

Brijs, J., Gräns, A., Hjelmstedt, P., Sandblom, E., van Nuland, N., Berg, C. and Axelsson, M. (2018). *In vivo* aerobic metabolism of the rainbow trout gut and the effects of an acute

temperature increase and stress event. *J. Exp. Biol.* **221**, jeb180703.

Britton, R. and Krehbiel, C. (1993). Nutrient metabolism by gut tissues. *J. Dairy Sci.* **76**, 2125–2131.

Brown, C. R. and Cameron, J. N. (1991a). The induction of specific dynamic action in channel catfish by infusion of essential amino acids. *Physiol. Zool.* **64**, 276–297.

Brown, C. R. and Cameron, J. N. (1991b). The relationship between specific dynamic action (SDA) and protein synthesis rates in the channel catfish. *Physiol. Zool.* **64**, 298–309.

Bucking, C. and Wood, C. M. (2006). Gastrointestinal processing of Na^+, Cl^-, and K^+ during digestion: implications for homeostatic balance in freshwater rainbow trout. *Am. J. Physiol. Integr. Comp. Physiol.* **291**, R1764–R1772.

Bucking, C. and Wood, C. M. (2008). The alkaline tide and ammonia excretion after voluntary feeding in freshwater rainbow trout. *J. Exp. Biol.* **211**, 2533–2541.

Bucking, C. and Wood, C. M. (2009). The effect of postprandial changes in pH along the gastrointestinal tract on the distribution of ions between the solid and fluid phases of chyme in rainbow trout. *Aquac. Nutr.* **15**, 282–296.

Bucking, C. and Wood, C. M. (2012). Digestion of a single meal affects gene expression of ion and ammonia transporters and glutamine synthetase activity in the gastrointestinal tract of freshwater rainbow trout. *J. Comp. Physiol. B Biochem. Syst. Environ. Physiol.* **182**, 341–350.

Bucking, C., Fitzpatrick, J. L., Nadella, S. R. and Wood, C. M. (2009). Post-prandial metabolic alkalosis in the seawater-acclimated trout: the alkaline tide comes in. *J. Exp. Biol.* **212**, 2159–2166.

Bucking, C., Landman, M. J. and Wood, C. M. (2010). The role of the kidney in

compensating the alkaline tide, electrolyte load, and fluid balance disturbance associated with feeding in the freshwater rainbow trout, *Oncorhynchus mykiss*. *Comp. Biochem. Physiol. - A Mol. Integr. Physiol.* **156**, 74–83.

Bucking, C., LeMoine, C. M., Craig, P. M. and Walsh, P. J. (2013a). Nitrogen metabolism of the intestine during digestion in a teleost fish, the plainfin midshipman (*Porichthys notatus*). *J. Exp. Biol.* **216**, 2821–2832.

Bucking, C., Edwards, S. L., Tickle, P., Smith, C. P., McDonald, M. D. and Walsh, P. J. (2013b). Immunohistochemical localization of urea and ammonia transporters in two confamilial fish species, the ureotelic gulf toadfish (*Opsanus beta*) and the ammoniotelic plainfin midshipman (*Porichthys notatus*). *Cell Tissue Res.* **352**, 623–637.

Busk, M., Overgaard, J., Hicks, J. W., Bennett, A. F. and Wang, T. (2000). Effects of feeding on arterial blood gases in the American alligator *Alligator mississippiensis*. *J. Exp. Biol.* **203**, 3117–3124.

Bustamante, S. A., Jodal, M., Nilsson, N. J. and Lundgren, O. (1989). Evidence for a countercurrent exchanger in the intestinal villi of suckling swine. *Acta Physiol. Scand.* **137**, 207–213.

Cameron, J. N. and Heisler, N. (1983). Studies of ammonia in the rainbow trout:Physico-chemical parameters, acid-base behaviour and respiratory clearance. *J. Exp. Biol.* **105**, 107–125.

Carrick, S. and Balment, R. J. (1983). The renin-angiotensin system and drinking in the euryhaline flounder, *Platichthys flesus*. *Gen. Comp. Endocrinol.* **51**, 423–433.

Carvalho, E. S. M., Gregório, S. F., Power, D. M., Canário, A. V. M. and Fuentes, J. (2012). Water absorption and bicarbonate secretion in the intestine of the sea bream are regulated

by transmembrane and soluble adenylyl cyclase stimulation. *J. Comp. Physiol. B Biochem. Syst. Environ. Physiol.* **182**, 1069–1080.

Chabot, D., Koenker, R. and Farrell, A. P. (2016). The measurement of specific dynamic action in fishes. *J. Fish Biol.* **88**, 152–172.

Chadwick, T. D. and Wright, P. A. (1999). Nitrogen excretion and expression of urea cycle enzymes in the Atlantic cod (*Gadus morhua* L.): A comparison of early life stages with adults. *J. Exp. Biol.* **202**, 2653–2662.

Chambrey, R., Geossens, D., Bourgeois, S., Picard, N., Bloch-Faure, M., Leviel, F., Geoffroy, V., Cambillau, M., Colin, Y., Paillard, M., et al. (2005). Genetic ablation of Rhbg in the mouse does not impair renal ammonium excretion. *Am. J. Physiol. - Ren. Physiol.* **289**, 1281–1290.

Chambrey, R., Goossens, D., Quentin, F. and Eladari, D. (2006). Rh glycoproteins in epithelial cells: lessons from rat and mice studies. *Transfus. Clin. Biol.* **13**, 154–158.

Chew, S. F., Wilson, J. M., Ip, Y. K. and Randall, D. J. (2005). Nitrogen Excretion And Defense Against Ammonia Toxicity. *Fish Physiol.* **21**, 307–395.

Clements, K. D., Gleeson, V. P. and Slaytor, M. (1994). Short-chain fatty acid metabolism in temperate herbivorous fish. *J. Comp. Physiol. B Biochem. Syst. Environ. Physiol.* **164**, 372–377.

Collie, N. L. and Ferraris, R. P. (1995). Nutrient fluxes and regulation in fish intestine. *Biochem. Mol. Biol. Fishes* **4**, 221–239.

Cooper, C. A. and Wilson, R. W. (2008). Post-prandial alkaline tide in freshwater rainbow trout: effects of meal anticipation on recovery from acid-base and ion regulatory disturbances. *J. Exp. Biol.* **211**, 2542–2550.

Cooper, C. A., Regan, M. D., Brauner, C. J., De Bastos, E. S. R. and Wilson, R. W. (2014). Osmoregulatory bicarbonate secretion exploits H^+-sensitive haemoglobins to autoregulate intestinal O_2 delivery in euryhaline teleosts. *J. Comp. Physiol. B Biochem. Syst. Environ. Physiol.* **184**, 865–876.

Couto, A., Peres, H., Oliva-Teles, A. and Enes, P. (2016). Screening of nutrient digestibility, glycaemic response and gut morphology alterations in gilthead seabream (*Sparus aurata*) fed whole cereal meals. *Aquaculture* **450**, 31–37.

Cowey, C. B. and Sargent, J. R. (1972). Fish nutrition. *Adv. Mar. Biol.* **10**, 383–494.

Cvancara, V. A. (1969). Comparative study of liver uricase activity in fresh-water teleosts. *Comp. Biochem. Physiol.* **28**, 725–732.

de Bruijn, I., Liu, Y., Wiegertjes, G. F. and Raaijmakers, J. M. (2018). Exploring fish microbial communities to mitigate emerging diseases in aquaculture. *FEMS Microbiol. Ecol.* **94**, 1–12.

Dejours, P. (1975). *Principles of Comparative Respiratory Physiology*. Amsterdam: North-Holland: Elsevier.

Dépêche, J., Gilles, R., Daufresne, S. and Chiapello, H. (1979). Urea content and urea production via the ornithine-urea cycle pathway during the ontogenic development of two teleost fishes. *Comp. Biochem. Physiol. - A Mol. Integr. Physiol.* **63**, 51–56.

Desai, A. R., Links, M. G., Collins, S. A., Mansfield, G. S., Drew, M. D., Van Kessel, A. G. and Hill, J. E. (2012). Effects of plant-based diets on the distal gut microbiome of rainbow trout (*Oncorhynchus mykiss*). *Aquaculture* **350**–**353**, 134–142.

Duée, P.-H., Darcy-Vrillon, B., Blachier, F. and Morel, M.-T. (1995). Fuel selection in intestinal cells. *Proc. Nutr. Soc.* **54**, 83–94.

Dupont-Prinet, A., Claireaux, G. and McKenzie, D. J. (2009). Effects of feeding and hypoxia on cardiac performance and gastrointestinal blood flow during critical speed swimming in the sea bass *Dicentrarchus labrax*. *Comp. Biochem. Physiol. - A Mol. Integr. Physiol.* **154**, 233–240.

Eliason, E. J., Kiessling, A., Karlsson, A., Djordjevic, B. and Farrell, A. P. (2007). Validation of the hepatic portal vein cannulation technique using Atlantic salmon *Salmo salar* L. *J. Fish Biol.* **71**, 290–297.

Eliason, E. J., Higgs, D. A. and Farrell, A. P. (2008). Postprandial gastrointestinal blood flow, oxygen consumption and heart rate in rainbow trout (*Oncorhynchus mykiss*). *Comp. Biochem. Physiol. - A Mol. Integr. Physiol.* **149**, 380–388.

Ellis, R. P., Urbina, M. A. and Wilson, R. W. (2017). Lessons from two high CO_2 worlds – future oceans and intensive aquaculture. *Glob. Chang. Biol.* **23**, 2141–2148.

Emerson, K., Russo, R. C., Lund, R. E. and Thurston, R. V. (1975). Aqueous ammonia equilibrium calculations: Effect of pH and temperature. *J. Fish. Res. Board Canada* **32**, 2379–2383.

Eom, J., Fehsenfeld, S. and Wood, C. M. (2020). Is ammonia excretion affected by gill ventilation in the rainbow trout Oncorhynchus mykiss? *Respir. Physiol. Neurobiol.* **275**,.

Esbaugh, A. J. and Grosell, M. (2014). Esophageal desalination is mediated by Na^+, H^+ exchanger-2 in the gulf toadfish (*Opsanus beta*). *Comp. Biochem. Physiol. - A Mol. Integr. Physiol.* **171**, 57–63.

Espey, M. G. (2013). Role of oxygen gradients in shaping redox relationships between the human intestine and its microbiota. *Free Radic. Biol. Med.* **55**, 130–140.

Evans, D. H., Piermarini, P. M. and Choe, K. P. (2005). The multifunctional fish gill:

Dominant site of gas exchange, osmoregulation, acid-base regulation, and excretion of nitrogenous waste. *Physiol. Rev.* **85**, 97–177.

Fara, J. W., Rubinstein, E. H. and Sonnenschein, R. R. (1972). Intestinal hormones in mesenteric agents vasodilation after intraduodenal. **223**, 1058–1067.

Farrell, A. P., Thorarensen, H., Axelsson, M., Crocker, C. E., Gamperl, A. K. and Cech, J. J. (2001). Gut blood flow in fish during exercise and severe hypercapnia. *Comp. Biochem. Physiol. - A Mol. Integr. Physiol.* **128**, 549–561.

Fehsenfeld, S. and Wood, C. M. (2018). Section-specific expression of acid-base and ammonia transporters in the kidney tubules of the goldfish *Carassius auratus* and their responses to feeding. *Am. J. Physiol. Physiol.* **315**, F1565–F1582.

Felskie, A. K., Anderson, P. M. and Wright, P. A. (1998). Expression and activity of carbamoyl phosphate synthetase III and ornithine urea cycle enzymes in various tissues of four fish species. *Comp. Biochem. Physiol. - B Biochem. Mol. Biol.* **119**, 355–364.

Ferlazzo, A., Carvalho, E. S. M., Gregorio, S. F., Power, D. M., Canario, A. V. M., Trischitta, F. and Fuentes, J. (2012). Prolactin regulates luminal bicarbonate secretion in the intestine of the sea bream (*Sparus aurata* L.). *J. Exp. Biol.* **215**, 3836–3844.

Ferreira, M. S., Wood, C. M., Harter, T. S., Dal Pont, G., Val, A. L. and Matthews, P. G. D. (2019). Metabolic fuel use after feeding in the zebrafish (*Danio rerio*): a respirometric analysis. *J. Exp. Biol.* **222**, jeb194217.

Fivelstad, S., Olsen, A. B., Åsgård, T., Baeverfjord, G., Rasmussen, T., Vindheim, T. and Stefansson, S. (2003). Long-term sublethal effects of carbon dioxide on Atlantic salmon smolts (*Salmo salar* L.): Ion regulation, haematology, element composition, nephrocalcinosis and growth parameters. *Aquaculture* **215**, 301–319.

Food and Agriculture Organization (2020). *The State of World Fisheries and Aquaculture*. Rome, Italy.

Forster, R. P. and Goldstein, L. (1969). Formation of excretory products. In *Fish Physiology* (ed. Hoar, W. S. and Randall, D. J.), pp. 313–350. New York: Academic Press.

Friedman, E. S., Bittinger, K., Esipova, T. V., Hou, L., Chau, L., Jiang, J., Mesaros, C., Lund, P. J., Liang, X., FitzGerald, G. A., et al. (2018). Microbes vs. chemistry in the origin of the anaerobic gut lumen. *Proc. Natl. Acad. Sci. U. S. A.* **115**, 4170–4175.

Fuentes, J. and Eddy, F. . (1997a). Drinking in freshwater, euryhaline and marine teleosts. In *Ionic Regulation in Animals* (ed. Hazon, N., Eddy, F. B., and Flik, G.), pp. 135–149. Heidelberg: Springer.

Fuentes, J. and Eddy, F. B. (1997b). Effect of manipulation of the renin-angiotensin system in control of drinking in juvenile Atlantic salmon (*Salmo salar* L) in fresh water and after transfer to sea water. *J. Comp. Physiol. - B Biochem. Syst. Environ. Physiol.* **167**, 438–443.

Fuentes, J., Soengas, J. L., Rey, P. and Rebolledo, E. (1997). Progressive transfer to seawater enhances intestinal and branchial Na^+-K^+-ATPase activity in non-anadromous rainbow trout. *Aquac. Int.* **5**, 217–227.

Fuentes, J., Power, D. M. and Canário, A. V. M. (2010). Parathyroid hormone-related protein-stanniocalcin antagonism in regulation of bicarbonate secretion and calcium precipitation in a marine fish intestine. *Am. J. Physiol. - Regul. Integr. Comp. Physiol.* **299**, 150–158.

Garrett, D. L., Pietsch, T. W., Utter, F. M. and Hauser, L. (2007). The hybrid sole *Inopsetta ischyra* (Teleostei: Pleuronectiformes: Pleuronectidae): hybrid or biological species? *Trans. Am. Fish. Soc.* **136**, 460–468.

Genz, J., Taylor, J. R. and Grosell, M. (2008). Effects of salinity on intestinal bicarbonate

secretion and compensatory regulation of acid-base balance in *Opsanus beta*. *J. Exp. Biol.* **211**, 2327–2335.

Ghoos, Y. F., Maes, B. D., Geypens, B. J., Mys, G., Hiele, M. I., Rutgeerts, P. J. and Vantrappen, G. (1993). Measurement of gastric emptying rate of solids by means of a carbon-labeled octanoic acid breath test. *Gastroenterology* **104**, 1640–1647.

Gips, C. H. (1973). Curve patterns after oral loading with ammonium acetate. *Clin. Chim. Acta* **46**, 415–418.

Gjevre, A. and Naess, L. I. masdal (1996). Intestinal Na^+/ K^+-ATPase activity in Salmonids. *Comp. Biochem. Physiol.* **115**, 159–168.

Goldstein, L. and Forster, R. O. Y. P. (1965). The role of uricolysis in the production of urea by fishes and other aquatic vertebrates. *Comp. Biochem. Physiol.* **14**, 567–576.

Goodrich, H. R., Bayley, M., Birgersson, L., Davison, W. G., Johannsson, O. E., Kim, A. B., Le My, P., Tinh, T. H., Thanh, P. N., Thanh, H. D. T., et al. (2020). Understanding the gastrointestinal physiology and responses to feeding in air-breathing Anabantiform fishes. *J. Fish Biol.* **96**, 986–1003.

Gräns, A., Albertsson, F., Axelsson, M. and Olsson, C. (2009a). Postprandial changes in enteric electrical activity and gut blood flow in rainbow trout (*Oncorhynchus mykiss*) acclimated to different temperatures. *J. Exp. Biol.* **212**, 2550–2557.

Gräns, A., Axelsson, M., Pitsillides, K., Olsson, C., Höjesjö, J., Kaufman, R. C. and Cech, J. J. (2009b). A fully implantable multi-channel biotelemetry system for measurement of blood flow and temperature: A first evaluation in the green sturgeon. *Hydrobiologia* **619**, 11–25.

Gregório, S. F., Carvalho, E. S. M., Encarnação, S., Wilson, J. M., Power, D. M., Canário,

A. V. M. and Fuentes, J. (2013). Adaptation to different salinities exposes functional specialization in the intestine of the sea bream (*Sparus aurata* L.). *J. Exp. Biol.* **216**, 470–479.

Gregório, S. F., Carvalho, E. S. M., Campinho, M. A., Power, D. M., Canário, A. V. M. and Fuentes, J. (2014). Endocrine regulation of carbonate precipitate formation in marine fish intestine by stanniocalcin and PTHrP. *J. Exp. Biol.* **217**, 1555–1562.

Grosell, M. (2006). Intestinal anion exchange in marine fish osmoregulation. *J. Exp. Biol.* **209**, 2813–2827.

Grosell, M. (2007). Intestinal transport processes in marine fish osmoregulation. In *Fish Osmoregulation* (ed. Baldisserotto, B., Mancera, J. M., and Kapoor, B. G.), pp. 332–357. New Hampshire: Science Pulishers Inc.

Grosell, M. (2011). The role of the gastrointestinal tract in salt and water balance. In *Fish Physiology: Multifunctional Gut* (ed. Grosell, M., Farrell, A., and Brauner, C.), pp. 136–165. Elsevier Inc.

Grosell, M. (2019). CO_2 and calcification processes in fish. In *Fish Physiology: Carbon Dioxide* (ed. Grosell, M., Munday, P. L., Farrell, A. P., and Brauner, C. J.), pp. 133–159. Elsevier Inc.

Grosell, M. and Genz, J. (2006). Ouabain-sensitive bicarbonate secretion and acid absorption by the marine teleost fish intestine play a role in osmoregulation. *Am. J. Physiol. - Regul. Integr. Comp. Physiol.* **291**, R1145–R1156.

Grosell, M. and Jensen, F. B. (1999). NO_2^- uptake and HCO_3^- excretion in the intestine of the European flounder (*Platichthys flesus*). *J. Exp. Biol.* **202**, 2103–10.

Grosell, M. and Wood, C. (2001). Branchial versus intestinal silver toxicity and uptake in the

marine teleost *Parophrys vetulus*. *J. Comp. Physiol. - B Biochem. Syst. Environ. Physiol.* **171**, 585–594.

Grosell, M., De Boeck, G., Johannsson, O. and Wood, C. M. (1999). The effects of silver on intestinal ion and acid-base regulation in the marine teleost fish, *Parophrys vetulus*. *Comp. Biochem. Physiol. - C Pharmacol. Toxicol. Endocrinol.* **124**, 259–270.

Grosell, M., O'Donnell, M. J. and Wood, C. M. (2000). Hepatic versus gallbladder bile composition: *in vivo* transport physiology of the gallbladder in rainbow trout. *Am. J. Physiol. Integr. Comp. Physiol.* **278**, R1674–R1684.

Grosell, M., Laliberte, C. N., Wood, S., Jensen, F. B. and Wood, C. M. (2001). Intestinal HCO_3^- secretion in marine teleost fish: Evidence for an apical rather than a basolateral Cl^-/HCO_3^- exchanger. *Fish Physiol. Biochem.* **24**, 81–95.

Grosell, M., Wood, C. M., Wilson, R. W., Bury, N. R., Hogstrand, C., Rankin, C. and Jensen, F. B. (2005). Bicarbonate secretion plays a role in chloride and water absorption of the European flounder intestine. *Am. J. Physiol. Integr. Comp. Physiol.* **288**, R936–R946.

Grosell, M., Gilmour, K. M. and Perry, S. F. (2007). Intestinal carbonic anhydrase, bicarbonate, and proton carriers play a role in the acclimation of rainbow trout to seawater. *Am. J. Physiol. Integr. Comp. Physiol.* **293**, R2099–R2111.

Grosell, M., Mager, E. M., Williams, C. and Taylor, J. R. (2009). High rates of HCO_3^- secretion and Cl^- absorption against adverse gradients in the marine teleost intestine: The involvement of an electrogenic anion exchanger and H^+-pump metabolon? *J. Exp. Biol.* **212**, 1684–1696.

Grosell, M., Farrell, A. P. and Brauner, C. J. (2011). *The mutifunctional gut of fish*. (ed. Grosell, M., Farrell, A., and Brauner, C.) Elsevier Inc.

Guffey, S., Esbaugh, A. and Grosell, M. (2011). Regulation of apical H^+-ATPase activity and intestinal HCO_3^- secretion in marine fish osmoregulation. *Am. J. Physiol. - Regul. Integr. Comp. Physiol.* **301**, 1682–1691.

Guo, F., Teo, L. and Chen, T. (1995). Effects of anaesthetics on the water parameters in a simulated transport experiment of platyfish, *Xiphophorus maculatus* (Günther). *Aquac. Res.* **26**, 265–271.

Hakvoort, T. B. M., He, Y., Kulik, W., Vermeulen, J. L. M., Duijst, S., Ruijter, J. M., Runge, J. H., Deutz, N. E. P., Koehler, S. E. and Lamers, W. H. (2017). Pivotal role of glutamine synthetase in ammonia detoxification. *Hepatology* **65**, 281–293.

Hamann, S., Herrera-Perez, J. J., Bundgaard, M., Alvarez-Leefmans, F. J. and Zeuthen, T. (2005). Water permeability of Na^+-K^+-$2Cl^-$ cotransporters in mammalian epithelial cells. *J. Physiol.* **568**, 123–135.

Handlogten, M. E., Hong, S. P., Zhang, L., Vander, A. W., Steinbaum, M. L., Campbell-Thompson, M. and Weiner, I. D. (2005). Expression of the ammonia transporter proteins Rh B glycoprotein and Rh C glycoprotein in the intestinal tract. *Am. J. Physiol. - Gastrointest. Liver Physiol.* **288**, 1036–1047.

Harder, W. (1975). *Anatomy of Fishes*. E. Schweizerbart'sche Verlagsbuchhandlung: Schweizerbart.

Heindler, F. M., Maes, G. E., Delerue-Ricard, S., Vanden Bavière, A., Hostens, K. and Volckaert, F. A. M. (2019). Diet composition and gut microbiome of 0-group European plaice *Pleuronectes platessa* L. - Strong homogeneity and subtle spatial and temporal differences. *J. Sea Res.* **144**, 67–77.

Hersey, S. J. and Sachs, G. (1995). Gastric acid secretion. *Physiol. Rev.* 155–189.

Heuer, R. M. and Grosell, M. (2016). Elevated CO_2 increases energetic cost and ion movement in the marine fish intestine. *Sci. Rep.* **6**, 1–8.

Higgins, H. L. (1914). The influence of food, posture, and other factors on the alveolar carbon dioxide tension in man. *Am. J. Physiol. Content* **34**, 114–126.

Hoseinifar, S. H., Sun, Y. Z. and Caipang, C. M. (2017). Short-chain fatty acids as feed supplements for sustainable aquaculture: an updated view. *Aquac. Res.* **48**, 1380–1391.

Huang, C. and Peng, J. (2005). Evolutionary conservation and diversification. *Proc. Natl. Acad. Sci.* **102**, 15512–15517.

Hung, C. Y. C., Tsui, K. N. T., Wilson, J. M., Nawata, C. M., Wood, C. M. and Wright, P. A. (2007). Rhesus glycoprotein gene expression in the mangrove killifish *Kryptolebias marmoratus* exposed to elevated environmental ammonia levels and air. *J. Exp. Biol.* **210**, 2419–2429.

Imler, M., Chabrier, G., Simon, C. and Schlienger, J. L. (1988). Intestinal ammonium production in the rat: The role of the colon, small intestine, and circulating glutamine. *Res. Exp. Med.* **188**, 1–7.

Ip, Y. K. and Chew, S. F. (2010). Ammonia production, excretion, toxicity, and defense in fish: A review. *Front. Physiol.* **1**, 1–20.

Iwama, G. K., McGeer, J. C. and Pawluk, M. P. (1989). The effects of five fish anaesthetics on acid–base balance, hematocrit, blood gases, cortisol, and adrenaline in rainbow trout. *Can. J. Zool.* **67**, 2065–2073.

James, L. A., Lunn, P. G. and Elia, M. (1998). Glutamine metabolism in the gastrointestinal tract of the rat assessed by the relative activities of glutaminase (*EC* 3.5.1.2) and glutamine synthetase (*EC* 6.3.1.2). *Br. J. Nutr.* **79**, 365–372.

Jensen, F. B. (2004). Red blood cell pH, the Bohr effect, and other oxygenation-linked phenomena in blood O_2 and CO_2 transport. *Acta Physiol. Scand.* **182**, 215–227.

Jensen, M. K., Madsen, S. S. and Kristiansen, R. (1998). Osmoregulation and salinity effects on the expression and activity of Na^+,K^+-ATPase in the gills of European sea bass, *Dicentrarchus labrax* (L.). *J. Exp. Zool.* **282**, 290–300.

Jobling, M. (1981). The influences of feeding on the metabolic rate of fishes: a short review. *J. Fish Biol.* **18**, 385–400.

Jodal, M. and Lundgren, O. (1986). Countercurrent mechanisms in the mammalian gastrointestinal tract. *Gastroenterology* **91**, 225–241.

Julsrud, E. A., Walsh, P. J. and Anderson, P. M. (1998). N-acetyl-L-glutamate and the urea cycle in gulf toadfish (*Opsanus beta*) and other fish. *Arch. Biochem. Biophys.* **350**, 55–60.

Jung, E. H., Eom, J., Brauner, C. J., Martinez-Ferreras, F. and Wood, C. M. (2020). The gaseous gastrointestinal tract of a seawater teleost, the English sole (*Parophrys vetulus*). *Comp. Biochem. Physiol. - A Mol. Integr. Physiol.* **247**, 110743.

Jung, E. H., Smich, J., Rubino, J. G. and Wood, C. M. (2021). An *in vitro* study of urea and ammonia production and transport by the intestinal tract of fed and fasted rainbow trout: responses to luminal glutamine and ammonia loading. *J. Comp. Physiol. B Biochem. Syst. Environ. Physiol.* **191**,.

Jung, E. H., Brauner, C. J. and Wood, C. M. (2022). Post-prandial respiratory gas and acid-base profiles in the gastrointestinal tract and its venous drainage in freshwater rainbow trout (*Oncorhynchus mykiss*) and seawater English sole (*Parophrys vetulus*). *Comp. Biochem. Physiol. - A Mol. Integr. Physiol.* **265**, 111123.

Kajimura, M., Croke, S. J., Glover, C. N. and Wood, C. M. (2004). Dogmas and

controversies in the handling of nitrogenous wastes: The effect of feeding and fasting on the excretion of ammonia, urea and other nitrogenous waste products in rainbow trout. *J. Exp. Biol.* **207**, 1993–2002.

Kajimura, M., Walsh, P. J., Mommsen, T. P. and Wood, C. M. (2006). The dogfish shark (*Squalus acanthias*) increases both hepatic and extrahepatic ornithine urea cycle enzyme activities for nitrogen conservation after feeding. *Physiol. Biochem. Zool.* **79**, 602–613.

Kalantar-Zadeh, K., Berean, K. J., Burgell, R. E., Muir, J. G. and Gibson, P. R. (2019). Intestinal gases: influence on gut disorders and the role of dietary manipulations. *Nat. Rev. Gastroenterol. Hepatol.* **16**, 733–747.

Kampen, E. J. and Zijlstra, W. G. (1961). Standardization of hemoglobinometry II. The hemiglobincyanide method. *Clin. Chim. Acta* **6**, 538–544.

Kapoor, B. G., Smit, H. J. and Verighina, I. A. (1975). The alimentary canal and digestion in teleosts. *Adv. Mar. Biol.* **13**, 109–239.

Karlsson, A., Eliason, E. J., Mydland, L. T., Farrell, A. P. and Kiessling, A. (2006). Postprandial changes in plasma free amino acid levels obtained simultaneously from the hepatic portal vein and the dorsal aorta in rainbow trout (*Oncorhynchus mykiss*). *J. Exp. Biol.* **209**, 4885–4894.

Kaushik, S. J. and de Oliva Teles, A. (1985). Effect of digestible energy on nitrogen and energy balance in rainbow trout. *Aquaculture* **50**, 89–101.

Kaushik, S. J., Dabrowski, K. R., Dabrowska, H., Olah, E. and Luquet, P. (1983). Utilization of dietary urea in rainbow trout. *Ann. Nutr. Metab.* **27**, 94–106.

Khademi, S., O'Connell, J., Remis, J., Robles-Colmenares, Y., Miercke, L. J. W. and Stroud, R. M. (2004). Mechanism of ammonia transport by Amt/MEP/Rh: Structure of

AmtB at 135 Å. *Science (80-.).* **305**, 1587–1594.

Knepper, M. A. and Agre, P. (2004). Visualizing the Dynamics. *Science (80-.).* **305**,.

Knoph, M. B. and MåsØval, K. (1996). Plasma ammonia and urea levels in Atlantic salmon farmed in sea water. *J. Fish Biol.* **49**, 165–168.

Koelz, H. R. (1992). Gastric acid in vertebrates. *Scand. J. Gastroenterol.* **27**, 2–6.

Kong, H., Edberg, D. D., Korte, J. J., Salo, W. L., Wright, P. A. and Anderson, P. M. (1998). Nitrogen excretion and expression of carbamoyl-phosphate synthetase III activity and mRNA in extrahepatic tissues of largemouth bass (*Micropterus salmoides*). *Arch. Biochem. Biophys.* **350**, 157–168.

Korte, J. J., Salo, W. L., Cabrera, V. M., Wright, P. A., Felskie, A. K. and Anderson, P. M. (1997). Expression of carbamoyl-phosphate synthetase III mRNA during the early stages of development and in muscle of adult rainbow trout (*Oncorhynchus mykiss*). *J. Biol. Chem.* **272**, 6270–6277.

Krogdahl, Å., Nordrum, S., Sørensen, M., Brudeseth, L. and Røsjø, C. (1999). Effects of diet composition on apparent nutrient absorption along the intestinal tract and of subsequent fasting on mucosal disaccharidase activities and plasma nutrient concentration in Atlantic salmon *Salmo salar* L. *Aquac. Nutr.* **5**, 121–133.

Krogdahl, Å., Sundby, A. and Bakke, A. A. . (2011). Gut Secretion and Digestion. In *Encyclopedia of Fish Physiology: from Genome to Environment* (ed. Farrell, A. P., Cech, J. J., Richards, J. G., and Stevens, E. D.), pp. 1301–1310. Elsevier Inc.

Kurbel, S., Kurbel, B. and Včev, A. (2006). Intestinal gases and flatulence: Possible causes of occurrence. *Med. Hypotheses* **67**, 235–239.

Lacy, B. E., Gabbard, S. L. and Crowell, M. D. (2011). Pathophysiology, evaluation, and

treatment of bloating: Hope, hype, or hot air? *Gastroenterol. Hepatol.* **7**, 729–739.

Lee, K. S., Kita, J. and Ishimatsu, A. (2003). Effects of lethal levels of environmental hypercapnia on cardiovascular and blood-gas status in yellowtail, *Seriola quinqueradiata*. *Zoolog. Sci.* **20**, 417–422.

Li, T., Li, H., Gatesoupe, F. J., She, R., Lin, Q., Yan, X., Li, J. and Li, X. (2017). Bacterial signatures of "Red-Operculum" disease in the gut of crucian carp (*Carassius auratus*). *Microb. Ecol.* **74**, 510–521.

Lie-Venema, H., Hakvoort, T. B., van Hemert, F. J., Moorman, A. F. and Lamers, W. H. (1998). Regulation of the spatiotemporal pattern of expression of the glutamine synthetase gene. *Prog. Nucleic Acid Res. Mol. Biol.* **61**, 243–308.

Liew, H. J., Sinha, A. K., Nawata, C. M., Blust, R., Wood, C. M. and De Boeck, G. (2013). Differential responses in ammonia excretion, sodium fluxes and gill permeability explain different sensitivities to acute high environmental ammonia in three freshwater teleosts. *Aquat. Toxicol.* **126**, 63–76.

Lin, H.-C. and Visek, W. J. (1991). Large intestinal pH and ammonia in rats: Dietary fat and protein interactions. *J. Nutr.* **121**, 832–843.

Lin, L. Y., Weng, C. F. and Hwang, P. P. (2001). Regulation of drinking rate in euryhaline tilapia larvae (*Oreochromis mossambicus*) during salinity challenges. *Physiol. Biochem. Zool.* **74**, 171–177.

Lindley, T. E., Scheiderer, C. L., Walsh, P. J., Wood, C. M., Bergman, H. L., Bergman, A. L., Laurent, P., Wilson, P. and Anderson, P. M. (1999). Muscle as the primary site of urea cycle enzyme activity in an alkaline lake-adapted tilapia, *Oreochromis alcalicus grahami*. *J. Biol. Chem.* **274**, 29858–29861.

Liu, H., Guo, X., Gooneratne, R., Lai, R., Zeng, C., Zhan, F. and Wang, W. (2016). The gut microbiome and degradation enzyme activity of wild freshwater fishes influenced by their trophic levels. *Sci. Rep.* **6**, 1–12.

Liu, L., Huh, J. R. and Shah, K. (2022). Microbiota and the gut-brain-axis: Implications for new therapeutic design in the CNS. *eBioMedicine* **77**, 103908.

Loo, D. D. F., Wright, E. M. and Zeuthen, T. (2002). Water pumps. *J. Physiol.* **542**, 53–60.

López Nadal, A., Ikeda-Ohtsubo, W., Sipkema, D., Peggs, D., McGurk, C., Forlenza, M., Wiegertjes, G. F. and Brugman, S. (2020). Feed, Microbiota, and Gut Immunity: Using the Zebrafish Model to Understand Fish Health. *Front. Immunol.* **11**,.

Loretz, C. A. (1995). Electrophysiology of ion transport in teleost intestinal cells. *Fish Physiol.* **14**, 25–56.

Macfarlane, S. and Macfarlane, G. T. (2003). Regulation of short-chain fatty acid production. *Proc. Nutr. Soc.* **62**, 67–72.

MacKay, W. C. and Janicki, R. (1979). Changes in the EEL intestine during seawater adaptation. *Comp. Biochem. Physiol. - A Mol. Integr. Physiol.* **62**, 757–761.

Marcaggi, P. and Coles, J. A. (2001). Ammonium in nervous tissue: Transport across cell membranes, fluxes from neurons to glial cells, and role in signalling. *Prog. Neurobiol.* **64**, 157–183.

Marshall, W. S. and Grosell, M. (2005). Ion transport, osmoregulation and acid–base balance. In *The Physiology of Fishes* (ed. Evans, D. H. and Claiborne, J. B.), pp. 177–230. Boca Raton: CRC Press.

Martinez, A.-S., Cutler, C. P., Wilson, G. D., Phillips, C., Hazon, N. and Cramb, G. (2005). Regulation of expression of two aquaporin homologs in the intestine of the European eel:

Effects of seawater acclimation and cortisol treatment. *Am. J. Physiol. Integr. Comp. Physiol.* **288**, R1733–R1743.

McCue, M. D. (2006). Specific dynamic action: A century of investigation. *Comp. Biochem. Physiol. - A Mol. Integr. Physiol.* **144**, 381–394.

McDonald, M. D. and Grosell, M. (2006). Maintaining osmotic balance with an aglomerular kidney. *Comp. Biochem. Physiol. - A Mol. Integr. Physiol.* **143**, 447–458.

McDonald, T. R. and Ward, J. M. (2016). Evolution of electrogenic ammonium transporters (AMTs). *Front. Plant Sci.* **7**, 1–9.

McDonald, D. G., Walker, R. L., Wilkes, P. R. and Wood, C. M. (1982). H^+ excretion in the marine teleost *Parophrys vetulus*. *J. Exp. Biol.* **98**, 403–414.

McDonald, M. D., Smith, C. P. and Walsh, P. J. (2006). The physiology and evolution of urea transport in fishes. *J. Membr. Biol.* **212**, 93–107.

McFarland, W. (1959). A study of the effects of anesthetics on the behavior and physiology of fishes. *Publ. Inst. Mar. Sci.* **6**, 23–55.

McNeil, B. I. and Matsumoto, K. (2019). The changing ocean and freshwater CO_2 system. In *Fish Physiology: Carbon Dioxide* (ed. Grosell, M., Munday, P. L., Farrell, A. P., and Brauner, C. J.), pp. 1–32. Elsevier Inc.

Mensink, P. B. F., Geelkerken, R. H., Huisman, A. B., Kuipers, E. J. and Kolkman, J. J. (2006). Effect of various test meals on gastric and jejunal carbon dioxide: A study in healthy subjects. *Scand. J. Gastroenterol.* **41**, 1290–1298.

Milligan, C. L. and Wood, C. M. (1987). Regulation of blood oxygen transport and red cell pHi after exhaustive activity in rainbow trout (*Salmo gairdneri*) and starry flounder (*Platichthys stellatus*). *J. Exp. Biol.* **133**, 263–282.

Mommsen, T. P., Busby, E. R., Von Schalburg, K. R., Evans, J. C., Osachoff, H. L. and Elliott, M. E. (2003a). Glutamine synthetase in tilapia gastrointestinal tract: Zonation, cDNA and induction by cortisol. *J. Comp. Physiol. B Biochem. Syst. Environ. Physiol.* **173**, 419–427.

Mommsen, T. P., Osachoff, H. L. and Elliott, M. E. (2003b). Metabolic zonation in teleost gastrointestinal tract: Effect of fasting and cortisol in tilapia. *J. Comp. Physiol. B Biochem. Syst. Environ. Physiol.* **173**, 409–418.

Moran, B. J. and Jackson, A. A. (1990). 15N-urea metabolism in the functioning human colon: luminal hydrolysis and mucosal permeability. *Gut* **31**, 454–457.

Mouillé, B., Robert, V. and Blachier, F. (2004). Adaptative increase of ornithine production and decrease of ammonia metabolism in rat colonocytes after hyperproteic diet ingestion. *Am. J. Physiol. - Gastrointest. Liver Physiol.* **287**, 344–351.

Mountfort, D. O., Campbell, J., Kendall, D. and Clements, K. D. (2002). Hindgut fermentation in three species of marine herbivorous fish. *Appl. Environ. Microbiol.* **68**, 1374–1380.

Movileanu, L., Flonta, M. L., Mihailescu, D. and Frangopol, P. T. (1998). Characteristics of ionic transport processes in fish intestinal epithelial cells. *BioSystems* **45**, 123–140.

Müller, T., Walter, B., Wirtz, A. and Burkovski, A. (2006). Ammonium toxicity in bacteria. *Curr. Microbiol.* **52**, 400–406.

Murray, B. W., Busby, E. R., Mommsen, T. P. and Wright, P. A. (2003). Evolution of glutamine synthetase in vertebrates: multiple glutamine synthetase genes expressed in rainbow trout (*Oncorhynchus mykiss*). *J. Exp. Biol.* **206**, 1511–1521.

Nawata, C. M., Hung, C. C. Y., Tsui, T. K. N., Wilson, J. M., Wright, P. A. and Wood, C.

M. (2007). Ammonia excretion in rainbow trout (*Oncorhynchus mykiss*): Evidence for Rh glycoprotein and H^+-ATPase involvement. *Physiol. Genomics* **31**, 463–474.

Nawata, C. M., Wood, C. M. and O'Donnell, M. J. (2010). Functional characterization of Rhesus glycoproteins from an ammoniotelic teleost, the rainbow trout, using oocyte expression and SIET analysis. *J. Exp. Biol.* **213**, 1049–1059.

Nayak, S. K. (2010). Role of gastrointestinal microbiota in fish. *Aquac. Res.* **41**, 1553–1573.

Nikinmaa, M. (2006). Gas transport. In *The Physiology of Fishes* (ed. Evans, D. H. and Claiborne, J. B.), pp. 153–174. Boca Raton: CRC Press.

Niv, Y. and Fraser, G. M. (2002). The alkaline tide phenomenon. *J. Clin. Gastroenterol.* **35**, 5–8.

Ohashi, Y., Igarashi, T., Kumazawa, F. and Fujisawa, T. (2007). Analysis of acetogenic bacteria in human feces with formyltetrahydrofolate synthetase sequences. *Biosci. Microflora* **26**, 37–40.

Oliphant, K. and Allen-Vercoe, E. (2019). Macronutrient metabolism by the human gut microbiome: Major fermentation by-products and their impact on host health. *Microbiome* **7**, 1–15.

Ou, M., Hamilton, T. J., Eom, J., Lyall, E. M., Gallup, J., Jiang, A., Lee, J., Close, D. A., Yun, S. S. and Brauner, C. J. (2015). Responses of pink salmon to CO_2-induced aquatic acidification. *Nat. Clim. Chang.* **5**, 950–957.

Papastamatiou, Y. P. and Lowe, C. G. (2005). Variations in gastric acid secretion during periods of fasting between two species of shark. *Comp. Biochem. Physiol. - A Mol. Integr. Physiol.* **141**, 210–214.

Pelster, B. (2021). Using the swimbladder as a respiratory organ and/or a buoyancy structure—

Benefits and consequences. *J. Exp. Zool. Part A Ecol. Integr. Physiol.* **335**, 831–842.

Pelster, B., Wood, C. M., Speers-Roesch, B., Driedzic, W. R., Almeida-Val, V. and Val, A. (2015). Gut transport characteristics in herbivorous and carnivorous serrasalmid fish from ion-poor Rio Negro water. *J. Comp. Physiol. B Biochem. Syst. Environ. Physiol.* **185**, 225–241.

Perrott, M. N., Grierson, C. E., Hazon, N. and Balment, R. J. (1992). Drinking behaviour in sea water and fresh water teleosts, the role of the renin-angiotensin system. *Fish Physiol. Biochem.* **10**, 161–168.

Perry, S. F. and Gilmour, K. M. (2006). Acid-base balance and CO_2 excretion in fish: Unanswered questions and emerging models. *Respir. Physiol. Neurobiol.* **154**, 199–215.

Perry, S. F. and Reid, S. D. (1992). Relationship between blood O2 content and catecholamine levels during hypoxia in rainbow trout and American eel. *Am. J. Physiol.* **263**, R240-9.

Perry, S. F., Braun, M. H., Genz, J., Vulesevic, B., Taylor, J., Grosell, M. and Gilmour, K. M. (2010). Acid-base regulation in the plainfin midshipman (*Porichthys notatus*): An aglomerular marine teleost. *J. Comp. Physiol. B Biochem. Syst. Environ. Physiol.* **180**, 1213–1225.

Pfaffl, M. W. (2001). A new mathematical model for relative quantification in real-time RT–PCR. *Nucleic Acids Res.* **29**, 2002–2007.

Raabe, W. (1990). Effects of NH_4^+ on the function of the CNS. In *Advances in experimental medicine and biology*, pp. 99–120.

Rahmatullah, M. and Boyde, T. R. C. (1980). Improvements in the determination of urea using diacetyl monoxime; methods with and without deproteinisation. *Clin. Chim. Acta* **107**, 3–9.

Raldúa, D., Otero, D., Fabra, M. and Cerdà, J. (2008). Differential localization and regulation

of two aquaporin-1 homologs in the intestinal epithelia of the marine teleost *Sparus aurata* . *Am. J. Physiol. Integr. Comp. Physiol.* **294**, R993–R1003.

Ramos, M. A., Gonçalves, J. F. M., Costas, B., Batista, S., Lochmann, R., Pires, M. A., Rema, P. and Ozório, R. O. A. (2017). Commercial Bacillus probiotic supplementation of rainbow trout (*Oncorhynchys mykiss*) and brown trout (*Salmo trutta*): Growth, immune responses and intestinal morphology. *Aquac. Res.* **48**, 2538–2549.

Randall, D. (2011). Excretion of Ammonia. In *Encyclopedia of Fish Physiology: From Genome to Environment* (ed. Farrell, A. P., Cech, J. J., Richards, J. G., and Stevens, E. D.), pp. 1427–1443. Elsevier Inc.

Randall, D. J. and Ip, Y. K. (2006). Ammonia as a respiratory gas in water and air-breathing fishes. *Respir. Physiol. Neurobiol.* **154**, 216–225.

Randall, D. J. and Tsui, T. K. . (2002). Ammonia toxicity in fish. *Mar. Pollut. Bull.* **45**, 17–23.

Randall, D. J. and Wright, P. A. (1987). Ammonia distribution and excretion in fish. *Fish Physiol. Biochem.* **3**, 107–120.

Randall, D. J., Wood, C. M., Perry, S. F., Bergman, H., Maloiy, G. M. O., Mommsen, T. P. and Wright, P. A. (1989). Urea excretion as a strategy for survival in a fish living in a very alkaline environment. *Nature* **337**, 165–166.

Rankin, J. C., Cobb, C. S., Frankling, S. C. and Brown, J. A. (2001). Circulating angiotensins in the river lamprey, *Lampetra fluviatilis*, acclimated to freshwater and seawater: Possible involvement in the regulation of drinking. *Comp. Biochem. Physiol. - B Biochem. Mol. Biol.* **129**, 311–318.

Remesar, X., Arola, L., Palou, A. and Alemany, M. (1985). Activities of amino acid metabolizing enzymes in the stomach and small intestine of developing rats. *Reprod. Nutr.*

Dev. **25**, 861–866.

Ringø, E., Løvmo, L., Kristiansen, M., Bakken, Y., Salinas, I., Myklebust, R., Olsen, R. E. and Mayhew, T. M. (2010). Lactic acid bacteria vs. pathogens in the gastrointestinal tract of fish: A review. *Aquac. Res.* **41**, 451–467.

Rodríguez, A., Gallardo, M. A., Gisbert, E., Santilari, S., Ibarz, A., Sánchez, J. and Castelló-Orvay, F. (2002). Osmoregulation in juvenile Siberian sturgeon (*Acipenser baerrii*). *Fish Physiol. Biochem.* **26**, 345–354.

Rogers, G. B., Keating, D. J., Young, R. L., Wong, M. L., Licinio, J. and Wesselingh, S. (2016). From gut dysbiosis to altered brain function and mental illness: Mechanisms and pathways. *Mol. Psychiatry* **21**, 738–748.

Root, R. W. (1931). The respiratory function of the blood of marine fishes. *Biol. Bull.* **61**, 427–456.

Rubino, J. G., Zimmer, A. M. and Wood, C. M. (2014). An *in vitro* analysis of intestinal ammonia handling in fasted and fed freshwater rainbow trout (*Oncorhynchus mykiss*). *J. Comp. Physiol. B Biochem. Syst. Environ. Physiol.* **184**, 91–105.

Rubino, J. G., Zimmer, A. M. and Wood, C. M. (2015). Intestinal ammonia transport in freshwater and seawater acclimated rainbow trout (*Oncorhynchus mykiss*): Evidence for a Na^+ coupled uptake mechanism. *Comp. Biochem. Physiol. - A Mol. Integr. Physiol.* **183**, 45–56.

Rubino, J. G., Wilson, J. M. and Wood, C. M. (2019). An *in vitro* analysis of intestinal ammonia transport in fasted and fed freshwater rainbow trout: roles of NKCC, K^+ channels, and Na^+, K^+ ATPase. *J. Comp. Physiol. B Biochem. Syst. Environ. Physiol.* **189**, 549–566.

Ruiz-Jarabo, I., Barany, A., Jerez-Cepa, I., Mancera, J. M. and Fuentes, J. (2017). Intestinal

response to salinity challenge in the Senegalese sole (*Solea senegalensis*). *Comp. Biochem. Physiol. - A Mol. Integr. Physiol.* **204**, 57–64.

Rummer, J. L. and Brauner, C. J. (2015). Root effect haemoglobins in fish may greatly enhance general oxygen delivery relative to other vertebrates. *PLoS One* **10**, 1–17.

Schmidt-Nielsen, B. (1958). Urea excretion in mammals. *Am. Physiol. Soc.* **38**, 139–168.

Secor, S. M. (2009). Specific dynamic action: A review of the postprandial metabolic response. *J. Comp. Physiol. B Biochem. Syst. Environ. Physiol.* **179**, 1–56.

Seidelin, M., Madsen, S. S., Blenstrup, H. and Tipsmark, C. K. (2000). Time-course changes in the expression of Na^+,K^+-ATPase in gills and pyloric caeca of brown trout (*Salmo trutta*) during acclimation to seawater. *Physiol. Biochem. Zool.* **73**, 446–453.

Seth, H. and Axelsson, M. (2010). Sympathetic, parasympathetic and enteric regulation of the gastrointestinal vasculature in rainbow trout (*Oncorhynchus mykiss*) under normal and postprandial conditions. *J. Exp. Biol.* **213**, 3118–3126.

Seth, H. and Axelsson, M. (2011). Integrated responses of the circulatory system to digestion. In *Encyclopedia of Fish Physiology: From Genome to Environment* (ed. Farrell, A. P., Cech, J. J., Richards, J. G., and Stevens, E. D.), pp. 1206–1214. Elsevier Inc.

Seth, H., Sandblom, E. and Axelsson, M. (2009). Nutrient-induced gastrointestinal hyperemia and specific dynamic action in rainbow trout (*Oncorhynchus mykiss*)—importance of proteins and lipids. *Am. J. Physiol. Integr. Comp. Physiol.* **296**, R345–R352.

Seth, H., Axelsson, M. and Farrell, A. P. (2011). The circulation and metabolism of the gastrointestinal tract. In *Fish Physiology: Multifunctional Gut* (ed. Grosell, M., Farrell, A. P , and Brauner, C. J), pp. 351–394. Elsevier Inc.

Sharon, G., Sampson, T. R., Geschwind, D. H. and Mazmanian, S. K. (2016). The Central nervous system and the gut microbiome. *Cell* **167**, 915–932.

Shepherd, A. P. and Kiel, J. W. (1992). A model of countercurrent shunting of oxygen in the intestinal villus. *Am. J. Physiol.* **262**, H1136-42.

Shigemura, M., Lecuona, E. and Sznajder, J. I. (2017). Effects of hypercapnia on the lung. *J. Physiol.* **595**, 2431–2437.

Skou, J. C. (1990). The energy coupled exchange of Na^+ for K^+ across the cell membrane. The Na^+, K^+-pump. *FEBS Lett.* **268**, 314–24.

Skou, J. C. and Esmann, M. (1992). The Na,K-ATPase. *J. Bioenerg. Biomembr.* **24**, 249–261.

Skov, P. V. (2019). CO_2 in aquaculture. In *Fish Physiology: Carbon Dioxide* (ed. Grosell, M., Munday, P. L., Farrell, A. P., and Brauner, C. J.), pp. 287–321. Elsevier Inc.

Smith, H. W. (1930). The absorption and excretion of water and salts by marine teleosts. *Am. J. Physiol.* 480–505.

Smith, C. P. and Wright, P. A. (1999). Molecular characterization of an elasmobranch urea transporter. *Am. Physiol. Soc.*

Söderström, V. and Nilsson, G. E. (2000). Brain blood flow during hypercapnia in fish: No role of nitric oxide. *Brain Res.* **857**, 207–211.

Soivio, A., Westman, K. and Nyholm, K. (1972). Improved method of dorsal aorta catheterization: Hematological effects followed for three weeks in rainbow trout (*Salmo gairdneri*). *Finnish Fish. Res.* **1**, 11–21.

Solbé, J. F. de L. G. and Shurben, D. G. (1989). Toxicity of ammonia to early life stages of rainbow trout (*Salmo gairdneri*). *Water Res.* **23**, 127–129.

Steggerda, F. R. (1968). Gastrointestinal gas following food consumption. *Ann. N. Y. Acad. Sci.*

150, 57–66.

Suarez, F., Furne, J., Springfield, J. and Levitt, M. (1997). Insights into human colonic physiology obtained from the study of flatus composition. *Am. J. Physiol.* **272**, G1028-33.

Summerskill, W. H. J. and Wolpert, E. (1970). Ammonia metabolism in the gut. *Am. J. Clin. Nutr.* **23**, 633–639.

Summerskill, W. H. J., Aoyagi, T. and Evans, W. B. (1966). Ammonia in the upper gastrointestinal tract of man: quantitations and relationships. *Gut* **7**, 497–501.

Sundh, H., Calabrese, S., Jutfelt, F., Niklasson, L., Olsen, R. E. and Sundell, K. (2011). Translocation of infectious pancreatic necrosis virus across the intestinal epithelium of Atlantic salmon (*Salmo salar* L.). *Aquaculture* **321**, 85–92.

Sundh, H., Gräns, A., Brijs, J., Sandblom, E., Axelsson, M., Berg, C. and Sundell, K. (2018). Effects of coeliacomesenteric blood flow reduction on intestinal barrier function in rainbow trout *Oncorhynchus mykiss*. *J. Fish Biol.* **93**, 519–527.

Takei, Y., Wong, M. K. S., Pipil, S., Ozaki, H., Suzuki, Y., Iwasaki, W. and Kusakabe, M. (2017). Molecular mechanisms underlying active desalination and low water permeability in the esophagus of eels acclimated to seawater. *Am. J. Physiol. - Regul. Integr. Comp. Physiol.* **312**, R231–R244.

Talwar, C., Nagar, S., Lal, R. and Negi, R. K. (2018). Fish gut microbiome: Current approaches and future perspectives. *Indian J. Microbiol.* **58**, 397–414.

Taylor, J. R. and Grosell, M. (2006). Feeding and osmoregulation: Dual function of the marine teleost intestine. *J. Exp. Biol.* **209**, 2939–2951.

Taylor, J. R. and Grosell, M. (2009). The intestinal response to feeding in seawater gulf toadfish, *Opsanus beta*, includes elevated base secretion and increased epithelial oxygen

consumption. *J. Exp. Biol.* **212**, 3873–3881.

Taylor, J. R., Whittamore, J. M., Wilson, R. W. and Grosell, M. (2007). Postprandial acid-base balance and ion regulation in freshwater and seawater-acclimated European flounder, *Platichthys flesus*. *J. Comp. Physiol. B Biochem. Syst. Environ. Physiol.* **177**, 597–608.

Taylor, J. R., Mager, E. M. and Grosell, M. (2010). Basolateral NBCe1 plays a rate-limiting role in transepithelial intestinal HCO_3^- secretion, contributing to marine fish osmoregulation. *J. Exp. Biol.* **213**, 459–468.

Terjesen, B. F., Finn, R. N., Norberg, B. and Ronnestad, I. (2002). Kinetics and fates of ammonia, urea, and uric acid during oocyte maturation and ontogeny of the Atlantic halibut (*Hippoglossus hippoglossus* L.). *Comp. Biochem. Physiol. - A Mol. Integr. Physiol.* **131**, 443–455.

Tetens, V. and Lykkeboe, G. (1985). Acute exposure of rainbow trout to mild and deep hypoxia: O_2 affinity and O_2 capacitance of arterial blood. *Respir. Physiol.* **61**, 221–235.

Thorarensen, H. and Farrell, A. P. (2006). Postprandial intestinal blood flow, metabolic rates, and exercise in Chinook salmon (*Oncorhynchus tshawytscha*). *Physiol. Biochem. Zool.* **79**, 688–694.

Thorarensen, H., McLean, E., Donaldson, E. M. and Farrell, A. P. (1991). The blood vasculature of the gastrointestinal tract in chinook, *Oncorhynchus tshawytscha* (Walbaum), and coho, *O. kisutch* (Walbaum), salmon. *J. Fish Biol.* **38**, 525–531.

Tiso, M. and Schechter, A. N. (2015). Nitrate reduction to nitrite, nitric oxide and ammonia by gut bacteria under physiological conditions. *PLoS One* **10**, 1–18.

Tng, Y. Y. M., Wee, N. L. J., Ip, Y. K. and Chew, S. F. (2008). Postprandial nitrogen metabolism and excretion in juvenile marble goby, *Oxyeleotris marmorata* (Bleeker, 1852).

Aquaculture **284**, 260–267.

Tomlin, J., Lowis, C., Read, N. W. and Tomlin, S. J. (1991). Investigation of normal flatus production in healthy volunteers. *Gut* **32**, 665–669.

Tran, N. T., Zhang, J., Xiong, F., Wang, G. T., Li, W. X. and Wu, S. G. (2018). Altered gut microbiota associated with intestinal disease in grass carp (*Ctenopharyngodon idellus*). *World J. Microbiol. Biotechnol.* **34**, 1–9.

Tresguerres, M., Parks, S. K., Wood, C. M. and Goss, G. G. (2007). V-H^+-ATPase translocation during blood alkalosis in dogfish gills: interaction with carbonic anhydrase and involvement in the postfeeding alkaline tide. *Am. J. Physiol. Integr. Comp. Physiol.* **292**, R2012–R2019.

Tsui, T. K. N., Randall, D. J., Chew, S. F., Jin, Y., Wilson, J. M. and Ip, Y. K. (2002). Accumulation of ammonia in the body and NH_3 volatilization from alkaline regions of the body surface during ammonia loading and exposure to air in the weather loach *Misgurnus anguillicaudatus*. *J. Exp. Biol.* **205**, 651–659.

Tsui, T. K. N., Hung, C. Y. C., Nawata, C. M., Wilson, J. M., Wright, P. A. and Wood, C. M. (2009). Ammonia transport in cultured gill epithelium of freshwater rainbow trout: The importance of Rhesus glycoproteins and the presence of an apical Na^+/NH_4^+ exchange complex. *J. Exp. Biol.* **212**, 878–892.

Tufts, B. and Perry, S. F. (1998). Carbon Dioxide Transport and Excretion. In *Fish Physiology: Fish Respiration* (ed. Tufts, B. L. and Perry, S. F.), pp. 229–281. New York: Academic Press.

Turner, L. A. and Bucking, C. (2019). The role of intestinal bacteria in the ammonia detoxification ability of teleost fish. *J. Exp. Biol.* **222**,.

Ussing, H. . (1949). The active ion transport through the isolated frog skin in the light of tracer studies. *Acta Physiol.* **17**, 1–37.

Vargas-Albores, F., Martínez-Córdova, L. R., Hernández-Mendoza, A., Cicala, F., Lago-Lestón, A. and Martínez-Porchas, M. (2021). Therapeutic modulation of fish gut microbiota, a feasible strategy for aquaculture? *Aquaculture* **544**,.

Vaugelade, P., Posho, L., Darcy-Vrillon, B., Bernard, F., Morel, M.-T. and Duee, P.-H. (1994). Intestinal oxygen uptake and glucose metabolism during nutrient absorption in the pig. *Proc. Soc. Exp. Biol. Med.* **207**, 309–316.

Verdouw, H., Van Echteld, C. J. A. and Dekkers, E. M. J. (1978). Ammonia determination based on indophenol formation with sodium salicylate. *Water Res.* **12**, 399–402.

Vince, A. J. and Burridge, S. M. (1980). Ammonia production by intestinal bacteria: the effects of lactose, lactulose and glucose. *J. Med. Microbiol.* **13**, 177–191.

Walsh, P. J., Heitz, M. J., Campbell, C. E., Cooper, G. J., Medina, M., Wang, Y. S., Goss, G. G., Vincek, V., Wood, C. M. and Smith, C. P. (2000). Molecular characterization of a urea transporter in the gill of the gulf toadfish (*Opsanus beta*). *J. Exp. Biol.* **203**, 2357–2364.

Walsh, P., Wang, Y., Campbell, C., Boeck, D. G. and Wood, C. (2001). Patterns of nitrogenous waste excretion and gill urea transporter mRNA expression in several species of marine fish. *Mar. Biol.* **139**, 839–844.

Wang, T., Busk, M. and Overgaard, J. (2001). The respiratory consequences of feeding in amphibians and reptiles. *Comp. Biochem. Physiol. - A Mol. Integr. Physiol.* **128**, 533–547.

Ward, J. B. J., Keely, S. J. and Keely, S. J. (2014). Oxygen in the regulation of intestinal epithelial transport. *J. Physiol.* **592**, 2473–2489.

Watters, K. W. and Smith, L. S. (1973). Respiratory dynamics of the starry flounder *Platichthys stellatus* in response to low oxygen and high temperature. *Mar. Biol.* **19**, 133–148.

Weihrauch, D., Wilkie, M. P. and Walsh, P. J. (2009). Ammonia and urea transporters in gills of fish and aquatic crustaceans. *J. Exp. Biol.* **212**, 1716–1730.

Weiner, I. D. (2006). Expression of the non-erythroid Rh glycoproteins in mammalian tissues. *Transfus. Clin. Biol.* **13**, 159–163.

Weiner, I. D. and Hamm, L. L. (2007). Molecular mechanisms of renal ammonia transport. *Annu. Rev. Physiol.* **69**, 317–340.

Weinrauch, A. M., Clifford, A. M. and Goss, G. G. (2018). Post-prandial physiology and intestinal morphology of the Pacific hagfish (*Eptatretus stoutii*). *J. Comp. Physiol. B Biochem. Syst. Environ. Physiol.* **188**, 101–112.

Wells, R. M. G. (2009). Blood-gas tansport and hemoglobin function: adaptations for functional and environmental hypoxia. In *Fish Physiology* (ed. Richards, J. G., Farrell, A. P., and Brauner, C. J.), pp. 255–299. San Diego: Elsevier Inc.

Wicks, B. J. and Randall, D. J. (2002a). The effect of feeding and fasting on ammonia toxicity in juvenile rainbow trout, *Oncorhynchus mykiss*. *Aquat. Toxicol.* **59**, 71–82.

Wicks, B. J. and Randall, D. J. (2002b). The effect of sub-lethal ammonia exposure on fed and unfed rainbow trout: The role of glutamine in regulation of ammonia. *Comp. Biochem. Physiol. - A Mol. Integr. Physiol.* **132**, 275–285.

Wideman, R. F., Hooge, D. M. and Cummings, K. R. (2003). Dietary sodium bicarbonate, cool temperatures, and feed withdrawal: Impact on arterial and venous blood-gas values in broilers. *Poult. Sci.* **82**, 560–570.

Wilkie, M. P., Clifford, A. M., Edwards, S. L. and Goss, G. G. (2017). Wide scope for ammonia and urea excretion in foraging Pacific hagfish. *Mar. Biol.* **164**, 1–10.

Wilson, R. W. and Grosell, M. (2003). Intestinal bicarbonate secretion in marine teleost fish - Source of bicarbonate, pH sensitivity, and consequences for whole animal acid-base and calcium homeostasis. *Biochim. Biophys. Acta - Biomembr.* 163–174.

Wilson, R. W., Gilmour, K. M., Henry, R. P. and Wood, C. M. (1996). Intestinal base excretion in the seawater-adapted rainbow trout: A role in acid-base balance? *J. Exp. Biol.* **199**, 2331–2343.

Wilson, R. W., Wilson, J. M. and Grosell, M. (2002). Intestinal bicarbonate secretion by marine teleost fish - Why and how? *Biochim. Biophys. Acta-Biomembranes* **1566**, 182–193.

Wolf, K. (1963). Physiological salines for fresh water teleosts. *Progress. Fish Cult.* **25**, 135–140.

Wolff, C. B. (2007). Normal cardiac output, oxygen delivery and oxygen extraction. In *Oxygen Transport to Tissue XXVIII* (ed. Maguire, D. J., Bruley, D. F., and Harrison, D. K.), pp. 169–182. Boston: Springer.

Wood, C. M. (2001). The influence of feeding, exercise, and temperature on nitrogen metabolism and excretion. In *Fish Physiology: Nitrogen Excretion* (ed. Anderson, P. A. and Wright, P. A.), pp. 201–238. Orlando, FL, U.S.A: Academic Press.

Wood, C. M. (2019). Internal spatial and temporal CO_2 dynamics: Fasting, feeding, drinking, and the alkaline tide. In *Fish Physiology: Carbon Dioxide* (ed. Grosell, M., Munday, P. L., Farrell, A. P., and Brauner, C. J.), pp. 245–286. Elsevier Inc.

Wood, C. M. and Eom, J. (2019). The internal CO_2 threat to fish: High PCO_2 in the digestive tract. *Proc. R. Soc. B Biol. Sci.* **286**,.

Wood, C. M. and Grosell, M. (2012). Independence of net water flux from paracellular

permeability in the intestine of *Fundulus heteroclitus*, a euryhaline teleost. *J. Exp. Biol.* **215**, 508–517.

Wood, C. M. and Nawata, C. M. (2011). A nose-to-nose comparison of the physiological and molecular responses of rainbow trout to high environmental ammonia in seawater *versus* freshwater. *J. Exp. Biol.* **214**, 3557–3569.

Wood, C. M., McMahon, B. R. and McDonald, D. G. (1979). Respiratory gas exchange in the resting starry flounder, *Platichthys stellatus*: a comparison with other teleosts. *J. Exp. Biol.* **78**, 167–179.

Wood, C. M., Turner, J. D. and Graham, M. S. (1983). Why do fish die after severe exercise? *J. Fish Biol.* **22**, 189–201.

Wood, C. M., Perry, S. F., Wright, P. A., Bergman, H. L. and Randall, D. J. (1989). Ammonia and urea dynamics in the Lake Magadi tilapia, a ureotelic teleost fish adapted to an extremely alkaline environment. *Respir. Physiol.* **77**, 1–20.

Wood, C. M., Hopkins, T. E., Hogstrand, C. and Walsh, P. J. (1995). Pulsatile urea excretion in the ureagenic toadfish Opsanus beta: an analysis of rates and routes. *J. Exp. Biol.* **198**, 1729–17241.

Wood, C. M., Kajimura, M., Mommsen, T. P. and Walsh, P. J. (2005). Alkaline tide and nitrogen conservation after feeding in an elasmobranch (*Squalus acanthias*). *J. Exp. Biol.* **208**, 2693–2705.

Wood, C. M., Bucking, C., Fitzpatrick, J. and Nadella, S. (2007). The alkaline tide goes out and the nitrogen stays in after feeding in the dogfish shark, *Squalus acanthias*. *Respir. Physiol. Neurobiol.* **159**, 163–170.

Wood, C. M., Iftikar, F. I., Scott, G. R., De Boeck, G., Sloman, K. A., Matey, V., Valdez

Domingos, F. X., Duarte, R. M., Almeida-Val, V. M. F. and Val, A. L. (2009). Regulation of gill transcellular permeability and renal function during acute hypoxia in the Amazonian oscar (*Astronotus ocellatus*): new angles to the osmorespiratory compromise. *J. Exp. Biol.* **212**, 1949–1964.

Wood, C. M., Bucking, C. and Grosell, M. (2010). Acid-base responses to feeding and intestinal Cl^- uptake in freshwater- and seawater-acclimated killifish, *Fundulus heteroclitus*, an agastric euryhaline teleost. *J. Exp. Biol.* **213**, 2681–2692.

Wood, C. M., Nawata, C. M., Wilson, J. M., Laurent, P., Chevalier, C., Bergman, H. L., Bianchini, A., Maina, J. N., Johannsson, O. E., Bianchini, L. F., et al. (2013). Rh proteins and NH_4^+-activated NH_4^+-ATPase in the Magadi tilapia (*Alcolapia grahami*), a 100% ureotelic teleost fish. *J. Exp. Biol.* **216**, 2998–3007.

Wood, C. M., Liew, H. J., De Boeck, G., Hoogenboom, J. L. and Anderson, W. G. (2019). Nitrogen handling in the elasmobranch gut: a role for microbial urease. *J. Exp. Biol.* **222**,.

Worrell, R. T., Merk, L. and Matthews, J. B. (2008). Ammonium transport in the colonic crypt cell line, T84: Role for Rhesus glycoproteins and NKCC1. *Am. J. Physiol. - Gastrointest. Liver Physiol.* **294**, 429–440.

Wright, P. A. and Wood, C. M. (2009). A new paradigm for ammonia excretion in aquatic animals: role of Rhesus (Rh) glycoproteins. *J. Exp. Biol.* **212**, 2303–2312.

Wright, P. A. and Wood, C. M. (2012). Seven things fish know about ammonia and we don't. *Respir. Physiol. Neurobiol.* **184**, 231–240.

Wright, P. A., Wood, C. M. and Randall, D. J. (1988). An *in vitro* and *in vivo* study of the distribution of ammonia between plasma and red cells of rainbow trout (*Salmo gairdneri*). *J. Exp. Biol.* **134**, 423–428.

Wright, P. A., Felskie, A. and Anderson, P. M. (1995). Induction of ornithine-urea cycle enzymes and nitrogen metabolism and excretion in rainbow trout (*Oncorhynchus mykiss*) during early life stages. *J. Exp. Biol.* **198**, 127–135.

Wright, P. A., Steele, S. L., Huitema, A. and Bernier, N. J. (2007). Induction of four glutamine synthetase genes in brain of rainbow trout in response to elevated environmental ammonia. *J. Exp. Biol.* **210**, 2905–2911.

Yen, J. T., Nienaber, J. A., Hill, D. A. and Pond, W. G. (1989). Oxygen consumption by portal vein-drained organs and by whole animal in conscious growing swine. *Proc. Soc. Exp. Biol. Med.* **190**, 393–398.

Zhang, X. J., Yang, W. M., Zhang, D. F., Li, T. T., Gong, X. N. and Li, A. H. (2015). Does the gastrointestinal tract serve as the infectious route of Aeromonas hydrophila in crucian carp (*Carassius carassius*)? *Aquac. Res.* **46**, 141–154.

Zimmer, A. M., Nawata, C. M. and Wood, C. M. (2010). Physiological and molecular analysis of the interactive effects of feeding and high environmental ammonia on branchial ammonia excretion and Na^+ uptake in freshwater rainbow trout. *J. Comp. Physiol. B Biochem. Syst. Environ. Physiol.* **180**, 1191–1204.

Zimmer, A. M., Wright, P. A. and Wood, C. M. (2017). Ammonia and urea handling by early life stages of fishes. *J. Exp. Biol.* **220**, 3843–3855.

Appendix

A.1 Intestinal Vasculature Potential Countercurrent Exchanger

Observation of the rainbow trout GIT confirmed a lack of intestinal villi, but the presence of circular folds that were regionally confined to the posterior intestine (Harder, 1975; Kapoor et al., 1975). Thus, this thesis focused on the posterior intestinal fold vasculature to investigate whether a potential countercurrent exchanger exists in fish, similar to that of mammals (Bernier-Latmani and Petrova, 2016). Corrosion casting (Giuvărăşteanu, 2007; Rogers et al., 2014) and a fluorescent dye technique (Ricard et al., 2009) were used on various sizes of rainbow trout and adult English sole. Then, either scanning electron microscopy (SEM) or confocal microscopy (single and two-photon) was employed to image the samples. Each approach yielded useful information, but also had its limitations, which will be discussed in the following sections.

Through a combination of these different techniques, I found that the serosal intestinal layer of the rainbow trout was lined with interconnected blood vessels (Figures S.7 & S.8; asterisks). On the mucosal side, the circular folds facing into the lumen in the posterior intestine were supplied with a larger blood vessel running parallel along the fold (Figures S.4 & S.7) and smaller blood vessels branching off perpendicularly (Figures S.4 & S.5 & S.6). These blood vessels projected toward the lumen, reaching down to a width < 5 μm at the tip, then returning back down (Figures S.4 & S.5) to form a row of blood vessel loops along the intestinal fold. English sole had a similar arrangement of rows of blood vessels within the posterior intestinal folds, with a network of interconnected capillary beds at the tip facing the lumen (Figure S.3). The distance between the afferent and efferent blood vessels of a single loop in rainbow trout was greater (~50-100 μm) than those known in the villi of mammals (20-30 μm; Jodal and Lundgren, 1986; Shepherd and Kiel, 1992). However, the intestinal folds of rainbow trout seem

to resemble mammalian villi epithelia fused together, with capillary beds similarly projecting toward the lumen. I conclude that it is possible that countercurrent exchange occurs between the afferent and efferent branches of the loops in fish, but this hypothesis needs to be investigated.

A.2 Casting and SEM

The experiments were conducted at the appropriate salinity at either UBC for fed FW rainbow trout (300 g) or at BMSC for fed SW English sole (300-400 g). All other experimental protocols were identical between the species. The fish was initially anaesthetized in a high dose of NaOH-neutralized MS-222 (> 0.3 g L^{-1}; Syndel Laboratories, Parksville, British Columbia, Canada), weighed and given a caudal injection of 1000 I.U. mL^{-1} heparin (Sigma-Aldrich, St. Louis, MO, USA) to prevent clotting. It was then placed on a surgery table and the gills were irrigated with 9 ˚C temperature-controlled anaesthetic water (~0.03 g L^{-1}). A 3-cm sagittal incision was made in-between the pectoral fins and the heart was exposed. PE50 tubing filled with heparinized (50 I.U. mL^{-1}) Cortland's saline without glucose (Wolf, 1963; See Table S.1 for composition) was inserted into the bulbus arteriosus, pushed forward, and tightly secured with a 2-0 silk thread. A small incision was made in the ventricle for drainage, and then slow perfusion with the heparinized Cortland's saline was started, using a 100-mL syringe *via* hand injection. After perfusion with a volume of saline approximately 3-fold the blood volume that was estimated at 5% of body mass (Olson, 1992). Mercox casting solution (Ladd Research, Williston, USA) at approximately 2-fold the blood volume was then injected as quickly as possible.

Following casting, the fish was kept in a warm water bath (~30-35 ˚C) for > 1 h for the casting solution to polymerize. The specimens were kept in a -20 ˚C freezer until maceration and microscopy. In rainbow trout, the fish was macerated as a whole animal in a strong basic solution

(30 % KOH), while in English sole, the intestine was carefully dissected out and tissues were macerated in the same strong basic solution. The casts were air-dried for > 24 h, then mounted on a metal platform with an adhesive tape to be sputter-coated with gold (Cressington 208HR High Resolution Sputter Coater) and observed at 15 kV in the SEM (Hitachi S-2600 SEM).

Figure S.1 is a photo of the whole animal vascular system of a rainbow trout casted with Mercox, showing a particularly structured and well-vascularized stomach and posterior intestine relative to other GIT sections. The dorsal and ventral intestinal veins are shown along the posterior intestine running longitudinally (Figure S.1; arrows), connected by circular loops of blood vessels. Overall, the cast was similar to the vasculature described in Thorarensen et al. (1991). The other parts of the intestine seemed to be less vascularized, however the breakage of the casts during preparation may have resulted in some loss of structure.

Figures S.2 & S.3 are SEM images of Mercox casts of rainbow trout and English sole posterior intestine respectively. Figure S.2 is a piece of the posterior intestinal cast taken from the whole animal cast of Figure S.1. In these samples, it was difficult to interpret the vascular structure facing the lumen of rainbow trout due to breakage of the casts (Figure S.2). English sole had rows of blood vessels projecting towards the lumen (Figure S.3) similar to those of rainbow trout observed using a different technique (Figure S.4). These blood vessels then formed interconnected capillary beds at the tip (Figure S.3). There were a few limitations with this approach. First, the brittle nature of Mercox caused breakage of the fine capillaries (< 20 μm) during maceration, making it difficult to obtain an intact cast to image. Secondly, precise morphometric measurements such as vessel diameters and intervascular distances were not achievable with SEM.

A.3 Microfil and single photon microscopy

To address the issue of the brittle nature of Mercox, a silicon-based casting solution Microfil (MV-122 yellow; Flow Tek Inc, Colorado, USA) was used on adult rainbow trout at UBC. Fed rainbow trout (100-150 g) were anaesthetized in a high dose of NaOH-neutralized MS-222 (> 0.3 g L^{-1}), weighed, transferred to the surgery table where the gills were irrigated with 9 ˚C temperature-controlled anaesthetic water (~0.03 g L^{-1}) throughout the experiment. A catheter (PE50) filled with heparinized (50 I.U. mL^{-1}) 0.9 % saline was inserted into the dorsal aorta (DA) by the method of Soivio et al. (1972). The fish was then injected *via* this catheter with 1 mL of 1000 I.U. mL^{-1} heparin and 0.01 M of papaverine (vasodilator; Sigma-Aldrich, St. Louis, MO, USA). A small incision was made in the ventricle for drainage, and then the whole vasculature was perfused with a volume of heparinized (50 I.U. mL^{-1}) 0.9 % saline equivalent to approximately 3-fold the blood volume *via* the DA catheter. This was done using a 100 mL-syringe for hand injection. Initial attempts included use of peristaltic pumps, but proved to supply insufficient pressure to give an adequate blood clearance and Microfil filling.

The Microfil casting solution was made with a modified ratio (30 g diluent, 10 g compound, 1 g of curing agent) to decrease viscosity and was injected through the DA catheter at a volume approximately equivalent to 2-fold the blood volume. The incision of the ventricle was sutured shut with silk thread and the DA catheter was tied in a knot to stop any solution from flowing out during polymerization. The specimen was transferred to a 4 ˚C fridge for at least 24 h to polymerize. The whole GIT was taken out, immersed in increasing concentrations of ethanol for 24 h at each step (25, 50, 75, 95 and 100 %), then immersed in 100% methyl salicylate for 24 h. The posterior intestinal folds were cut out under a stereoscope with small surgical scissors (Figure S.4). The images in Figure S.4 support the presence of blood vessel loops in circular

intestinal folds, as seen in Figure S.1, with better filling of the smaller blood vessels than Mercox. Each of the folds had branches of blood vessels projecting towards the lumen.

Sections of the casts were imaged confocally using an Olympus FV1000 Confocal Microscope in z-stack series at 25X (Figures S.5 & S.6). As can be seen in Figures S.5 and S.6, an afferent blood vessel (~5–10 μm in width) projected towards the lumen, looped back down at the tip of the fold, and joined the major blood vessel lining the fold in the serosa. The distances between the afferent and efferent blood vessels of the loops were anywhere from ~50–100 μm. The capillaries at the tip of the fold were < 5 μm in width, just enough for erythrocytes to squeeze through (Witeska, 2013). Although this was the best combination of techniques that gave a better visualization of the vasculature, it also did not give a complete filling of the capillaries even with a reduced viscosity casting solution.

A.4 Fluorescent dye and two-photon microscopy

Fed juvenile rainbow trout (20-25 g) were anaesthetized with NaOH-neutralized MS-222 (0.1–0.2 g L^{-1}) and weighed. A caudal injection of 50 μL of heparinized (1000 I.U. mL^{-1}) rhodamine B-dextran (0.02 g mL^{-1}; Sigma-Aldrich, St. Louis, MO, USA) was given with a 100 μL Hamilton syringe. Fish were transferred back to the anaesthetic water for 10 min for the rhodamine to circulate in the vascular system. Another caudal injection of 100 μL of 0.1 mg mL^{-1} atropine (Sigma-Aldrich, St. Louis, MO, USA) was given to immobilize the smooth muscle of the GIT and the fish was transferred to the anaesthetic water for 20 min. The fish was euthanized in an overdose of MS-222 (> 0.3 g L^{-1}), the peritoneal cavity was revealed, and the rectum was tied with silk thread. Then, 100 μL of 0.002 g mL^{-1} fluorescein isothiocyanate (FITC; Sigma-Aldrich, St. Louis, MO, USA) was injected into the lumen through the pyloric sphincter. The

posterior intestine was tied to make gut sacs (Figure S.7), and then imaged from the serosal surfaces confocally using an Olympus FV1000 Confocal Microscope in z-stack series at 25X (Figure S.8).

These images, again, confirmed the larger blood vessels (~50–100 μm) lining the circular folds in the posterior intestine of rainbow trout (Figure S.7) that give rise to the vasculature seen in Figures S.4, S.5 & S.6. The serosal wall was also lined with smaller blood vessels (~10 μm; shown with asterisks in Figures S.7 & S.8). However, the two-photon microscopy did not give enough depth penetration from the serosa into the lumen to visualize the vasculature within the folds.

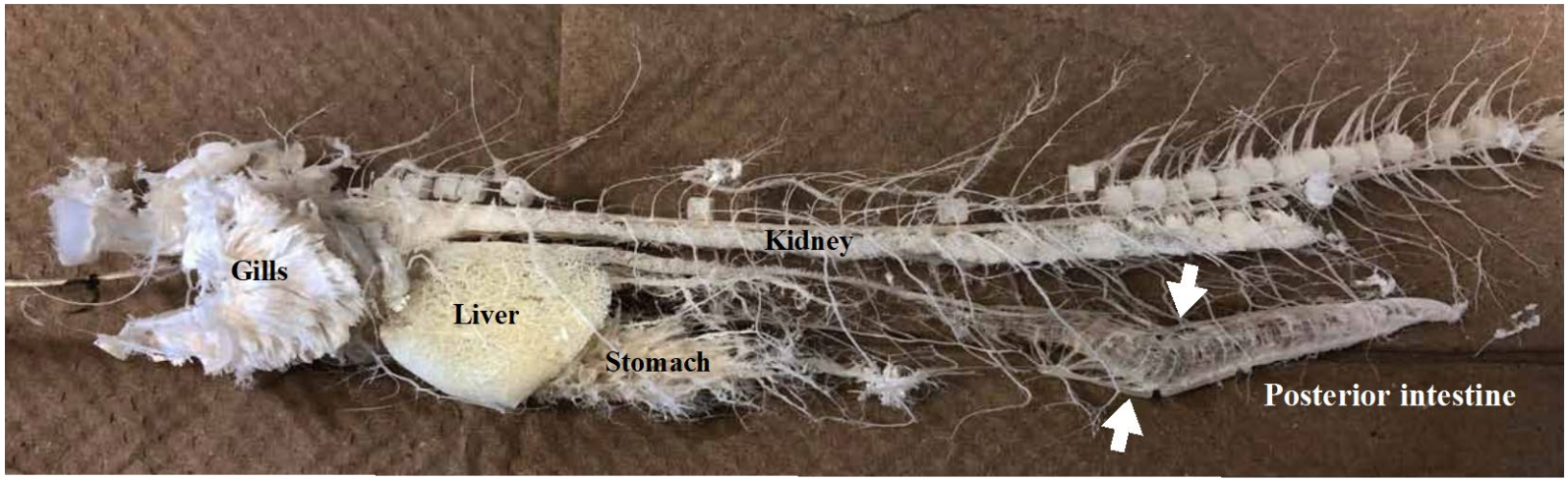

Figure S.1 Rainbow trout vasculature cast using Mercox. Only the posterior section of the intestine remains post maceration due to its more structured, highly vascularized circular intestinal folds. The dorsal and ventral intestinal veins are shown with arrows.

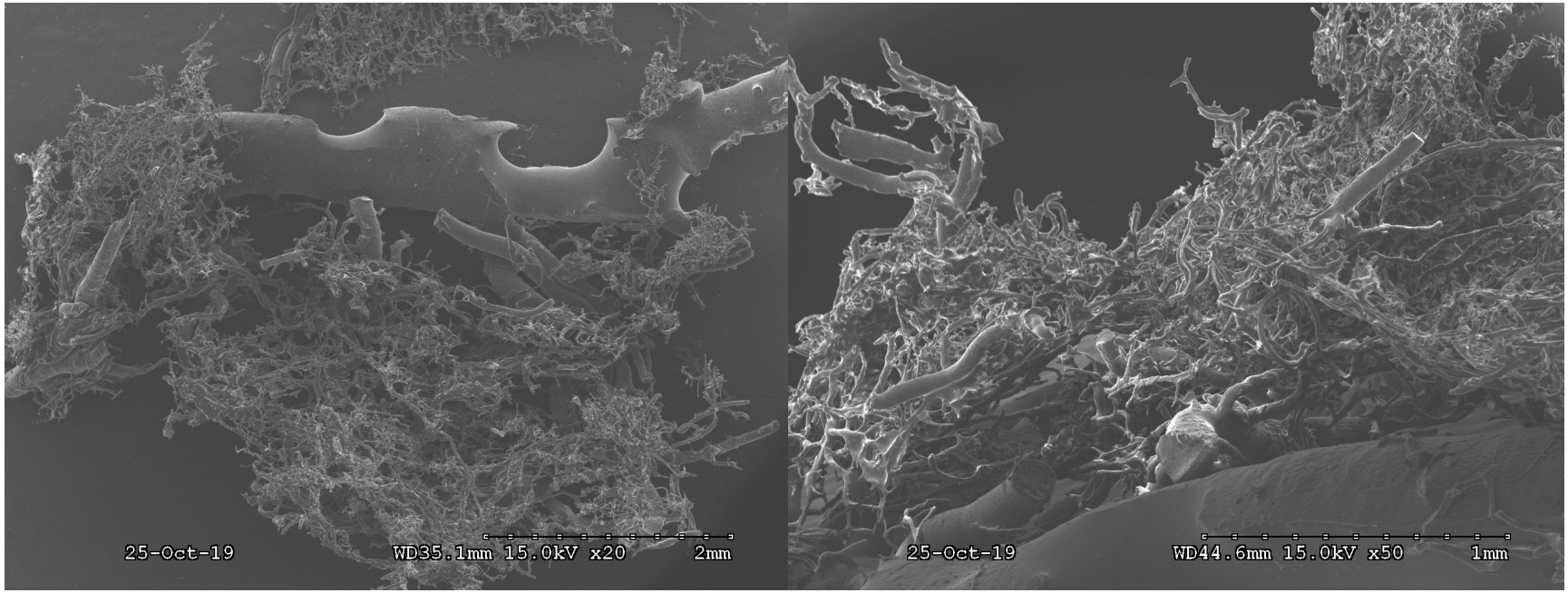

Figure S.2 Mercox cast of the rainbow trout posterior intestinal vasculature from Figure S.1 viewed under SEM. The length of the dotted line represents the relative scale on each image. The left image is a top down view from the lumen to the serosa, and the larger vessel at the top representing the ventral subintestinal vein. On the right image, the lumen is the top left corner and the serosa is the bottom right corner. A network of smaller blood vessels branch off from the ventral subintestinal vein and project toward the lumen. The majority of the smaller blood vessels were broken off during maceration, preventing visualization of the complete network orientation.

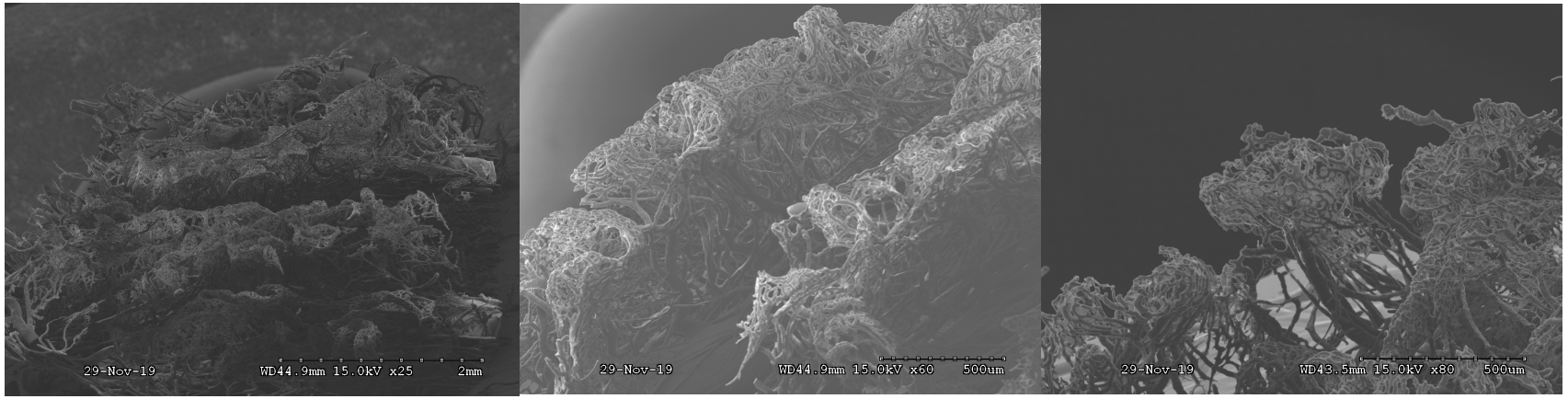

Figure S.3 Mercox cast of the English sole posterior intestinal vasculature viewed under SEM. The length of the dotted line represents the relative scale on each image. The left image is a top down view from the lumen to the serosa, showing a network of blood vessels within the intestinal folds running horizontally. The centre and right images are magnified images of the blood vessels branching into the lumen (top left). The blood vessels are organized in a tree-like fashion with vessels branching straight into the lumen, forming a network of round, interconnected capillary beds at the tip.

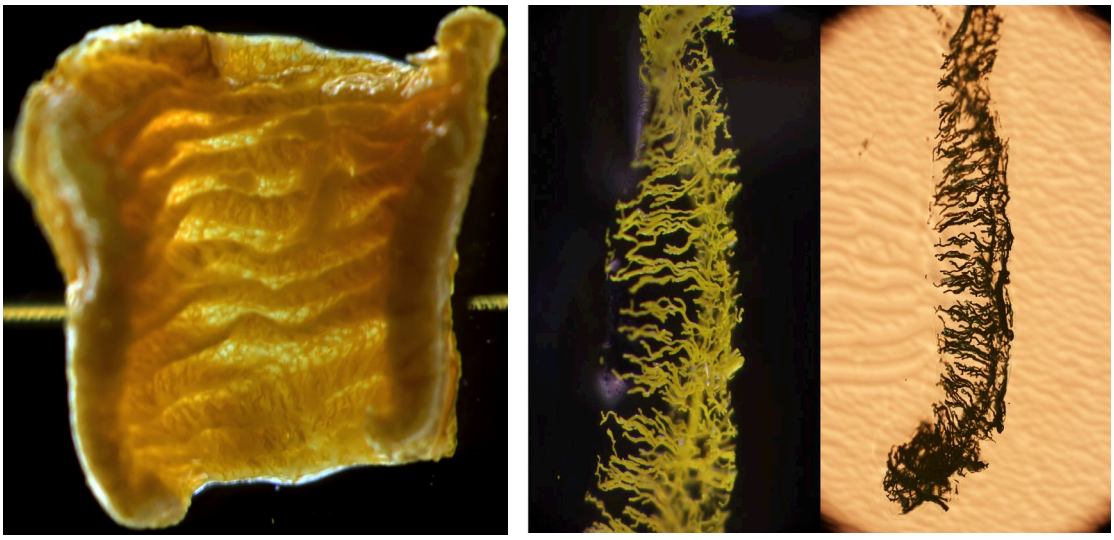

Figure S.4 Microfil filled vasculature of rainbow trout posterior intestinal folds with tissue clearing viewed under stereoscope. The left photo is a sagittal sectioning of the posterior intestine, showing the circular intestinal folds running horizontally. The right photos are of a single intestinal fold dissected out from the left and laid flat with the left sides facing the lumen. Blood vessels branching towards the lumen from the larger blood vessel(s) of each fold are seen.

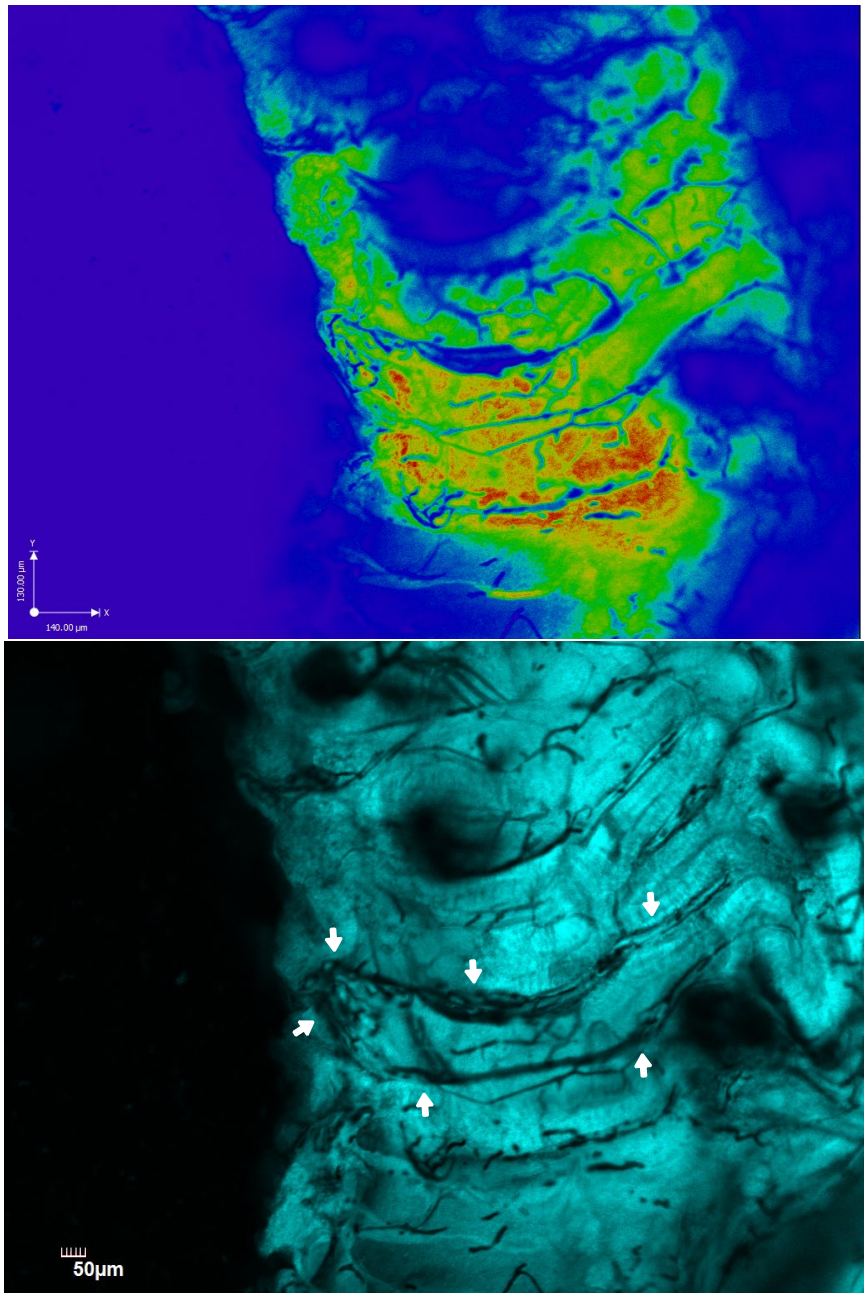

Figure S.5 Negative fluorescence of the Microfil filled vasculature in a single posterior intestinal fold of rainbow trout shown in Figure S.4 viewed under a single-photon microscope. Two images are of the same location with different colour channels. The left side is facing the lumen. Arrows on the second image show a vascular loop starting from the serosal side (right) to the lumen (left) then coming back to the serosal side The blood vessel is ~5-10 µm in width.

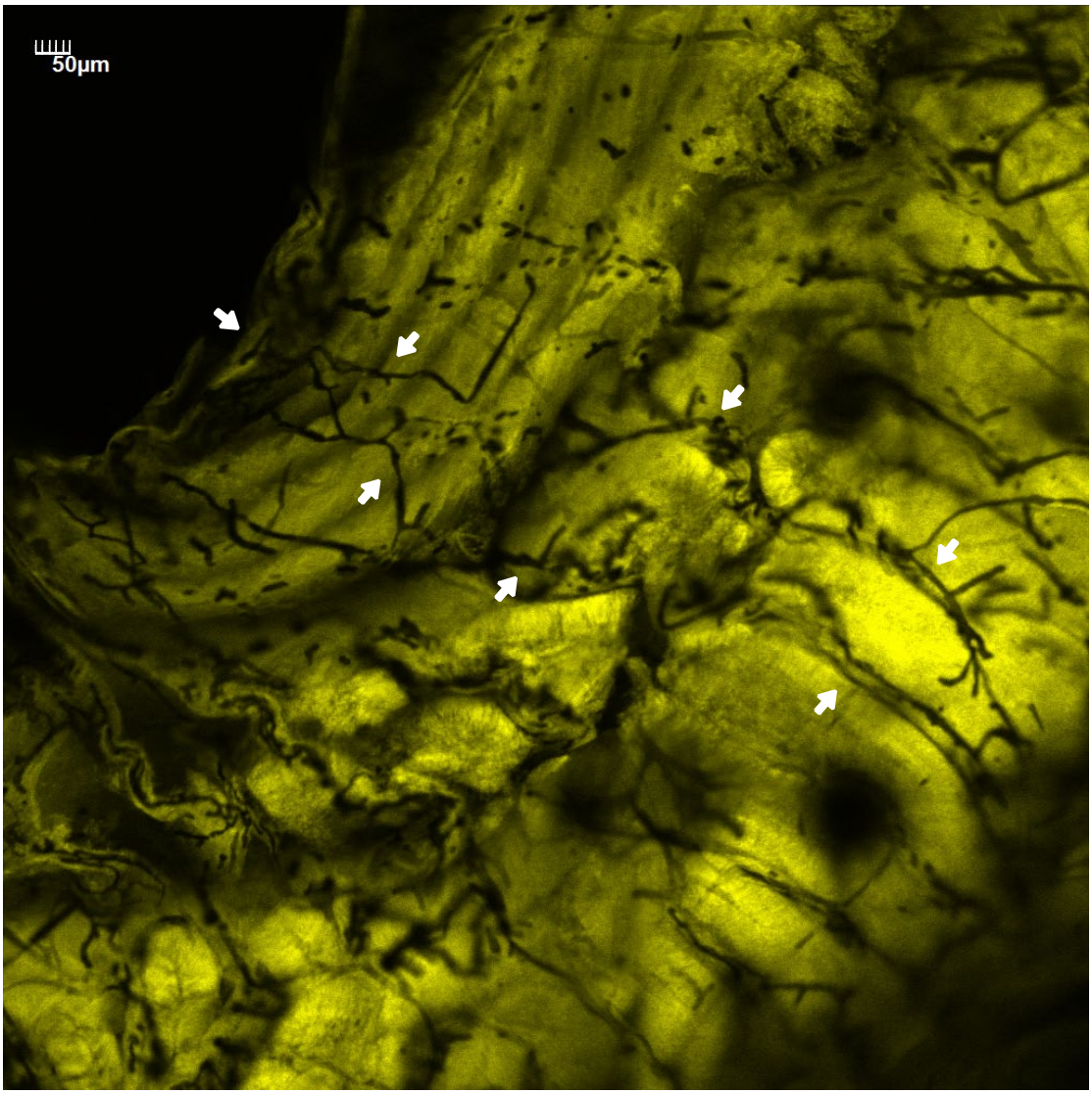

Figure S.6 Negative fluorescence of the Microfil filled vasculature in a single posterior intestinal fold of rainbow trout shown in Figure S.4 viewed under a single-photon microscope. The top left corner is facing the lumen. Arrows show a potential vascular loop starting from the serosal side (bottom right) to the lumen (top left) then coming back to the serosal side. The blood vessel at the tip is < 5 µm in width.

Figure S.7 Posterior intestine sac of juvenile rainbow trout injected with rhodamine in the vascular system and fluorescein filled lumen viewed under a stereoscope. The second photo is a magnification of the blood vessels. Blood vessels lining the circular folds are shown with black arrows. White asterisks (*) show smaller blood vessels lining the serosal wall.

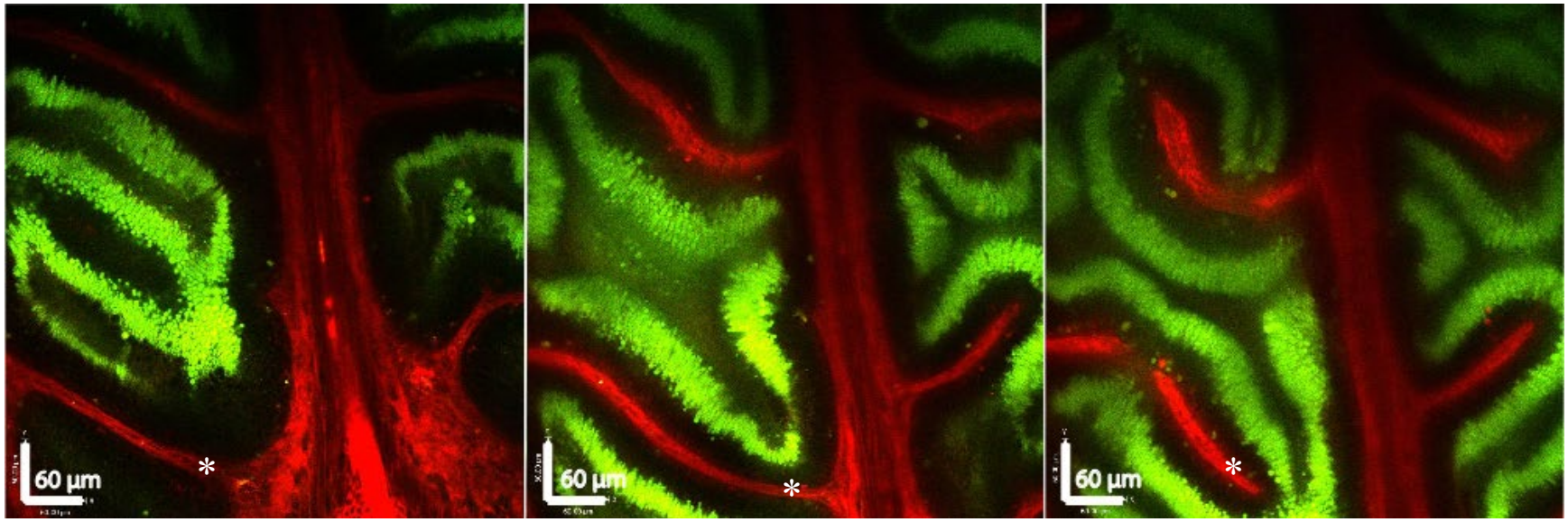

Figure S.8 Two-photon microscopy images of the posterior intestinal sacs shown in Figure S.7. Starting from the left panel, approximately 180, 200 and 240 µm in depth from the serosa into the lumen. The blood vessels stained with rhodamine (red) and the lumen stained with fluorescein (green). The larger blood vessel (~50-100 µm) running vertically in the images is the circular fold blood vessel, also shown with black arrows in Figure S.7. White asterisk (*) indicates the smaller blood vessels (~10 µm) lining the serosal wall as shown in Figure S.7. Due to the limitation with the depth penetration, imaging beyond 240 µm from the serosa was difficult, thus the vascular network within the intestinal fold is not seen in these images.

Table S.1 Ionic composition and pH of Cortland's saline. Concentrations given in mM.

NaCl	124
KCl	5.1
$CaCl_2$	1.6
$MgSO_4$	0.9
$NaHCO_3$	11.9
NaH_2PO_4	3
Glucose	5.5 (C.2; C.4; C.5) or 0 (C.6; Appendix)
pH	7.4

A.5 Supporting references

Bernier-Latmani, J. and Petrova, T. V. (2016). High-resolution 3D analysis of mouse small-intestinal stroma. *Nat. Protoc.* **11**, 1617–1629.

Giuvărăşteanu, I. (2007). Scanning electron microscopy of vascular corrosion casts-standard method for studying microvessels. *Rom. J. Morphol. Embryol.* **48**, 257–261.

Harder, W. (1975). *Anatomy of Fishes*. E. Schweizerbart'sche Verlagsbuchhandlung: Schweizerbart.

Jodal, M. and Lundgren, O. (1986). Countercurrent mechanisms in the mammalian gastrointestinal tract. *Gastroenterology* **91**, 225–241.

Kapoor, B. G., Smit, H. J. and Verighina, I. A. (1975). The alimentary canal and digestion in teleosts. *Adv. Mar. Biol.* **13**, 109–239.

Olson, K. R. (1992). Blood and extracellular fluid volume regulation: Role of the renin-angiotensin system, kallikrein-kinin system, and atrial natriuretic peptides. In *Fish Physiology: The Cardiovascular System* (ed. Hoar, W., Randall, D., and Farrell, A.), pp. 135–254. San Diego: Academic.

Ricard, C., Fernández, M., Gastaldo, J., Dupin, L., Somveille, L., Farion, R., Requardt, H., Vial, J. C., Elleaume, H., Segebarth, C., et al. (2009). Short-term effects of synchrotron irradiation on vasculature and tissue in healthy mouse brain. *J. Synchrotron Radiat.* **16**, 477–483.

Rogers, M. P., Sherman, R. L. and Spieler, R. E. (2014). Studying vascularization in fishes using corrosion casting and microscopy: a Review. *Microsc. Adv. Sci. Res. Educ.* 95–102.

Shepherd, A. P. and Kiel, J. W. (1992). A model of countercurrent shunting of oxygen in the intestinal villus. *Am. J. Physiol.* **262**, H1136-42.

Soivio, A., Westman, K. and Nyholm, K. (1972). Improved method of dorsal aorta catheterization: Hematological effects followed for three weeks in rainbow trout (*Salmo gairdneri*). *Finnish Fish. Res.* **1**, 11–21.

Thorarensen, H., McLean, E., Donaldson, E. M. and Farrell, A. P. (1991). The blood vasculature of the gastrointestinal tract in chinook, *Oncorhynchus tshawytscha* (Walbaum), and coho, *O. kisutch* (Walbaum), salmon. *J. Fish Biol.* **38**, 525–531.

Witeska, M. (2013). Erythrocytes in teleost fishes: A review. *Zool. Ecol.* **23**, 275–281.

Wolf, K. (1963). Physiological salines for fresh water teleosts. *Progress. Fish Cult.* **25**, 135–140.